The HKIE
Geotechnical Division
36th annual seminar 2016

Reclamation:

Challenges and beyond

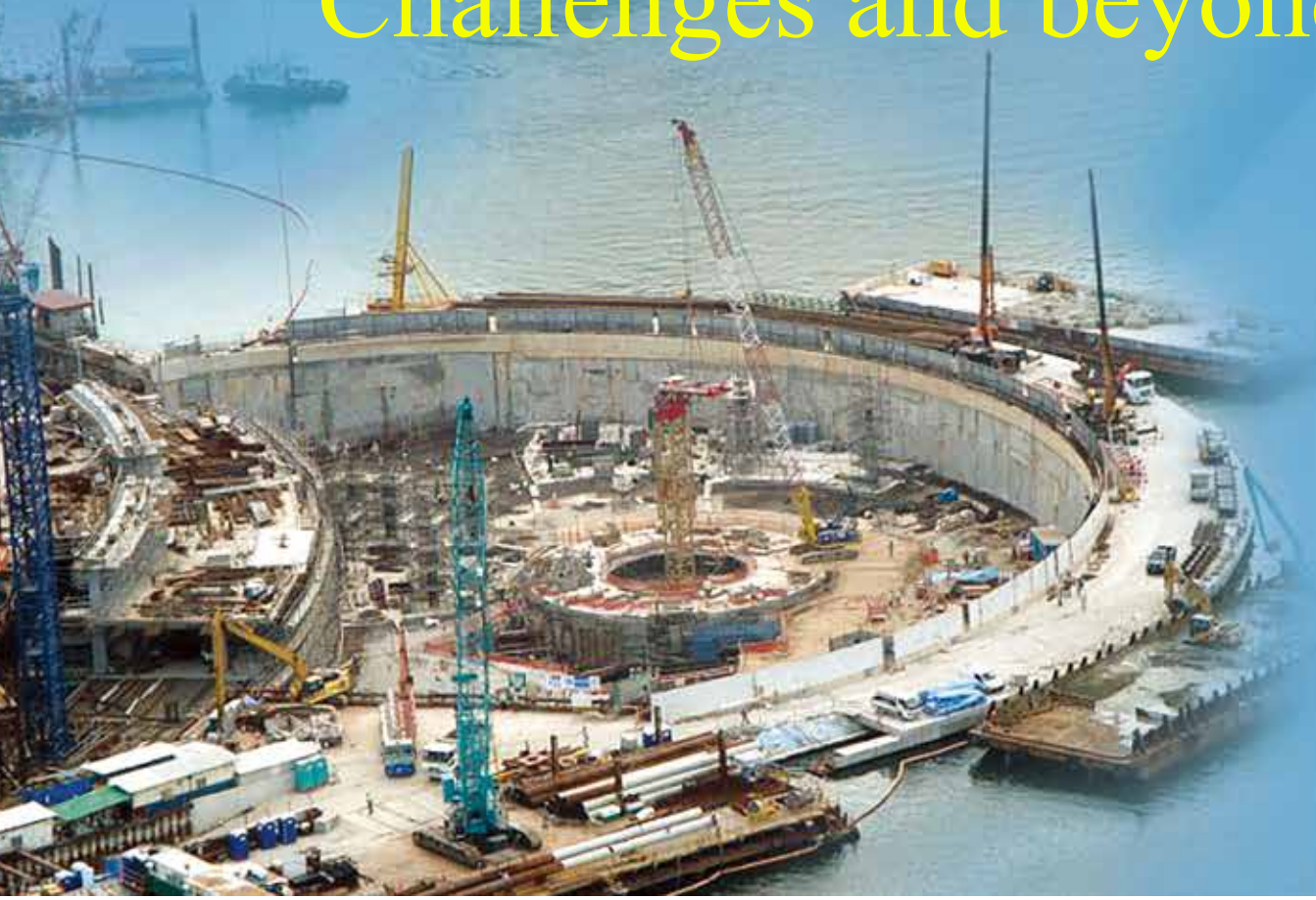

HKIE THE HONG KONG INSTITUTION OF ENGINEERS 香港工程師學會
Geotechnical Division 岩土分部

Co-organiser
HKGES 香港岩土工程學會 Since 2003

Supporting Organisations
HKIE THE HONG KONG INSTITUTION OF ENGINEERS Civil Division
HKIE THE HONG KONG INSTITUTION OF ENGINEERS Structural Division

FUGRO
CONSTANTLY EVOLVING

Fugro works with you, supporting each stage of your reclamation project, identifying and overcoming environmental, logistical and technical challenges.

Fugro are pleased to sponsor the HKIE Geotechnical Division 36th Annual Seminar.

www.fugro.com

華益土力有限公司
Lam Geotechnics Limited
Ground Investigation & Instrumentation Professionals

業務範圍包括:
Services Include:

※ 陸地及海上地質勘探
Land and Marine Ground Investigation

※ 陸地及海上靜力觸探試驗
Land and Marine CPT

※ 土力儀器安裝及監測
Geotechnical Instrumentation and Monitoring

※ 環境取樣、監測及審核
Environmental Sampling, Monitoring and Audit

※ 在線數據報告
Online Database Reporting

11/F, Centre Point, 181-185 Gloucester Road, Wanchai, Hong Kong
香港灣仔告士打道 181-185 號 中怡大廈 11 樓
Tel: (852) 2882-3939 Fax: (852) 2882-3331 Email: info@lamgeo.com Website: www.lamgeo.com

A city's metamorphosis

Raising land from sea is not a miracle — Arup created an oasis on reclaimed land with a navigable seawater canal system in Korea's Songdo International Business District, a youthful business gateway in north-east Asia.

40 YEARS IN HONG KONG | ARUP

TREVI
Foundation Specialists

Trevi Group is a worldwide leader in the field of ground engineering (special foundations, tunnel excavation, ground consolidation and the building and marketing of special rigs and equipment relevant to this engineering sector with its manufacturing division); the Group is also active in the drilling sector (oil, gas and water) both in the production of plant and the supply of services and in the construction of automated underground car parks.

The Group was established in Cesena (Italy) in 1957 and today has more than 50 subsidiary companies all over the world.

Its success is due to the vertical integration of the main divisions making up the Group:

- **Trevi**, the division that supplies special services in the field of ground engineering,
- **Petreven**, the oil drilling division of the Group,
- **Soilmec**, the division that produces and develops plant and machinery for ground engineering,
- **Drillmec,** the division that produces and develops drilling rigs (oil, gas and water).

The main activities of **Trevi Construction Co Ltd** in Hong Kong are:

1) Jet Grouting for ground improvement for basement excavation work and tunnelling work,
2) Ground Anchors, permanent and temporary,
3) Pipe Pile Installation,
4) Micro-piles (mini-piles),
5) All types of grouting including pressure, compaction, fissure, etc with cement and chemical based grout,
6) Ground freezing.

HK/2010/02
HK – Zhuhai – Macao Bridge HK Boundary Crossing Facilities – Reclamation Works

Trevi Construction Co Ltd
7/F, Sun Kwong Industrial Building, 1059 – 1061 Tung Chau West Street, Lai Chi Kok, Kowloon.
Tel : 2116 6966 Fax : 2117 0229 Email : info@trevihk.com Website : www.trevispa.com

ISO 9001:2008

MOTT MACDONALD

Pushing the boundaries of land

We have been supporting the delivery of innovative reclamation and land formation solutions in Hong Kong for over 30 years. For the Three-Runway System at the Hong Kong International Airport, we introduced ground improvement by deep cement mixing as a technically viable, sustainable alternative to dredging which will minimise environmental impact.

Opening opportunities with connected thinking

Mott MacDonald
T +852 2828 5757
E marketing.mmhk@mottmac.com
W mottmac.hk

我們的主要業務包括：
Our Business includes:

- 基礎工程
  Foundation Works
- 斜坡及擋土牆長遠防治山泥傾瀉工程
  Construction of Landslip Preventive and Mitigation Works to Slopes and Retaining Walls
- 道路及渠務工程
  Roads and Drainage
- 水務工程
  Waterworks
- 地盤平整工程
  Site Formation

中国地质工程集团公司
CHINA GEO-ENGINEERING CORPORATION

香港灣仔港灣道 30 號新鴻基中心 24 樓 2421-25 室
Rm. 2421-25, 24/F., Sun Hung Kai Centre, 30 Harbour Road, Wanchai, Hong Kong
Tel: (852) 2511 9001 Fax: (852) 2580 0697

包容 誠信 創新 奉獻

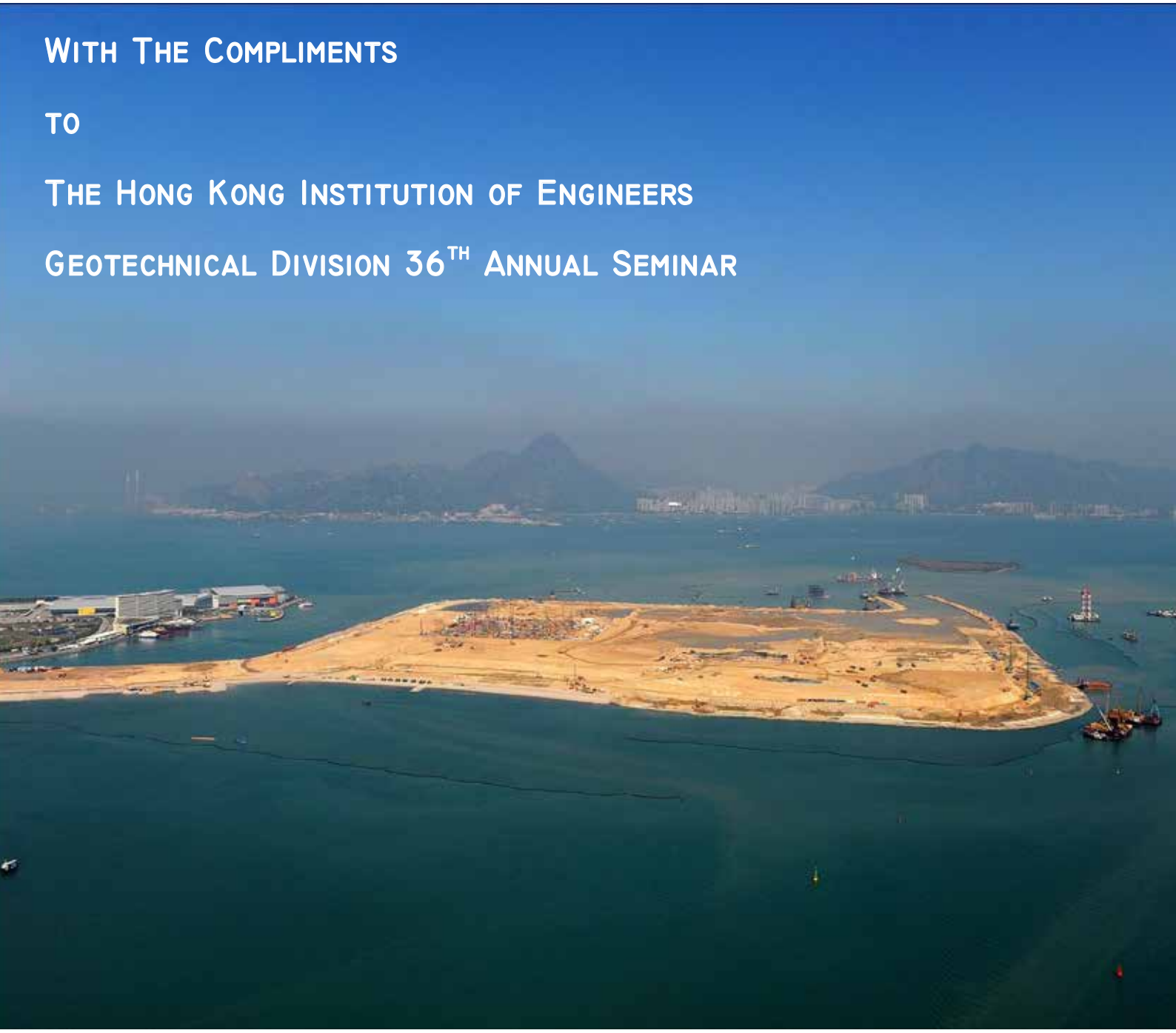

中國港湾 CHINA HARBOUR

BUSINESS ENVIRONMENT COUNCIL 商界環保協會 CORPORATE MEMBER

5 years+ 商界展關懷 caringcompany

中 國 港 灣 工 程 有 限 責 任 公 司

CHINA HARBOUR ENGINEERING COMPANY LIMITED

香港北角英皇道 370-374 號振華大廈 19 樓

19/F, China Harbour Building, 370-374 King's Road, North Point, Hong Kong

AECOM

Built to deliver a better world.

Tuen Mun - Chek Lap Kok Link

Central – Wan Chai Bypass

Wan Chai Development Phase II

From Chek Lap Kok Airport, Kwai Chung Container Terminals, Central-Wan Chai Bypass, Wan Chai Development Phase II to Tuen Mun – Chek Lap Kok Link, our reclamation work is transformative. We make a positive, lasting impact by applying our global reach, innovative approach, connected expertise and delivery excellence to solve complex, evolving challenges - challenges that can only be solved by a company like ours. One with deep roots and diverse perspectives. One with the people, technology and vision to deliver what others can only imagine.
We are AECOM – built to deliver a better world.

www.aecom.com

Dextra

WORLD LEADER | IN GEOTECHNICAL ENGINEERING FOR 30+ YEARS

GEOGRIDS For Walls & Slopes Reinforcement

Tensar®




GEOGRIDS For Subgrade Stabilization & Pavement Optimization



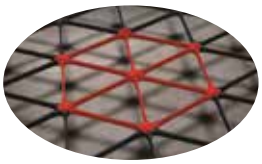

ANCHORS

GFRP ROCK-BOLTS

GFRP SOIL-NAIL

GFRP TIE-BACK

ASTEC


SOFT-EYE

CONSTRUCTION

INSTALLATION

BREAK-THROUGH

DEXTRA PACIFIC LIMITED
Tel: (852) 2845 7766 Fax: (852) 2586 1656
E-mail: dplbuilding@dextragroup.com
Website: www.dextragroup.com

ARCADIS Design & Consultancy for natural and built assets

Starting with Deep Market Insights

Designed by Sector Professionals
Creating Exceptional and Sustainable Outcomes

Arcadis is the leading global Design & Consultancy firm for natural and built assets. Applying our deep market sector insights and collective design, consultancy, engineering, project and cost management services, we work in partnership with our clients to deliver exceptional and sustainable outcomes throughout the lifecycle of their natural and built assets.

We are 27,000 people active in over 70 countries that generate €3.4 billion in revenues. Within Asia we can call upon the skills and resource of almost 6,000 professionals based throughout the region.

We support UN-Habitat with knowledge and expertise to improve the quality of life in rapidly growing cities around the world.

For more information please contact:
T: (852) 2911 2233
E: hyder.hk@ arcadis.com
www.arcadis.com

康和建築工程有限公司
Konwall Construction & Engineering Co., Ltd

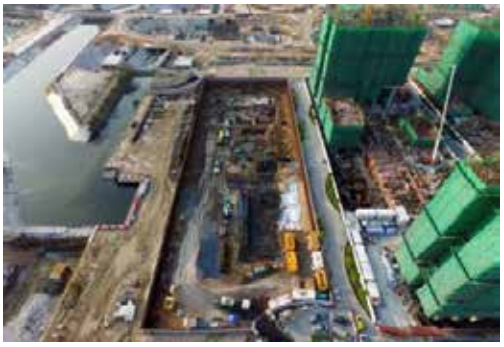

Buildings Department

- Registered General Building Contractor
- Registered Specialist Contractor in the Foundation Works Category
- Registered Specialist Contractor in the Demolition Works Category
- Registered Specialist Contractor in the Ground investigation Field Works Category

Development Bureau

- Approved Specialist Land Piling Contractor (Group II) for Public Works
- Approved Site Formation Contractor (Group B Probationary) for Public Works

Unit 1003, K. Wah Centre, 191 Java Road, North Point, Hong Kong 香港北角渣華道 191 號嘉華國際中心 1003 室 Tel: 2563 1233 Fax : 2561 7122

Civil Engineering Contractor Specializing in Foundation & Site Investigation Works

VIBRO 惠保(香港)有限公司
VIBRO (H.K.) LIMITED
新創建集團成員 Member of NWS Holdings

11/F., Chevalier Commercial Centre,
No. 8 Wang Hoi Road, Kowloon Bay, Hong Kong
Tel: (852)2137-5500 Fax: (852)2137-5599
Website: http://www.vibro.com.hk Email: email@vibro.com.hk

泰昇集團
TYSAN GROUP
泰昇地基工程有限公司
TYSAN FOUNDATION LIMITED
泰昇地基土力工程有限公司
TYSAN FOUNDATION GEOTECHNICAL LIMITED

ISO 9001: 2008 Certificate No.: CC 111
ISO 14001: 2004 Certificate No.: CC 3315
OHSAS 18001: 2007 Certificate No.: CC 3316
ISO 50001: 2011 Certificate No.: CC 5697

香港黃竹坑香葉道2號One Island South 20樓
20/F One Island South, 2 Heung Yip Road, Wong Chuk Hang, Hong Kong.
電話 Tel: (852) 2882 3632 傳真 Fax: (852) 2808 0565
網址 Website: http://www.tysan.com

泰昇地基工程有限公司
泰昇地基土力工程有限公司
業務覆蓋香港及澳門，專注地基工程，主要提供設計及建造服務，包括地盤勘察、海陸鑽孔樁／打樁、迷你樁、鑽孔工程、地腳、樁帽及地庫工程、地盤平整、泥釘及斜坡之防護工程。

Tysan Foundation Limited
Tysan Foundation Geotechnical Limited
spcialise in foundation works with businesses covering Hong Kong and Macau area. We provide services on design and construction which include site investigation, land & marine bored/driven piling, mini-piling, pre-boring work, footing, pile cap & basement construction, site formation, soil nail and slope protection work.

LAMBETH

Distinctly Different





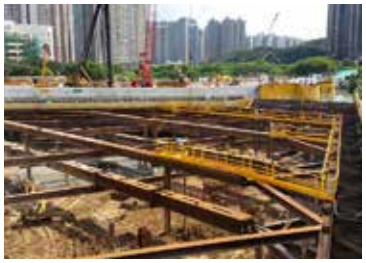

Lambeth brings together the diverse experience of operations, planning, commercial and design professionals – from within Gammon and Balfour Beatty – ensures it remains at the forefront of new techniques and new thinking. We set the standard for both innovation and technological advancement in building, civil, environmental, foundations, geotechnical and safety disciplines.

A member of the Gammon Group

28/F Devon House, Taikoo Place, 979 King's Road, Hong Kong Tel: 2516 8823 Fax: 2516 6352

An award of the Hong Kong geotechnical profession

The HKIE Geotechnical Paper Award

(see inner pages for a report on the 2016 Award)

Proceedings of the 36th Annual Seminar
Geotechnical Division, The Hong Kong Institution of Engineers

Reclamation: Challenges and Beyond

3 June 2016
Hong Kong

Jointly organised by:
Geotechnical Division, The Hong Kong Institution of Engineers
The Hong Kong Geotechnical Society

Supported by:
Civil & Structural Divisions, The Hong Kong Institution of Engineers

Captions of Figures on the Front Cover

Top Left to Right:

1) Example of Ground Stabilisation using Hexagonal Geogrids over Extremely Soft Soils in Malaysia (By courtesy of Tensar International Limited, Malaysia)
2) Site Overview during Ground Improvement Works in Cotai, Macau SAR (By courtesy of Ban Lam, Halcrow China Limited, and Benaim Limited)

Bottom Left to Right:

3) Aerial View of the Power Plant on Reclaimed land in Operation in Malaysia (By courtesy of Golder Associates (HK))
4) Dry Bottom-feed Columns Installed for a Dockyard using Purpose-built Rigs in Malaysia (By courtesy of Keller Group plc, Keller ASEAN, and Keller AsiaPacific Ltd)

Background:

Deep Excavation in Semi-Circular Cofferdam next to Sea Shore on Reclaimed Land in Singapore (By courtesy of Ove Arup & Partners Hong Kong Limited)

Soft copy of the proceedings can be downloaded from the HKIE Geotechnical Division's website http://hkieged.org/geodiv/annualseminar.aspx

ORGANISING COMMITTEE

Chairman
Ir James Sze

Members
Ir Lily Chan
Ir Warren Dou
Ir David Lai
Ir Chris Lee
Dr Andy Leung
Ir Clifford Phung
Ir K P Yim
Ir Jack Yiu
Ir Ringo Yu

Technical Sub-committee
Ir Dr Johnny Cheuk
Ir Warren Dou
Ir Dr Julian Kwan
Ir David Lai
Ir Dr S W Lee
Dr Andy Leung
Ir Clifford Phung
Ir Jack Yiu

Published by:
Geotechnical Division
The Hong Kong Institution of Engineers
9/F., Island Beverley, 1 Great George Street, Causeway Bay, Hong Kong
Tel: 2895 4446 Fax: 2577 7791

Printed in Hong Kong

FOREWORD

The reclamation of land from the ocean has long been used in Hong Kong to expand the limited supply of developable land. Numerous land reclamation projects were successfully carried out to create buildable land. Many new towns such as Sha Tin, Tai Po, Tuen Mun, Ma On Shan, and Tseung Kwan O were built on reclaimed land and so were both the old airport at Kai Tak and the current Hong Kong International Airport at Chek Lap Kok. Many of these reclamations involved dredging of the soft marine deposit on the surface of the seabed, in order to reduce the risk of instability during reclamation. With the increasing awareness and current standards on environmental protection, there are high expectations both from the regulating authority and the general public for reclamation works to have minimal impact on the marine environment. This implies that the reclamation design has to deal with, one way or the other, the soft mud in-situ. This is typically one of the key challenges facing geotechnical engineers when it comes to reclamation design, especially when the seabed level is deep and the thickness of the soft mud is significant.

The 36th Annual Seminar of the Geotechnical Division has a theme on "Reclamation: Challenges and beyond". It aims to take stock on the challenges facing the geotechnical profession, and to provide a platform for geotechnical practitioners and academics to impart the recent advancements on reclamation practices. The proceedings contain two keynote papers by Prof. C.F. Leung and Prof. Mark Randolph who are renowned experts on soft soil and offshore engineering respectively. The topics of the other papers span across a wide spectrum or topics covering marine geology, ground treatment techniques, constitutive modelling and reclamation case studies.

On behalf of the Geotechnical Division, I would like to thank the Hong Kong Geotechnical Society (HKGES) for jointly organising this seminar, and the HKIE Civil Division and Structural Division for their support. I am grateful to our Guest-of-Honour, Ir HON Chi Keung JP, Permanent Secretary for Development (Works), and our Keynote Speakers, Prof. C.F. Leung and Prof. Mark Randolph. I would also like to express my gratitude to the authors and speakers contributing to this seminar and the Organising Committee, under the leadership of Ir James Sze, for their excellent efforts in making this seminar a great success.

Ir Patrick A Chao
Chairman, Geotechnical Division
Hong Kong Institution of Engineers (2015/2016 Session)
June 2016

The HKIE Geotechnical Paper Award

In the proceedings of the 34th Annual Seminar of the Geotechnical Division of the institution, I reported on the Award scheme and the outcome of the 2014 selection exercise. I wish to update you on the matter.

The 2016 exercise opened for entries on 1 December 2015. By the end of the nomination period on 31 January 2016, there were seventeen entries. This is less than in the first exercise in 2014, but the papers are likewise all of very high quality.

An Assessment Board was formed to look at the entries. It is chaired by the Chairman of the Geotechnical Division Committee (GDC), and comprises the Deputy Chairman of GDC, together with five members from a standing Assessment Board Penal of eminent members of the geotechnical profession. The Assessment Board hence comprises Ir Patrick Chao, Ir James Sze, Ir Dr CK Lau, Ir KW Leung, Ir Dr Victor Li, Ir CM Wong and Ir YC Chan.

We continued the code of strict confidentiality introduced in the 2014 exercise, to facilitate frank and critical views from members, and to assure those who entered papers that the entries will be handled with discretion and upmost fairness. Assessment Board members received information on a need-to-know basis. They passed views to a designated member of the Board who then redirect it to members of differing views upon removal of any identity tags, for response or adjustment of views. This was repeated until no new points came up. The final decision on winners was by secret ballot with the summary of anonymous views in hand. This permits the Board to develop in-depth appreciation of the relative strength and specialties of the contending papers, with time to ponder and dig up supporting information, and with room for contention without tension. It ensures that all papers are given fair consideration for the best to come out.

Members of the Assessment Board Panel were selected to form the Board with in mind, among other things, avoidance of perceived conflict of interest. Such facility is not possible in respect of the Chairman and Deputy Chairman of GDC, who join the Board by nature of their office. In the present exercise, both have peers from their firms who are co-authors of the entries. To minimize possible conflict of interest, they took part in sharing of views on the papers, but abstained from the secret voting in which winners were selected.

The voting found two papers to be equally strong, in respect of their potential to advance local geotechnical practice and their quality of writing for the readership of practicing geotechnical engineers. It was not possible to place one ahead of the other with confidence. The Board therefore selected both for the Award, as follows.

Almog, E., Mangione, M. and Cachia, G. (2015) Ground relaxation in segmental lining design using the convergence-confinement method. Proceedings of the Underground Design and Construction Conference 2015, IOM3, Hong Kong Branch, pp335-345

The paper describes a methodology for designing linings for TBM tunnels, as applied to a recently completed tunnel project. It is based on the convergence-confinement method which is still receiving research attentions though introduced decades ago. The methodology distinguishes itself by a simple but insightful extension to the latest thoughts on the method, to account for the effect of face pressure, a key parameter for controlling closed-face TBM. The paper appeared to have been written with presumed tunneling knowledge of readers. With the systematic description of evolving ideas on the method, their application and finally the back-analyses from the tunnel project, and with the succinct conclusions and the compact set of reference, an average geotechnical engineer should be able to follow the arguments and judge on the strength of the methodology. There are places that the paper was too sketchy, but the drive for brevity for the limit space of a proceedings paper could be understood. There are also occasional typo mistakes including two affecting equations. Let readers be aware.

Kwan, J.S.H., Chan, S.L., Cheuk, J.C.Y. and Koo, R.C.H. (2014) A case study on an open hillside landslide impacting on a flexible rockfall barrier at Jordan Valley, Hong Kong. Landslides, Springer-Verlag Berlin Heidelerg, Vol 11, pp1037-1050

The paper documented in detail the first local case of response of a flexible barrier to open hillside landslide debris. It reviewed succinctly the state of the art of flexible barrier design to support a back-analysis. Observations on improving local practice were put forward. Although flexible barrier design technology has since advanced significantly, most of the paper's observations remain relevant and the paper provides a faithful record of its time and a milestone against which the rapid progress of technology could be visualized. The detailed record could be used to calibrate newer design technology. The paper is carefully structured and amply illustrated to bring the subject to readers of a wide range of background knowledge.

Each winner is to keep a trophy until the time of the next award exercise. Each of the authors of a winning paper is to receive for his personal retention a plaque based on the trophy and also a certificate. These are presented in the annual seminar for which this set of proceedings is produced.

Further information of the Award can be found in http://hkieged.org/geodiv/geopaperaward.aspx, the official webpage.

Y C Chan

Secretary, Assessment Board

The 2016 HKIE Geotechnical Paper Award

June 2016

ACKNOWLEDGEMENTS

The Organising Committee would like to acknowledge the support of Civil and Structural Divisions of HKIE and express sincere gratitude to the following sponsors for their generous support of the Seminar:-

Keller Foundations (SE Asia) Pte Ltd.
Intrafor Hong Kong Limited
Fugro Holdings (Hong Kong) Limited
Arup
Lam Geotechnics Limited
Earth Products China Ltd.
AECOM Asia Co Ltd.
Arcadis
Atkins China Limited
China Geo-Engineering Corporation
China Harbour Engineering Company Ltd.
Dextra Pacific Ltd.
Mott MacDonald Hong Kong Ltd.
Trevi Construction Co., Ltd.
Konwall Construction & Engineering Co., Ltd.
Lambeth Associates Limited
Nippon Steel & Sumikin Bussan (HK) Co., Ltd.
Tysan Foundation Limited
Vibro (H.K.) Limited

TABLE OF CONTENTS

Land Reclamation and Ground Improvement: Singapore Experience

C.F. Leung
Centre for Soft Ground Engineering, National University of Singapore, Singapore

ABSTRACT

With extensive land reclamation in the past several decades, the land area of Singapore has increased by over 20%. This paper highlights the development and challenges of land reclamation works in Singapore. These include the placement of fills on soft sea beds and the lack of suitable fill materials for land reclamation. The salient findings from existing and ongoing research studies on land reclamation are presented. In addition, the environmental concerns for new reclamation works are briefly discussed. Before land reclamation, it is necessary to construct protection bunds around the perimeter of the site to be reclaimed. The problems faced in the bund construction on soft soils are highlighted. For reclamation works such as the development of new container terminal ports, permanent wharf front structures are required and the challenges faced in its construction on difficult ground conditions are highlighted. As soft soils are prominent in Singapore, ground improvements works are necessary before the new reclaimed land can be used for development. The historical development of ground improvement works on reclaimed lands underlain by sandy, clayey and mixed grounds are presented.

1 INTRODUCTION

For the past several decades, Singapore population has grown from just 2.1 million in 1970 to 5.53 million in 2015. To cope with increasing population and economic activities, Singapore has developed its Master Plan since 1950s with regular reviews and updates. The latest 2014 edition (URA 2014) is the 9th of the series. The major development for the present phase includes the expansion of the Changi Airport with new mega passenger terminal and runway, the construction of new container ports in Tuas in the west to replace the existing ports and the construction of several new subway lines. Singapore is a small country with its land area of just about 590 square kilometers in 1970. As part of the previous master plans, extensive land reclamation had been carried out and the land area has grown by over 20% with a land area of 719 square kilometers in 2015.

This paper provides an overview on existing and ongoing land reclamation works in Singapore. The challenges faced in the works and how they are overcome are presented. With extensive land reclamation works in the past decades, there are currently shortage of suitable reclaimed fill materials. Research studies on employing alternate land reclamation fills such as construction waste materials, soils dredged from the seabed and improvement of weak reclamation fills are highlighted in this paper. For general reclamation works, perimeter bunds need to be constructed. As soft soils are prominent in Singapore, the problems of constructing such bunds on soft grounds are presented. A large portion of ongoing land reclamation works in Singapore deal with the construction of new container port terminals. Permanent wharf front structures need to be constructed. The challenges faced for the construction of such structures on complex seabed conditions are discussed. Before the reclaimed land can be developed, the land with underlying in-situ soft soils needs to be improved and strengthened. The advancement of ground improvement works in sandy grounds, clayey grounds and mixed grounds are presented in this paper.

2 LAND RECLAMATION

Choa (1991) presented the major land reclamation projects for the development of Changi Airport and port in Singapore during the Hong Kong Annual Geotechnical Seminar in 1991. He highlighted that land reclamation in Singapore dated back to 19th century. As thick soft soils are abundant along the coasts of Singapore, he reported the problems faced while reclaiming land for the Changi airport particularly for the second runway which rested on soft soils with variable strengths and thicknesses.

In 1991, extensive land reclamation was ongoing for the construction of Hong Kong's Chek Lap Kok Airport. The development of the airport including its challenging ground conditions and the difficulties in land reclamation are well documented (Plant et al. 1998). The issues of creep of the thick sand fill was discussed in detail by Pickles & Tosen (1998) and the residual settlement of the Hong Kong airport was examined by Zhao et al. (2011). In view of the above, the issue of possible long term settlement of reclaimed land in deep waters had drawn attention to the geotechnical community of Singapore.

2.1 Reclamation on soft grounds

Plate 1 shows a typical land reclamation work in progress in Singapore with a large part of the protection perimeter bund constructed first. Barges with reclamation fills are brought inside the bund area to place the fills till the highest possible elevation, typically at high tide elevation. The remaining fills will be placed by pumping the fill materials from outside the bund into the reclaimed area till the intended reclaimed fill reaching the desired top elevation plus allowance for the estimated settlement of the fill and in-situ soils under the new fill. For a big reclaimed area, the correct estimation of settlement of a reclaimed land is crucial as a relatively small underestimation of settlement of in-situ soils under the reclaimed fill could cost the contractor millions of dollars for a lump sum contract.

Plate 1: Typical land reclamation work in progress

In the early days, land reclamation might not be successful due to presence of very soft in-situ clay at the seabed. In such case, the very soft clay often heaved up causing the so-called 'mud heave' phenomenon. As an example, land reclamation using sand fill was not successful at some parts of a large reclamation site and there was a dispute between the client and the contractor. The contractor was not proficient from the client's view point while the very difficult in-situ soil conditions were the reason put forward by the contractor. Experts were invited to evaluate the causes of the problem and additional extensive site investigation was carried out to establish the detailed soil profile and properties. In-situ vane shear tests were carried out as the main investigation tool as it was difficult to obtain undisturbed very soft soil samples. The undrained shear strength

values were compared with those of unconsolidated undrained triaxial compression tests conducted on the limited number of undisturbed soil samples that could be collected at the site.

Based on the soil plasticity index values, it was established that Bjerrum's (1972) correction factor of 0.75 should be applied to correct all the vane shear strength values. It was found that such correction was reasonable as the corrected vane shear strength agreed with the limited undrained shear strength values from triaxial tests. A summary of a typical soil strength profile is shown in Figure 1. It is evident that the top 5 m of in-situ soil was extremely soft having a very low unit weight of 12.6 kN/m^3 and an average undrained shear strength of only about 3 kPa.

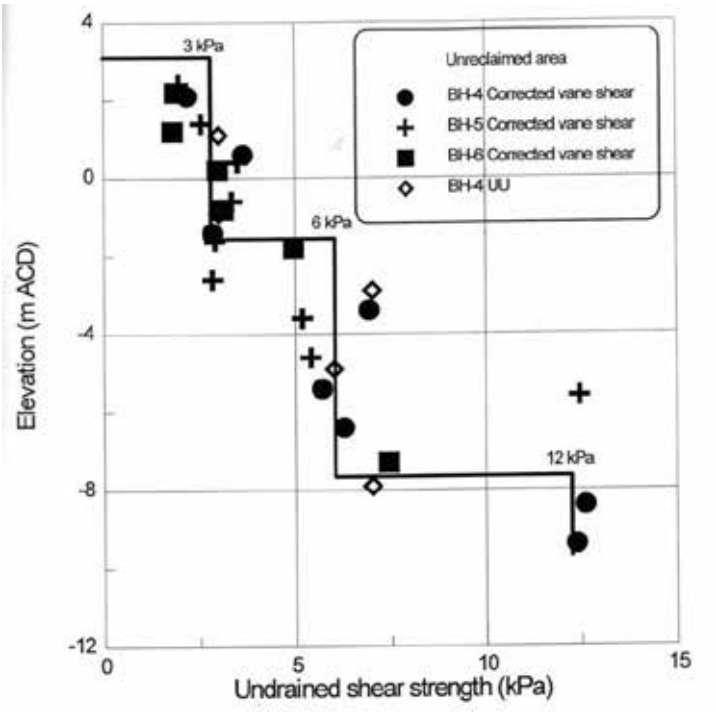

Figure 1: Soil strength profile after extensive soil investigation

In view of presence of soft clay, the reclamation contract specified that the fill height should not exceed 1 m for every fill height increment. Slope stability analyses revealed that global stability was not an issue as long as the 1-m fill height did not possess a slope angle exceeding 30^o which could be readily achievable for the loose sand fill at the site. Table 1 shows a summary of the global slope stability analyses. However, bearing capacity was established to be an issue as the 'unexpected' very low soil strength of 3 kPa could not support the relatively small fill increment height of 1 m. A summary of the bearing capacity calculations is shown in Table 2. As the contract allowed 1-m fill height increment, the contractor was judged to be not at fault and the main cause of the land reclamation failure at some parts of the site was due to the presence of the 'unexpected' very soft clay on the seabed at the locations which was not revealed from the soil investigation reports provided at the tender stage.

Table 1: Summary of global stability analyses

Hydraulic fill height	Maximum safe slope angle (^{o})	Maximum slope gradient	Safety factor based on angle of response of sand fill
1.0 m	30	1:1.73	1.68
1.5 m	30	1:1.73	1.12
2.0 m	4.1	1:14	1.00
3.0 m	3.2	1:18	1.00

Table 2: Summary of magnitude of critical fill height from bearing capacity calculations (Assume strip footing and safety factor =1)

Undrained soil strength (kPa)	3	4	5	6	7	8
No surcharge	0.91 m	1.21 m	1.51 m	1.81 m	2.12 m	2.42 m
Surcharge 5 kPa	0.61 m	0.91 m	1.21 m	1.51 m	1.82 m	2.12 m

After the land reclamation for the present Changi airport in the 1970s, reclamation was further extended to the east of the airport in 1990s and termed as the Changi East reclamation project. In fact the present ongoing extension of the Changi Airport new mega terminal and runway are located in the western part of this site. An area of ultra-soft slurry pond was encountered which was extremely difficult to reclaim. Chu et al. (2009) described in detail the very careful approach to achieve a workable reclamation scheme for the silt pond. Figure 2 shows that the in-situ soils had extremely high water content and very low undrained shear strength of between 1 to 6 kPa up to 20 m depth. The soil strength is as soft as that described earlier in this paper but with the very soft soil extending to greater depth. To make the reclamation successful, sand spreader systems shown in Figure 3 were used to first sprinkle the sand on the soft clay systematically and slowly such that the ultra-soft soils would not heave. Once a certain thickness of the sand fill with sufficient strength is achieved, light weight machines were sent onto the sand fill to install flexible vertical drains into the soft clay such that water can be squeezed out of the clay to make the clay stronger. Once this first stage is completed, the process was repeated with further sand fill being placed. With more water being squeezed out from the clay using new drains installed, the improved soft clay can hence withstand the fill loading and the land reclamation was thus successful.

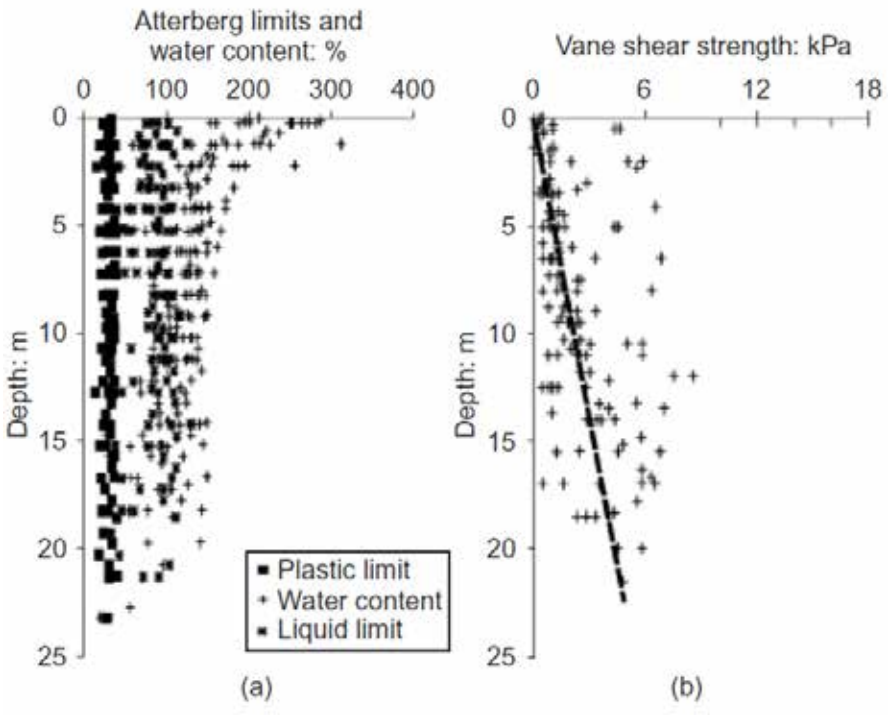

Figure 2: Variations of soil parameters with depth (after Chu et al. 2009)

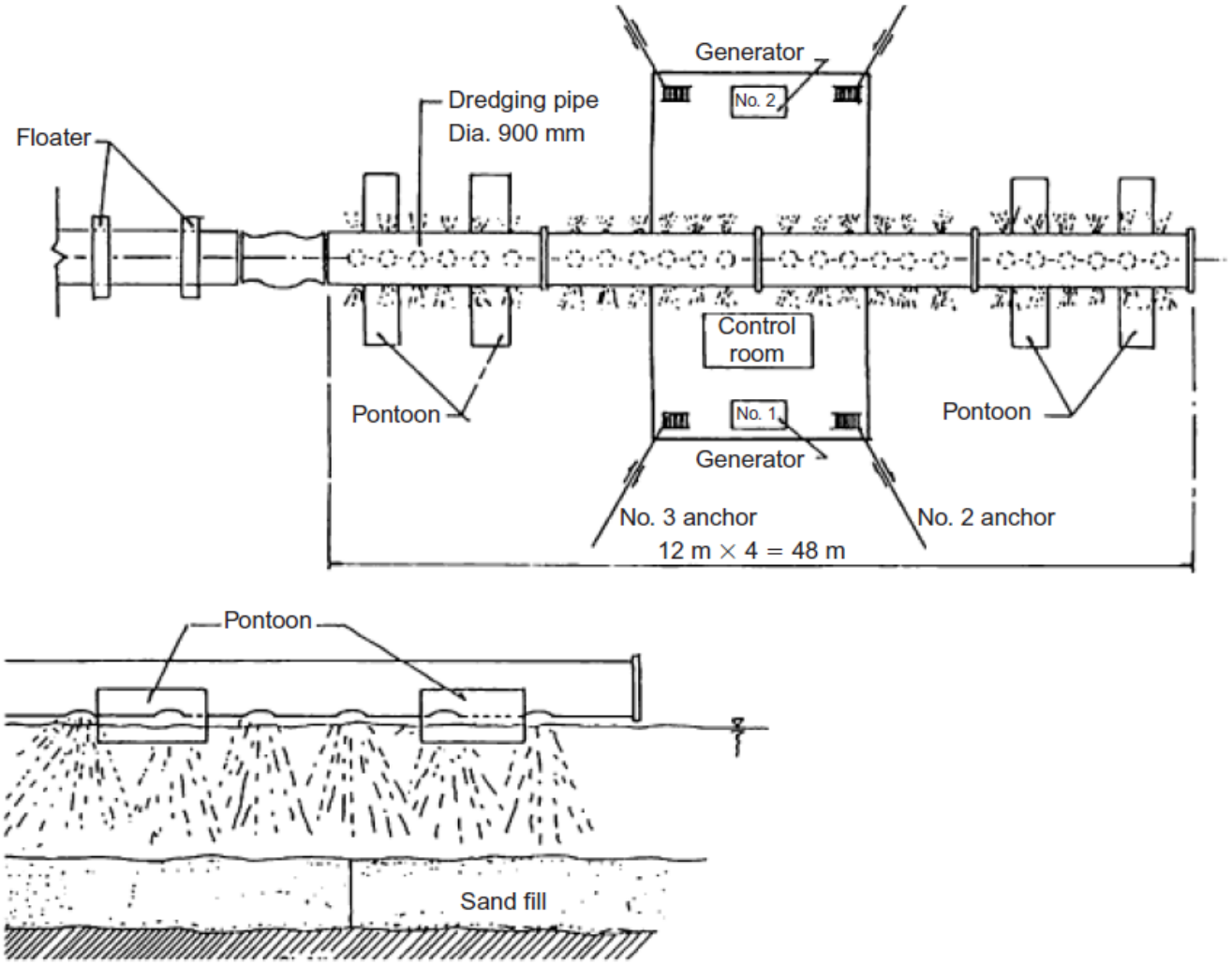

Figure 3: Sand spreader system (after Chu et al. 2009)

2.2 Reclamation fills

In the 1960s, hill cut materials were mainly employed as the fill materials for land reclamation. As Singapore is a relatively flat island, the hill cut materials were soon exhausted. Sand dredged from the seabed was then used for the land reclamation of the present Changi Airport. As reclamation sites became bigger in plan and in considerably deeper waters, large amount of fill materials were required in recent land reclamation works and there was severe shortage of 'good' reclaimed fills. Alternate fills other than sandy soils need to be explored for land reclamation. One of the first major study was the sand-clay sandwich scheme for land reclamation. Figure 4 shows a schematic of such scheme reported by Lee et al. (1990). Essentially sand was sprinkled at the site such that the clay underneath would not heave. Once a minimum thickness of sand was reached, clayey fills could be placed and the process repeated till the final reclaimed height with adjustment for the settlement of the sandwiched clay and in-situ soils. The sand layers served as horizontal drainages that could speed up the consolidation of the sandwiched clay fill.

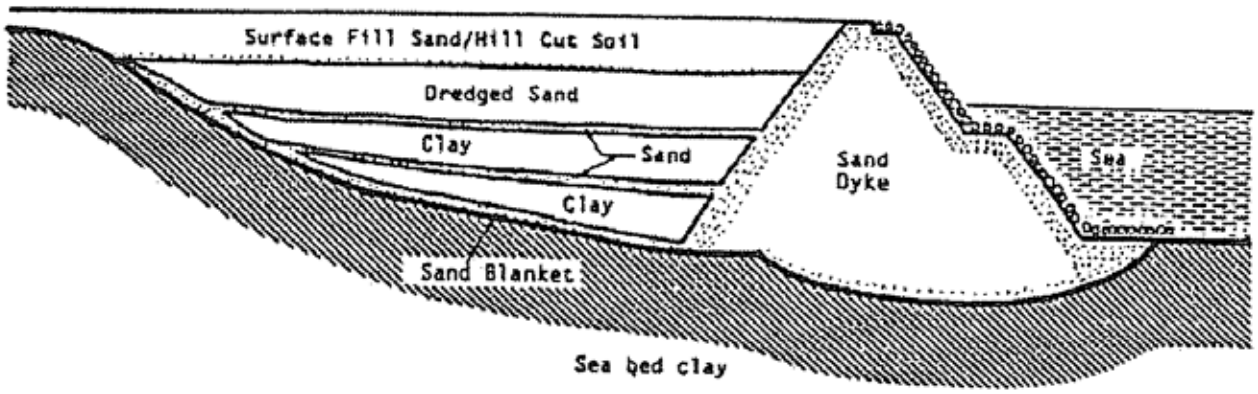

Figure 4: Sand-clay sandwich reclamation scheme (after Lee et al. 1990)

Singapore economy is rapidly growing with many deep excavation and tunneling activities. In addition, it needs to dredge its seabed regularly to maintain the depth of its navigation channels. There are abundance of construction waste soils and dredged materials and finding dumping grounds for such materials can be difficult for a small country like Singapore. It is certainly attractive to use the above waste soils for land reclamation. In fact, all the present ongoing land reclamation projects specify that they must receive the waste soils which are classified as 'bad earth' (soft soils) and 'good earth' (stiff soils). For the use of soft soils for land reclamation, the problems lie with difficulties in making land reclamation successful as highlighted earlier in this paper. In addition, the settlement of the soft soil fills and the in-situ soft soils must be considered. Ground improvement is often necessary to accelerate the settlement of the fills and the in-situ soils.

In some cases, the seabed may consist of residual soils which are stiff and over-consolidated in nature. It is thus attractive to use stiff soils (good earth) for land reclamation but this could pose other problems. Stiff soils often form lumps and the placement in lumpy fills would create voids between the clay lumps. The closing up of the voids is a great concern and engineers certainly would like the voids being closed up during fill placement rather than under working conditions. Plate 2 shows a large stiff clay lump dredged from the seabed and Figure 5 shows a schematic of lumpy fill system with voids between stiff clay lumps. The settlement process of such lumpy fill can be complex as it consists of the closing up of inter-lump voids and consolidation settlement of the clay lumps.

Plate 2: Large stiff clay lump dredged from seabed

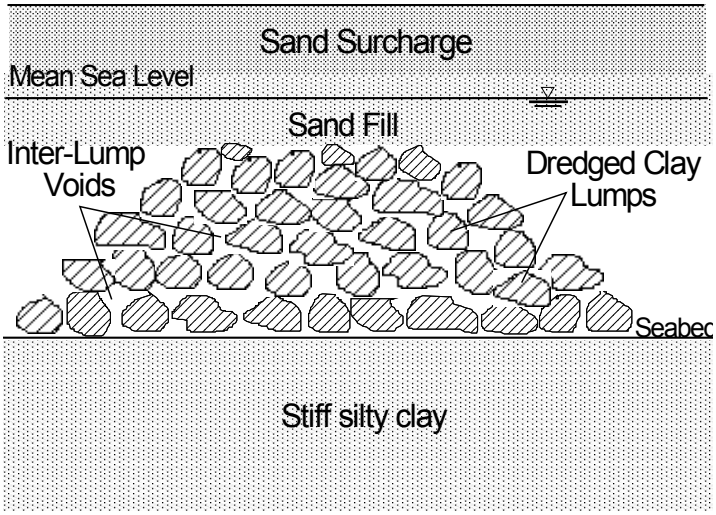

Figure 5: Lumpy fill system (after Leung et al. 2001)

Conventional large scale one-dimensional consolidation tests were conducted to observe the movements and rotations of the clay lumps using pins attached to selected clay lumps before the test. Figure 6 shows the visualization of the movements and rotations of spherical clay lumps. As expected, the upper lumps had moved down and rotated by a much larger amount as compared to those of lower lumps. However, the lower lumps deformed significantly more as compared to the upper lumps as they experienced considerably higher overburden stresses. Upon higher loading, the lower lumps were observed to be crushed and further deformation took place. Leung et al. (2001) described the test results and observations in detail.

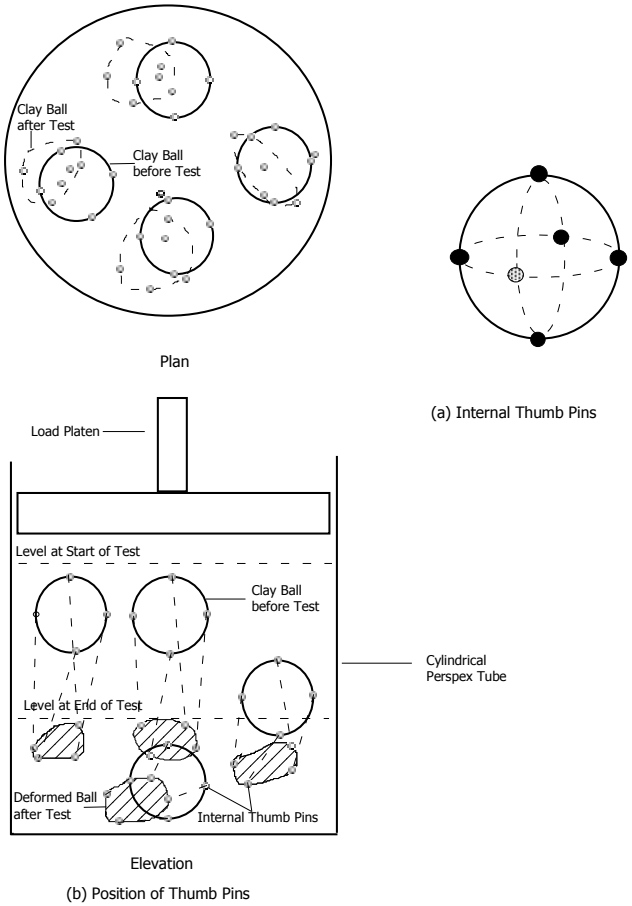

Figure 6: Movements and rotations of clay lumps (after Leung et al. 2001)

To further investigate the lumpy fill behavior, centrifuge model tests were conducted at 100g on the National University of Singapore geotechnical centrifuge (Plate 3). Centrifuge modeling has advantages that under forced gravitational field, the prototype soil stresses can be appropriately simulated and the time for soil consolidation can be accelerated by a factor of $1:N^2$ where N is the gravitational field. As an example, for centrifuge tests conducted at 100g, 1 day consolidation time in model scale is equivalent to 10,000 days (27.4 years) in prototype time.

Figure 7 shows the centrifuge model set up which consists of a strong box. High resolution photographs could be taken regular during the test through the front Perspex window. Details of the centrifuge model set-up were presented in Leung et al. (2001).To facilitate double drainage for soil consolidation, 40-mm thick uniform coarse sand was placed at the bottom of the strong box. The simulated prototype fill was 30 m by 21 m in plan and 18 m thick at 100g.

Plate 3: National University of Singapore Geotechnical Centrifuge

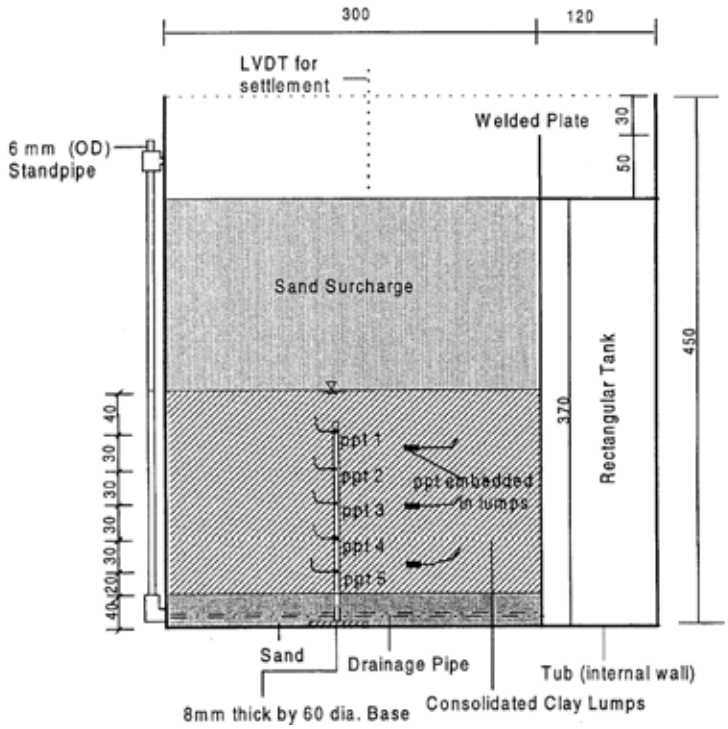

Figure 7: Centrifuge model setup of lumpy fill study (after Leung et al. 2001)

As the clay lumps could be of different shapes and sizes, spherical, cubical and irregular shape model lumps of 1 cm^3 volume (prototype scale 1 m^3) were first simulated with the model lumps prepared from the clay bed using knives and specially made spades. The clay lumps were uniformly placed in the model container in layers. After the placement of clay lumps, rubber tube inlets were inserted by the sides of the model container such that de-aired water could be drained into the clay lumps in-flight. The variation of surface settlement strains (settlement/original thickness) with time for clay lumps of irregular, spherical and cubic shapes under 120 kPa loading is shown in Figure 8. It is observed that the fill made up of spherical lumps experienced smaller settlement strain compared to cubical and irregular shape lumpy fills. This is due to spherical lumps having a more stable open structure that effectively form a densely packed structure within the lumpy fill.

The results illustrate that the shape of lump greatly affects the consolidation behavior of the lumpy fill. The void ratio of the lumpy fill system e_{sys} at the end of the tests at 100g for spherical, irregularly and cubical shaped lumps were determined to be 1.09, 1.09 and 1.16, respectively. Hence the final void ratio after both self-weight and surcharge consolidation is similar. It can be deduced that the settlement of the lumpy fill is mainly caused by the closing-up of inter-lump voids and the settlement due to lateral spreading of the lumps is not significant. The voids between the clay lumps were observed to be almost closed under a relatively small surcharge pressure of 40 kPa. The results of further studies on lumpy fill consolidation were reported by Robinson et al. (2005).

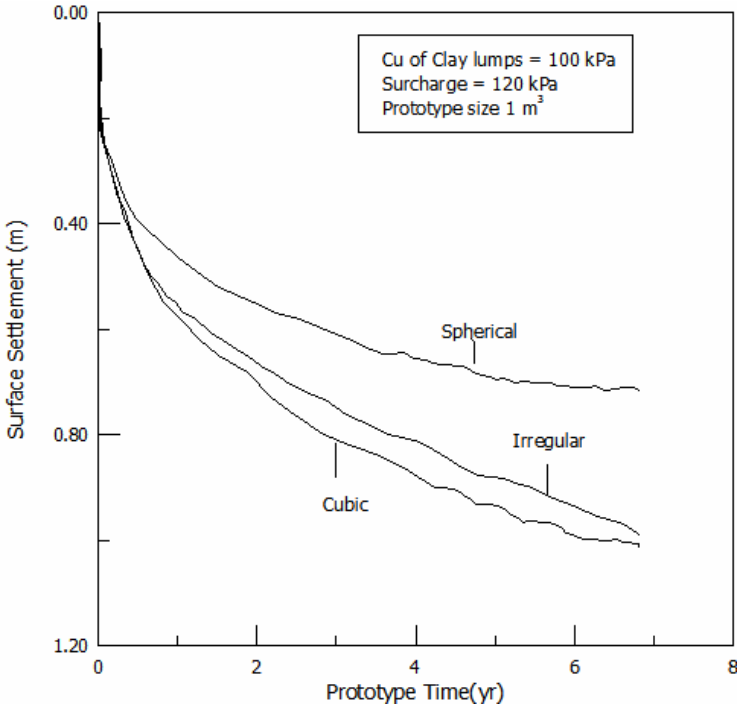

Figure 8: Settlement-time plots for lumps of different shapes (after Leung et al. 2001)

Cement mixed soil is being explored as possible alternate fill materials for land reclamation in Singapore. If successful, this would greatly reduce the use of sand as fill materials. In Japan, the use of stabilized clay slurry with a small amount of cement as reclamation fill had been explored in the recent Haneda Airport extension (Morohoshi et al., 2010) and Chubu Airport construction (Kitazume and Satoh, 2005). Tan et al. (2011) reported the first pilot study of using cemented mixed slurry to build part of the containment bund in Tekong, an island off the northeast coast Singapore. Under the tropical environment of Singapore, the issue of high ambient temperature and its impact on the curing temperature were investigated. The study focused on the early strength gain of the mixed soil under elevated temperature experienced in Singapore. Figure 9 shows the effect of curing temperature ranging from 20° to 50° on strength gain of cemented mixed soils with time. It is evident that a relatively low temperature of 20° is not effective with time while the difference is not so

significant between 35° and 50°. As the quantity of mixing is very large for a land reclamation project, it is important to have an early effective quality control to achieve a workable design of appropriate cement mix.

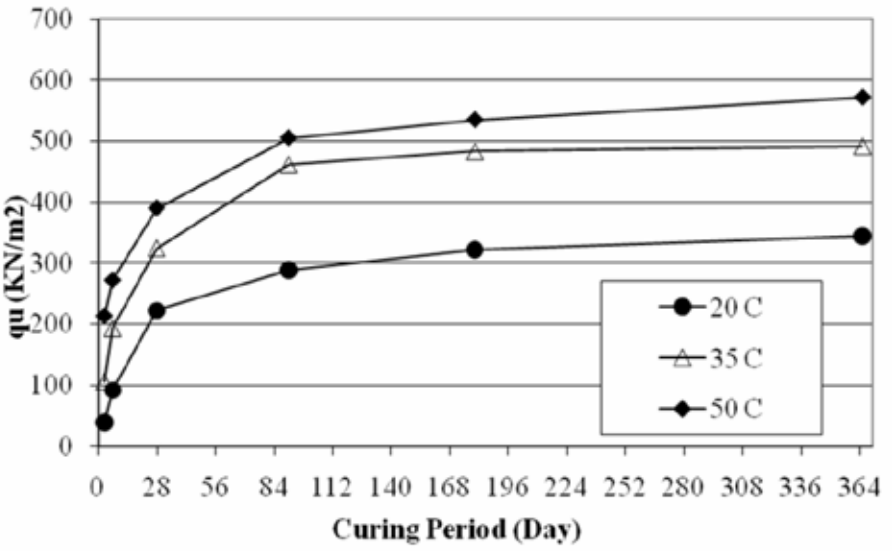

Figure 9: Effect of curing temperature on strength gain of cement mixed soils (after Tan et al. 2011)

3 WATER FRONT STRUCTURES

3.1 Reclamation perimeter bund

Reclamation perimeter bunds are built to reduce the environmental impacts on adjacent areas and the loss of fill materials. In the early days, the soft clay would be removed and replaced by sand and the sand key formed became the foundation for the perimeter bund. Without the sand key foundation, the bund might not be stable due to global slope instability. However, such approach would result in large amount of soft clay to be disposed elsewhere and it was often difficult to find dumping grounds to receive the waste soils. To reduce the amount of sand and spoil materials, sand compaction piles were installed as the foundation for the bund. Such method generally enjoyed high success rate.

However, bund failure was observed at a site along the curved section of the perimeter bund for a reclamation project. Experts were engaged to establish the cause of the bund failure. Details of the study were presented in Leung et al. (2006). Figure 10 shows a section of the bund. An independent analysis confirmed that the original global slope stability evaluation had indeed achieved a minimum desired safety factor of at least 1.5. Further analyses were carried out to investigate the various factors that could degrade the global stability. These include the extent and strength of the in-situ marine clay, the shifting of the alignment of the sand compaction pile foundation relative to the bund, overfill by the contractor, bund gradient and water line within the bund. It has been established that the alignment of the sand compaction pile foundation relative to the bund is the most influential affecting the bund stability rather than other factors. It should be noted that it would be challenging for the contractor to achieve an accurate alignment between the bund and the foundation along a curved section in view of harsh operating conditions in an open sea. Figure 11 shows the gradual increase in the soil yielding zone when the bund-foundation misalignment increases.

It was found that a shift in the relative alignment between the foundation and the fund would not be sufficient to cause the bund failure. Further analyses revealed that if the marine clay were thicker and weaker, the global instability safety factor would further reduce. As such, the combination of bund misalignment and weaker/deeper marine clay was established to be the vital factor of the bund failure. Figure 12 shows that under such adverse combinations, the global stability safety factor would reduce to below unity.

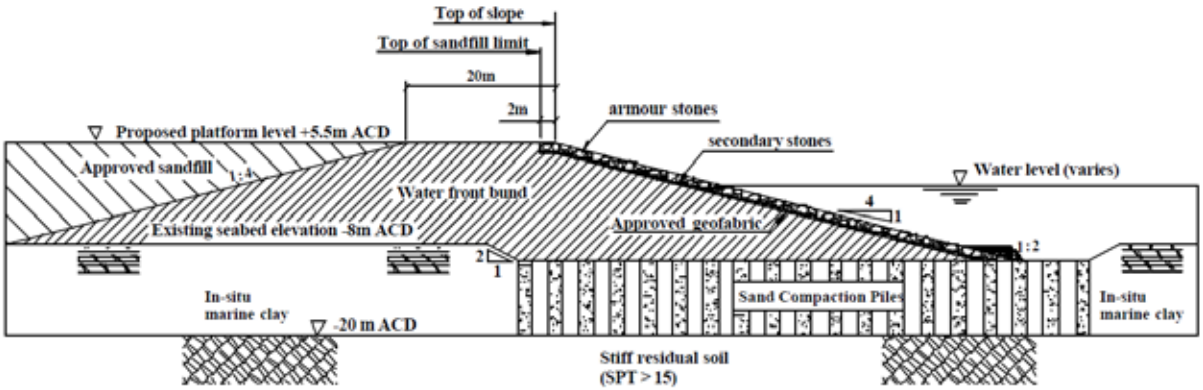

Figure 10: Typical cross-section of bund and the sand compaction pile foundation (after Leung et al. 2006)

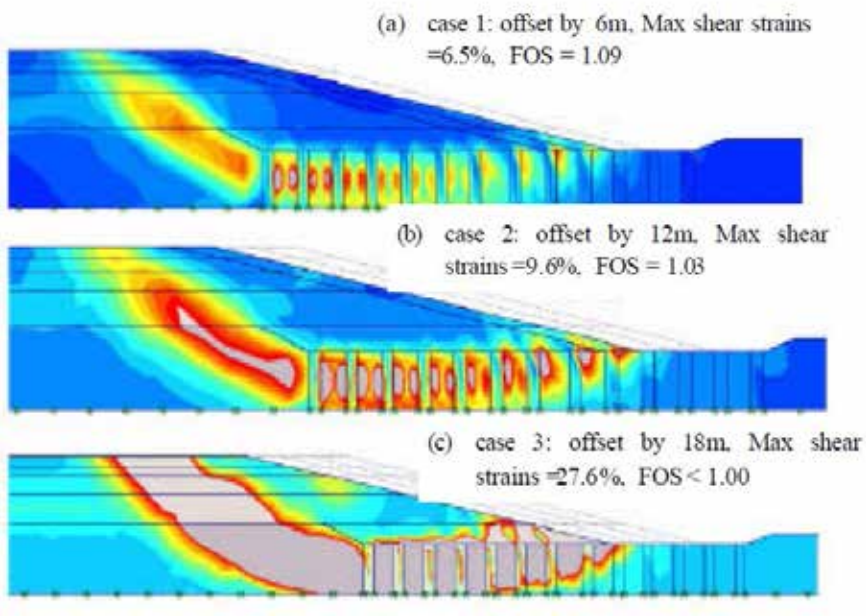

Figure 11: Soil yielding zone for different bund-foundation misalignment (after Leung et al. 2006)

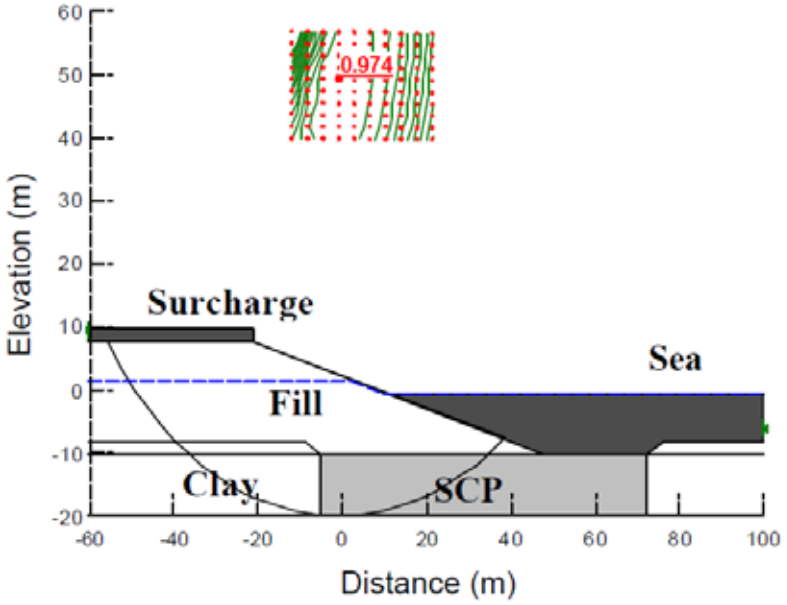

Figure 12: Global stability of bund slope under a combination of adverse conditions (after Leung et al. 2006)

3.2 Container port wharf front structures

Singapore is one of the busier container ports in the world. The latest master plan proposed to build new container terminal ports in Tuas in the western part of Singapore such that the first generation ports located close to the central business district can be redeveloped for commercial purposes. Since 1990s, the construction of new container port started in Pasir Pajang (located in the south of Singapore main land) with its last phase being completed recently. Traditionally piled decks were used as the wharf front structures (Leung 2014). For the new container ports, gravity caissons have been employed as the wharf front structures instead. Although gravity caisson wharf front structures are more expensive than piled deck wharf front structures, the former is chosen as any subsequent change in land use can be better dealt with.

Figure 13 shows a schematic of gravity caisson wharf front structure supported on sand compaction pile foundation which were installed to very stiff soils. The movement of the caisson during port operation is a major concern as the front leg of the quay crane rests on the caisson while the rear leg is supported on piles. The caissons were preloaded with intended working loads plus 20% surcharge to eliminate the initial slacks of the foundation. The loads were removed and the working load were then applied again to monitor the vertical and lateral caisson movements under simulated working loads. The monitoring of the caisson vertical and lateral movements was reported by Tan et al. (1999).

At one stretch of the port, the elevation of the very stiff soils were found to be highly variable, see Figure 14. The differential movements of adjacent caissons under rapidly changing sand compaction pile (SCP) lengths were a concern to the geotechnical engineers. The monitoring instruments placed at the back of the caisson were often damaged by the land reclamation works behind the caisson and an important performance indicator of the caisson tilt could not be evaluated. In view of this, finite element analyses were conducted to back analyzing the measured data to obtain the caisson tilt assuming the caisson moved as a rigid body. The simulation of 3-dimensioanl sand compaction pile foundation system in the two-dimensional analysis are presented by Leung and Shen (2008). The horizontal caisson movement is made of sliding movement and tilt. The summary of the composition of caisson sliding movement and tilt obtained from the back analyses for the stretch of caissons are shown in Figure 15. It is evident that sliding movement of the caisson contributes to a significant portion of the caisson horizontal movement.

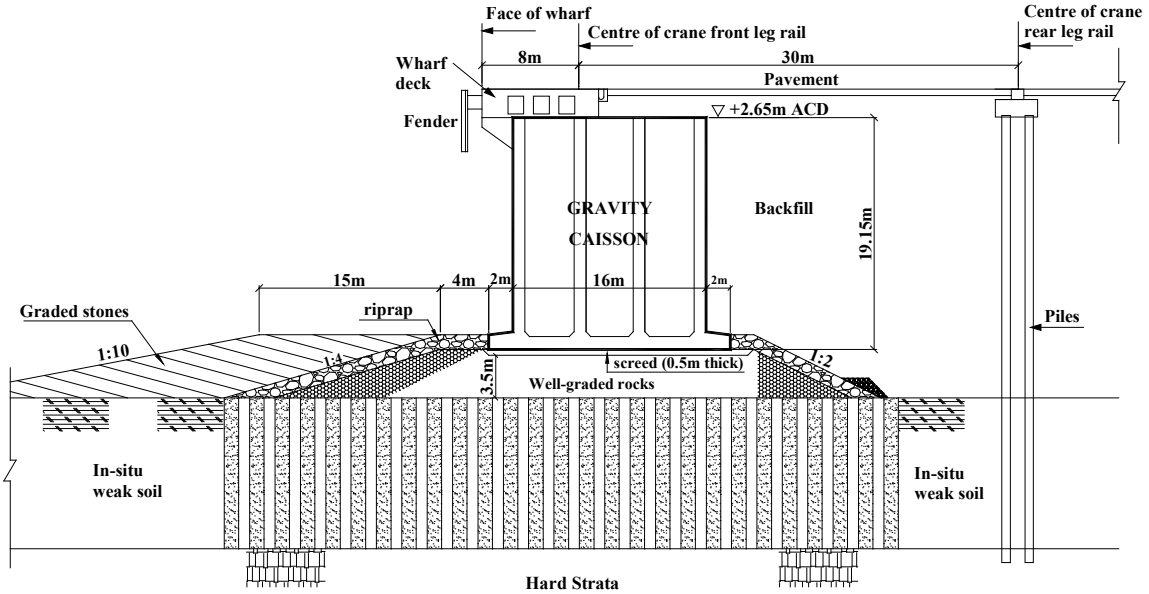

Figure 13: Cross-section of gravity caisson wharf front structures (after Leung and Shen 2008)

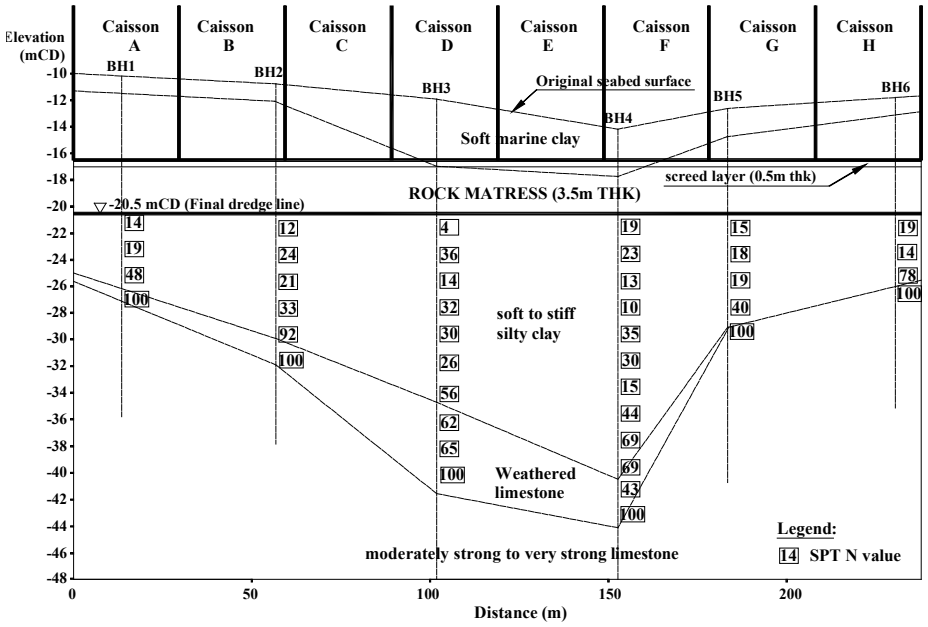

Figure 14: Stretch of caisson with highly variable soil profile (after Leung et al. 2008)

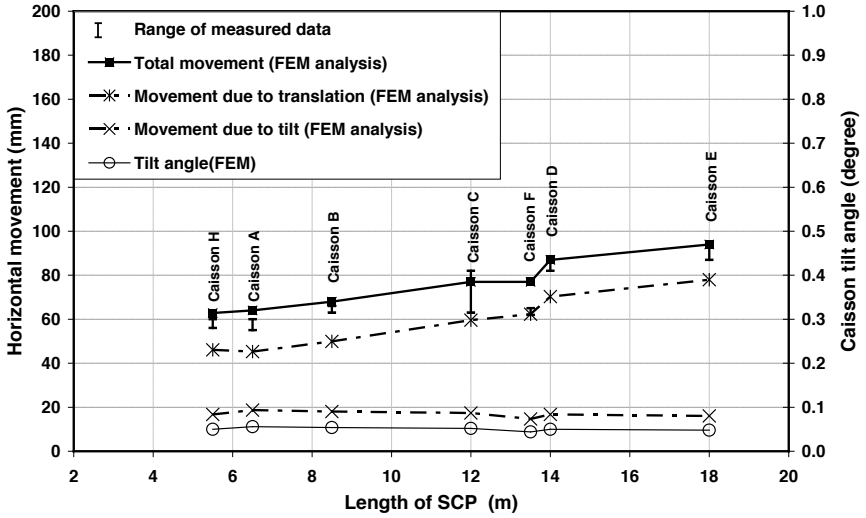

Figure 15: Comparison of predicted and measured caisson horizontal movements for different sand compaction pile SCP lengths (after Leung et al. 2008)

4 GROUND IMPROVEMENT

With presence of thick soft soils beneath reclamation fills, ground improvement is often necessary before the land can be released for development. In the early days, dynamic compaction, vibro floatation and Muller resonance compaction were attempted to compact the sand fill (Choa et al. 1979, Choa 1980). However, they were found to be effective only for the relatively shallow sand fill depths. To accelerate the consolidation of in-situ soft clay, sand drains were used. For the Changi Airport development, it was found to be too time consuming and not economical to use sand drains in a large scale. Flexible drains were used after successful field trials.

4.1 Vertical flexible drains

Since the Changi Airport development in the late 1970s, flexible band drains were commonly employed to accelerate the consolidation of in-situ soft marine clay. For the Changi Airport and Changi East reclamation (Plate 4) projects, extensive field trials were carried out to determine the necessary drain spacing for different thicknesses of in-situ soft clay. These were reported in detail by Choa et al. (1981) who noted that the pore pressures became stagnant in the marine clay at 3 m to 6 m above the ground water table when closely spaced prefabricated drains were installed. They attributed the above to (a) location of piezometers in relation to drain grid and horizontal drainage layer, (b) variation of compressibility of clay before and after passing the critical pressure and (c) existence of back pressure in the untreated areas of reclamation adjacent to the treated areas.

An important verification procedure for ground improvement of in-situ soft clay is whether the clay has gained enough strength to withstand the anticipated fill and additional loading. The preconsolidation pressure obtained from 1-dimensional consolidation tests, the undrained shear strength from undrained uncosolidated triaxial compression tests or vane shear tests and the moisture content before and after improvement were compared. It was established that inconclusive findings were often reached when comparing the preconsolidation pressure and moisture content values before and after ground improvement. On the other hand, the undrained shear strength measurements before and after improvement often revealed marked strength improvement of the soft clay, as illustrated in Figure 16 which was reported by Choa (1991). In the current on-going ground improvement works for reclaimed lands in Singapore, the same observation still maintains with the shear strength measurements being the most effective evaluation tool to gauge the strength improvement of the soft clay after ground improvement.

Plate 4: Large scale installation of flexible drains (Photograph courtesy of Prof J Chu)

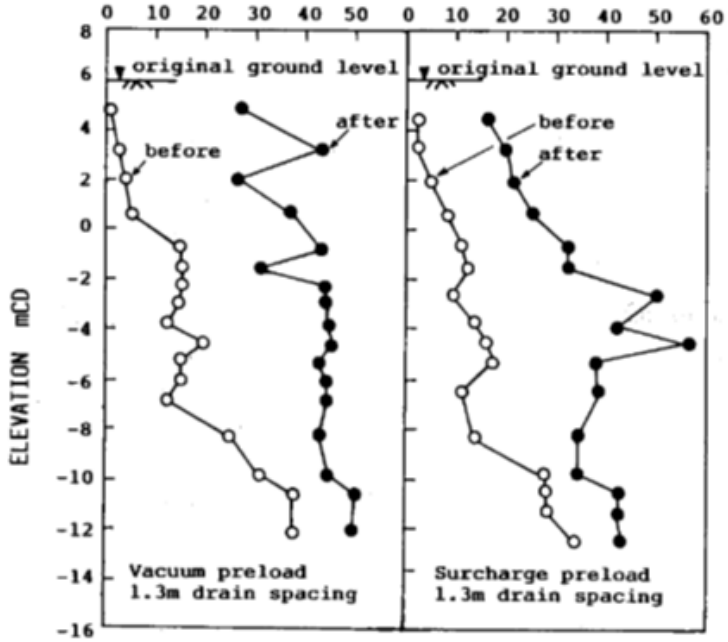

Figure 16: Comparison of vane shear strength before and after ground improvement (after Choa 1991)

4.2 Vibro Replacement

To support heavier loads without the use of deep foundation, stone columns can be employed. The principle of stone column design was presented by Priebe (1995). Essentially the bearing capacity of the improved ground is derived from the strength of the composite area of in-situ soils and stone columns. The cost of such improvement method often depends on the availability of the stones which can be costly. In Singapore, concrete from demolished buildings has been employed to replace stones. This is certainly environmental friendly as the waste concrete can be reused and also economical as stones need not be used.

As discussed earlier in this paper, sand compaction piles or sand keys were commonly used to support perimeter sand bunds for land reclamation in Singapore. It was reported that a part of the sand bund in a reclamation project could not be stabilized by sand key, as any dredging of the soft clay would affect the stability of the adjoining sand bund. Leong and Raju (2007) and Raju (2009) reported that the underlying soft marine clay was up to 15 m thick having undrained shear strengths from 15 kPa to 30 kPa. As the soft clay had to be stabilized in-situ, offshore vibro replacement was carried out. The "Gravel Jet" system was used to install the columns with stones pumping through a hose to the top of vibrator up to 25 m above seawater level. Once in the stone chamber, the stones were forced down the tubes by compressed air, see Figure 17. A total of 43,000 m of columns with 55,000 m^3 of stone were installed in the soft clay.

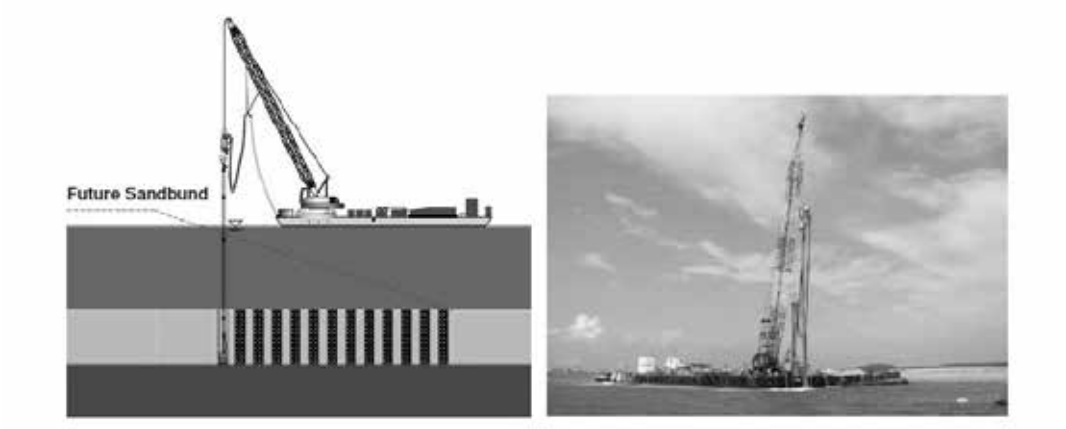

Figure 17: Vibro replacement carried out under sand bund (after Raju 2009)

4.3 Vibrocompaction

If there is no in-situ soft clay in some parts of a reclaimed land, the sand fill can be treated by vibro compaction in these parts. Although compaction was attempted to improve the sand fill for the Changi Airport and Changi East reclamation projects, it was found that such improvement would only be effective to limited depths. With the advancement of technology and equipment, modern vibro compaction can be effective to great depth. Singapore is one to busiest oil and chemical refinery in the world, it has been building hundreds of new oil and chemical storage tanks in its Jurong Island. The tanks are getting taller and wider. Vibrocompaction has been employed to improve the thick sand fill to support the tank instead of using deep foundation. Figure 18 shows a schematic of the scheme. Details of the principle and its equipment are given in Leung et al. (2015). The verification of the success of vibrocompaction is to evaluate the cone presentation resistance profile which must exceed those specified in the performance specifications in the contract. It has been found that owing to presence of soft clay lenses within the sand fill, the cone penetration resistance at certain elevations may not be achieved. In view of this, the average of the cone resistance profile is used instead to verify the success of the vibrocompaction in some contracts.

The tanks will be subjected to hydrostatic tests upon completion and the results need to fulfill the global and local settlement as well as tilt specified by API (2009 & 2013). A typical test results is shown in Figure 19 which reveals the tank settlement is relatively large but it falls within the API specifications. In most of the on-going tank farm projects, ground improvement using vibro compaction is often considered as the preferred foundation option rather than deep foundation. Vibrocompaction is typically faster and more economical as compared to deep foundation.

4.4 Mixed ground conditions

In places where both the reclaimed sand fill and in-situ soft clay need to be improved, hybrid methods are often employed. For a very large industrial building under heavy machinery loading of over 500 m long and 70 m wide (Plate 5), the subsurface comprises thick reclaimed sand fill but overlain with several meters of soft marine clay at 27 m below the ground level at certain locations. Piled foundation was first proposed but it was found to be too costly with negative skin friction consideration and also too time consuming. Ground

improvement specialist contractors were invited to evaluate whether ground improvement can be adopted to support the heavily loaded huge industrial building.

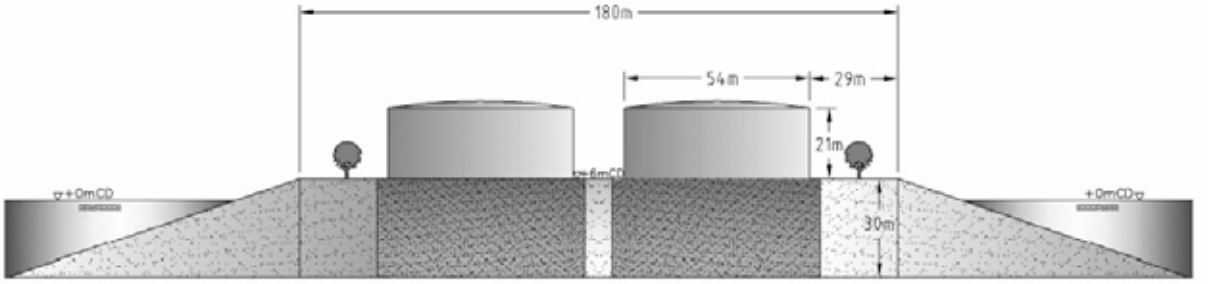

Figure 18: Schematic of vibro compaction scheme (after Raju & Daramalinggam 2007)

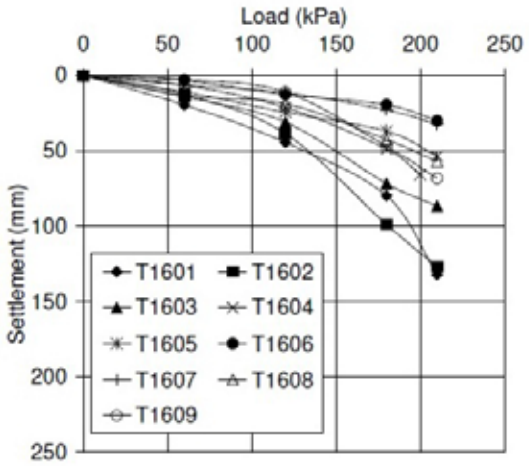

Figure 19: Typical hydro test results (after Raju & Daramalinggam 2007)

Plate 5: Heavily loaded industrial building built on reclaimed land (photograph taken upon completion)

The solution was to install deep flexible drains to improve the deep marine clay before carrying out vibrocompaction to improve the thick sand fill. A schematic of the ground improvement scheme is shown in Figure 20 revealing surcharge was applied to accelerate the settlement of the marine clay. The installation of deep drains using special powerful machinery was successful for the first time in Singapore. A comparison of the predicted and measured settlement of the marine clay upon ground improvement is shown in Figure 21. To

ensure required degree of consolidation has been achieved, the surcharge was removed and the ground settlement was monitored which verified that the ground settlement had more or less stabilized.

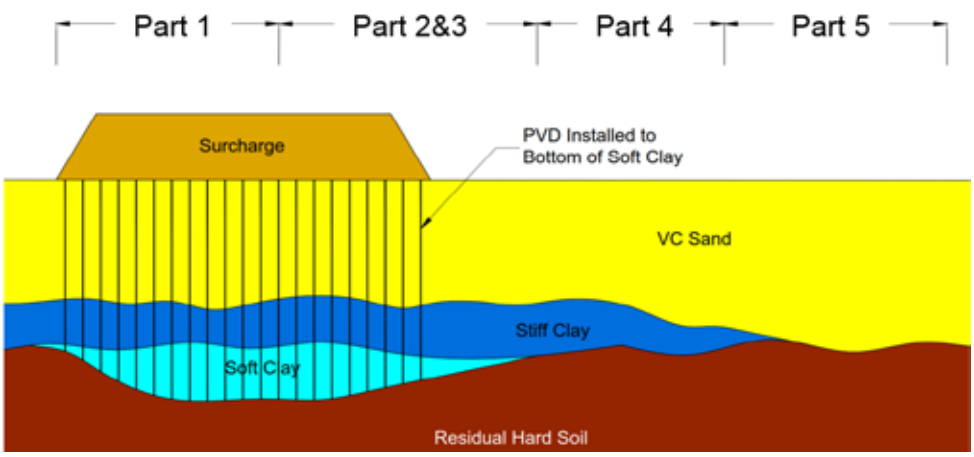

Figure 20: Schematic of ground improvement scheme (after Leung & Raju 2015)

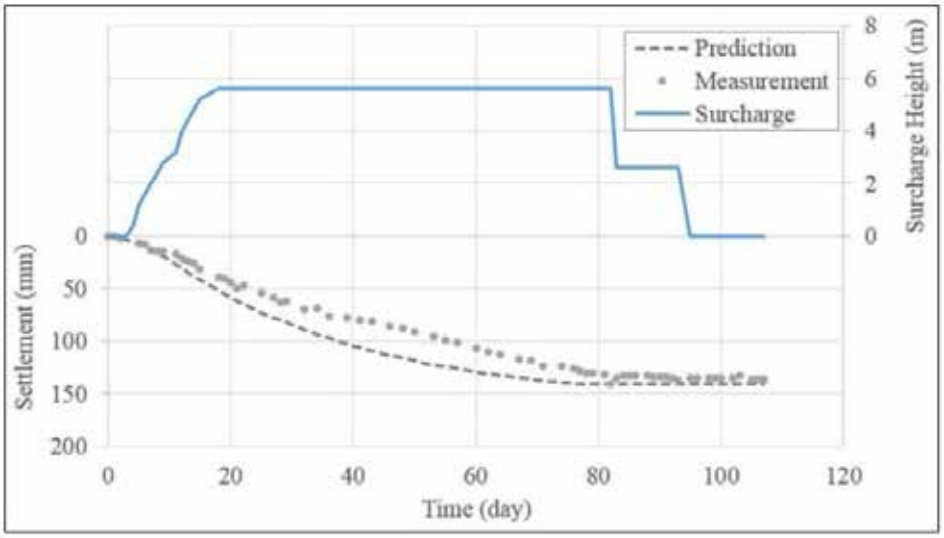

Figure 21: Comparison of predicted and measured ground settlement (after Leung & Raju 2015)

A 6-storey low-rise residential buildings with single level basement was built on reclaimed land in Sentosa Island. The subsurface conditions can be divided into 3 zones. Piled foundation was adopted for Zone A as the sand was silty/clayey beneath 10 m depth. No ground improvement or piling was deemed necessary for Zone B as the ground comprised 3 m to 4 m of loose sand followed by stiff clay. For Zone C, the sand fill was about 4 m to 5 m depth underlain by soft clay of up to 8 m thick. The decision was to support the structure on a raft foundation with the soft clay being mixed in-situ forming deep mixing columns (DSM). Figure 22 shows a schematic of the ground improvement scheme. The construction of DSM was of shorter duration and cheaper as compared to deep foundation. The replacement ratio of the columns varied from 25% to 35% depending on the loading intensity. To satisfy settlement requirements, the DSM columns were required to achieve an unconfined compressive strength of 1 MPa and a secant Young's modulus of 150 MPa. Unconfined compression tests conducted on vertical core samples from the DSM columns revealed that the average unconfined compressive strength was 2.7 MPa and the average modulus was 390 MPa. Under 180 kPa plate test load, the reported settlement was less than 10 mm. After the completion of the building (Plate 6), the observed settlement was less than 25 mm.

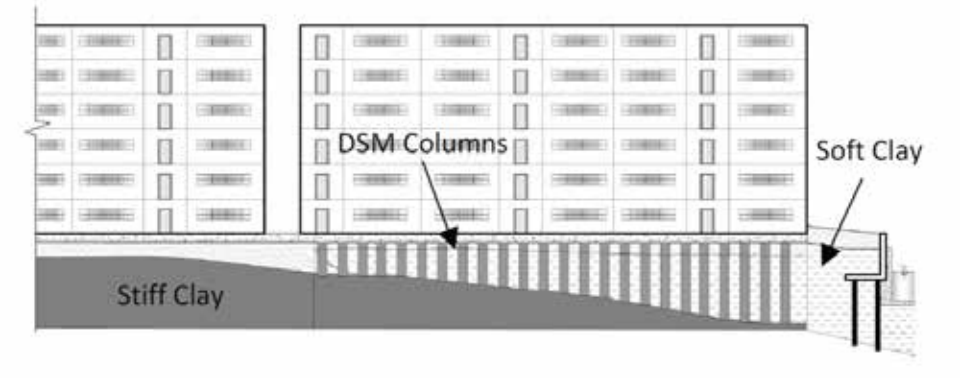

Figure 22: Schematic of ground improvement scheme (after Raju 2009)

Plate 6: Completed luxury residential building on reclaimed land supported by improved ground without deep foundation (photograph courtesy of Keller Singapore)

Leung and Raju (2015) reported that vibrocompaction had been successfully employed to improve the thick loose sandy soils in India. The improved ground was employed as the foundation supporting 13 blocks of 14-storey residential buildings in a seismic active area. It was of the view that such improved ground would provide better resistance against earthquake as compared to piled foundation installed through loose sand. It should be noted that ground improvement methods, equipment and technologies have advanced significantly in recent years and is expected to continue to advance and improve. As an example, vacuum consolidation trials are ongoing in several land reclamation projects in Singapore. Although vacuum consolidation has been employed successfully employed for ground improvement of very soft to soft soils in many countries such as China, the technique is relatively new in Singapore. Chu et al. (2015) reported the principle of vacuum consolidation and several case histories.

This paper highlighted the ground improvement commonly used in marine geotechnical projects in Singapore. Ground improvement works were often carried out by specialist contractors which have different skills and expertise. There are many other ground improvement methods available such as deep mixing, control modus columns, grouting, just to name a few. Important factors on the selection of appropriate ground improvement technique to be considered include the local ground conditions, the availability of improved materials such as stones or sand locally, and the availability of equipment as well as the expertise of specialist contractors.

5 IMPACTS ON ENVIRONMENT

In the early days, Singapore was a developing country and less attention was paid to the impacts of land reclamation on the environment. Since the turn of the century, people are more concerned about the environment and environmental impact assessment needs to be conducted for new land reclamation projects. The impacts on many aspects of the environment such as water pollution, sea lives and others on Singapore and its neighboring countries would be examined. As an example, land reclamation was planned in 2005 for the expansion of an offshore soil and chemical refinery site. Danish Hydraulic Institute (DHI, 2016) was engaged to carry out an environmental impact assessment study on the proposed land reclamation. The challenges listed for the study included the problems concerning reclamation on the environment, how to assess probable loss of biodiversity in the vicinity during reclamation, and long term impacts on marine habitats. Environmental monitoring and management plan (EMMP) was proposed to analyze the impact of land reclamation on the environment. This would enable the early detection of unexpected impacts on the environment as well as action to be taken to mitigate such impacts on marine habitats. Action was taken to relocate the corals to other locations and to carry out real time monitoring on sediment spill and habitat monitoring such as seagrass and mangroves during reclamation.

6 CONCLUSIONS

This paper provides an overview on land reclamation and related ground improvement works in Singapore. Creating new lands is vital for the economic and population growth of Singapore. Difficulties in the construction of water front structures in soft and thick marine clay for land reclamation and new container terminal works are presented. The challenges faced and how they are overcome concerning reclaiming land on very soft seabed are discussed. As sandy soils are in short supply, the explorations of using construction waste soils, dredged materials and cement mixed soil as alternate reclaimed fill are ongoing. Case histories on such research studies are presented in this paper. Ground improvement techniques in improving the reclaimed fills and in-situ soft soils are presented. For improvement using flexible drains, the undrained shear strength measurements are found to be most reliable in verifying the improvement of soft clay. For an improved ground to carry heavy loads without the use of deep foundation, vibrocompaction is established to be effective in improving the granular sand fills while stone columns can be used to reinforce soft soils. Hybrid approaches need to be considered for mixed ground conditions. Finally a case study on the conduct of environmental impact assessment for a recent land reclamation project in Singapore is highlighted.

ACKNOWLEDGEMENTS

Singapore has carried out extensive land reclamation in the past several decades. Many researchers and engineers from the tertiary institutions and industry had made significant contributions to the advancement of land reclamation methods and related ground improvement works. Owing to paper length constraint, this article only manages to provide overview of selected research and case studies.

REFERENCES

American Petroleum Institute (API), 2009. *API Standard 653 – Tank Inspection, Repair, Alternation & Reconstruction,* 4th Edition. API Publishing Services.

American Petroleum Institute (API), 2013. *API Standard 650 – Welded Tanks for Oil Storage*, 12th Edition. API Publishing Services.

Bjerrum, A.B. 1972. Settlement on soft ground. *Proc ASCE Specialty Conference on Performance of Earth and Earth Supported Structure,* 2, 1-54.

Choa, V. 1980. Geotechnical aspects of a hydraulic fill reclamation. *Proc. 6th Southeast Conf. on Soil Engr., Taipei,* 1, 469-484.

Choa, V. 1991. Reclamation on soft ground for airport and port development. *Proc. HKIE Annual Geotechnical Seminar, Hong Kong,* 1-32.

Choa, V., Karunaratne, G.P., Ramaswamy, S.D., Vijiaratnam, A. & Lee, S.L. 1979. Compaction of sand fill at Changi Airport. *Proc. 6th Asian Reg. Conf. on Soil Mech. and Fdn. Engr., Singapore*, 1, 137-140.

Choa, V., Karunaratne, G.P., Ramaswamy, S.D., Vijiaratnam, A. & Lee, S.L. 1981. Drain performance in

Changi marine clay. *Proc. 10th Intl. Conf. on Soil Mech. and Fdn. Engr., Stockholm*, 3, 623-626.
Chu, J., Bo, M.W., & Arulrajah, A. 2009. Reclamation of a slurry pond in Singapore. *Proc ICE Geotech. Engr.,* 162(1): 13-20.
Chu, J., Guo, W. & Yan, S. 2015. Recent development and applications in vacuum preloading method for soft soil improvement. In Leung, C.F., Ku, T. & Chain, S.C. (eds), *Advances in Soft Ground Engineering, Singapore*, Keynote lecture, 67-81.
Danish Hydraulic Institute, 2016. Reclaiming the land, protecting the environment. *www.dhigroup.com*.
Kitzaume, M. & Satoh, T. 2005. Quality control in Central Japan International Airport construction, *Proc. ICE Ground Improvement*, 9(2), 59-66.
Lee, S.L., Karunaratne, G.P., Yong, K.Y., Tan, S.A., Tan, T.S. & Vijiaratnam, A. (1990). Development in land reclamation. *Proc. 1990 Convention of Instn. Engr., Singapore,* 13-20.
Leong, K.W. & Raju, V.R. 2007. The Construction and Performance of Foundations using Vibro Techniques for an Oil Storage Terminal in Singapore, *Proc.16th Southeast Asian Geotech. Conf., Kuala Lumpur*, 585–590.
Leung, C.F. 2012. Ground improvement techniques for land reclamation: Singapore experience. In Indraratna, B., Rujikiatkamjorn, C. & Vinod, J.S. (eds), *Proc. on Ground Improvement and Ground Control, Wollongong,* Special Lecture, 193-208.
Leung, C.F. 2014. Historical development of container port wharf front structure in Singapore. In Grabe, J. (eds), *Ports for Container Ships of Future Generations, Hamburg,* 199-210.
Leung, C.F., Wong, J. C., Manivanann, R., & Tan, S. A. 2001. Experimental evaluation of consolidation behavior of stiff clay lumps in reclamation fill." *Geotech. Testing J.* 24(2): 145-156.
Leung, C.F., Tan, S.A. & Shen, R.F. 2006. Prediction versus performance of land reclamation bund. *Proc. 16th Int Conf on Soil Mech. & Geotech Engr., Osaka,* Invited presentation, Post conference volume appendix CD ROM.
Leung, C.F. & Shen, R.F. 2008. Performance of gravity caissons on sand compaction piles, *Canadian Geotechnical Journal*, 393-407.
Leung, C.F. & Raju, V.R. 2015. Optimum foundation solutions with ground improvement. In Leung, C.F., Ku, T. & Chain, S.C. (eds), *Advances in Soft Ground Engineering, Singapore*, Special Lecture, 85-103.
Leung, C.F., Yee, Y.W. & Leong, K.W. 2015. Principle and case histories of deep vibro techniques. In Indraratna, B., Chu, J. & Rujikiatkamjorn, C. (eds), *Compaction, Grouting & Geosynthetics*, Chapter 11, 337-364. Elsevier.
Morohoshi, K. et al. 2010. Design and long-term monitoring of Tokyo International Airport extension project constructed on soft ground. *Geotechnical and Geological Engineering*, 28(3), 223-232.
Pickles, A.R, & Tosen, R, 1998. Settlement of reclaimed land for the Hong Kong International Airport, *Proc ICE Geotechnical Engineering*, 131, 191-209.
Plant, G.W., Covil, C.S. & Hughes R.A. (eds) 1998. *Site preparation for the new Hong Kong International Airport.* Thomas Telford.
Preibe, H.J., 1995. The design of vibro replacement. *Ground Engr.*, 28(10): 31-37.
Raju, V.R. 2009. Ground improvement - principles and applications in Asia. In Leung, C.F., Chu, J. & Shen, R.F. (eds), *Proc. Ground Improvement Tech. and Case Histories, Singapore*, Keynote Lecture, 43-65.
Raju, V.R. and Daramalinggam. J. 2007. Optimized foundation systems using deep vibro techniques for large tank farms. *Proc. 13th Asian Reg. Conf. on Soil Mech. and Fdn. Engr.*, Kolkata.
Robinson, R.G., Tan, T.S., Dasari, G.R., Leung, C.F. & Vijayakumar, A. 2005. Experimental Study of the Behavior of a Lumpy Fill of Soft Clay. *Intl. J. of Geomechanics* 5(2): 125-137.
Tan, A., Wong, Y.K., Lay, K.H. & Leung, C.F. 1999. Performance of Gravity Caissons. In Leung C.F., Tan, S.A. & Phoon, K.K. (eds), *Proc. Field Measurements in Geomechanics, Singapore*, 297-302.
Tan, T.S., Lu, Y.T., Phoon, K.K. & Karthikeyan, M. 2011. Innovative approaches in land reclamation in Singapore. In Phoon, K.K., Goh, S.H., Shen, R.F. and Zhu, H. (eds). *Proc. Advances in Ground Tech. and Geo-information, Singapore,* Keynote lecture, 85-102.
Urban Redevelopment Authority, 2014. *Master plan, 2014*. www.ura.gov.sg
Zhao, Q., Lin, H., Gao, W., Zebker, H.A., Chen, A. & Yeung, K. 2011. InSAR detection of residual settlement of an ocean reclamation engineering project: a case study of Hong Kong international airport. *Journal of Oceanogr*, 67, 415-426.

Design Issues for Steel Pipe Piles for Coastal Structures and Offshore Wind Turbines

M.F. Randolph
Centre for Offshore Foundation Systems
The University of Western Australia

ABSTRACT

Steel pipe piles are widely used both onshore and offshore because of their good bending response and ease of installation. They are generally driven open-ended, although internal plates or even complete end-closures may be used to improve their bearing capacity. The lecture draws together a number of design issues that pertain to open-ended steel piles. These range from axial capacity considerations, in comparison with similar closed ended piles, to extrusion buckling of pipe piles. Particular emphasis in the lecture will be placed on design of the ultra large diameter monopiles now being used in European waters for offshore wind turbines, where rotational stiffness is critical. The vulnerability of pipe piles to damage during installation will be illustrated through case studies showing progressive distortion of the pile tip, and the possible triggers for damage will be discussed.

1 INTRODUCTION

In the urban environment, driven piles have tended to be replaced by different forms of cast in situ pile, for example bored or continuous flight auger piles. However, for coastal and offshore applications driven piles are still widely used, since the environmental issues associated with noise and vibration arising from pile driving are of reduced concern. In particular, driven steel pipe piles offer an attractive foundation solution, since most coastal and offshore applications involve significant lateral loading, where the good bending response of steel pipe piles is of benefit.

Typically (and almost universally for offshore applications) steel pipe piles are driven open-ended, resulting in much reduced lateral soil displacement by comparison with a closed-ended or solid pile. In sands and other free-draining granular deposits, i.e. where pile installation occurs in a nominally drained manner with minimal excess pore pressures retained in the surrounding soil, the reduced lateral soil displacement will lead to significantly lower axial capacity than for a closed-ended pile. This may not be an issue if the operational loads are dominated by lateral loading, but can be an important consideration in assessing required pile penetration in uniform or layered granular stratigraphies.

Under lateral loading, most driven piles are relatively long by comparison with the zone over which significant lateral resistance is transferred to the soil. As such, the critical design consideration is generally that of ensuring sufficient plastic moment capacity of the pile section, which will often necessitate thickening the wall of pipe piles in the vicinity of the ground or seabed surface, extending to a depth of 3 to 5 diameters. Exceptions to this include the rather stubby (length to diameter ratios less than 5 or 6) suction caissons used routinely for deepwater anchors (Andersen et al. 2005) and, of particular consideration here, the large diameter monopiles used to support offshore wind turbines. In the case of offshore monopiles, the lateral loading is applied above sea-level, resulting in substantial bending moments near the seabed surface and requiring increased wall thickness in that region. However, a more critical design criterion for monopiles is the rotation stiffness of the pile, both to ensure rotations are less than the serviceability limit, but also to

ensure that the natural frequency of the combined pile, column and turbine system is separated from frequencies of either high energy wave loading or the turbine rotation (Arany et al. 2014; Bhattacharya 2014).

Apart from regions where the pile wall thickness is increased to provide the required plastic moment capacity, the diameter to wall thickness ratio generally decreases with increasing pile diameter, for both economic reasons (minimizing the required volume of steel) and for feasibility of fabrication. However, for large diameter monopiles, this trend results in piles with extremely low hoop stiffness and radial buckling resistance. This renders the pile vulnerable to damage, and gradually accumulating distortion of the cross-section during installation in medium to dense granular deposits or soft rocks.

The paper expands on the various design issues mentioned above, discussing relevant calculation approaches and presenting design charts for simplified soil stratigraphies. Particular emphasis is placed on design considerations for offshore wind monopiles, and analysis techniques at evaluating the potential for such piles to undergo tip distortion during installation through heterogeneous layered soil profiles. Case studies are presented where cumulative distortion, termed 'extrusion buckling', was found to have occurred, and the mechanism of extrusion buckling is discussed.

2 INSTALLATION AND AXIAL CAPACITY

The relative volume of soil displaced during pile driving, and the resulting changes in radial stress are illustrated in Figure 1 (after White el al. 2005). The ratio of displaced soil volume to the gross installed volume of the pile is referred to as the area ratio, A_r. For a solid or closed-ended pile this would be unity, while for a typical offshore steel pile, with a diameter (D) to wall thickness (t) ratio of D/t ~ 40, the area ratio would be about 0.1, assuming a perfect 'coring' soil plug. If the central soil plug is depressed below the original ground surface, then additional soil displacement must occur at some stage during the penetration, resulting in stress changes intermediate between the closed-ended and (perfectly coring) open-ended installation.

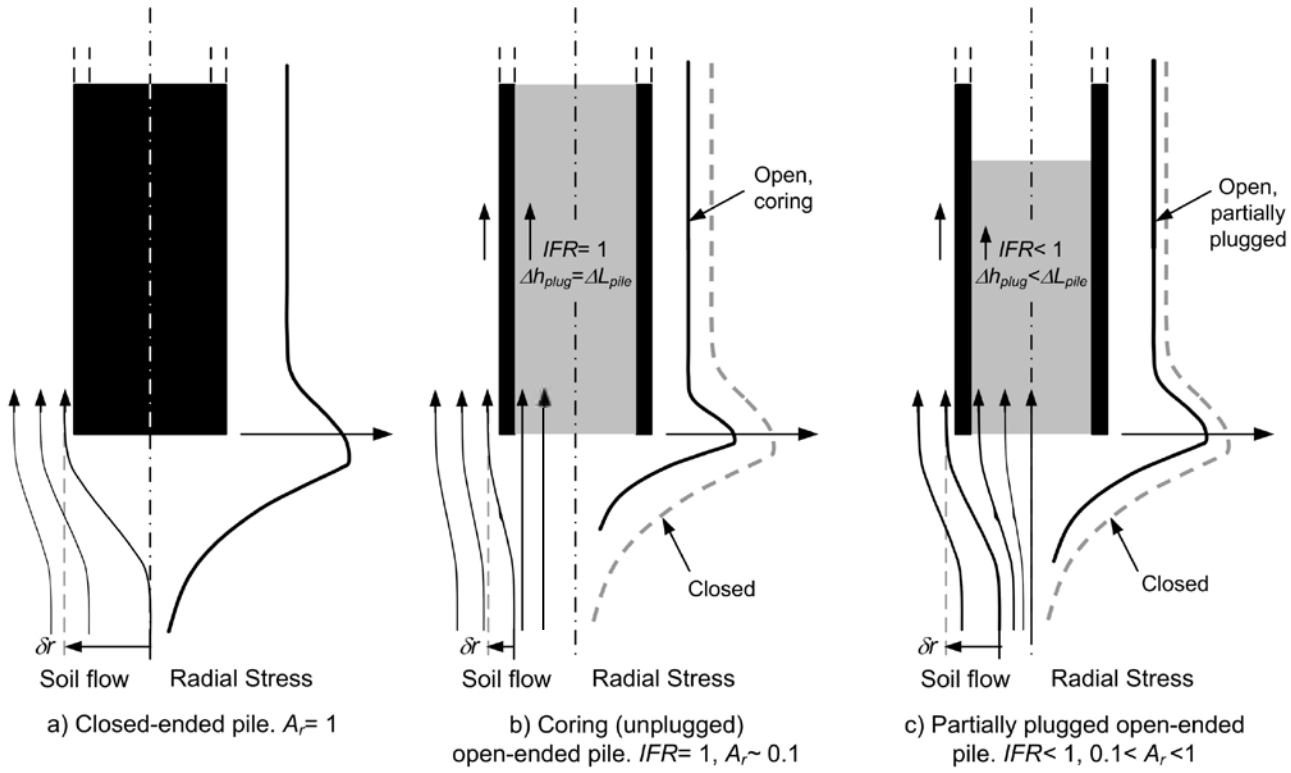

Figure 1: Schematic of soil streamlines and radial stress changes during piles installation

The degree of 'soil plugging' may be quantified by the incremental filling ratio (IFR), which is the ratio of the incremental increase in soil plug height to the incremental penetration of the pile. IFR would equal unity for a perfectly coring pile, and (on average) be less than unity where the soil plug length is less than the pile penetration. In practice, the soil plug height is rarely (if ever) monitored during pile driving, so only an average value of IFR may be estimated – by measuring the final soil plug height. From a design perspective, a value of IFR of unity is generally assumed for open-ended piles, since that results in the lowest radial stress changes and hence lowest pile capacity. The area ratio (for IFR = 1) may be expressed as

$$A_r = 1 - \left(\frac{D_i}{D}\right)^2 \approx \frac{D/t}{4} \quad (1)$$

where D_i is the internal diameter of the pile.

In practice, open-ended piles generally drive in an 'unplugged' manner (i.e. with the soil plug advancing up the inside of the pile, with IFR ~ 1) because of the high inertial resistance of the soil plug (Liyanapathirana et al. 2001; Dean & Deokiesingh 2012). Exceptions occur as a pile is driven through a strong layer of soil into weaker material, where the reduction in end-bearing resistance may lead to the pile driving more as a plugged pile (with reduced IFR). However, the reduction in IFR generally occurs only for limited further pile penetration before unplugged conditions are re-established.

2.1 Soil resistance during driving

The soil resistance during driving, often referred to as 'SRD', may be assessed using similar approaches as are used for estimating the long-term static axial pile capacity. However, there are two important differences: firstly, during driving the mode of penetration is essentially open-ended, so the soil resistance comprises internal and external shaft friction together with end-bearing on the pile annulus; secondly, in fine grained soils the shaft friction (both internal and external) will typically be much lower than the long term value, due to the effects of remoulding and retention of excess pore pressure in the soil adjacent to the pile surface.

In lightly overconsolidated clays, a common approach is to assume the shaft friction during driving is similar to the remoulded strength of the clay, so potentially 20 to 40 % of the long term shaft friction, with equal internal and external shaft friction. By contrast, in free draining granular soils, back-analysis of stress-wave data suggests that the internal friction is extremely low over most of the soil plug length apart from over the lower 1 or 2 diameters when the internal friction may be comparable (or even higher) than the external friction.

As a practical approach, the internal shaft friction may be taken as a fixed proportion of the external shaft friction, with the latter calculated using static axial pile capacity methods but reduced for the effects of set-up (consolidation for fine-grained soils and aging for granular deposits). In granular deposits that proportion is typically taken as about 50 % (Stevens et al. 1982; Alm & Hamre 2001; Schneider and Harmon 2010), although correlations from case histories suggest even lower proportions may be appropriate (Byrne et al. 2012). Given that the aim of a drivability analysis is to identify an appropriate hammer size that will be sufficient to drive the pile to the target penetration, adoption of an internal to external friction ratio of 0.5 in granular deposits should prove a safe approach.

2.2 Static axial capacity

Just as open-ended piles are not expected to 'plug' during driving, by contrast under static loading they will generally plug except for piles with very low ratios of embedded length (L) to diameter. In fine-grained soils, simple consideration of the static equilibrium of the soil plug is sufficient to demonstrate that 'plugged' failure (i.e. without further penetration of the top of the soil plug up the inside of the pile) will occur for L/D greater than 3 to 5, depending on the ratio of internal shaft friction to the in situ shear strength of the soil. For free-draining granular deposits, where the potential end bearing resistance is high, it might be expected that higher L/D ratios would be needed to ensure plugged response. However, a reverse silo effect operates within the pile, with the shearing resistance proportional to the local (average) vertical effective stress within the soil plug (Figure 2). This leads to an exponential growth in the magnitude of plug resistance, q_{plug} that may be mobilized with increasing soil plug length, h_p, according to (Randolph et al. 1991, 1992):

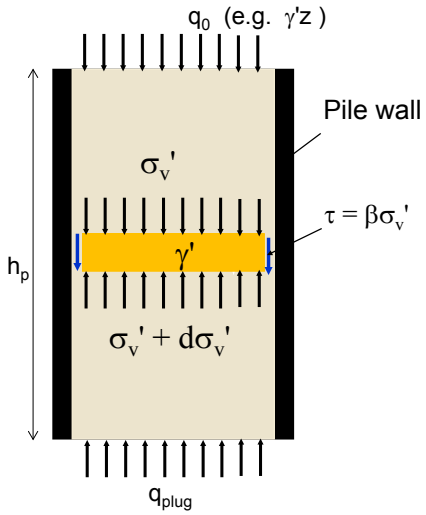

Figure 2: Equilibrium of the soil plug for granular deposit

$$\frac{q_{plug}}{q_0} \le e^{4\beta h_p / D_i} \tag{2}$$

where q_0 is the surcharge pressure acting at a distance h_p from the pile tip. Even for conservative estimates of the friction ratio β, the limiting value of q_{plug} rises exponentially from around 10 to 50 as the normalized 'active' plug length, h_p/D_i, increases from 3 to 5.

Traditionally, pile shaft friction and end-bearing values in granular soils have been expressed in terms of the ambient vertical effective stress, σ'_{v0}, through earth pressure ratios, K, and end-bearing factors, N_q. However, extensive research undertaken in the 1980s and early 1990s demonstrated two main principles:

1. The cone resistance, q_c, provides much better correlations for both end-bearing and shaft friction.
2. The ratio of shaft friction to cone resistance at a given depth is a maximum value as the pile tip passes through that depth, but then decreases as a function of the length of pile driven past that location, a process referred to as 'friction fatigue' (Alm & Hamre 2001) or 'friction degradation'.

These principles are now adopted in modern approaches to estimating the axial capacity of piles in sand (Jardine et al. 2005; Lehane et al. 2005; Schneider et al. 2008; Xu et al. 2008).

Figure 3 shows results from field measurements that illustrate the effects of friction degradation (data from Lehane et al. 1993). The profiles of shaft friction follow qualitatively the shape of the cone resistance profile, but with decreasing ratios of τ_s/q_c with increasing distance h from the pile tip. Friction degradation may be attributed to the effects of cyclic shearing between pile and soil, much as may be measured in a cyclic shear-box test carried out under conditions of constant normal stiffness (see Figure 4, following DeJong et al. 2006).

Best-fit correlations of shaft friction from an extensive database of field pile tests may be expressed in the form: (API 2011)

$$\frac{\tau_s}{q_c} = S\left(\frac{\sigma''_{v0}}{p_a}\right)^a A_r^b \left[\max\left(\frac{h}{\nu D},1\right)\right]^{-c} F_t \tan\delta \tag{3}$$

where p_a is a reference pressure of 100 kPa, δ is the pile-soil friction angle and F_t is unity for compression loading, but reduced to 0.75 for tensile axial loading. The coefficient S and exponents a, b and c vary slightly among different methods, but a typical set (Lehane et al. 2005) is S = 0.021, a = 0, b = 0.3, c = 0.5, ν = 2. Note that the coefficient S represents the radial stress ratio, σ'_r/q_c, adjacent to the pile shaft immediately behind the pile tip, with a value of around 2 % for a closed-ended pile (A_r = 1). The reduction factor for a typical open-ended pile with $A_r \sim 0.1$ is close to 0.5. The square root reduction in shaft friction ratio with increasing h/D gives a decrease by a factor of 2 for h/D = 4, and a factor of 5 for h/D = 25.

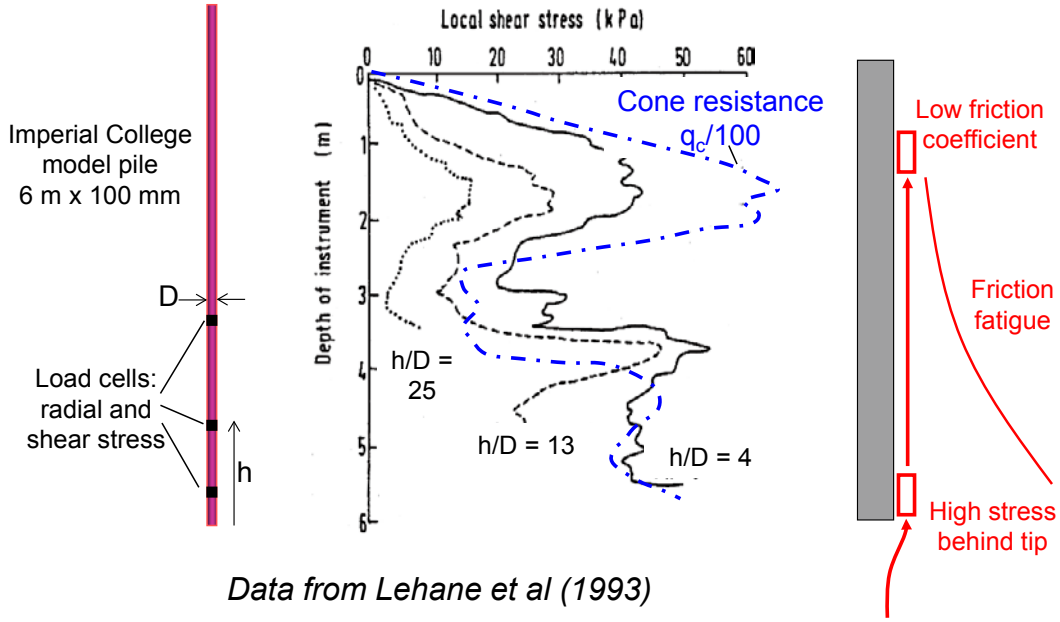

Figure 3: Illustration of the effects of friction fatigue from field measurements

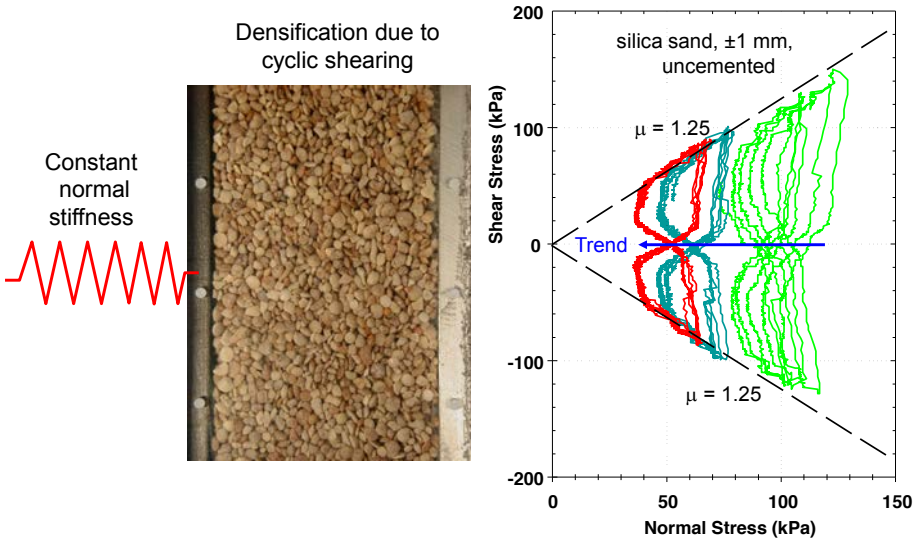

Figure 4: Results from laboratory constant normal stiffness cyclic shearing tests

Corresponding recommendations for design values of end bearing suggest an approximately linear trend of decreasing q_b/q_c with decreasing area ratio, according to (Lehane et al. 2005; Xu et al. 2008)

$$\frac{q_{b,0.1}}{q_c} = 0.15 + 0.45A_r \tag{4}$$

The design end bearing is denoted $q_{b,0.1}$ to reflect the resistance that can be mobilized within a limited displacement of 10 % of the pile diameter (0.1D). The main reasons for the lower proportion of q_c for open-ended piles ($q_{b,01}/q_c \sim 0.2$) compared with closed-ended piles ($q_{b,01}/q_c \sim 0.6$) are: (a) the much lower level of residual stresses typically developed during open-ended pile installation (Randolph 2003); and (b) the greater compliance of the tip response of an open-ended pile because of compression of the soil plug (Lehane & Randolph 2002).

In applying the design equations (3) and (4) it is necessary to consider the detailed stratigraphic fluctuations in cone resistance q_c, taking appropriate averages above and below the pile tip. This is discussed in some detail by Xu and Lehane (2005), who point out that, in profiles where q_c varies smoothly, averaging q_c over ±1.5D relative to the pile tip is sufficient. By contrast, in zones where q_c shows significant fluctuations the so-called 'Dutch' averaging method, which may extend up to 8D above the pile tip and 4D below, leads to better correlations of $q_{b,01}/q_c$.

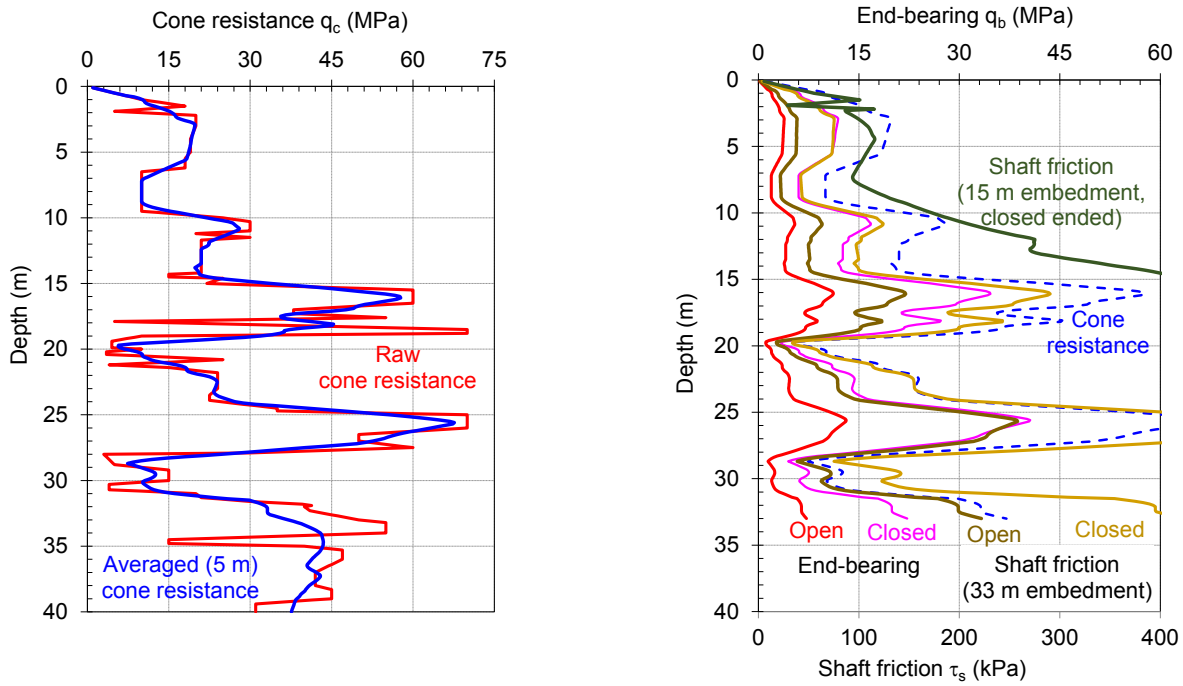

(a) Raw and averaged q_c profile (b) Shaft friction and end-bearing profiles

Figure 5: Comparison of shaft friction and end-bearing profiles for open-ended and closed-ended piles

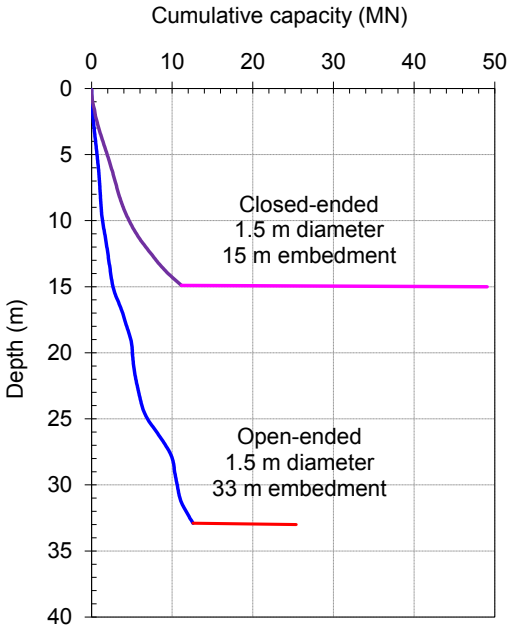

Figure 6: Profiles of cumulative axial pile capacity

An illustration of the design approach described above is shown in Figures 5 and 6 for a typical profile of relatively dense sand interbedded with looser zones of silty sand. The cone resistance profile has been smoothed over ±2.5 m relative to the tip of a notional 1.5 m diameter pile. Profiles of shaft friction and end-bearing are presented in Figure 5b for open-ended (with $A_r = 0.2$) and closed-ended piles, with shaft friction profiles for the latter presented for pile embedment of 15 m and 33 m. For a given embedment, the cumulative capacity of an open-ended pile is around 40 % of that for a closed-ended pile. In addition, the effects of friction degradation are such that, for this particular soil profile, a closed-ended pile embedded to 15 m (10D) could develop double the capacity of an open-ended pile embedded to 33 m (22D), as illustrated in Figure 6.

3 LATERAL PILE RESPONSE

As noted earlier, steel pipe piles are an attractive foundation choice for a wide range of applications in coastal constructions, particularly for wharfs, mooring dolphins and bridge foundations, owing to their relatively high bending stiffness and plastic moment compared with an equivalent diameter concrete pile. However, perhaps the most topical application of steel pipe piles is in the offshore wind industry, where extremely large diameter 'monopiles' have provided the primary foundation choice for developments in European coastal waters of the North Sea.

Typical geometries for offshore wind turbine monopiles are indicated in Figure 7. Diameters of the embedded sections range between 4 and 8 m, with an increasing trend chronologically, reflecting increases in turbine power (and size) and also in water depths. A corresponding trend has been the increase in typical diameter to wall thickness (D/t) ratios. Although the wall thickness is generally increased in the vicinity of the soil surface, where the bending moments are highest, over much of the monopile length D/t ratios lie between 60 and 120, so significantly greater than values of around 40 used historically in the offshore oil and gas industry.

Perhaps the largest monopiles installed to date have been those for the Gode Wind farm off the coast of Germany in the North Sea (Figure 8). The monopiles were 7.5 m in diameter, with wall thickness of around 75 mm over much of their length (Schroeder et al. 2015). The water depth at the location was around 30 m, with the critical design loads acting about 40 m above the seabed. The monopiles were designed with embedment depths around 28 to 32 m (3.8 to 4.2D). Schroeder et al. (2015) provide interesting insights into differences between conventional load transfer (p-y) curve analyses and more sophisticated three-dimensional finite element analyses.

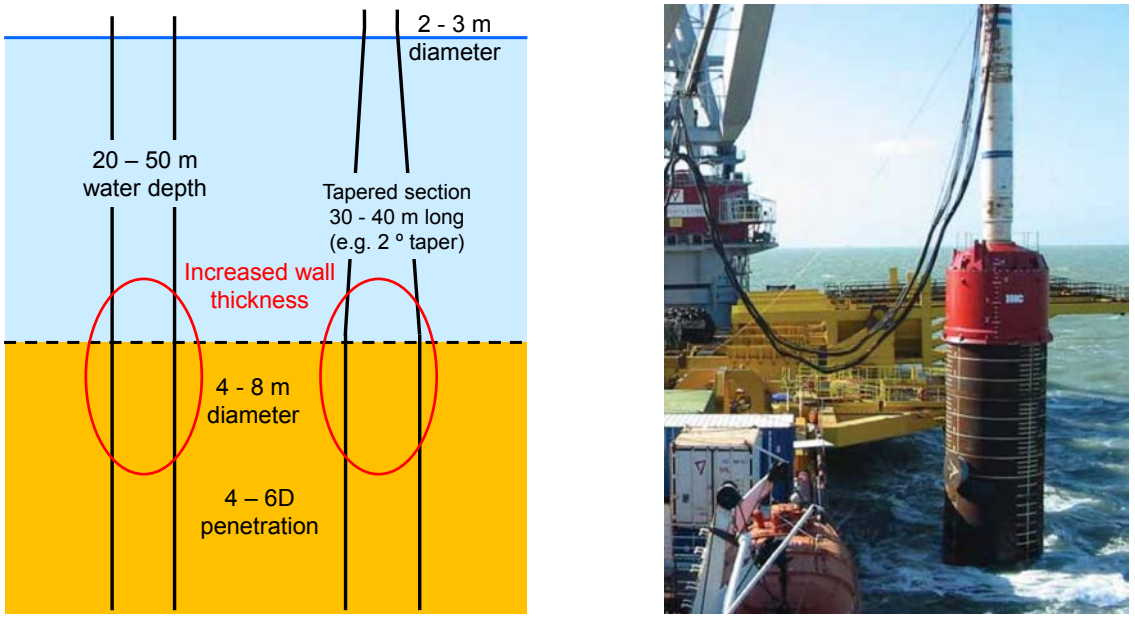

(a) Schematic of typical geometries (b) Driving of a 6 m diameter monopile

Figure 7: Monopiles for offshore wind turbines

Figure 8: Photograph of 7.5 m diameter monopiles for the Gode Wind farm

The failure mode of short (low L/D) piles under lateral loading is that of rigid body rotation about a point typically 70-80 % of the embedded depth. Initial sizing of the pile may be achieved using simple limit equilibrium techniques (e.g. Broms 1964a, b). However, design of monopiles is largely undertaken using load transfer analysis, although with some additional restraining springs applied at the tip of the monopile (in view of the low L/D ratio). In practice, base shearing contributes little to the lateral capacity except for L/D ratios below 2. Non-linear load transfer (p-y) curves are generally based on those recommended in ISO (2007) or API (2011), although recent studies have proposed new forms of p-y curve derived from the cone resistance (Suryasentana & Lehane 2014). In cemented soils and soft rocks, attention should be paid to brittleness in the load transfer response, which can lead to significant reductions in ultimate capacity (Erbrich 2004).

3.1 Lateral stiffness at small displacements

Considerable attention has been paid to the monopile stiffness, in particular the rotational stiffness, under operating load levels, partly owing to tight serviceability tolerances on turbine rotation (typically about 0.5 º of rotation) and partly in order to ensure that the natural frequency of the combined monopile, column and turbine system does not conflict with the high energy frequency of waves, or the rotational frequency of the turbine or an individual blade. Typically, the critical wave frequency will be around 0.1 Hz, the turbine frequency perhaps 0.15 to 0.3 Hz, and the individual blade frequency 3 times higher. The natural frequency of a typical turbine installation with monopile foundation will generally lie in the range 0.3 to 0.4 Hz, so falling between the turbine rotational frequency and that of individual blades (Zaaijer 2003; Bhattacharya 2014).

Simple elastic solutions for the lateral response of piles are useful to assess the foundation contribution to the natural frequency, and also gauge the rotational stiffness of monopiles in the initial stages of design. Such solutions are often presented using an equivalent 'solid pile' modulus, E_p, which for a steel pipe pile varies from about $0.2E_{steel}$ down to $0.1E_{steel}$ as the D/t ratio increases from 40 to 80. Depending on the pile-soil stiffness ratio and the L/D ratio of the pile, the pile response may be classified as 'rigid', 'intermediate' or 'flexible', with the intermediate range defined by (Randolph 1981; Carter & Kulhawy 1992).

$$0.05\left(\frac{E_p}{G_c}\right)^{0.5} < \frac{L}{D} < \left(\frac{E_p}{G_c}\right)^{2/7} \tag{5}$$

where G_c is the average modified shear modulus over the lesser of the pile embedment or the critical pile length given by the right hand limit (i.e. $L_c/D = (E_p/G_c)^{2/7}$ - see Figure 9).

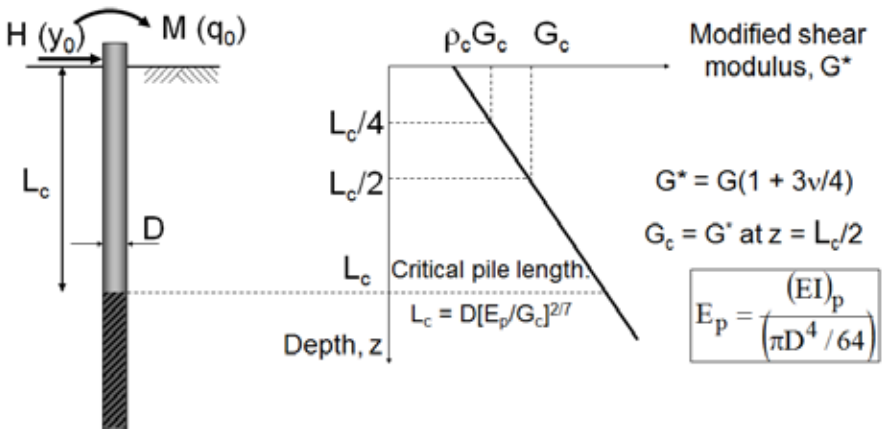

Figure 9: General conditions for lateral response of pile

Expressions for the pile head displacement and rotation for the extremes of pile response are

$$\begin{aligned} y_0 &= 0.4\frac{H}{G_c/D}\left(\frac{2L}{D}\right)^{-1/3} + 0.3\frac{M}{G_c/D^2}\left(\frac{2L}{D}\right)^{-7/8} \\ \theta_0 &= 0.3\frac{H}{G_c/D^2}\left(\frac{2L}{D}\right)^{-7/8} + 0.8\frac{M}{G_c/D^3}\left(\frac{2L}{D}\right)^{-5/3} \end{aligned} \tag{6}$$

for rigid pile response in homogeneous soil, so $G_c = G^*$ (Carter & Kulhawy 1992), and

$$\begin{aligned} y_0 &= \frac{(E_p/G_c)^{1/7}}{\rho_c G_c}\left[0.27\frac{H}{L_c/2} + 0.30\frac{M}{(L_c/2)^2}\right] \\ \theta_0 &= \frac{(E_p/G_c)^{1/7}}{\rho_c G_c}\left[0.30\frac{H}{(L_c/2)^2} + 0.80\sqrt{\rho_c}\,\frac{M}{(L_c/2)^3}\right] \end{aligned} \tag{7}$$

for flexible pile response (Randolph 1981).

It may also be convenient to consider the pile stiffness matrix, as opposed to the above compliance matrices. For the case of a pile close to or longer than its critical length, this may be expressed simply as

$$\begin{Bmatrix} H \\ M/L_c \end{Bmatrix} = G_c D^2 \sqrt{L_c/D}\begin{bmatrix} 3.2^* & -0.6 \\ -0.6 & 0.27 \end{bmatrix}\begin{Bmatrix} u_0/D \\ (L_c/D)\theta_0 \end{Bmatrix} \tag{8}$$

where the asterisked term should be replaced by 2.2 for soil where the modulus increases proportionally with depth (i.e. $\rho_c = 0.5$, according to Figure 9). Manipulation of equations (7) or (8) allows the rotational stiffness of a monopile to be expressed as (assuming homogeneous soil modulus) as

$$\frac{H}{\theta_0} = \frac{(L_c/D)^{1.5}}{1.2+6.4e/L_c} G_c D^2 = \frac{E_p{}^{3/7} G_c{}^{4/7}}{1.2+6.4e/L_c} D^2 = K_{H\theta} E_p{}^{3/7} G_c{}^{4/7} D^2 \quad (9)$$

where e is the eccentricity of the applied load above the seabed. For typical values of e/L_c, the stiffness coefficient $K_{H\theta}$ lies within a relatively narrow range of 0.1 to 0.15. The form of the right hand side of equation (9) shows the relative contribution to the rotational stiffness of the pile from pile modulus, E_p, modified soil shear modulus, G_c, and pile diameter, D.

Equations (6) and (7) may also be expressed as design charts for pile lateral stiffness as a function of pile-soil stiffness, E_p/G, and embedded normalized length, L/D. Two examples are shown in Figures 10 and 11, both for homogeneous soil shear modulus, G, and Poisson's ratio $\nu = 0.3$. The first example is for conditions where the pile head is restrained from rotation at the ground surface, such as might be the case for a bridge abutment. The pile head stiffness is normalized as H/u_0GD. The second, which is more applicable to monopile design, is for a high loading eccentricity where the applied moment at seabed level is M = 5HD. The normalized stiffness is expressed in terms of $H/\theta_e GD^2$, where θ_0 is the rotation at seabed level. The design charts show the effect of increasing L/D. For a given pile-soil stiffness ratio, the pile response changes gradually from rigid to flexible, beyond which limit the pile stiffness remains constant with further increase in normalized pile length L/D.

The form of the plots of pile stiffness against L/D, suggests that an appropriate design strategy for monopiles would be to adopt a pile length that is close to the critical pile length, L_c (given by the right hand limit of equation (5)). For piles shorter than that, the stiffness decreases relatively sharply with decreasing pile length. Typical pile-soil stiffness ratios, E_p/G, for the relatively stiff soils of the North Sea lie in the range 50 to 300, suggesting minimum values of normalized pile length of 3 to 5. These are consistent with typical geometries adopted in practice.

For comparison, additional (dashed) design lines are shown in Figures 10 and 11 for pile stiffness calculated using a Winkler spring model for the soil (i.e. as would be obtained from the initial pile response using a load transfer approach). The relative positions of pairs of 'continuum' and 'Winkler' curves, with the Winkler spring constant taken as k = 4.5G, suggest that values of equivalent load transfer spring stiffness in the range 4 to 5 times the shear modulus of the soil give broadly consistent values of pile head stiffness. However, the ratio k/G to obtain 'exact' correspondence changes with the pile geometry (L/D), pile-soil stiffness (E_p/G) and also the loading eccentricity (M/HD).

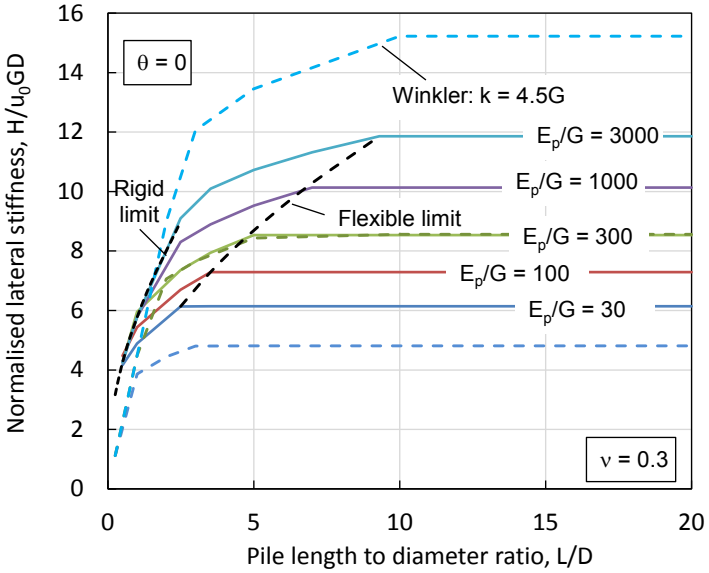

Figure 10: Pile head lateral stiffness for restrained-head pile

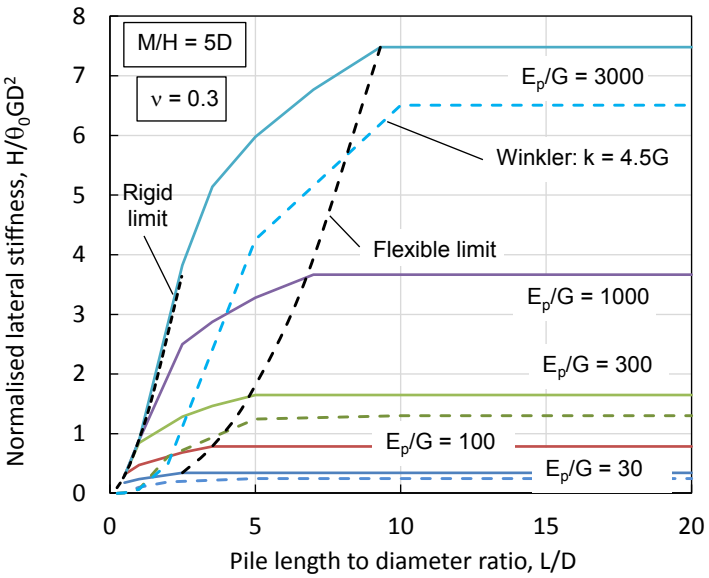

Figure 11: Pile lateral stiffness at load application point for high loading eccentricity

3.2 Effects of cyclic loading

The effects of cyclic loading are an important aspect of design, particularly where serviceability limits on cumulative displacements or rotations are tight. In fine-grained soils, cyclic loading will result in excess pore pressure generation and strength reduction in the soils adjacent to the pile. In turn, increased lateral displacement of the pile will be required in order to mobilize sufficient soil resistance to balance the applied loading. Much the same happens in free-draining soil, except that the cyclic loading tends to cause densification of the soil. Under symmetric loading, the soil stiffness will tend to increase, but under biased loading incremental deformations occur, even though the secant stiffness of each load-displacement cycle may increase.

Typical data from laboratory model tests are shown in Figure 12 (Leblanc et al. 2010). The incremental rotation, normalized by the rotation induced at maximum moment during the first cycle, increased linearly with the logarithm of the number of cycles. Results from tests conducted with different combinations of maximum and minimum cyclic moment (normalized by the ultimate moment capacity, M_u) followed similar linear trends, but offset from each other. This allowed Leblanc et al. (2010) to express the incremental moment as a function of key loading ratios.

Other testing programs at field scale, or on a geotechnical centrifuge, have shown similar quasi-linear trends in incremental movement as a function of the logarithm of number of cycles, although for very large numbers of cycles the trends can diverge towards either failure or shakedown, with the former exacerbated by varying the plane of the lateral loading (Dührkop & Grabe 2008; Li et al. 2010; Rudolph et al. 2014).

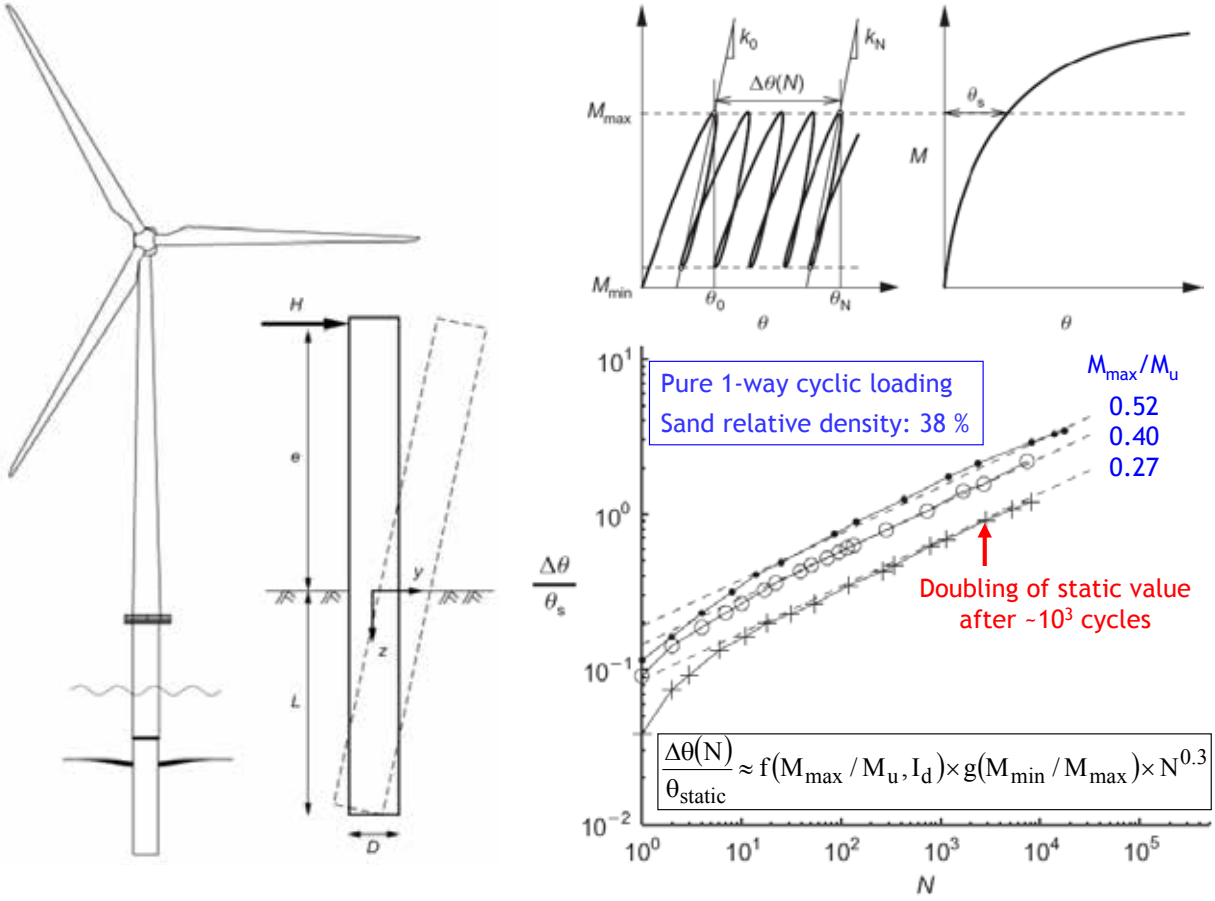

(a) Schematic of offshore wind turbine (b) Definition and data for incremental rotation

Figure 12: Example of incremental rotation under cyclic moment loading

3.3 Alternative foundation systems

Although monopiles have proved the most widespread foundation type for offshore wind farms, alternative approaches have been considered, as illustrated in Figure 13 (from Byrne & Houlsby 2003). Suction caissons have been considered extensively, either as separate foundations for a multi-pod structure, or as a single large diameter unit. A key design concern for suction caissons, particularly in sands, is their performance under the action of cyclic loading that results in tensile stresses at the base of the caisson. These may be sustained through transient negative excess pore pressures, but the cycling of stresses between compression and tension will cause accumulation of positive residual pore pressures, potentially allowing the caisson to undergo excessive displacements (Bye et al. 1995; Randolph et al. 2005).

However, of relevance here are different arrangements of conventional (smaller diameter) piles to replace the single large diameter monopile. Independent piles may be used to stabilize a multi-pod structure, such as used for the Borkum wind farm (Figure 14a, from Merritt et al. 2012), or in the form of a ring surrounding the turbine column (Figure 14b). In either case, the high moments from wind and wave loading are carried by axial 'push-pull' of the piles, which is somewhat more robust in respect of cumulative movements arising from cyclic loading compared with a low aspect ratio monopile.

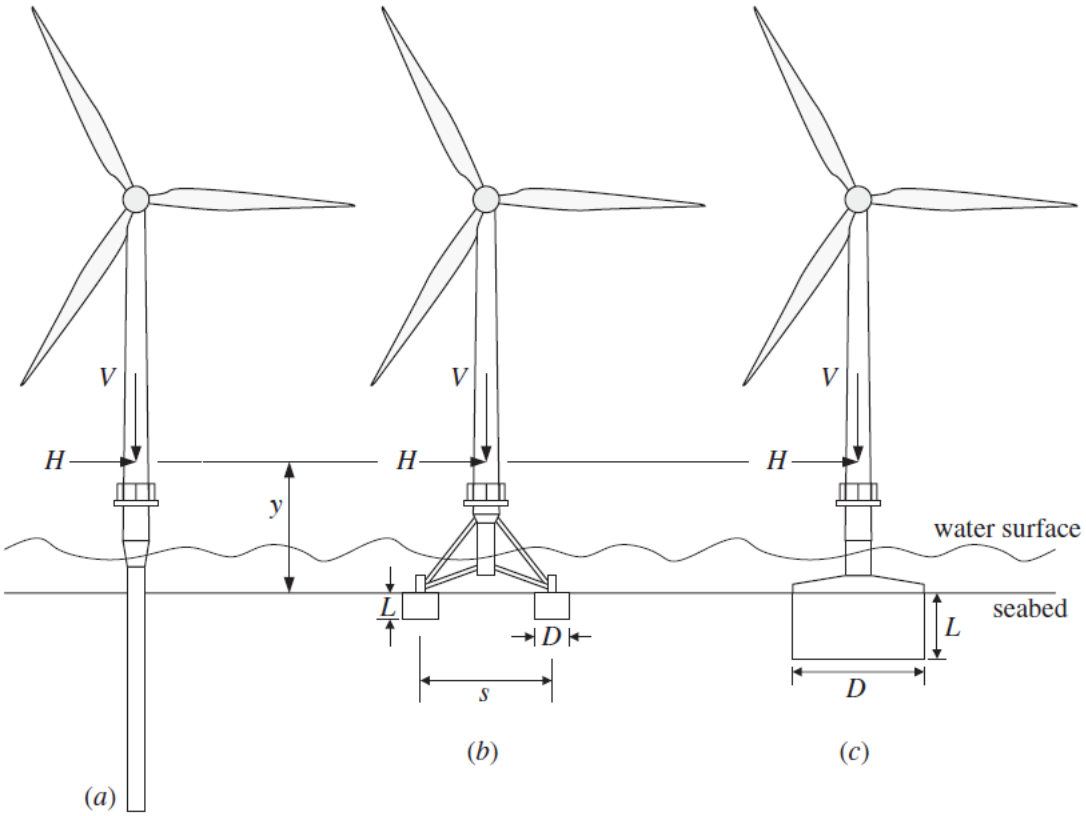

Figure 13: Alternative foundation concepts for offshore wind turbines

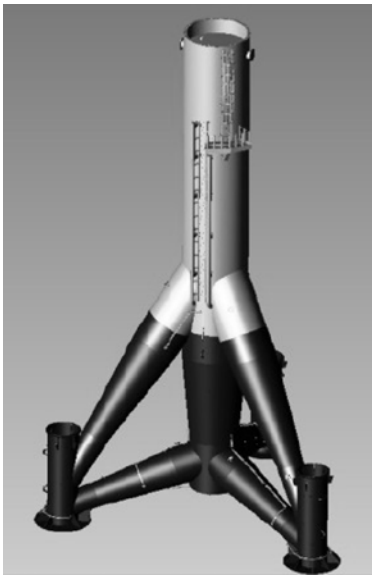

(a) Piled tripod structure (Merritt et al. 2012)

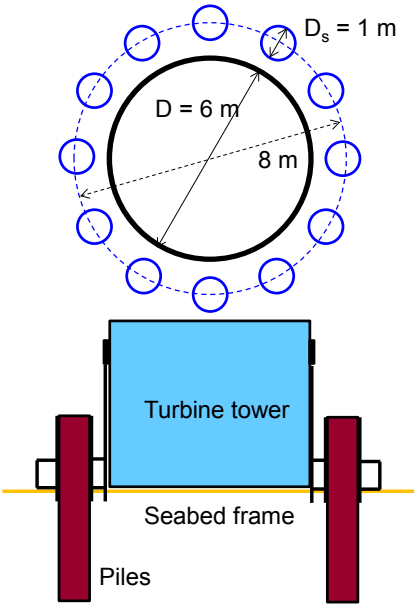

(b) Ring of piles

Figure 14: Alternative pile arrangements for offshore wind turbine foundations

It is interesting to consider the amount of steel and relative rotational stiffness of the foundation configurations in Figure 14, compared with a large (6 m) diameter monopile, as summarized in Table 1. The pile dimensions for the tripod are based broadly on the Borkum wind farm structure (Merritt et al. 2012). That structure has by far the highest rotational stiffness, an order of magnitude greater than for the two other

configurations as a result of its large footprint, but requires the most steel (especially once the tripod structure itself is allowed for). By comparison, the ring of piles has the least steel and a higher rotational stiffness than the monopile. As noted above, an advantage of the tripod and ring configurations is that the moments are carried by axial push-pull action of the piles, which is likely to reduce incremental rotation under cyclic loading. In addition, the strength mobilization ratio in the steel (from the maximum bending moments within the piles or monopile) for the tripod and ring configurations is only about 30 % of that for the monopile.

Table 1: Comparison of different foundation configurations for offshore wind farms

Foundation Configuration	Diameter and embedment (m)	L/D and D/t ratios	Steel volume per unit length (m^2)	Rotational * Stiffness (GN)
Monopile	6 × 30	5 and 75	1.5	2.2
Tripod structure	2.5 × 30	12 and 40	1.5	26.3
Ring of 12 piles	1 × 30	30 and 40	0.9	3.3

* Nominal value for load eccentricity of 40 m above the seabed and soil shear modulus of G = 5z MPa

4 VULNERABILITY OF PIPE PILES TO TIP DISTORTION AND EXTRUSION BUCKLING

Piles are vulnerable to damage during driving into strong soils or weak rock. This may often go undetected, with the only indication being a driving resistance that deviates from the expected profile. Figure 15 shows examples from onshore pile driving. In one case tip buckling of an H-pile has occurred due to encountering unweathered basalt at a shallower depth than anticipated; in the other case a thin-walled casing has become distorted during driving, possibly due to encountering a buried object within made ground. Progressive elliptical (and beyond) distortion of pipe piles in the offshore environment has been identified on several occasions, and two well-studied case studies are summarized briefly below.

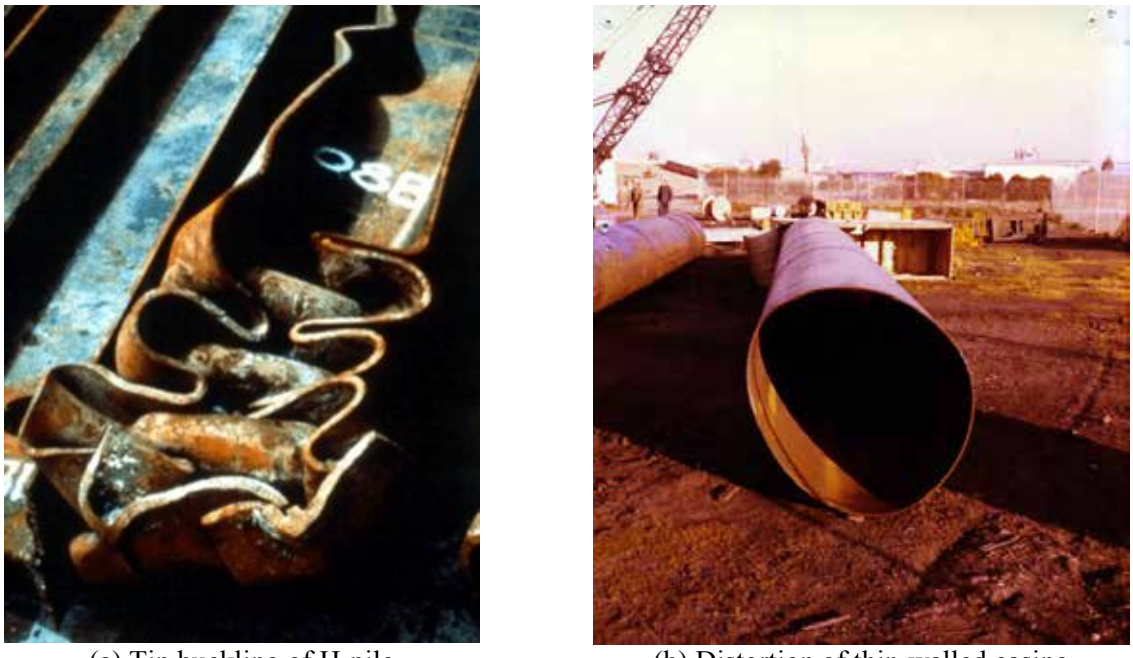

(a) Tip buckling of H-pile (b) Distortion of thin-walled casing

Figure 15: Examples of damage during driving

(a) View from the air

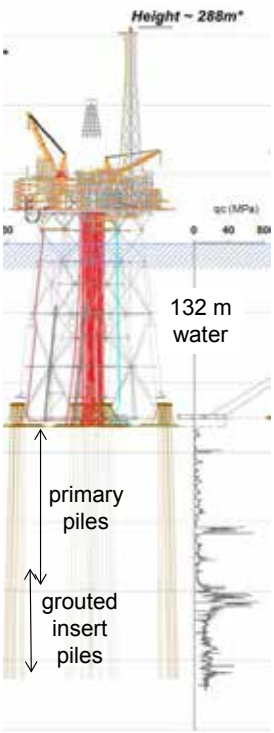

(b) Elevation of platform and foundations

Figure 16: Overview of Goodwyn A platform on North-West Shelf of Australia

4.1 Case study 1: Goodwyn A

The Goodwyn A platform was installed on the North-West Shelf of Australia in the late 1980s. The seabed comprised relatively low strength calcareous silt and sand layers down to a depth of about 110 m, below which calcarenite was found. Given the low shaft capacity of driven piles in calcareous soils, the adopted foundation design consisted of primary piles driven through the uncemented sediments, below which grouted insert piles were to provide the main axial support (Figure 16). The platform included 20 piles, 5 at each corner of the jacket structure, with diameter 2.65 m and wall thickness 45 mm (D/t = 59). However, when attempts were made to drill out the soil plug within the driven primary piles, to enable construction of the grouted insert piles, it was found that 16 of the 20 piles had undergone progressive distortion to the extent that the pile tips had become almost closed into a peanut shape. The distortion started at about the depth of a layer of cemented material (3 to 5 m thick, with cone resistance upwards of 60 MPa) embedded within the calcareous silt and sand layers (Figure 17).

In order to understand the process of what is now referred to as ‘extrusion buckling’, a numerical technique (BASIL) was developed within ABAQUS (Barbour & Erbrich 1995; Erbrich et al. 2010). The pile-soil interaction is represented by layers of ‘hair’ springs distributed around (and along the length of) the embedded section of the pile (Figure 18a). The zero force and displacement for each spring is taken from the point where the pile tip ‘cuts’ the hair spring. As the pile advances further, any forced radial movement of the spring (for example, if the pile wall is not parallel to the direction of advance) will invoke a force acting on the pile wall.

The analysis typically starts with the pile pre-embedded to some depth, and with the pile tip distorted according to the shape of a radial buckle (mode 1), with the maximum out of roundness adjusted in a parametric fashion, but typically 0.5 to 2 % of the pile radius. Typical fabrication tolerances specified for out of roundness are a maximum deviation from a true circle of ~0.5 % of the pile radius (DNV 2010). The pile is then advanced through the sets of soil springs, each of which has been pre-assigned an appropriate non-linear load-displacement response curve.

An example outcome from a BASIL simulation of extrusion buckling of a Goodwyn A pile is shown in Figure 19 (see also Erbrich et al. 2010). In order to achieve the progressive distortion, an initial out of roundness of 25 mm (1.9 % of the pile radius) was needed, which is somewhat outside the specified tolerance.

It was concluded that, notwithstanding any limitations of the numerical analysis, some external factor such as collision with the conical entry guides during stabbing of the piles, must have led to initial damage to the pile tip prior to installation.

At the time of the Goodwyn A platform installation, the pile D/t ratio of 59 was somewhat greater than in routine practice in the offshore oil and gas industry. However, as discussed later, many of the very large diameter monopiles used in the offshore wind industry have adopted even higher D/t ratios.

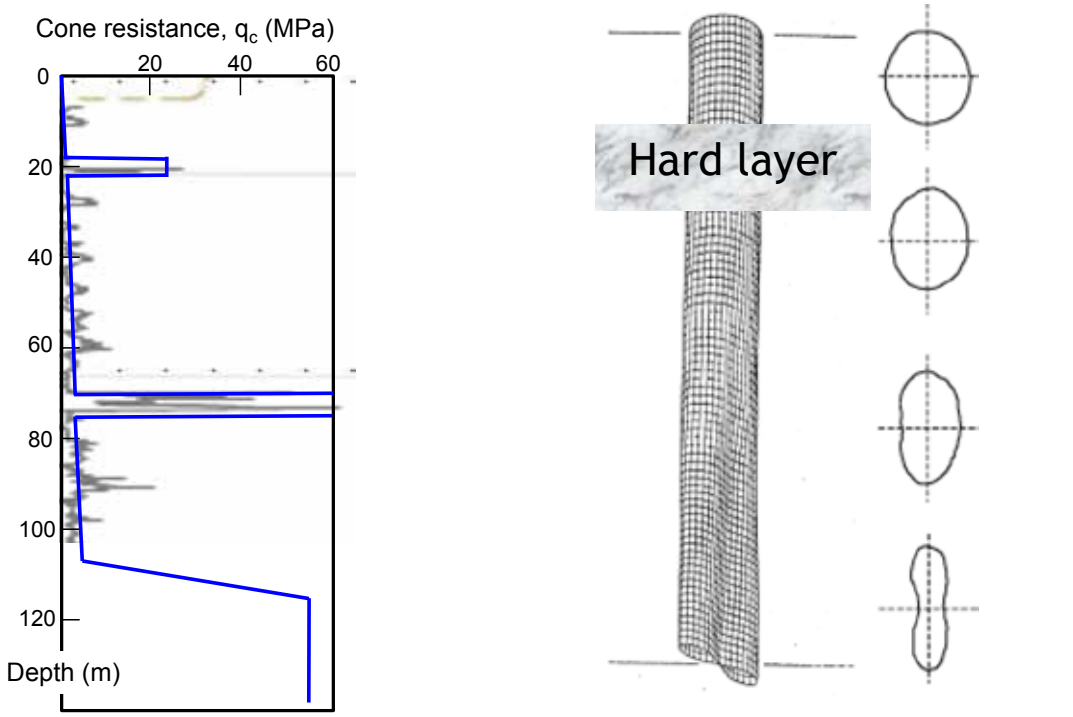

(a) Profile of cone resistance (b) Progressive pile distortion below hard layer

Figure 17: Soil strength profile and measured growth in pile distortion

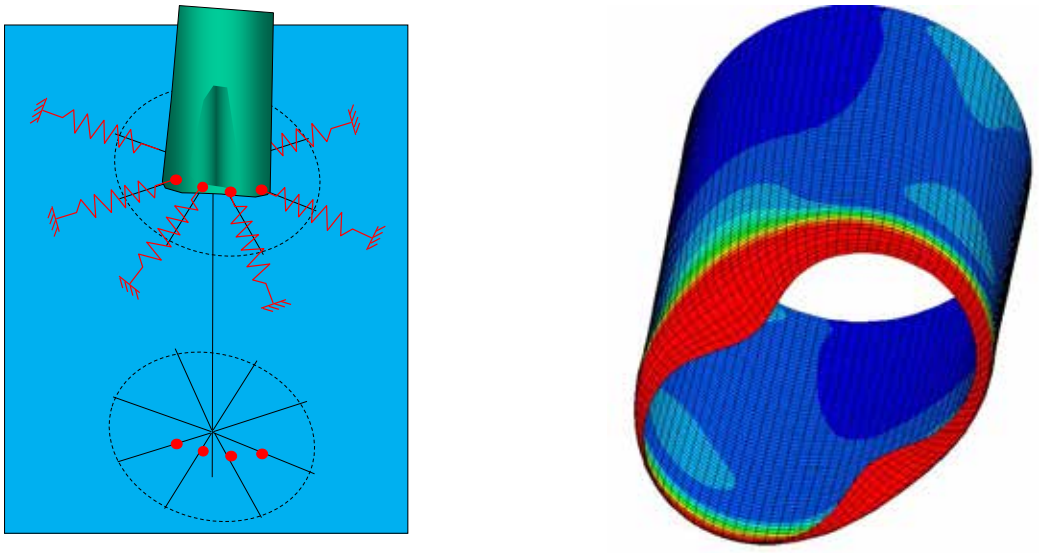

(a) Soil represented as 'hair' springs (b) Initial imperfection (exaggerated)

Figure 18: Numerical modelling approach to investigate extrusion buckling

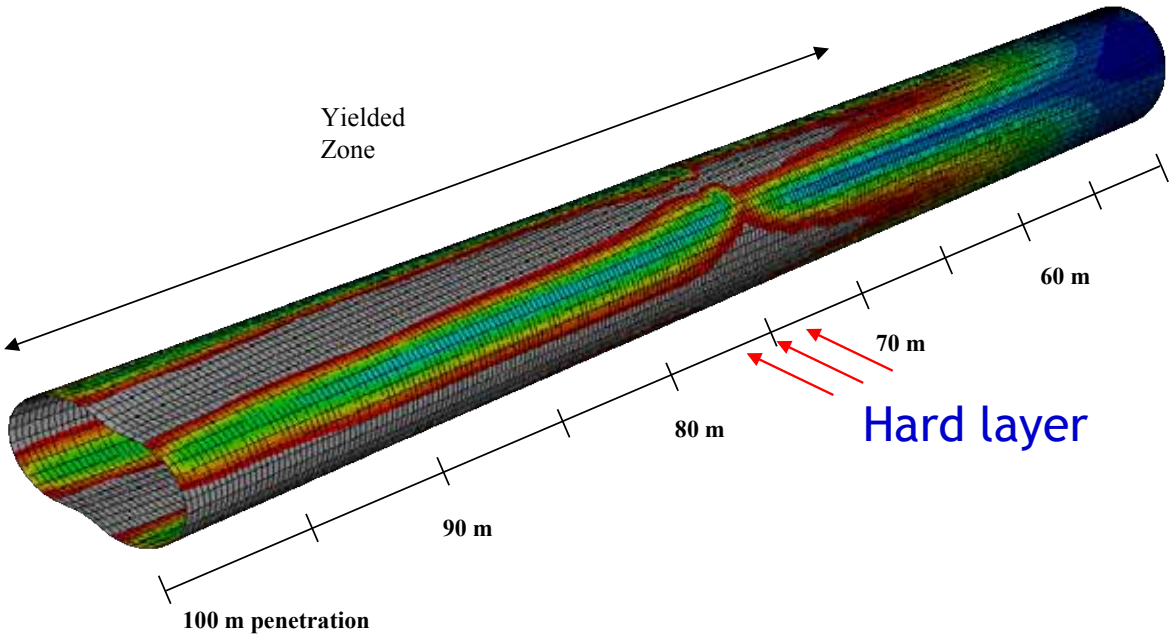

Figure 19: Example pattern of plastic strains for a pile pushed 25 m beyond the hard layer

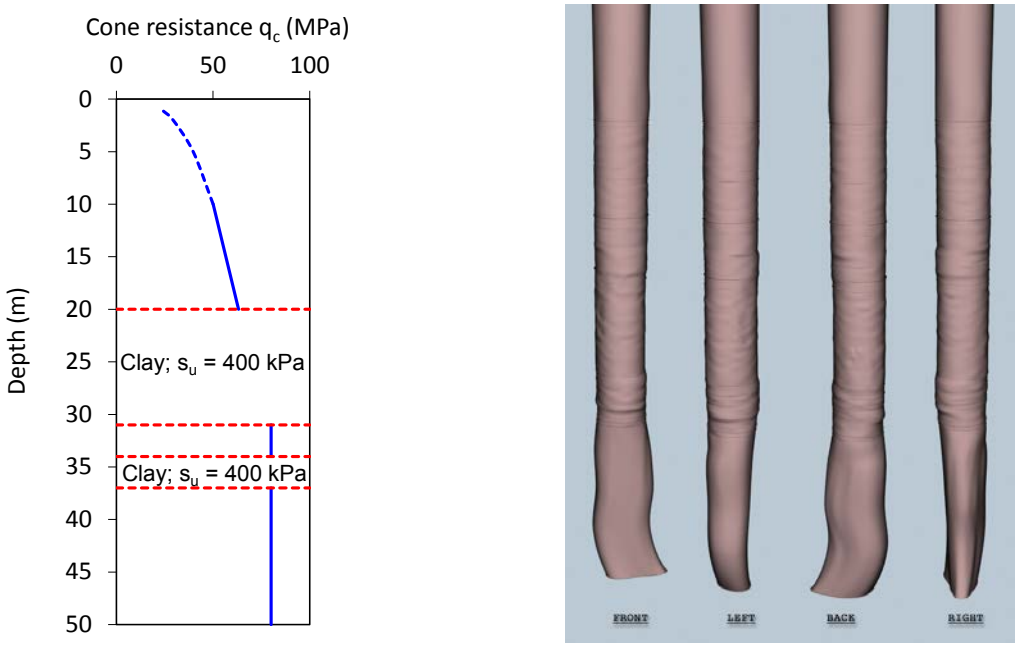

(a) Simplified cone profile (b) Typical distortion of lower part of pile

Figure 20: Soil profile and surveyed pile distortion for Valhall

4.2 Case study 2: Valhall, North Sea

The Valhall water injection platform was installed in the North Sea in 2002, but encountered problems when 5 or the 8 piles reached refusal at penetrations between 45 and 55 m, compared with the target penetration of around 70 m (Alm et al. 2004). The premature refusal meant that external weld beads, and the profiled variations in pile wall thickness, were then not at their anticipated design depths relative to the jacket structure. Investigations revealed that the piles that met refusal had undergone extrusion buckling to the extent that the tips were almost closed (Figure 20). The soil stratigraphy below about 37 m comprised very dense

sands, with cone resistances estimated as about 80 MPa. The piles were 2.44 m in diameter, with a wall thickness of 60 mm (so D/t of 40), hence consistent with routine practice.

During investigations into the cause of the pile distortion, attention focused on what might seem a relatively minor design detail, in the form of an external chamfer that was applied to the pile tips (Figure 21). In the context of the 2.44 m pile diameter, it is perhaps surprising that this detail could have such ramifications for pile installation. However, analysis suggested that there may indeed be significant differences in the external (and possibly internal) radial stresses that act on the pile wall.

Figure 22 shows schematically a comparison of the external radial stresses that may arise for blunt tipped and chamfered tip piles. For the former, radial stresses near the pile tip are expected to be near the lower end of 1 to 2 % of the cone resistance q_c (see equation (3)). However, for a chamfered tip, radial stresses will increase over the length of the chamfer as the external soil is pushed laterally, and also the reduction at the transition to the vertical wall will be relatively small. As such, stresses near the pile tip may be as high as 2 to 3 % of q_c, potentially as much as a factor of 3 greater than for a blunt tipped pile. In addition, for a chamfered pile tip there will be reduced tendency for soil to be forced inside the pile shaft (since the tip of the pile is thinner compared with a blunt tipped pile), leading to reduced internal radial stresses.

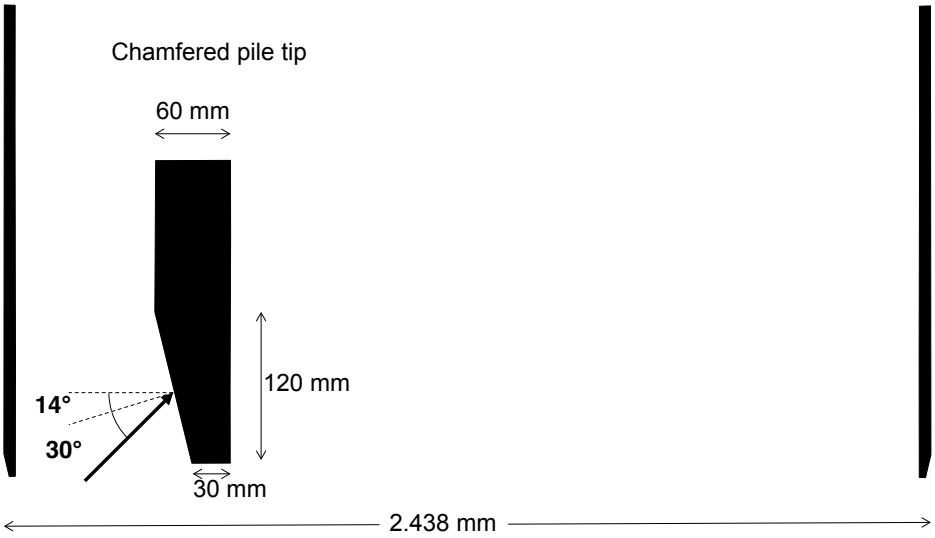

Figure 21: Detail of chamfered pile tip

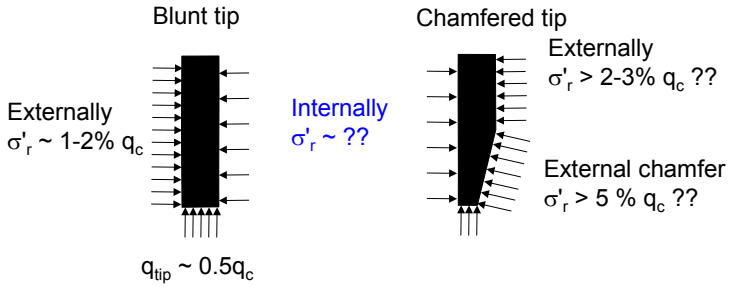

Figure 22: Effect of chamfer on external radial stresses

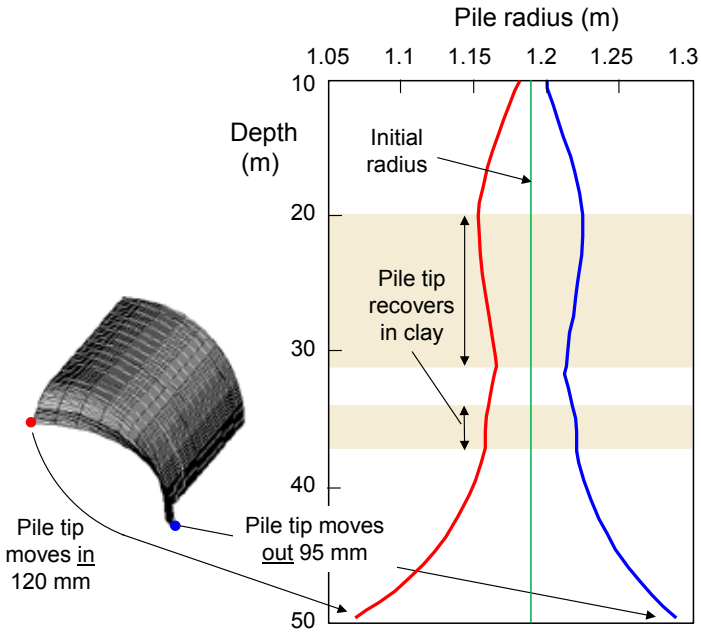

Figure 23: Soil profile and surveyed pile distortion for Valhall

Analyses using BASIL were carried out to explore conditions for triggering extrusion buckling, allowing for the radial stress enhancement of the chamfered tip. Figure 23 (Erbrich, private communication) shows example output for an initial out of roundness of 0.8 % of the pile radius. The pile was pre-embedded to 10 m and then pushed to a penetration of 50 m. Although full collapse was not achieved, significant outward (in one plane) and inward (in a perpendicular plane) movements occurred, hence initiating extrusion buckling.

4.3 Initiation and propagation of extrusion buckling

Extrusion buckling can be initiated during driving of pipe piles by a variety of conditions that include:

(1) initial out of roundness of the pile cross-section with non-verticality of the pile wall;
(2) high differential internal and external stresses acting on the pile wall from the soil;
(3) heterogeneous soil conditions.

In each case, it is necessary for the soil to be sufficiently stiff to overcome the elastic hoop stiffness of the steel, and also to be capable of generating differential radial stresses of sufficient magnitude. Conditions (1) and (2), respectively, are considered the primary causes of the pile distortion discussed above in Case studies 1 and 2. Clearly any plastic distortion of the circularity of the pile section near the tip would be expected to propagate further during driving through strong soils. Equally, if the differential stresses across the pile wall exceed the radial buckling pressure (the Bresse pressure, HSE 2001), then potential instability of the pile circularity can be initiated.

The effect of heterogeneous soil conditions is illustrated in Figure 24. An eccentric zone of stronger soil, or just a layer dipping relative to the horizontal, will tend to apply localized pressure across one plane of the cross-section. For high D/t ratios the hoop stiffness of the pile can be significantly lower than the corresponding soil stiffness, hence the soil will distort the pile rather than the other way round. Such heterogeneous conditions are particularly germane to offshore wind developments in the North Sea, where interbedded zones of silt to very dense sounds are frequently encountered, with high likelihood of variations in strength across the diameter of a monopile.

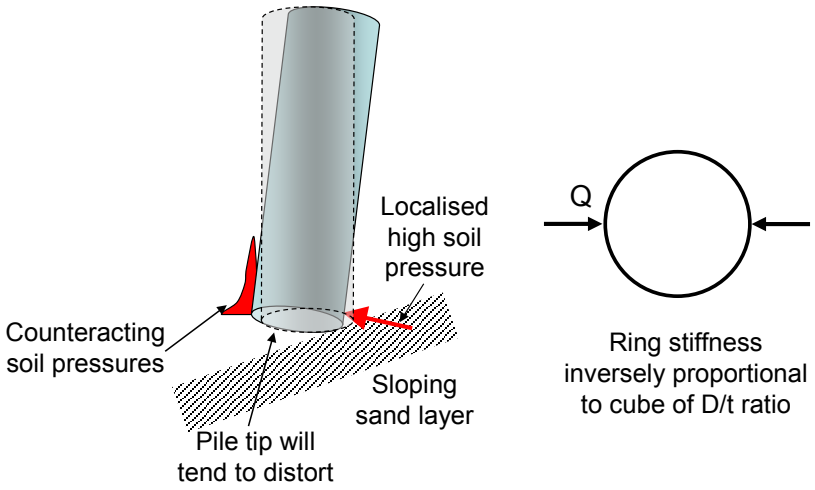

Figure 24: Initiation of pile tip distortion in heterogeneous soil

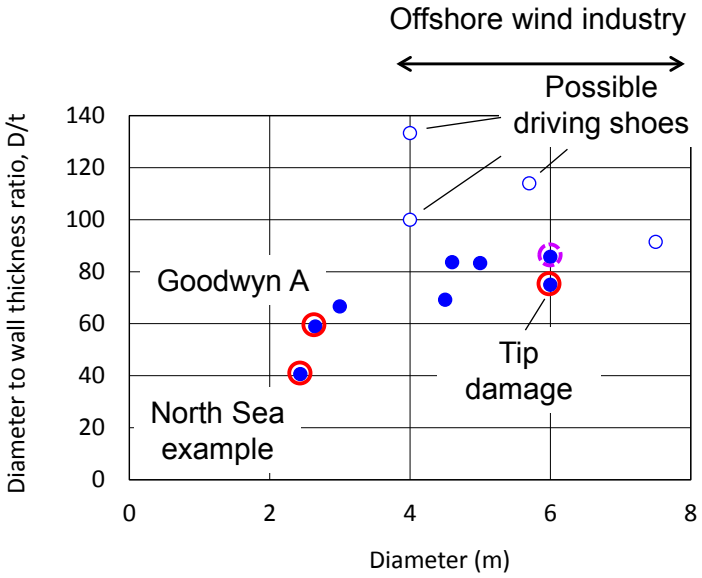

Figure 25: Trends in pile geometry in offshore wind industry

The hoop stiffness and critical radial buckling pressure are given by

$$\text{Hoop stiffnes (Figure 22)}: \quad \frac{Q}{\delta E_{steel}} = \frac{9.85}{(D/t)^3}$$

$$\text{Critical Bresse pressure}: \quad \frac{p_e}{E_{steel}} = \frac{2}{(D/t)^3} \qquad (10)$$

Both quantities are inversely proportional to the cube of the diameter to wall thickness ratio (D/t). Data for diameter to wall thickness ratio as a function of pile diameter are shown in Figure 25, from which a clear trend emerges of increasing D/t with increasing diameter. (Note that, for some of the larger diameter piles, details of any driving shoe (with thickened wall) are not publically available.) Marked on Figure 25 are cases where extrusion buckling of the pile tip has occurred, or in one case where it may be inferred from sharply increased driving resistance well above upper bound predictions.

For a D/t ratio of 80, the hoop stiffness and critical Bresse pressures calculated from equation (10) would be about 4 MPa and 0.8 MPa respectively. The latter figure is of the same order of magnitude as the external radial stresses expected in relatively uniform layers of dense sand with cone resistance in excess of 50 MPa,

but the low hoop stiffness is the more critical factor in initiation of pile tip distortion. The hoop stiffness may be compared with the initial gradient of a load transfer curve for lateral pile response. This would exceed the pile hoop stiffness for soil with shear modulus greater than about 1 MPa – so easily satisfied in all but quite soft soils. This is consistent with a similar assessment, although for somewhat thicker walled piles, by Aldridge et al. (2005).

For heterogeneous or dipping soil layers such as shown in Figure 24, localized increased soil stresses across the relevant vertical plane will initiate distortion of the pile tip, provided the soil stiffness is sufficiently high. Extrusion buckling is then likely to proceed, since minor distortion exacerbates the increased external stresses in that plane, while increased internal stresses will be generated across the perpendicular plane. The process is illustrated in Figure 26, considering a situation where the originally circular pile section has been distorted into an elliptical shape. If the pile wall at any given location around the tip attempts to advance vertically as the pile penetrates further, the external stresses will be increased further across the minor axis of the ellipse, while the internal stresses will be increased across the major axis of the ellipse. This provides a feedback loop, which will instead encourage the pile wall to advance parallel to its current direction in each vertical plane (see dashed arrows in Figure 26). The only external indication that the pile has started to undergo extrusion buckling may be increasing deviation of the driving resistance from predictions.

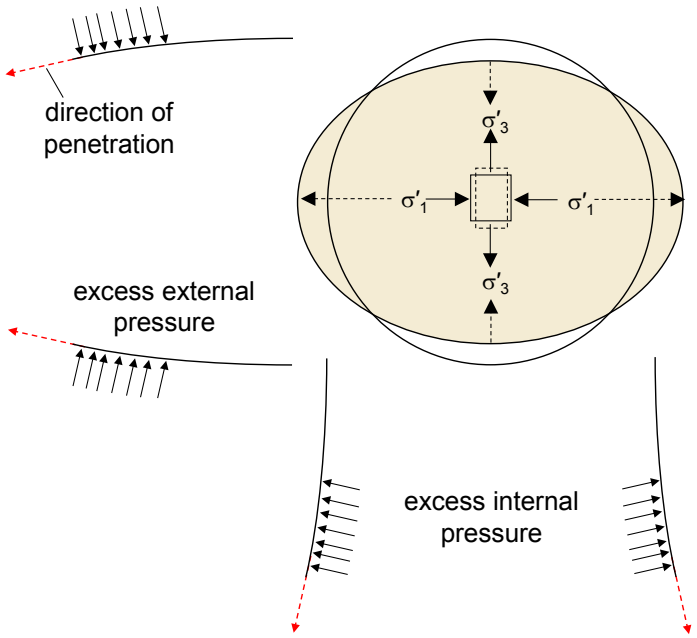

Figure 26: Schematic of extrusion buckling kinematics

In summary, open-ended piles are vulnerable to tip distortion leading to extrusion buckling. Tight fabrication tolerances, and construction procedures that eliminate damage to the pile tip during up-ending and initiating pile driving, are necessary in order to limit the potential for asymmetric differential radial stresses to develop around the pile. The greatest danger is the occurrence of heterogeneous soil conditions across the diameter of the pile, since they could distort the pile tip circularity. Relatively small displacements, of the order of the pile wall thickness, are sufficient to cause yield of the pile wall, further reducing the hoop stiffness. Careful checks are needed at the design stage to ensure that the diameter to wall thickness ratio at the pile tip provides sufficient hoop stiffness of the pile for the soil conditions anticipated at the site.

5 CONCLUDING REMARKS

Steel pipe piles are used extensively in coastal and offshore applications, and also as foundations for bridge piers, because of their ability to withstand bending moments arising from lateral loads. The majority are driven open-ended, allowing a soil plug to advance up the inside of the pile during installation. Modern design

approaches for driven piles in granular deposits have expressed engineering parameters such as the unit shaft friction and end bearing resistance in terms of the cone resistance profile deduced from in situ testing. They have also advanced understanding of friction degradation that arises due to cyclic shearing between pile and soil during driving, and also of the reduction in shaft friction and end bearing resistance for open-ended piles compared with similar diameter closed-ended piles. This can have a significant effect on the required penetration depth of the pile to achieve a given design axial capacity.

The offshore wind industry has adopted steel pipe piles as one of the primary foundation types on which to mount wind turbine columns. Relatively stubby piles are needed, given the low weight of the structures, but in order to provide sufficient rotational stiffness very large diameters are required for the so-called 'monopiles' with recent designs reaching diameters of 6 to 8 m. The failure mode for such piles is one of rigid body rotation, as opposed to the development of a plastic hinge. Since the rotational stiffness under operational conditions is of primary concern, simple elastic solutions may be used during the early stages of design to evaluate the required pile size for given loading conditions. An appropriate design principle is to adopt embedded lengths for the monopile that are around the 'critical' length under lateral loading.

In the offshore oil and gas and wind industries there have been a number of well documented instances where damage, with increasing elliptical distortion of the pile tip, has occurred progressively as the pile was driven, a process referred to as extrusion buckling. Two case studies were presented here, illustrating this form of damage. In the offshore wind industry, along with the increasingly large diameters of the monopiles, there has been a trend of increasing diameter to wall thickness ratios (D/t). The dramatic reduction in hoop stiffness of the pile that results from increasing D/t has exacerbated the vulnerability for extrusion buckling to occur, particularly in the rather heterogeneous soil conditions that pertain in the North Sea.

ACKNOWLEDGEMENTS

The work forms part of the activities of the Centre for Offshore Foundation Systems (COFS), currently supported as a node of the Australian Research Council Centre of Excellence for Geotechnical Science and Engineering and through the Fugro Chair in Geotechnics, the Lloyd's Register Foundation Chair and Centre of Excellence in Offshore Foundations and the Shell EMI Chair in Offshore Engineering. The author would like to acknowledge the value of discussions with colleagues in Fugro, in particular Carl Erbrich.

REFERENCES

Aldridge, T.R. Carrington, T.M. & Kee, N.R. 2005. Propagation of pile tip damage during installation. *Proc. of International Symposium on Offshore Geotechnics*, *Perth*, Taylor & Francis, 823-827.

Alm, T. & Hamre, L. 2001. Soil model for pile driveability based on CPT interpretations. *Proc. of 15th International Conference on Soil Mechanics and Geotechnical Engineering*, *Istanbul*, 2: 1297-1302.

Alm, T., Snell, R.O., Hampson, K.M. & Olaussen, A. 2004. Design and installation of the Valhall piggyback structures. *Proc. of Offshore Technology Conference, Houston*, Paper OTC 16294.

Andersen, K.H., Murff, J.D., Randolph, M.F., Clukey, E., Erbrich, C.T., Jostad H.P., Hansen, B., Aubeny, C.P., Sharma, P. & Supachawarote, C. 2005. Suction anchors for deepwater applications. *Proc. of International Symposium on Offshore Geotechnics, Perth*, Taylor & Francis, 3-30.

API. 2011. *Recommended Practice 2GEO Geotechnical and Foundation Design Considerations*, 1st Edition, American Petroleum Institute, Washington.

Arany, L., Bhattacharya, S., Adhikari, S., Hogan, S.J. & Macdonald, J. 2015. An analytical model to predict the natural frequency of offshore wind turbines on three-spring flexible foundations using two different beam models. *Soil Dynamics and Earthquake Engineering*, 74: 40-45.

Barbour, R. & Erbrich, C.T. 1995. Analysis of soil skirt interaction during installation of bucket foundations using ABAQUS. *Proc. Of ABAQUS Users Conference*, *Paris.*

Bhattacharya, S. 2014. Challenges in design of foundations for offshore wind turbines. *IET Engineering and Technology Reference*, doi: 10.1049/etr.2014.0041.

Broms, B.B. 1964a. Lateral resistance of piles in cohesive soils. *Journal Soil Mechanics and Foundations Division*, *ASCE*, 90(SM2): 27-63.

Broms, B.B. 1964b. Lateral resistance of piles in cohesionless soils. *Journal Soil Mechanics and Foundations Division*, *ASCE*, 90(SM3): 123-156.

Bye, A., Erbrich, C., Rognlien, B. & Tjelta, T.I. 1995. Geotechnical design of bucket foundations. *Proc. of Offshore Technology Conference, Houston*, Paper OTC 7793.

Byrne, T., Doherty, P., Gavin, K. & Overy, R. (2012). Comparison of pile driveability methods in North Sea sand. *Proc. of Offshore Site Investigation and Geotechnics: Integrated Technologies - Present and Future*, *Society for Underwater Technology, London, UK*, 481-488.

Byrne, B.W. & Houlsby, G.T. 2003. Foundations for offshore wind turbines. *Phil. Trans. R. Soc. Lond. A*, 361: 2909-2930.

Carter, J.P. & Kulhawy, F.H. 1992. Analysis of laterally loaded shafts in rock, *Journal of Geotechnical Engineering Division*, *ASCE*, 118(6): 839-855.

Dean, E.T.R. & Deokiesingh, S. (2012) Plugging criterion for offshore pipe pile drivability. *Géotechnique*, 63(9): 796-800.

DeJong, J.T., White, D.J. & Randolph, M.F. 2006. Microscale evolution of soil-structure interface behaviour during CNS cyclic shearing using PIV. *Soils and Foundations*, 46(1): 15-28.

DNV 2010. *Fabrication and Testing of Offshore Structures, Offshore Standard DNV-OS-C401*, Det Norske Veritas, Oslo.

Dührkop, J. & Grabe, J. 2008. Monopilegründungen von Offshore-Windenergieanlagen - Zum Einfluss einer veränderlichen zyklischen Lastangriffsrichtung. *Bautechnik*, 85(5): 317–321.

Erbrich, C.T. 2004. A new method for the design of laterally loaded anchor piles in soft rock. *Proc. of Offshore Technology Conference*, *Houston, Texas*, Paper OTC 16441.

Erbrich, C.T., Barbosa-Cruz, E. & Barbour, R. 2010. Soil-pile interaction during extrusion of an initially deformed pile. *Proc. of 2nd International Symposium on Offshore Geotechnics*, *Perth*, 489-494, Taylor & Francis, London, Australia.

HSE 2001. *A Study of Pile Fatigue During Driving and In-Service and of Pile Tip Integrity*. Offshore Technology Report 2001/018, Health and Safety Executive, UK, published by Her Majesty's Stationery Office, Norwich.

ISO. 2007. *Petroleum and natural gas industries — Fixed Steel Offshore Structures*, 1st Edition. International Standard 19902, International Standards Organisation Standard, Geneva.

Jardine, R.J., Chow, F.C., Overy, R. & Standing, J. 2005. *ICP Design Methods for Driven Piles in Sands and Clays*. Thomas Telford, London. ISBN 0 7277 3272 2.

LeBlanc, C., Houlsby, G.T. & Byrne, B.W. 2010. Response of stiff piles in sand to long-term cyclic lateral loading. *Géotechnique*, 60(2): 79–90.

Lehane, B.M., Jardine, R.J., Bond, A.J. & Frank, R. 1993. Mechanisms of shaft friction in sand from instrumented pile tests, *Journal of Geotechnical Engineering Division*, *ASCE*, 119(1): 19-35.

Lehane B.M. & Randolph M.F. 2002. Evaluation of a minimum base resistance for driven pipe piles in siliceous sand. *Journal of Geotechnical Engineering Division*, *ASCE*, 128(3): 198-205.

Lehane, B.M., Schneider, J.A. & Xu, X. 2005. *A Review of Design Methods for Offshore Driven Piles in Siliceous Sand*. Research Report Geo:05358, Geomechanics Group, The University of Western Australia.

Li, Z., Haigh, S.K. & Bolton, M.D. 2010. Centrifuge modeling of monopile under cyclic lateral loads. *Proc. of 7th International Conference on Physical Modelling in Geotechnics (ICPMG 2010)*, Taylor & Francis, London, 965–970.

Liyanapathirana, D. S., Deeks, A. J. & Randolph, M. F. 2001. Numerical modelling of the driving response of thin-walled open-ended piles. *International Journal of Numerical and Analytical Methods in Geomechanics*, 25(9): 933–953.

Randolph M.F. 1981. The response of flexible piles to lateral loading. *Géotechnique*, 31(2): 247-259.

Randolph, M.F. 2003. 43rd Rankine Lecture: Science and empiricism in pile foundation design. *Géotechnique*, 53(10): 847-875.

Randolph, M.F., Cassidy, M.J., Gourvenec, S. & Erbrich, C.J. 2005. Challenges of offshore geotechnical engineering, State of the Art paper. *Proc. of International Conference on Soil Mechanics and Foundation Engineering*, Osaka, Taylor & Francis, London, 1: 123-176.

Randolph, M.F., Leong, E.C. & Houlsby, G.T. 1991. One dimensional analysis of soil plugs in pipe piles. *Géotechnique*, 41(4): 587-598.

Randolph M.F., May M., Leong E.C., Hyden A.M. & Murff J.D. (1992). Soil plug response in open ended pipe piles. *Journal of Geotechnical Engineering Division,* ASCE, 118(GT5): 743-759.

Rudolph, C., Bienen, B. & Grabe, J. 2014. Effect of variation of the loading direction on the displacement accumulation of large-diameter piles under cyclic lateral loading in sand. *Canadian Geotechnical Journal*, 51: 1196-1206.

Schneider, J.A. & Harmon, I.A. 2010. Analyzing drivability of open ended piles in very dense sands. *Journal of the Deep Foundation Institute*, 4(1): 3-15.

Schneider, J.A., Xu, X. & Lehane, B.M. 2008. Database assessment of CPT-based design methods for axial capacity of driven piles in siliceous sands. *Journal of Geotechnical and Geoenvironmental Engineering*, ASCE, 134(9): 1227–1244.

Schroeder, F.C., Merritt, A.S., Sørensen, K.W., Muir Wood, A., Thilsted, C.L. & Potts, D.M. 2015. Predicting monopile behaviour for the Gode Wind offshore wind farm. *Proc. of 3rd International Symposium on Offshore Geotechnics*, Oslo, 735-740, Taylor & Francis, London.

Stevens, R.S, Wiltsie, E.A, & Turton, T.H. 1982. Evaluating pile drivability for hard clay, very dense sand, and rock. *Proc. of Annual Offshore Technology Conference*, *Houston, Texas*: 465-469.

Suryasentana, S.K. & Lehane, B.M. 2014. Numerical derivation of CPT-based p-y curves for piles in sand. *Géotechnique*, 64(3): 186–194.

Vaitkunaite, E., Nielsen, B.N. & Ibsen, L.B. 2015. Comparison of design methods for axially loaded buckets in sand. *Proc. of 3rd International Symposium on Offshore Geotechnics*, Oslo, 735-740, Taylor & Francis, London, 331-336.

Xu, X.T., Schneider, J.A. & Lehane, B.M. 2008. Cone penetration test (CPT) methods for end-bearing assessment of open- and closed-ended driven piles in siliceous sand. *Canadian Geotechnical Journal*, 45(1): 1130–1141.

White, D.J., Schneider, J.A. & Lehane, B.M. 2005. The influence of effective area ratio on shaft friction of displacement piles in sand. *Proc. of International Symposium on Frontiers in Offshore Geotechnics*, *Perth, Australia*, 741–747, Taylor & Francis, London.

Zaaijer, M.B. 2003. *Comparison of monopile, tripod, suction bucket and gravity base design for a 6 MW turbine*. Delft University of Technology, Report to DOWEC project, Dutch Ministry of Economic Affairs.

A New Simplified Hypothesis B Method for Calculating Consolidation Settlement of Clayey Soils Exhibiting Creep

Jian-Hua YIN
Department of Civil and Environmental Engineering,
The Hong Kong Polytechnic University, Hong Kong, China

ABSTRACT

This paper introduces a new simplified Hypothesis B method for calculating consolidation settlement of clayey soils exhibiting creep. This paper presents example applications of this method for calculating settlements of one layer of Hong Kong Marine Deposits (HKMD) with creep. The validation of this method is examined by comparing calculated settlements with settlements from two fully coupled finite element (FE) consolidation analyses. It is found that curves calculated using this new simplified Hypothesis B method with a factor α=0.8 are close to curves from two Finite Element (FE) model simulations with the smallest relative errors. In overall, settlements calculated using Hypothesis A method are smaller than those from the two FE simulations with large relative errors for the same HKMD layer. This paper also introduces the extension of this new method for one layer to multiple layers. Settlements of two cases of double soil layers are calculated using the extended method and are compared with settlements from a fully coupled finite element consolidation analysis and Hypothesis A. It is found again that Hypothesis A method underestimates the settlement a lot; while curves calculated using the extended new simplified Hypothesis B method with Zhu and Yin (2005) for U_a are very close to curves from the fully coupled FE consolidation analysis.

1 INTRODUCTION

The creep is defined as deformation under a constant load or stress. It is well known that many materials have creep deformation. For example, if a dead weight is placed on the top of a plastic bottle, a few days later, the bottle will suffer compression deformation. If a large dead weight is placed on a concrete cube, this cube will have compression deformation with time. The larger the load and the higher the temperature, the larger the creep deformation of the concrete cube. If a clayey soil specimen is subjected to a constant stress in an oedometer ring (or a specimen in a triaxial cell), this specimen will exhibit compression strain with time. In summary, creep deformation exists in many engineering materials. This is the fact. The physical and chemical mechanisms (or causes) of creep are different for different engineering materials. For clayey soils, the causes of creep are due to four levels of factors: (a) viscous adsorbed water in double layers on clay plates, (b) viscous re-arrangement and sliding of clay plates, (c) viscous deformation (maybe small) of clay plates, and (d) viscous deformation (large) of clay skeleton (structural frameworks formed by soil solid partials).

Consolidation is a coupled process of dissipation of excess porewater pressure and compression of the soil skeleton. Creep deformation of soil skeleton during and after the consolidation process will result in both short-term and long-term settlements. Settlements are an important issue for foundation or reclamation designs. Creep contributes a lot to these settlements, especially post-construction settlements. Therefore, creep settlements or deformation of clayey soils must be considered and shall be carefully and reliably calculated.

1.1 Hypothesis A method

The consolidation settlement in this paper is for the case of one-dimensional straining (1D straining) condition with constant soil properties for each layer. The conventional Hypothesis A method for the calculation of consolidation settlement has the following assumptions:

(a) There exists a so-called "End-of-Primary" (EOP) point between "primary" consolidation period and "secondary" compression without excess porewater pressure (u_e=0) with the corresponding time t_{EOP}.
(b) There is no creep compression during the "primary" consolidation period; but the creep compression occurs only in the "secondary" compression starting at t_{EOP} (see Figure 1).
(c) The creep compression occurs in the "secondary" compression period can be described by the "secondary" consolidation coefficient $C_{\alpha e}$ which is $C_{\alpha e} = -\Delta e / \Delta \log t$, where e is void ratio and t is the duration time of the present loading (see Figure 1). The mathematical equation of the method based on Hypothesis A for the calculation of the total consolidation settlement S_{totalA} in the field is:

$$S_{totalA} = S_{"primary"} + S_{"secondary"} = \begin{cases} U_v S_f & for \quad t < t_{EOP,field} \\ U_v S_f + \dfrac{C_{\alpha e}}{1+e_o} \log\left(\dfrac{t}{t_{EOP,field}}\right) H & for \quad t > t_{EOP,field} \end{cases} \tag{1}$$

where $S_{"primary"}$ is the "primary" consolidation settlement at time t and is equal to $U_v S_f$ in which U_v is the average degree of consolidation and S_f is the final "primary" settlement. In Eq.(1), e_o is the initial void ratio. The "secondary" compression settlement is $S_{"secondary"} = [C_{\alpha e}/(1+e_o)]\log(t/t_{EOP,field})H$ and is calculated since $t > t_{EOP,field}$ which is the time at "EOP" in the field condition. The $t_{EOP,field}$ is dependent on the thickness of the soil layer and hydraulic permeability of the soil. The two main problems in Eq.(1) are as follows:

(a) The separation of the "primary" consolidation period and "secondary" compression period is subjective and not accurate. According to the Tergazhi's 1-D consolidation theory, the time corresponding to excess porewater pressure u_e=0, that is, U_v=100%, is infinite, that is, $t_{EOP,field}$ shall be infinite. To get around this problem, it is often assumed that the time corresponding to $U_v \geq 98\%$ is the time $t_{EOP,field}$ at "EOP".
(b) There is no creep when time $t < t_{EOP,field}$ as shown in Eq.(1), that is, no creep in the "primary" consolidation; however creep occurs right after $t_{EOP,field}$ as "secondary" compression.

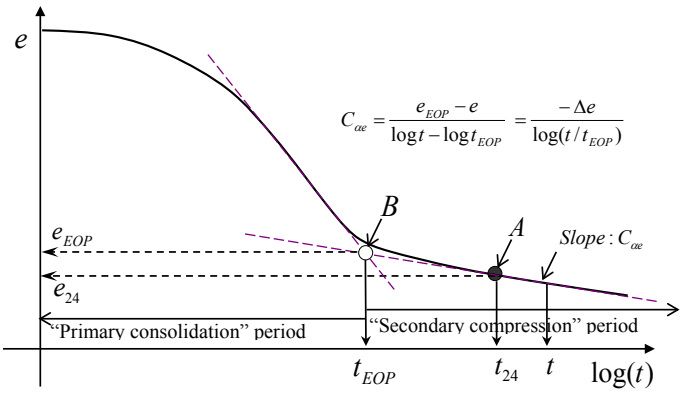

Figure 1: Curve of void ratio versus log (time) and "secondary" compression coefficient

In fact, under the action of the effective stress, the skeleton of a clayey soil exhibits viscous deformation, or ongoing settlement in 1-D straining case. Even in the "primary" consolidation period, there are effective stresses. The rate of creep compression depends on the state of consolidation such as normal consolidation or over-consolidation. Therefore, due to the exclusion of creep compression in the "primary" consolidation period, the method based on Hypothesis A normally underestimates the total consolidation settlement.

1.2 Hypothesis B method

The method based on Hypothesis B does not need these assumptions in Hypothesis A. The method based on Hypothesis B is a coupled consolidation analysis using a proper constitutive relationship for the time-dependent stress-strain behavior of clayey soils. The time-dependent compression of the clay skeleton, for example, creep in the "primary" consolidation, is naturally included in the coupled consolidation analysis. The equations of the method based Hypothesis B is briefly described here. From the mass continuity condition:

$$\frac{k}{\gamma_w}\frac{\partial^2 u_e}{\partial z^2} = -\frac{\partial \varepsilon_z}{\partial t} \tag{2}$$

where k is the vertical hydraulic conductivity; γ_w is the unit weight of water; u_e is the excess porewater pressure; and ε_z is the vertical strain. There are two unknowns in Eq.(2), that is, u_e, ε_z. A constitutive model equation is needed.

Yin and Graham (1989, 1994) developed, validated, and applied a 1D Elastic Visco-Plastic (1D EVP) constitutive model for the time-dependent stress-strain behavior of clayey soils. The 1D EVP constitutive model equation is:

$$\dot{\varepsilon}_z = \frac{\kappa}{V}\frac{\dot{\sigma}'_z}{\sigma'_z} + \frac{\psi}{Vt_o}\exp\left[-(\varepsilon_z - \varepsilon_{zo}^{ep})\frac{V}{\psi}\right]\left(\frac{\sigma'_z}{\sigma'_{zo}}\right)^{\lambda/\psi} \tag{3}$$

where $\dot{\varepsilon}_z$ and ε_z are the vertical strain rate and strain; $\dot{\sigma}'_z$ and σ'_z are the vertical effective stress rate and effective stress; V is equal to (1+e_o), called specific volume; κ/V together is considered to be one parameter related the elastic compression of the soil; The three parameters λ/V, ε_{zo}^{ep}, σ'_{zo} define a "reference time line" (Yin and Graham 1989, 1994) and are related to the normal compression line of the soil; and the two parameters ψ/V and t_o are related to the creep compression of the soil. The 1D EVP model in Eq.(3) is an extension of the Maxwell's linear elastic visco-plastic model in which a linear elastic spring is connected to a linear viscous dash pot (Yin 2015). By solving Eq.(2) together with Eq.(3), we can obtain the excess porewater pressure u_e, from which, we can obtain the effective stress σ'_z, the vertical strain ε_z and the total settlement S_{totalB} of the soil layer (Yin and Graham 1996). One limitation of the above rigorous Hypothesis B method is that a numerical method is needed to solve a set of non-linear partial different equations and a computer program for this method is needed. Such computer program is still not readily available to engineers or difficult for them to use. The main objective of this paper is to introduce a new simplified Hypothesis B method for spread-sheet calculation of consolidation settlements of clayey soils with creep.

2 BRIEF DESCRIPTION OF THE SIMPLIFIED HYPOTHESIS B METHOD FOR ONE LAYER

Figure 2 shows relationship of void ratio (or strain) and log(effective stress) with different consolidation state for 1-F straining (oedometer) condition. The new simplified Hypothesis B method for the calculation of the total consolidation settlement S_{totalB} for 1-D straining condition in Figure 2 is expressed as:

$$\begin{aligned} S_{totalB} &= S_{"primary"} + S_{creep} \\ &= U_v S_f + [\alpha S_{creep,f} + (1-\alpha) S_{"secondary"}] \quad for \quad all \quad t \geq 1\,day \quad (t \geq t_{EOP,field} \; for \; S_{"secondary"}) \end{aligned} \tag{4}$$

We explain how to determine all parameters in Eq.(4) as follows:

(a) Determination of the "primary" consolidation settlement $S_{"primary"}$

$S_{"primary"}$ is calculated in a conventional way, $S_{"primary"} = U_v S_f$ where U_v is the vertical average degree of consolidation and can be obtained from suitable charts, equations, and approximate equations (see example later). The S_f in Eq.(4) is normally calculated using the "swelling" index C_e, that is, unloading/reloading (or the over-consolidation compression) slope and compression index C_c using the compression data from oedometer tests with 1 day (24 hours) duration under each load. The duration of 1 day has been included creep occurred already during 24 hours of loading. This is why the time t shall be equal or larger than 1 day in Eq.(4). The final settlements S_f in Eq.(4) for four cases are calculated as follows (see Yin 2016):

(*i*) *Loading from Point 1 to Point* 2*:*

$$S_f = \Delta\varepsilon_{z,1-2} H = \frac{C_e}{1+e_o} \log(\frac{\sigma'_{z2}}{\sigma'_{z1}}) H \tag{5a}$$

The $\Delta\varepsilon_{z,1-2}$ is the vertical strain increase due to stress increases from σ'_{z1} to σ'_{z2}. Similar strain increase symbols are used in the following equations.

(*ii*) *Loading from Point 1 to Point* 4*:*

$$S_f = \Delta\varepsilon_{z,1-4} H = [\frac{C_e}{1+e_o} log(\frac{\sigma'_{zp}}{\sigma'_{z1}}) + \frac{C_c}{1+e_o} log(\frac{\sigma'_{z4}}{\sigma'_{zp}})] H \tag{5b}$$

(*iii*) *Unloading from Point* 4 *to Point* 6*:*

$$S_f = \Delta\varepsilon_{z,4-6} H = \frac{C_e}{1+e_o} \log(\frac{\sigma'_{z6}}{\sigma'_{z4}}) H \le 0 \tag{5c}$$

(*iv*) *Reloading from Point* 6 *to Point* 5*:*

$$S_f = \Delta\varepsilon_{z,6-5} H = \frac{C_e}{1+e_o} \log(\frac{\sigma'_{z5}}{\sigma'_{z6}}) H \ge 0 \tag{5d}$$

(b) Determination of the creep settlement S_{creep}

The creep settlement is $S_{creep} = [\alpha S_{creep,f} + (1-\alpha) S_{"secondary"}]$. $S_{"secondary"}$ is the same as that in Eq.(1) and $t_{EOP,field}$ is the time at $U_v = 98\%$. $S_{"secondary"}$ can be calculated in the same way by using Hypothesis A method (see example later). $S_{"secondary"}$ occurs for $t \ge t_{EOP,field}$. $S_{creep,f}$ is the creep settlement under the final effective vertical stress without excess pore water pressure coupling. For example, if the loading is increased from Point 1 to Point 4 (see Figure 2), $S_{creep,f}$ is calculated by assuming to be the creep under the effective stress at Point 4, ignoring the pore water pressure. In this way, real creep settlement will be over-estimated. This is why we introduce a parameter α . The parameter α is shall be in the range from 0 to 1, that is, $0 \le \alpha \le 1$. If $\alpha = 1$, Eq.(4) becomes the old Yin's simplified Hypothesis B method (Yin 2011). If $\alpha = 0$, Eq.(4) becomes Hypothesis A method in Eq.(1). The most suitable value α will be determined by comparing calculated settlement using Eq.(4) with settlements from coupled consolidation analysis. It is found later in this paper that if $\alpha = 0.8$, the settlements calculated using this new simplified Hypothesis B method are closer to the settlements from the fully coupled consolidation modelling (Yin 2016; Yin and Feng 2016; Feng and Yin 2016). Comparing Eq.(4) to Eq.(1), it is seen that the creep settlement S_{creep} is included for the loading

time $t \geq 1\,\text{day}$, that is, creep compression occurs from the beginning. The details of calculating $S_{creep,f}$ for different stress-strain states are explain below.

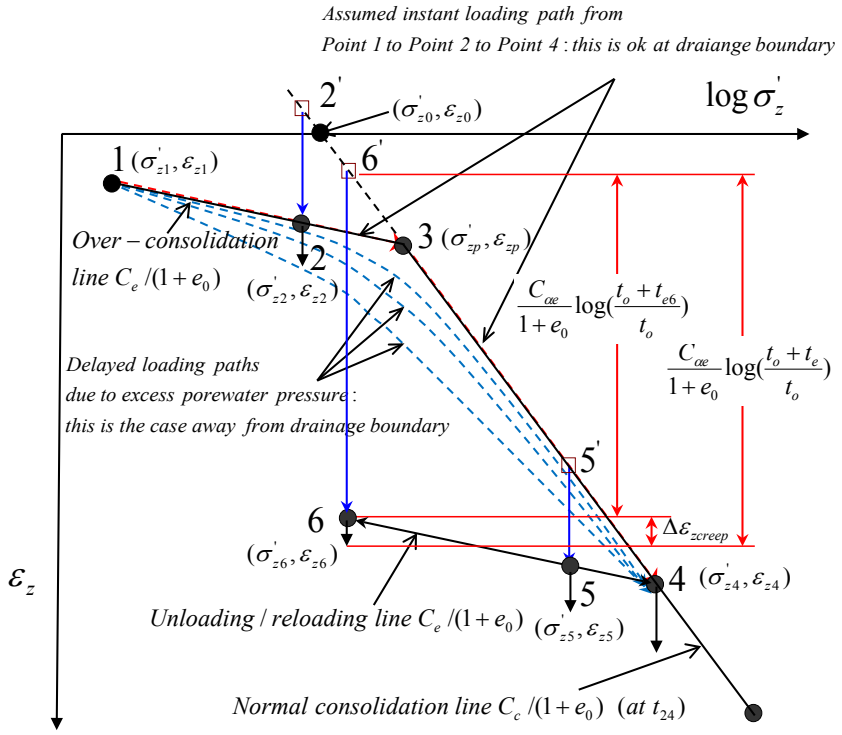

Figure 2: Relationship of void ratio (or strain) and log(effective stress) with different consolidation states

(*i*) *Final stress is on normal consolidation line* (*NCL or state*)

$$S_{creep,f} = \frac{C_{\alpha e}}{1+e_0}\log(\frac{t_o+t_e}{t_o})H \tag{6a}$$

where H is the thickness of the soil layer. In this case, the "equivalent time" $t_e = t - t_o$, where t is duration time of the current total vertical stress.

(*ii*) *Final stress is on over – consolidation line* (*or state*)

According to the definition of "equivalent time" (Yin and Graham 1989, 1994), the creep strain rate at the present Point 2, no matter how to get this point in real situation, can be considered to reach Point 2 from Point 2' on the extension of the normal consolidation line (NCL) by creep with an "equivalent time" value t_{e2}. According Eq.(8), the strain at Point 2 ε_{z2} can be calculated as:

$$\varepsilon_{z2} = \varepsilon_{zp} + \frac{C_c}{V}\log\frac{\sigma'_{z2}}{\sigma'_{zp}} + \frac{C_{\alpha e}}{V}\log\frac{t_0+t_{e2}}{t_o} \tag{6b}$$

From the above, we have:

$$\log\frac{t_0+t_{e2}}{t_o}=(\varepsilon_{z2}-\varepsilon_{zp})\frac{V}{C_{\alpha e}}-\frac{C_c}{C_{\alpha e}}\log\frac{\sigma'_{z2}}{\sigma'_{zp}}$$

$$\therefore\frac{t_0+t_{e2}}{t_o}=10^{\left[(\varepsilon_{z2}-\varepsilon_{zp})\frac{V}{C_{\alpha e}}+\log(\frac{\sigma'_{z2}}{\sigma'_{zp}})^{-\frac{C_c}{C_{\alpha e}}}\right]}=10^{\left[(\varepsilon_{z2}-\varepsilon_{zp})\frac{V}{C_{\alpha e}}\right]}\times(\frac{\sigma'_{z2}}{\sigma'_{zp}})^{-\frac{C_c}{C_{\alpha e}}}$$

From which, we obtain:

$$t_{e2}=t_o\times10^{(\varepsilon_{z2}-\varepsilon_{zp})\frac{V}{C_{\alpha e}}}(\frac{\sigma'_{z2}}{\sigma'_{zp}})^{-\frac{C_c}{C_{\alpha e}}}-t_o \tag{6c}$$

It is seen from Eq.(6c) that the equivalent time t_{e2} at Point 2 is uniquely related to the stress-strain point $(\sigma'_{z2},\varepsilon_{z2})$. The final creep settlement in Eq.(4) is:

$$S_{creep,f}=\frac{C_{\alpha e}}{1+e_0}\log(\frac{t_o+t_e}{t_o+t_{e2}})H \tag{6d}$$

The relationship between t_e and the creep duration time *t* under the stress σ'_{z2} is $t_e=t_{e2}+t-t_o$. Using this relation in Eq.(6d), we have:

$$S_{creep,f}=\frac{C_{\alpha e}}{1+e_0}\log(\frac{t+t_{e2}}{t_o+t_{e2}})H \tag{6e}$$

Taking the same approach, the creep at Point 6 (say unloading from Point 4 to Point 6), we have:

$$S_{creep,f}=\frac{C_{\alpha e}}{1+e_0}\log(\frac{t+t_{e6}}{t_o+t_{e6}})H \tag{6f}$$

The creep at Point 5 (say reloading from Point 6 to Point 5), we have:

$$S_{creep,f}=\frac{C_{\alpha e}}{1+e_0}\log(\frac{t+t_{e5}}{t_o+t_{e5}})H \tag{6g}$$

It is noted that the duration time t and creep settlement above are for this load increment only.

3 EXAMPLE APPLICATIONS OF THE NEW SIMPLIFIED HYPOTHESIS B METHOD FOR ONE LAYER

Yin (2016) gives one example how to use this new simplified Hypothesis B method for calculating the consolidation settlement of a soil layer when the soil in normal or over-consolidated stress-strain state.

Example 1: The thickness *H* of a HKMD is 10m with double drainage in 1D straining. Other parameters are Table 1. Calculate final settlements after 10 years of loading for three loading cases (Point 1 to Point 4, Point 1 to Point 2, and re-loading from Point 6 to Point 5). The loading is assumed suddenly applied.

Table 1: Soil parameters & stress-strain state

$C_e = 0.07$	$C_c = 0.5$	$C_{\alpha e} = 0.018$
$e_o = 1$ $V = 1 + e_o = 2$	$C_v = 0.488$ (m^2/yr)	$t_o = 1(day)$
$\sigma'_{z1} = 30\text{kPa}$ $\varepsilon_{z1} = 0.001$ $= 0.1\%$	$\sigma'_{z2} = 40\text{kPa}$ $\varepsilon_{z2} = 0.0054$ $= 0.54\%$	$\sigma'_{zp} = 60\text{kPa}$ $\varepsilon_{zp} = 0.0115$ $= 1.15\%$
$\sigma'_{z4} = 120\text{kPa}$ $\varepsilon_{z4} = 0.0868$ $= 8.68\%$	$\sigma'_{z5} = 100\text{kPa}$ $\varepsilon_{z5} = 0.0840$ $= 8.40\%$	$\sigma'_{z6} = 50\text{kPa}$ $\varepsilon_{z6} = 0.0735$ $= 7.35\%$

Solution:

(i) Loading from Point 1 to Point 4 which is in a normal consolidation state

$$S_f = \frac{C_e}{1+e_o}\log\frac{\sigma'_{zp}}{\sigma'_{z1}}H + \frac{C_c}{1+e_o}\log\frac{\sigma'_{z4}}{\sigma'_{zp}}H$$

$$= (\frac{0.07}{2}\log\frac{60}{30} + \frac{0.5}{2}\log\frac{120}{60})\times 10 = 0.858\text{m}$$

For t=10 years and using Eq.(6a):

$$S_{creep,f} = \frac{C_{\alpha e}}{1+e_0}\log(\frac{t_o + t_e}{t_o})H =$$

$$= \frac{0.018}{2}\log(\frac{1+365\times 10 - 1}{1})\times 10 = 0.3206\text{m}$$

$$d = 10/2 = 5\text{m}, T_v = tC_v/d^2 = 10\times 0.488/5^2 = 0.1952; U_v \approx \sqrt{4\times T_v/\pi} = \sqrt{4\times 0.1952/3.14} = 0.4987$$

$$\because U_v = 49.87\% < 98\% \quad \therefore S_{"secondary"} = 0$$

$$S_{totalB} = U_v S_f + [(\alpha S_{creep,f} + (1-\alpha)S_{"secondary"})] = 0.4987\times 0.858 + [0.8\times 0.3206 + (1-0.8)\times 0] = 0.6844\text{m}$$

(ii) Loading from Point 1 to Point 2 which is on an over-consolidation state (assume C_v no change)

$$S_f = \frac{C_e}{1+e_o}\log\frac{\sigma'_{z2}}{\sigma'_{z1}}H = \frac{0.07}{2}\log\frac{40}{30}\times 10 = 0.0437\text{m}$$

The equivalent time at Point 2 is calculated using Eq.(6c):

$$t_{e2} = t_o \times 10^{\left[(\varepsilon_{z2}-\varepsilon_{zp})\frac{V}{C_{\alpha e}}\right]}(\frac{\sigma'_{z2}}{\sigma'_{zp}})^{-\frac{C_c}{C_{\alpha e}}} - t_o = 10^{\left[(0.0054-0.0115)\frac{2}{0.018}\right]}(\frac{40}{60})^{-\frac{0.5}{0.018}} - 1 = 16354(day)$$

For t=10 years and using Eq.(6e):

$$S_{creep,f} = \frac{C_{\alpha e}}{1+e_0}\log(\frac{t + t_{e2}}{t_o + t_{e2}})H = \frac{0.018}{2}\log(\frac{365\times 10 + 16354}{1+16354})\times 10 = 0.00787\text{m}$$

$$d = 10/2 = 5\text{m}, T_v = tC_v/d^2 = 10 \times 0.488/5^2 = 0.1952, U_v \approx \sqrt{4 \times T_v/\pi} = \sqrt{4 \times 0.1952/3.14} = 0.4987$$
$$\because U_v = 49.87\% < 98\% \quad \therefore S_{"\text{sec}\,ondary"} = 0$$
$$S_{totalB} = U_v S_f + [(\alpha S_{creep,f} + (1-\alpha) S_{"\text{sec}\,ondary"})] = 0.4987 \times 0.0437 + [0.8 \times 0.00787 + (1-0.8) \times 0] = 0.0281\text{m}$$

(iii) Re-loading from Point 6 to Point 5 which is on an over-consolidation state (assume C_v no change)

$$S_f = \frac{C_e}{1+e_o} \log \frac{\sigma'_{z5}}{\sigma'_{z6}} H = \frac{0.07}{2} \log \frac{100}{50} \times 10 = 0.1054\text{m}$$

The equivalent time at Point 5 is calculated using Eq.(6c):

$$t_{e5} = t_o \times 10^{\left[(\varepsilon_{z5} - \varepsilon_{zp}) \frac{V}{C_{\alpha e}}\right]} \left(\frac{\sigma'_{z5}}{\sigma'_{zp}}\right)^{-\frac{C_c}{C_{\alpha e}}} - t_o = 10^{\left[(0.084-0.0115) \frac{2}{0.018}\right]} \left(\frac{100}{60}\right)^{-\frac{0.5}{0.018}} - 1 = 76.18(day)$$

For t=10 years and using Eq.(6g):

$$S_{creep,f} = \frac{C_{\alpha e}}{1+e_0} \log\left(\frac{\text{t} + t_{\text{e5}}}{\text{t}_\text{o} + t_{\text{e5}}}\right) H = \frac{0.018}{2} \log\left(\frac{365 \times 10 + 76.18}{1 + 76.18}\right) \times 10 = 0.1515\text{m}$$
$$d = 10/2 = 5\text{m}, T_v = tC_v/d^2 = 10 \times 0.488/5^2 = 0.1952, U_v \approx \sqrt{4 \times T_v/\pi} = \sqrt{4 \times 0.1952/3.14} = 0.4987$$
$$\because U_v = 49.87\% < 98\% \quad \therefore S_{"\text{sec}\,ondary"} = 0$$
$$S_{totalB} = U_v S_f + [(\alpha S_{creep,f} + (1-\alpha) S_{"\text{sec}\,ondary"})] = 0.4987 \times 0.1054 + [0.8 \times 0.1515 + (1-0.8) \times 0] = 0.1738\text{m}$$

Example 2: For the first case in Example 1 (loading from Point 1 to Point 4), calculate the curves of settlement and time using Hypothesis A method and the new simplified Hypothesis B method.

Solution:

For Hypothesis A method, Eq.(1) is used. For $U_v = 0.98 = 98\%$,

$T_v \approx -0.933 \log(1 - 0.98) - 0.085 = 1.500$.

The time $t_{EOP,field} = T_v \times d^2 / C_v = 1.500 \times 5^2 / 0.488 = 76.844 years = = 28048.16 days$.

Using this $t_{EOP,field}$ value in Eq.(1), the calculated settlement S_{totalA} is listed in Table 2 and shown in Figure 3.

For the new simplified Hypothesis B method, Eq.(4) and Eq.(6a) are used to calculate the settlement. All calculated values are listed in Table 2 and shown in Figure 3. It is seen from Table 2 and Figure 3 that Hypothesis A method underestimate the settlement a lot.

Eq.(4) can be extended to the case with vertical drains installed in one layer of a soil. In this case, U_v in Eq.(4) is replaced by the average degree of consolidation combing vertical (U_v) and radial consolidation (U_r), that is, $U = 1 - (1 - U_v)(1 - U_r)$. The calculation of creep settlement is the same as before.

Table 2: Settlements calculated using Hypothesis A method and the new simplified Hypothesis B method

t=(day)	T_V=	U_v	U_v*S_f (m)	$S_{creep,f}$ (m)	$S_{"secondary"}$ (m)	S_{totalA} (m)	S_{totalB} (m)
1	5.34795E-05	0.008254	0.007082	0.027093	0	0.007082	0.028756
2	0.000106959	0.011673	0.010015	0.042941	0	0.010015	0.044368
4	0.000213918	0.016508	0.014164	0.062907	0	0.014164	0.06449
8	0.000427836	0.023346	0.02003	0.085882	0	0.02003	0.088736
16	0.000855671	0.033016	0.028327	0.11074	0	0.028327	0.11692
32	0.001711342	0.046691	0.040061	0.136666	0	0.040061	0.149394
64	0.003422685	0.066031	0.056655	0.163162	0	0.056655	0.187184
128	0.00684537	0.093382	0.080122	0.189953	0	0.080122	0.232084
256	0.01369074	0.132062	0.113309	0.216894	0	0.113309	0.286825
512	0.027381479	0.186764	0.160244	0.243911	0	0.160244	0.355372
1024	0.054762959	0.264124	0.226619	0.270965	0	0.226619	0.443391
1825	0.0976	0.352606	0.302536	0.293535	0	0.302536	0.537364
2737.5	0.1464	0.431853	0.37053	0.309376	0	0.37053	0.618031
4106.25	0.2196	0.528909	0.453804	0.32522	0	0.453804	0.71398
6159.375	0.3294	0.640382	0.549448	0.341065	0	0.549448	0.8223
9239.063	0.4941	0.760495	0.652505	0.356911	0	0.652505	0.938034
13858.59	0.74115	0.869826	0.746311	0.372758	0	0.746311	1.044517
20787.89	1.111725	0.94784	0.813247	0.388605	0	0.813247	1.124131
28048.16	1.500000228	0.979993	0.840834	0.400313	0	0.840834	1.161084
42072.24	2.250000342	0.996857	0.855303	0.416161	0.015848213	0.871152	1.191402
63108.36	3.375000513	0.999804	0.857832	0.432008	0.031696427	0.889529	1.209778
94662.54	5.062500769	0.999997	0.857997	0.447856	0.04754464	0.905542	1.225791
141993.8	7.593751154	1	0.858	0.463705	0.063392853	0.921393	1.241642
212990.7	11.39062673	1	0.858	0.479553	0.079241067	0.937241	1.25749
319486.1	17.0859401	1	0.858	0.495401	0.09508928	0.953089	1.273338
479229.1	25.62891014	1	0.858	0.511249	0.110937493	0.968937	1.289187
718843.7	38.44336522	1	0.858	0.527097	0.126785707	0.984786	1.305035
1078265	57.66504783	1	0.858	0.542945	0.14263392	1.000634	1.320883
1617398	86.49757174	1	0.858	0.558794	0.158482133	1.016482	1.336731
2426097	129.7463576	1	0.858	0.574642	0.174330346	1.03233	1.352579
3639146	194.6195364	1	0.858	0.59049	0.19017856	1.048179	1.368428
5458719	291.9293046	1	0.858	0.606338	0.206026773	1.064027	1.384276
8188079	437.8939569	1	0.858	0.622186	0.221874986	1.079875	1.400124
12282118	656.8409354	1	0.858	0.638035	0.2377232	1.095723	1.415972
18423177	985.2614031	1	0.858	0.653883	0.253571413	1.111571	1.431821
27634765	1477.892105	1	0.858	0.669731	0.269419626	1.12742	1.447669

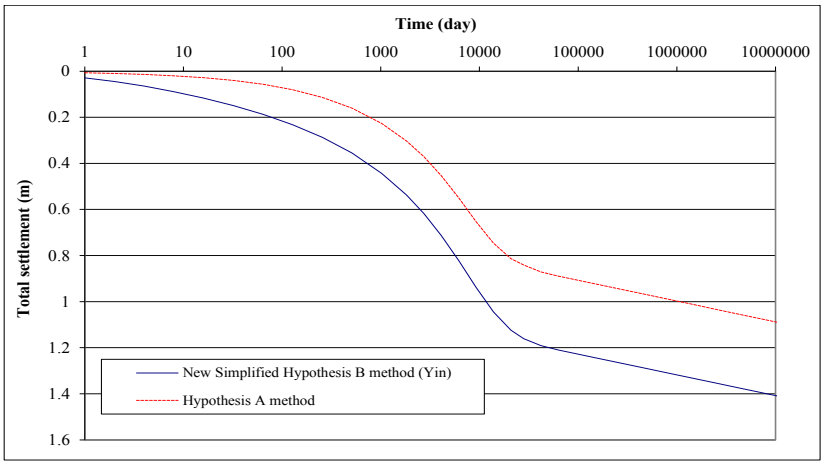

Figure 3: Curves of settlement versus log(time) calculated using Hypothesis A method and the new simplified Hypothesis B method

4 VALIDATION OF THE NEW SIMPLIFIED HYPOTHESIS B METHOD FOR ONE LAYER

Yin and Feng (2016) reported settlements calculated using the old simplified Hypothesis B method ($S_{totalB-old}$) (Yin 2011), Hypothesis A method (S_{totalA}), two Finite Element (FE) simulations by using Consol (Zhu and Yin 1999) and PLAXIS (Vermeer and Neher 1999; Plaxis 2015), and the new simplified Hypothesis B method ($S_{totalB-new}$) for three soil layers (2m, 4m, and 8m) of HKMD. The bottom of the layers is considered

impermeable. Values of parameters used in Hypothesis A method and the new simplified Hypothesis B method are listed in Table 3. Other parameters and values used in Consol (Zhu and Yin 1999) and PLAXIS (2015) can be found in Yin and Feng (2016). The top is applied suddenly by 20 kPa of uniform surcharge.

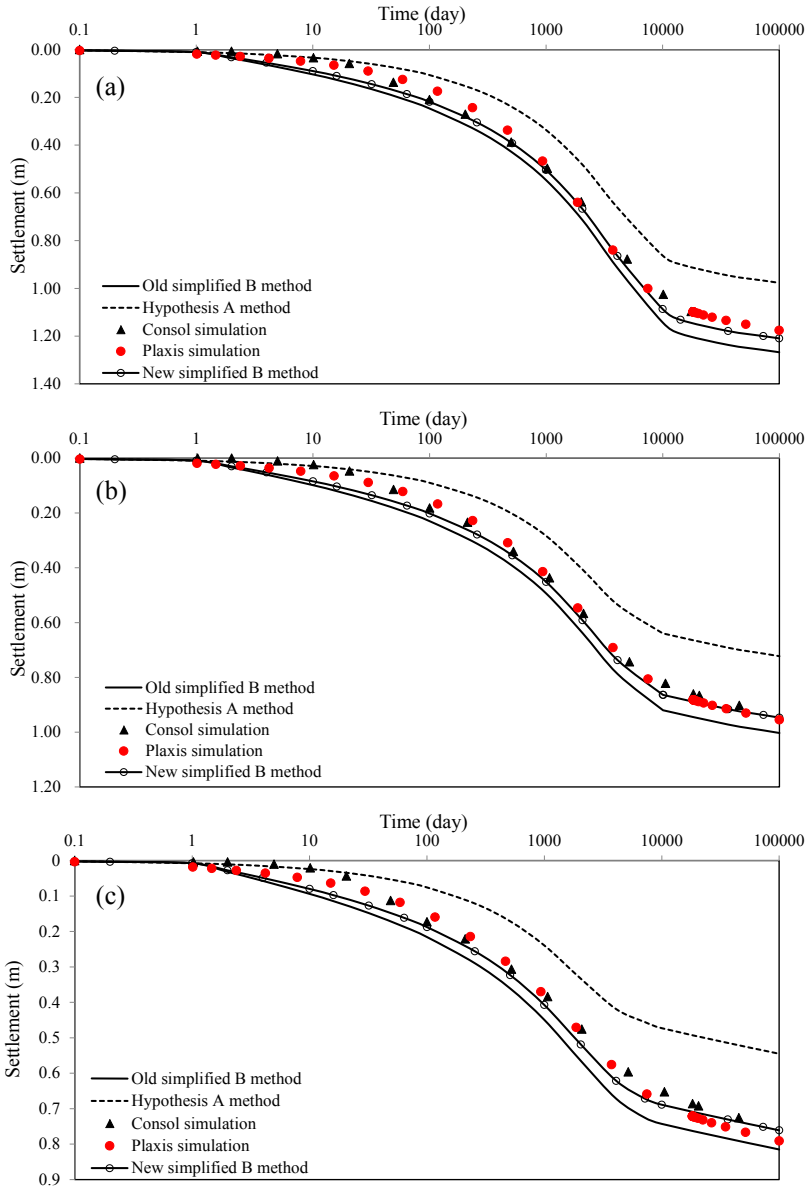

Figure 4: Comparison of settlement-log(time) curves from the old simplified Hypothesis B method, Hypothesis A method, two FE models, and the new simplified Hypothesis B method for 4 m thick layer: (a) OCR=1; (b) OCR=1.5; and (c) OCR=2

Figure 4 shows a comparison of settlement-log(time) curves from the old simplified Hypothesis B method, Hypothesis A method, two FE models, and the new simplified Hypothesis B method ($\alpha = 0.8$) for 4 m thick layer: (a) OCR=1; (b) OCR=1.5; and (c) OCR=2.

Comparing with the FE results in Figure 4, Hypothesis A method ($\alpha = 0$) underestimates the total settlement; while the old simplified Hypothesis B method ($\alpha = 1$) (Yin 2011) over-estimates the total settlement. In overall, the settlement curves calculated using the new simplified Hypothesis B method ($\alpha = 0.8$) is much closer to curves computed using Plaxis (2015) and Consol (Zhu and Yin 1999, 2000) when compared to other two methods. Plaxis simulation results with the soft soil creep model are in good consistence and agreement with results from Consol analysis using the 1D EVP model (Yin and Graham

1989, 1994). The FE models are for fully coupled consolidation analysis of soils with creep and shall be credible as the rigorous Hypothesis B method. From the comparison the validation of this new simplified Hypothesis B method is confirmed for this case. More validations can be found in Yin and Feng (2016).

Table 3: Values of parameters used in Hypothesis A method and the new simplified Hypothesis B method

γ_{clay} (kN/m^3)	w_i (%)		OCR	C_e	C_c	$C_{\alpha e}$	V	t_0 (day)	k_v (m/day)
15	100		1, 1.5, 2	0.0913	1.4624	0.0639	3.65	1	1.90×10^{-4}

5 EXTENSION OF THE NEW SIMPLIFIED HYPOTHESIS B METHOD FOR ONE LAYER TO MULTUPLE LAYERS

Feng and Yin (2016) recently has extended the new simplified Hypothesis B method in Eq.(4) for one layer to multiple layers. The extended new simplified Hypothesis B method is:

$$\begin{aligned} S_{totalB} &= \sum_{i=1}^{n} S_{"primary"i} + \sum_{i=1}^{n} S_{creepi} = U_a \sum_{i=1}^{n} S_{fi} + \sum_{i=1}^{n} [\alpha S_{creep,fi} + (1-\alpha) S_{"secondary"i}] \\ &= U_a \sum_{i=1}^{n} \varepsilon_{fi} H_i + \sum_{i}^{n} \{[\alpha \varepsilon_{creep,fi} + (1-\alpha)\varepsilon_{"secondary"i}] H_i\} \quad for\ t \geq 1day\ (t \geq t_{EOP,field}\ for\ S_{"secondary"i}) \end{aligned} \tag{7}$$

where $\sum_{i=1}^{n} S_{"primary"i}$ is the "primary" consolidation settlement of n soil layers, U_a and $\sum_{i=1}^{n} S_{fi}$ are the average degree of consolidation and the total "primary" consolidation settlement of n soil layers, $\sum_{i=1}^{n} S_{creepi}$ is the total creep settlement of n soil layers, $\sum_{i=1}^{n} S_{creep,fi}$ $\sum_{i=1}^{n} S_{"secondary"i}$ are the total final creep settlement and the total "secondary" consolidation settlement of n soil layers.

In the previous study, Yin and Feng [3] suggested α 0.8 for a single soil layer. In the study of this paper, Feng and Yin (2016) have found that α is related to Over-Consolidation Ratio (OCR) and can be taken as $\alpha = 0.4 + 0.2\text{OCR}$. For OCR = 1, 1.5, and 2, we have $\alpha = 0.6, 0.7, 0.8$. The verification of these α values can be seen in Figure 5 with a comparison with FE simulation results of two layered soils. Eqs. (6a) to (6f) are also used to determine the final creep compression $\varepsilon_{creep,f}$ and then creep settlement $S_{creep,f}$ of a soil in each layer under different stress-strain states. Another important issue is how to correctly determine the average degree of consolidation, m_v for multiple soil layers.

Feng and Yin (2016) has presented four double layer soil profile cases with three OCRs and comparisons of calculated values using the extended method with values from Plaxis (2015). For more details and values of parameters, please see Feng and Yin (2016). This paper presents two profile cases with OCR=1.5. Figures 5(a) and 5(b) show profiles of double soil layers for Plaxis simulation with free drainage in the top and impermeable in the bottom: (a) Case I(4m) and (b) Case II(4m). Figures 5(c) and 5(d) show comparison of curves from FE simulation and from the extended new simplified Hypothesis B method for 4m thick double soil layers with OCR=1.5. For 4m thick double soil layers with OCR =1, 1.5, and 2, it is found that the values of *relative error* are from 0.9% to 10.3% for the new simplified Hypothesis B method using Zhu and Yin method (2005) for U_a and from 0.7% to 35.5% for the new simplified Hypothesis B method using US Navy method (US Department of the Navy 1982) for U_a. However, values of *relative error* are from 10.1% to 50.4% for the Hypothesis A method with US Navy method for U_a. Again, the Hypothesis A method underestimates the consolidation settlement a lot.

6 CONCLUSIONS

From the presentation and discussion above, the following conclusions are presented:

(a) Creep settlements of clayey soils during and after the "primary" consolidation must be considered in geotechnical designs and shall be properly calculated.
(b) The Hypothesis A method underestimates consolidation settlements a lot since the creep settlements during the "primary" consolidation is not included.
(c) The new simplified Hypothesis B method has been validated by comparing with fully coupled consolation modelling with a suitable time-dependent constitutive model for clayey soils.
(d) The new simplified Hypothesis B method and the extended method are all very simple by spread-sheet calculation and are suitable for calculating consolidation settlements of one layer and two layers of clayey soils exhibiting creep with good accuracy.

ACKNOWLEDGEMENT

The work in this paper is supported by a research grant (project No. 51278442) from National Natural Science Foundation of China (NSFC), a general research fund (GRF) (project No. PolyU 152196/14E) from Research Grants Council (RGC) of Hong Kong Special Administrative Region Government of China, grants (4-BCAW, G-YM28, G-YN97, B-Q43L) from The Hong Kong Polytechnic University, China.

REFERENCES

Feng, W.Q. and Yin, J.H. 2016. A new simplified hypothesis b method for calculating consolidation settlements of double soil layers exhibiting creep. *Submitted to International Journal for Numerical and Analytical Method in Geomethanics* (under the first review).

Plaxis 2015. *Software and manuals of PLAXIS (Version 2015)*. Plaxis bv, Computerlaan 14, 2628 XK Delft, The Netherlands

US Department of the Navy 1982. *Soil mechanics design manual 7.1*. NAVFAC DM-7.1. US Department of the Navy, Arlington, Va.

Vermeer, P.A. and Neher, H.P. 1999. A soft soil model that accounts for creep. *In proceedings of Beyond 2000 in Computational Geotechnics 10 Years of Plaxis International, Balkema*, 249-261.

Yin, J.H. 2011. From constitutive modeling to development of laboratory testing and optical fiber sensor monitoring technologies, *Chinese J of Geotechnical Engineering*, 33(1), 1~15. (14th "Huang Wen-Xi Lecture" in China).

Yin, J.H. 2015. Fundamental issues on constitutive modelling of the time-dependent stress-strain behavior of geomaterials. *International Journal of Geomechanics*, 15(5), A4015002, 1~9.

Yin, J.H. 2016. *Advanced Geotechnical Design (Lecture 1: Consolidation of soils in 1-D, 2-D and 3-D)*. Department of Civil and Environmental Engineering, The Hong Kong Polytechnic University.

Yin, J.H. and Feng, W.Q. 2016. A new simplified method and its verification for calculation of consolidation settlement of a clayey soil with creep. *Submitted to Canadian Geotechnical Journal* (under the third review).

Yin, J.-H. and Graham, J. 1989. Visco-elastic-plastic modeling of one-dimensional time-dependent behavior of clays. *Canadian Geotechnical Journal*, 26, 199-209.

Yin, J.-H. and Graham, J. 1994. Equivalent times and one-dimensional elastic visco-plastic modeling of time-dependent stress-strain behavior of clays. *Canadian Geotechnical Journal*, 31, 42-52.

Yin, J-H and Graham J. 1996. Elastic visco-plastic modelling of one-dimensional consolidation. *Géotechnique*, 46(3): 515-527.

Zhu, G.F. and Yin, J.-H. 1999. Finite element analysis of consolidation of layered clay soils using an elastic visco-plastic model. *Int'l J. of Num. and Ana. Methods in Geomechanics*, Vol.23, 355-374.

Zhu, G-F, and Yin, J-H.2005. Solution charts for the consolidation of double soil layers. *Canadian geotechnical journal*, 42(3): 949-956.

Zhu, G.F., Yin, J.H., and Graham, J. 2000. Consolidation modelling of soils under the test embankment at Chek Lap Kok International Airport in Hong Kong using a simplified finite element method", *Canadian Geotechnical Journal*, Vol.38, No.2, 349-363.

Grouted Jetted Precast Reinforced Concrete Piling Technology for No Dredge Seawall and Land Reclamation in Hong Kong

Quentin Z. Q. Yue
Department of Civil Engineering, The University of Hong Kong, Hong Kong

ABSTRACT

Seawall and reclaiming land in Hong Kong have to be robust, cost-effective and environmental-friendly. To achieve this goal, this paper introduces an innovative technology of originality for design and construction of continuous and impermeable seawall and land reclamation environmental-friendly and cost-effectively. It is called the grouted jetted precast reinforced concrete piling (GJPRCP) technology. It is briefly introduced at first. Applications are given for illustration afterward. The idea of GJPRCP based no dredge seawall and reclamation is presented and discussed with illustration of conceptual design and construction steps. It can form continuous and impermeable and robust reinforced concrete structural seawall. The seawall can be used as a continuous impermeable cofferdam and a diaphragm during the construction stage. Brief examination and discussion of both the practice of conventional dredge seawall and reclamation and the adoption of no dredge seawall and reclamation in Hong Kong can show that because of their high structural rigidity, the GJPRCP based no dredge seawall and reclamation can be acceptable, feasible and applicable in Hong Kong.

1 INTRODUCTION

Hong Kong is a small territory of about 1104 km2 land area and 1651 km2 sea area. Because of population growth, it has an ever-increasing demand for land to cope with development. Cutting into hillside and reclaiming the sea have been the two dominant methods in forming new lands for development. However, there is a limited land reclamation practice in Hong Kong over last 15 years. Therefore, the theme of this 36th Annual Seminar of the HKIE Geotechnical Division is "Reclamation: Challenge and Beyond". It is to capture and showcase the achievement that we have made in reclamation projects in recent years. It also provides a platform to share new knowledge and techniques that will enable engineers to meet the demand and tackle the challenges in the near future and beyond.

For land reclamation over the sea, a stable and robust seawall is an essential and necessary structure to protect a reclaimed land from erosion against wave and current actions(CEO 2002a, 2002b, 2004). The seawall can be a deep seated reinforced concrete retaining structure to confine and protect the soil fill of reclaimed land. Furthermore, the seawall and reclamation should be cost-effective and environmental-friendly. Hence, this paper aims to introduce an innovative technology of originality for design and construction of continuous and impermeable seawall and land reclamation environmental-friendly and cost-effectively. This technology is the so-called grouted jetted precast reinforced concrete piling (GJPRCP). Details can be found in the two papers by Xu et al. (2004, 2006). Other related materials and history can be found in the cited references (McVay, et al. 2014; Shestopal, et al. 1959; Tsinker 1988; Hameed et al. 2000). It is expected that this technology can be accepted and adopted by our geotechnical engineering community in Hong Kong.

The paper is outlined as follows. The GJPRCP technology is briefly introduced at first. Some application cases are given afterward. Thirdly, an idea for GJPRCP based no dredge seawall and reclamation is discussed. Its conceptual design and construction steps are described accordingly. Basically, the GJPRCP technology can

form continuous and impermeable and robust reinforced concrete structural seawall. It can be used as a continuous impermeable cofferdam and a diaphragm during the construction stage. The function of a cofferdam is for treating and improving in-situ soft marine mud ground within the reclaimed seabed before filling soils for reclaiming land. The function of a diaphragm wall is to retain the compacted fill soils and protect the sea wave and current actions.

2 GJPRCP TECHNOLOGY

2.1 Set up

The GJPRCP technology is shown in Figure 1. It consists of a floating platform with a crane to lift the pile and two pump systems. The pile sinks vertically into water and soil at the chosen position by its own weight and the pressurized water jetting. One of the two pump systems is for jetting the water and the other is for grouting.

The pipe of various cross-sections has a steel pipe passing its center from head to toe vertically (Figure 2). This central pipe can be either temporary or permanent. It is connected to a horizontal nozzle pipe at the pile toe. The toe pipe has many small nozzles of 3 mm diameter and regular pattern. As a result, the soil beneath the pile toe can be liquefied and vertically cut. The disturbed gap between the sheet pile and the undisturbed soil is relatively small, typically 10 to 20 mm wide. The central pipe can be connected to a plastic hose for transferring its pressurized water from the water pump to the toe nozzle pipe. The pressurized water can be vertically jetted into the soil via the nozzles.

A steel I-beam and a steel tube are casted along one of the two connecting side surfaces, respectively (Figures 2 and 4). The tube has a narrow opening slightly wider than the I-beam web but much narrower than the I-beam flange. The tube inner width is larger than the I-beam flange. The tube inner length is longer than the half of the I-beam height. Each of the two side surfaces has two semi-circular hole channels around the I-beam or the tube (Figure 4). The I-beam, tube and the semi-circular hole channels are ended at some meters above the pile toe, as shown in Figure 2(e).

2.2 Sinking pile by jetting

The quiet process of sinking the precast pile by water jetting is shown in Figure 5. The crane erects the pile vertically and let its seating on the seabed surface. Then the pressurized water flow is pumped into the plastic hose-central pipe-nozzle pipeline and released via the nozzles into the soil. The pumping pressure is about 1.5 to 2.0 MPa. The total water discharge rate is about 50 to 80 liters per second. The soil immediately beneath the pile toe is loosened and liquefied by jetting. The pile sinks into the liquefied soil by its own weight until the design depth. Once the first pile is installed, a similar process is used to install the second pile. The installation of two connected precast reinforced concrete piles is also shown in Figure 5. The I-beam of the second pile is inserted into the tube of the first pile. This process is repeated with all subsequent piles.

2.3 Grouting for connecting and stabilizing piles

As shown in Figure 6(a), the two adjacent piles are initially connected with the I-beam inside the tube. The gap space between the two adjacent piles is filled with liquefied mud, which has to be cleaned before grouting. Each of the two cylindrical holes are firstly sealed completely with a grout-filled cylindrical plastic bag of the hole length. Once the liquid grout in the two plastic bags is hardened, the mud water within the tube can be washed and cleaned. A steel pipe with a toe nozzle is inserted into the rectangular tube until its toe and used for pumping clean water to flush the mud out of the tube and gap within the two grouted bags. As shown in Figure 6(b), liquid grout is then pumped into the tube toe via a steel pipe. The liquid grout gradually fills up the tube and the gap from bottom to top. The grouting is stopped when the liquid grout begins to flow out of the tube head. To enhance pile strength, the toe nozzle pipe, the central pipe and the contact zone between the pile toe and the soil beneath should be grouted. Clean water can be used to wash and clean the pipes. Fresh grout is then pumped into the toe pipe to fill these spaces. The central steel pipe, if it is a temporary pipe, may be retrieved for cost saving before cleaning and grouting. If it is a permanent pile, the pipe can be used as a reinforcement for the pile and seawall. Lastly, the soils of 10 to 20 mm close to the pile walls can be disturbed and loosened. They can be strengthened with grouting (Figure 6(c)).

The above GJPRCP method can be summarized as following steps. Reinforced concrete piles shall be designed and pre-casted. Water jetting is used to drive the pile into the soil platform. The connection zone between two piles and the surrounding disturbed soils should be grouted. The internal pipes should be grouted and pile caps should be casted in-situ.

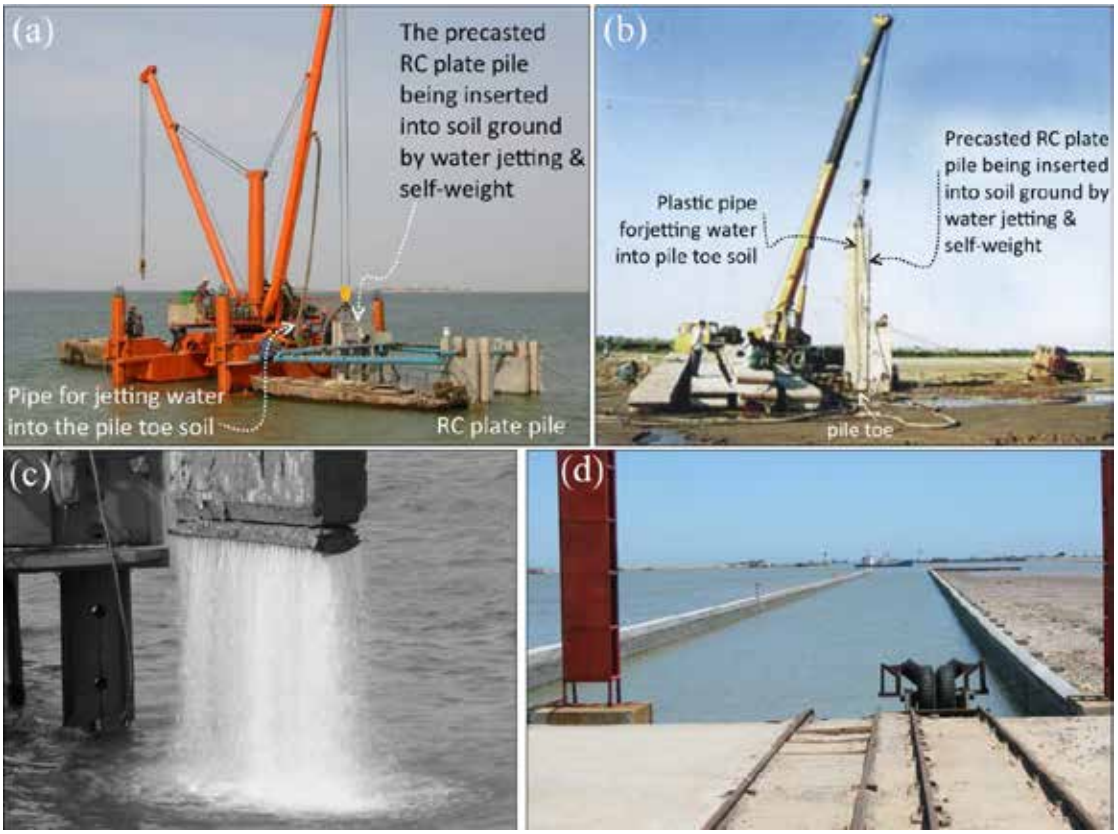

Figure 1: The grouted jetted reinforced concrete piling technology and results

(a) Piling on floating platform; (b) Piling on soft soil ground; (c) Vertical jetting of pressurized water from small nozzles at pile toe; (d) Seawall by GJPRCP

Figure 2: Various and flexible design of precast reinforced concrete piles for jetting and grouting installation

3 APPLICATIONS

The GJPRCP technology has been applied to many projects in Mainland China. They include seawall, breakwater, bridges, piers, port-bank, river embankment, reservoir embankment, division dike, baffle dike, conduit, underground water tanks, and small islands, as shown in Figure 1(d), Figures, 7 8 and 9. Figure 1(d) shows the GJPRCP seawall in Tianjian Port. It is 9.5 m long and 4.5 m buried in soil.

In particular, Figure 7(a) shows a GJPRCP breakwater built in July 1998 at a coastal site in northern China on the shore of the Bohai Sea. Its aim was to determine whether this breakwater could resist heavy seabed erosion. It was located 30 m outside the main embankment. Figure 7(b) shows its design details. A T-shaped pile was also used for supporting. Each pile was 1.2 m wide, 0.3 m thick and 16.0 m long. A pile cap was constructed using cast-in-place method. It is still standing there. The wastewater treatment tanks in Figure 8(c) was constructed in 2000. Each tank was 3.5 m deep, 15 m wide and 56 m long. The tank-wall has been impermeable and functioning well for many years.

Other applications GJPRCP technology can be found in a research project report recently made by McVay et al. (2014) in USA (see also Figure 3(c)).

Figure 3: Flexible design of head and toe of precast reinforced concrete piles for jetting and grouting installation

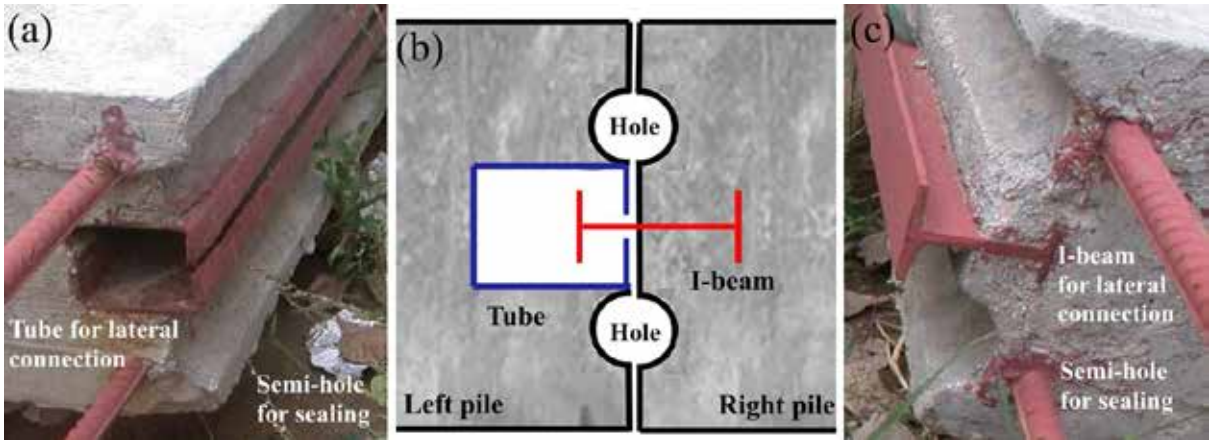

Figure 4: Steel tube or I-beam and two semi-circular hole on one side surface of pile for connection with grout in-situ

(a) Female side wall with steel tube and two semi-holes; (b) Connection arrangement of a male side wall with a female side wall; (c) Male side wall with I-beam and two semi-holes

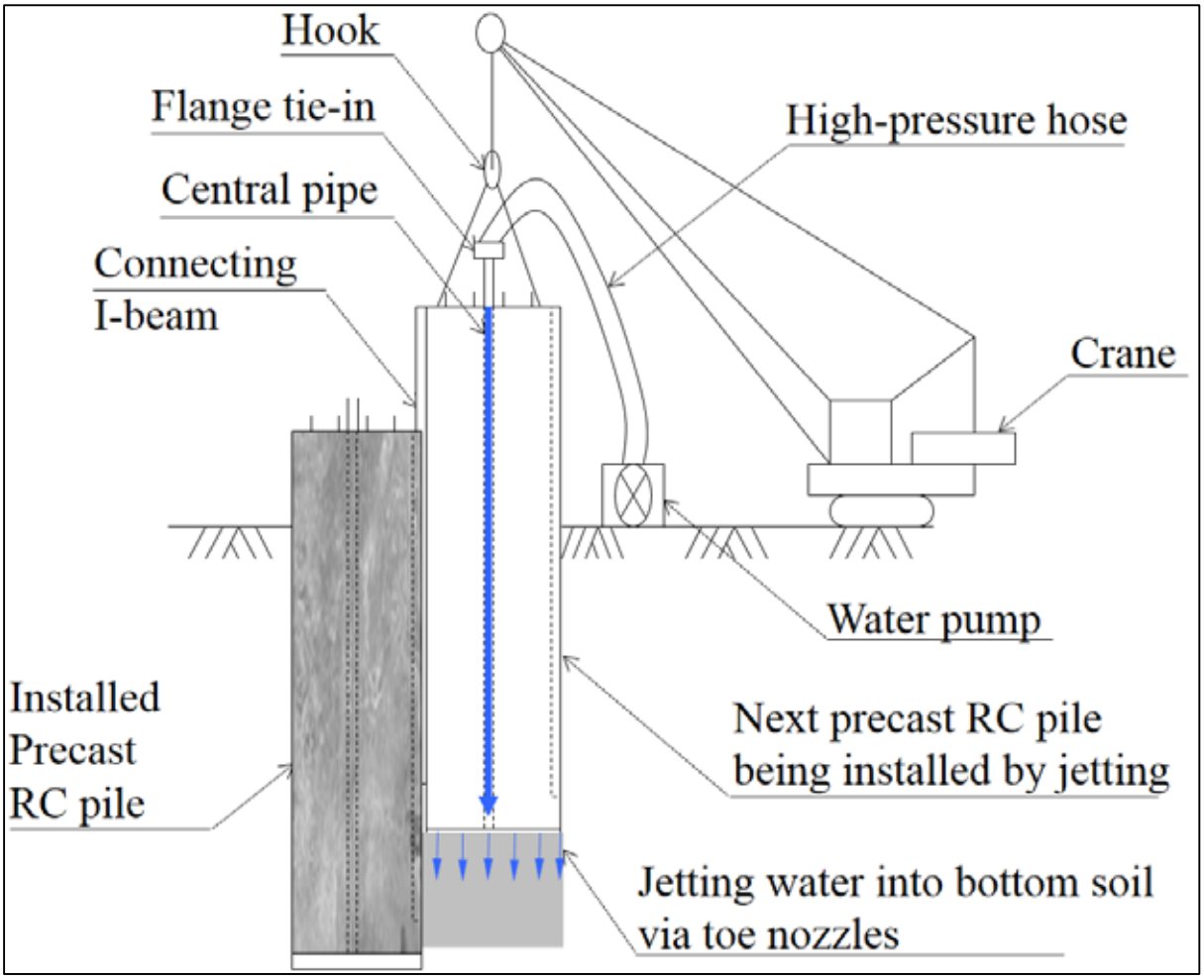

Figure 5: Installation of two connected rectangular precast reinforced concrete piles with jetting of pressurized water from pile head into the toe nozzles via the central pipe

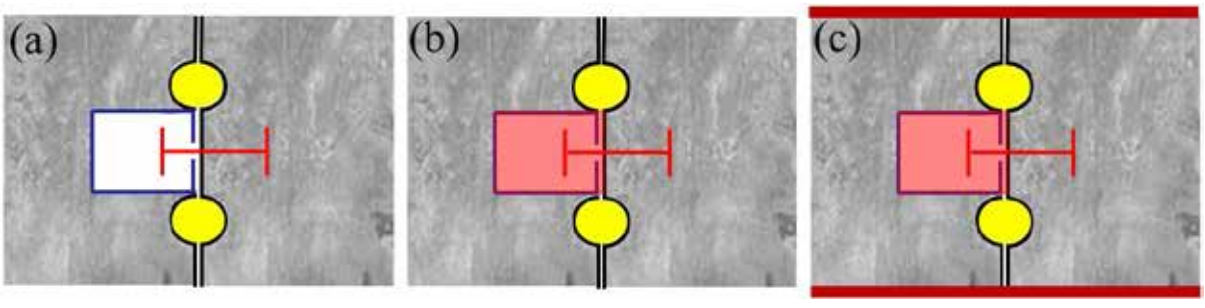

Figure 6: Lateral connection of a male side wall with I-beam and a female side wall with tube by in-situ grouting

(a) In-situ grouting the two circular holes within the male and female side walls with plastic bag; (b) In-situ grouting the gap within the tube; (c) In-situ grouting the longitudinal side wall with adjacent soil

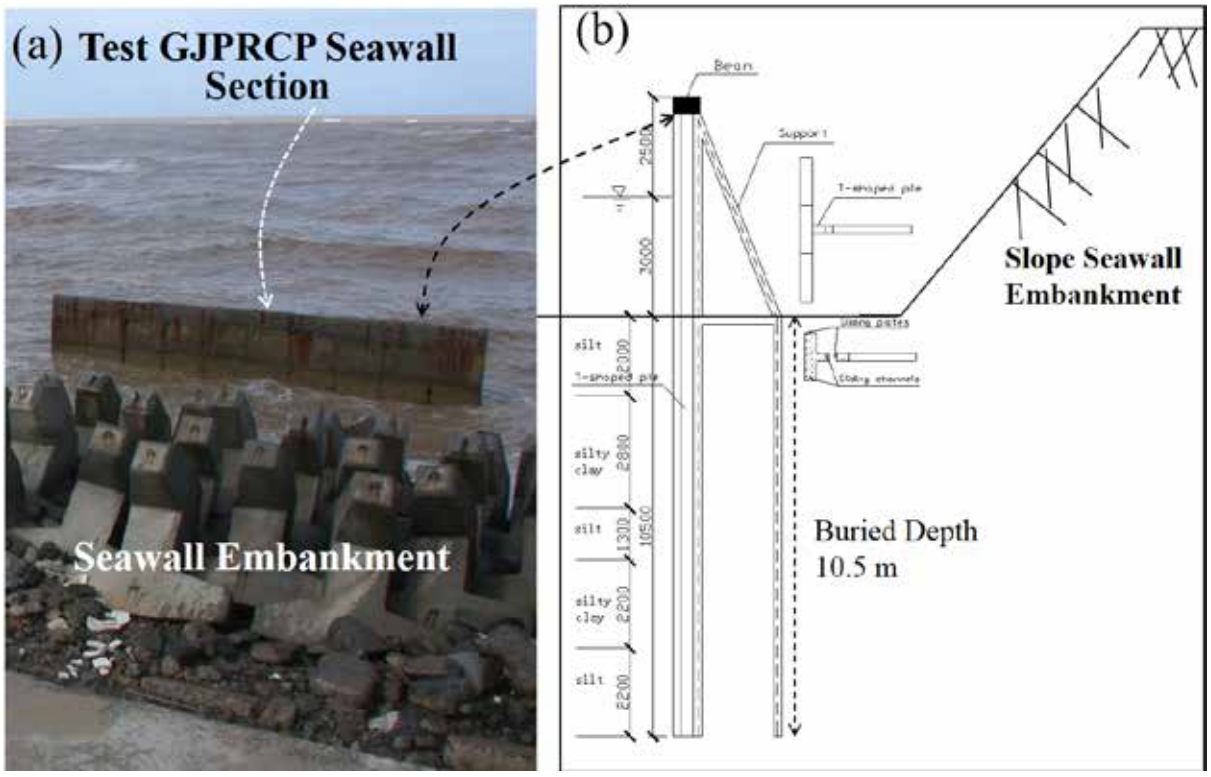

Figure 7: Design details of a test section of a grout jetted precast reinforced concrete pile seawall in front of a main seawall embankment

(a) Photograph showing the seawall condition in 2003; (b) Cross-section details of the seawall

Figure 8: Application cases of GJPRCP technology

(a) Bridge piles; (b) Pier piles; (c) Walls of waste water treatment tanks; (d) Port on river; (e) Control lock for water discharge

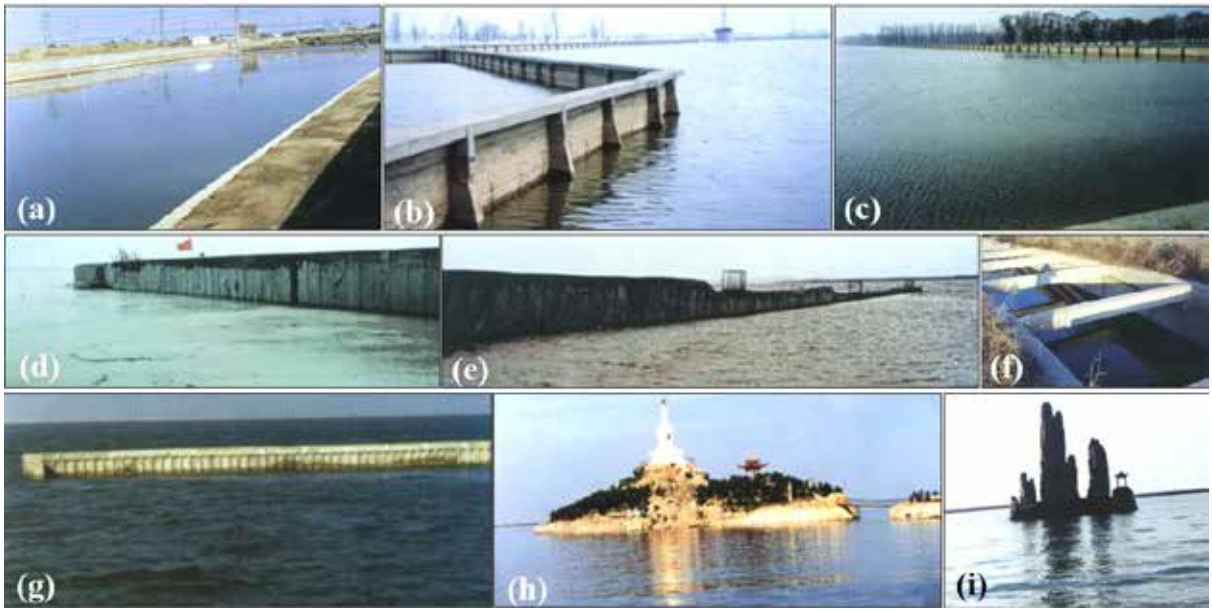

Figure 9: Further application cases of GJPRCP technology

(a) River embankment; (b) Division dike in river; (c) Reservoir-wall; (d) Baffle dike; (e) Baffle dike; (f) water supply conduit; (g) Breakwater; (h) Island-wall; (i) Caisson-mount on lake

4 GJPRCP-BASED NO DREDGE SEAWALL AND RECLAMATION

4.1 General

The seawater depth in Hong Kong is about 5 to 10 m. Its typical seabed soil and rock conditions are a top layer of soft marine deposit of 10 to 30 m thick, overlying alluvium, residual soil, completely decomposed rock and bedrock (Lumb and Holt 1968; GEO 1988). The marine deposit is too soft to support any structures (Li et al. 2005a, 2005b; Yue et al. 1994a, 1994b). The many successful applications of the GJPRCP technology have demonstrated that the design and construction and installation of the precast reinforce concrete piles are flexible, effective, efficient and economic. The piles are structurally and continuously jointed and connected. They can form a continuous, impermeable and rigid seawall and can function as a cofferdam with underground diaphragm wall during construction and a permanent RC structured rigid seawall retaining the fill materials for the reclaimed land. A conceptual idea for the design and construction process of such no dredge seawall and reclamation is shown in Figures 10 to 14 on the basis of the general guide by GEO (1984, 1994). They can be briefed as follows.

4.2 Structural design and stability checking

At first, conventional ground investigation and laboratory testing have to be carried out along the seawall alignment to define the seawater depth, the thickness and physical and mechanical properties of the marine mud deposit, the alluvia, residual soils, CDG or CDV, and/or bedrocks. Next, the precast RC seawall structure and stability have to be calculated and designed according to the three geotechnical cross-section models in Figure 14. The first model is to check the stability and structure of the JGPRCP seawall when it is used as the cofferdam during pumping and expelling seawater out of the sealed space within the seawall. The second model is to check the stability and structure of the JGPRCP seawall when it is used as a cofferdam during treatment of soft marine mud with the cofferdam. The third model is to check the stability and structure of the JGPRCP seawall when it is used as the permanent seawall during soil filling of the cofferdam space up to the designed ground level of +2.5 mPD and after completion of the land reclamation works. Accordingly, the reinforcements and concrete

properties and cross-section dimensions and lengths of the piles can be determined. The size and length of the I-beam and tube can be determined so that an impermeable seawall can be formed. It is noted that the seawall can be formed with either single layer of the connected piles (Figure 12) or double layers of the connected piles (Figure 13). The double layered pile seawall can be used as a temporary paved road for ground vehicle transportation.

4.3 Construction steps

The construction process of the GJPRCP based no dredge seawall and reclamation is shown in Figures 10 to 13. Controlling rectangular pile groups (caissons) can be installed at first for working platforms and for stability at critical and isolated locations along the seawall in the sea. The seawall piles are installed for continuous and impermeable connection between each of the two pile groups. Then the seawater is pumped out of the cofferdam formed by the seawall. Subsequently, the soft marine mud within the cofferdam is improved via conventional vacuum preloading with wick drains (Li et al. 2005a, 2005b). Some backfill sand can be added afterward and gradually for increasing the mud consolidation process. The backfilling can be carried out with compaction for reducing the fill voids and increase its strength and deformation moduli. It will be completed until the designed ground level is reached. During these construction processes, the seawall movements and ground settlements should be monitored and measured. Additional piles can be added to the seawall system if necessary. The actual founding level of each pile toe depth can be determined via pre-probing of a steel pipe with a toe nozzle. This steel pipe can be sunk into the soil ground via jetting of pressured water stream, similar to the pile jetting.

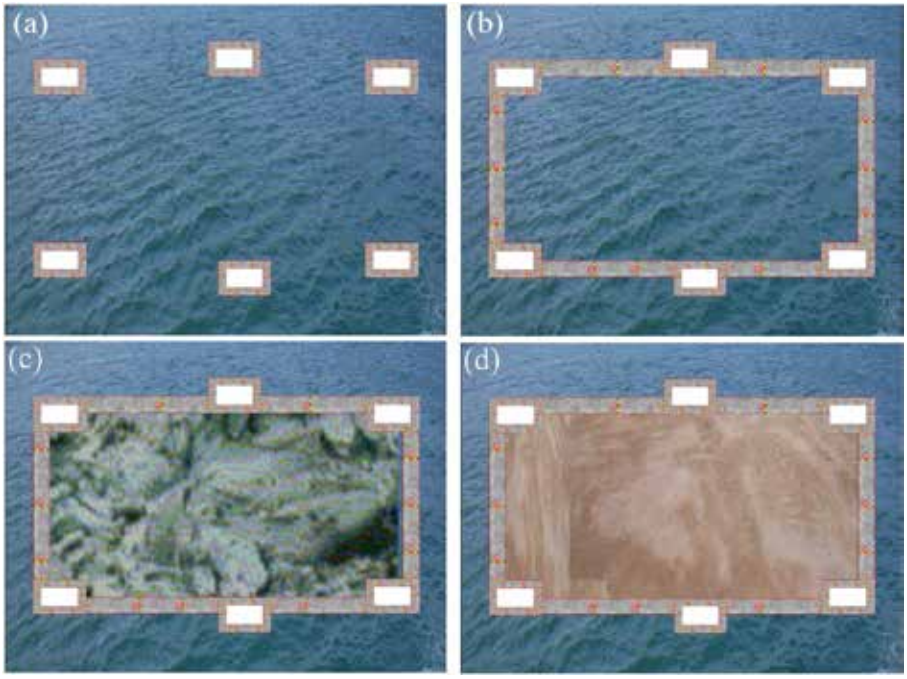

Figure 10: Plan view of a conceptual design and construction process of land reclamation of island on sea with GJPRCP technology

(a) Step A: Installation of six controlling rectangular pile groups; (b) Step B: Installation of wall piles for continuous and impermeable connection between each two pile groups; (c) Pumping water out of the connected pile wall cofferdam and improving the soft marine mud via vacuum preloading with wick drains; (d) Filling the empty space of the cofferdam with general fill or sand fills with compaction

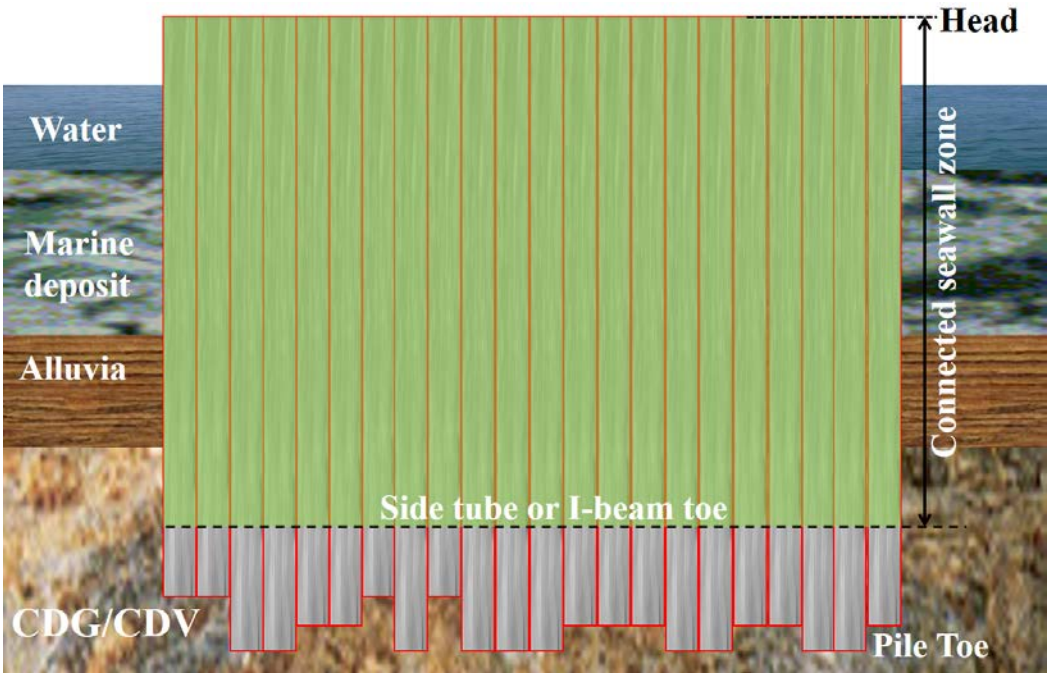

Figure 11: Longitudinal cross-section of the conceptual seawall with GJPRCP technology

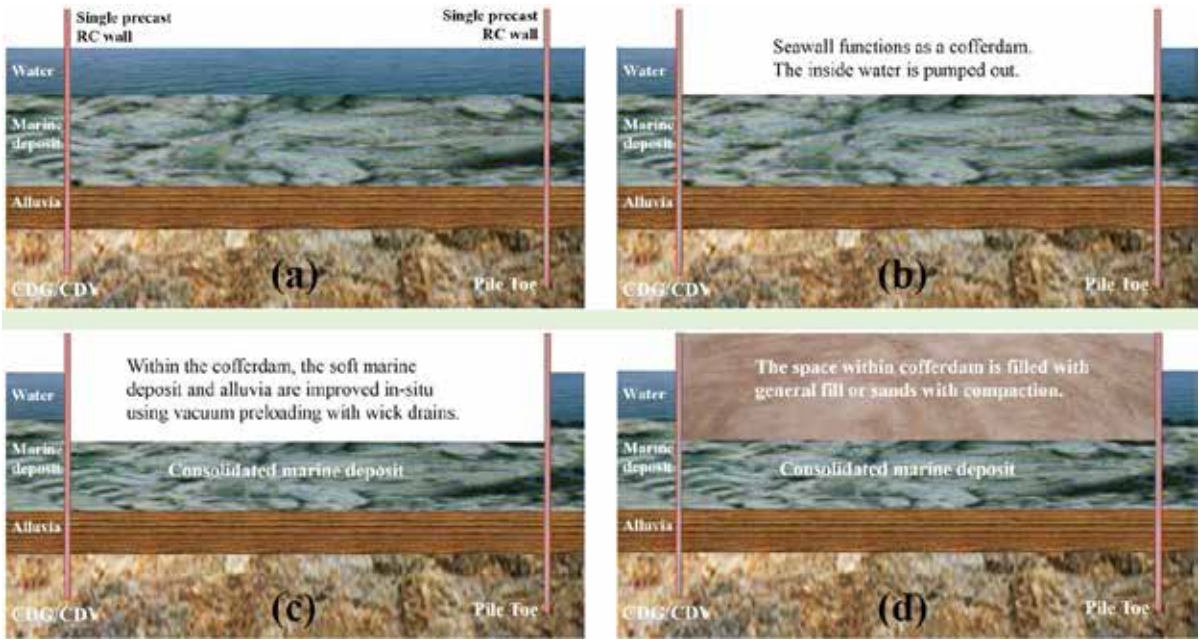

Figure 12: Lateral cross-sections of the conceptual seawall design and construction with single pile wall

(a) Step 1: Installation of controlling rectangular pile groups and single connecting rectangular piles with in-situ grouting for impermeability; (b) Step 2: Pumping seawater out of the cofferdam formed with the vertical seawalls; (c) Step 3: Consolidating the soft marine mud within the cofferdam via vacuum preloading with wick drains; (d) Step 4: Filling the empty space within the cofferdam with general soils or sand fills and in-situ compaction

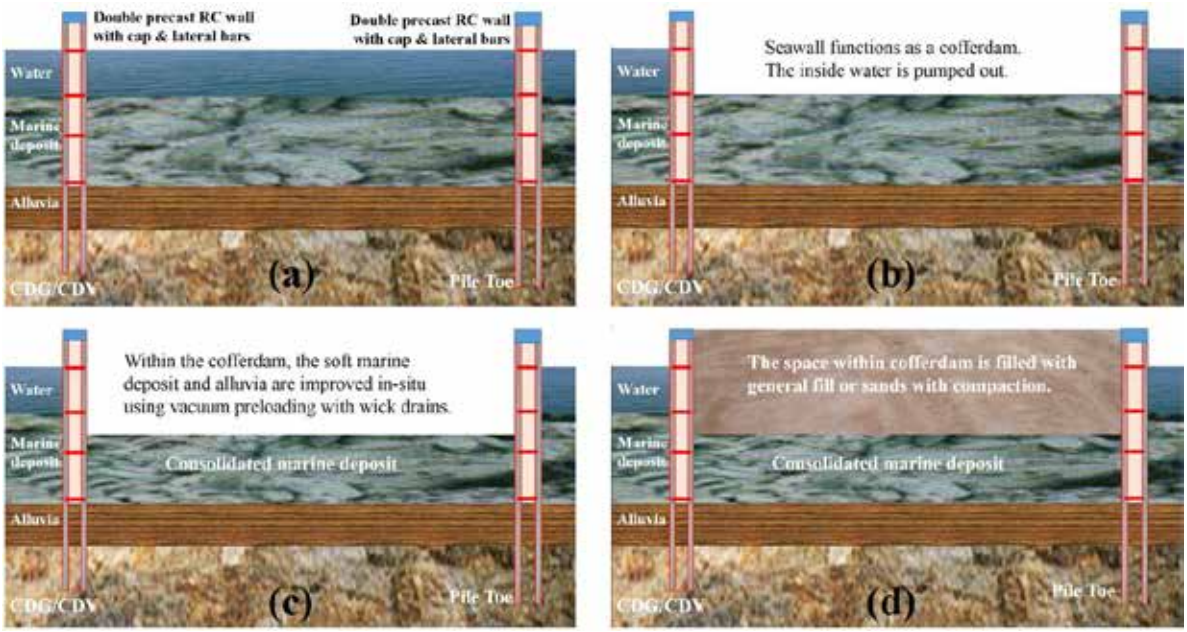

Figure 13: Lateral cross-sections of the conceptual seawall design and construction with connected double pile walls

(a) Step 1: Installation of controlling rectangular pile groups and two rows of connecting rectangular piles with in-situ grouting for impermeability; (b) Step 2: Pumping seawater out of the cofferdam formed with the vertical seawalls; (c) Step 3: Consolidating the soft marine mud within the cofferdam via vacuum preloading with wick drains; (d) Step 4: Filling the empty space within the cofferdam with general soils or sand fills and in-situ compaction

5 APPLICABILITY IN HONG KONG

5.1 Conventional dredge seawall and reclamation and concerns

The conventional reclamation practice is to dredge the thick soft marine deposit, build the seawalls and fill the enclosed space by sand (CEO 2002a, 2002b, 2004; Li et al. 2005a, 2005b). This conventional approach has many shortcomings in terms of adverse environmental effects, shortage of dumping site for dredged mud and large deformation and/or failure of conventional seawalls.

The seawalls can be vertical or sloping and include concrete blockwork seawalls, caisson seawalls, wave absorption vertical seawalls and rubble mound sloping seawalls. They also need to dredge the thick soft marine deposit and fill with sand and fractured rock aggregates. The concerns on environmental impacts have made extreme difficulty to be used again. These impacts are similar to reclaiming and include dredging and dumping of marine mud, impacts on water quality and ecology and marine traffic of large amount of backfilling materials.

5.2 The first and only no dredge seawall and reclamation and concerns

Therefore, no dredge reclamation for both seawall construction and reclaiming land have been accepted and adopted in recent years. The advantages of no dredge reclamation include significant reductions of dredging and dumping and suspended particles, as well as reductions of backfilling material and construction marine traffic by 50%. The first and only example is the HK$7 billion Hong Kong Boundary Facilities (HKBCF) reclamation. It is a key element of the Hong Kong Zhuhai Macau bridge (HZMB) infrastructure.

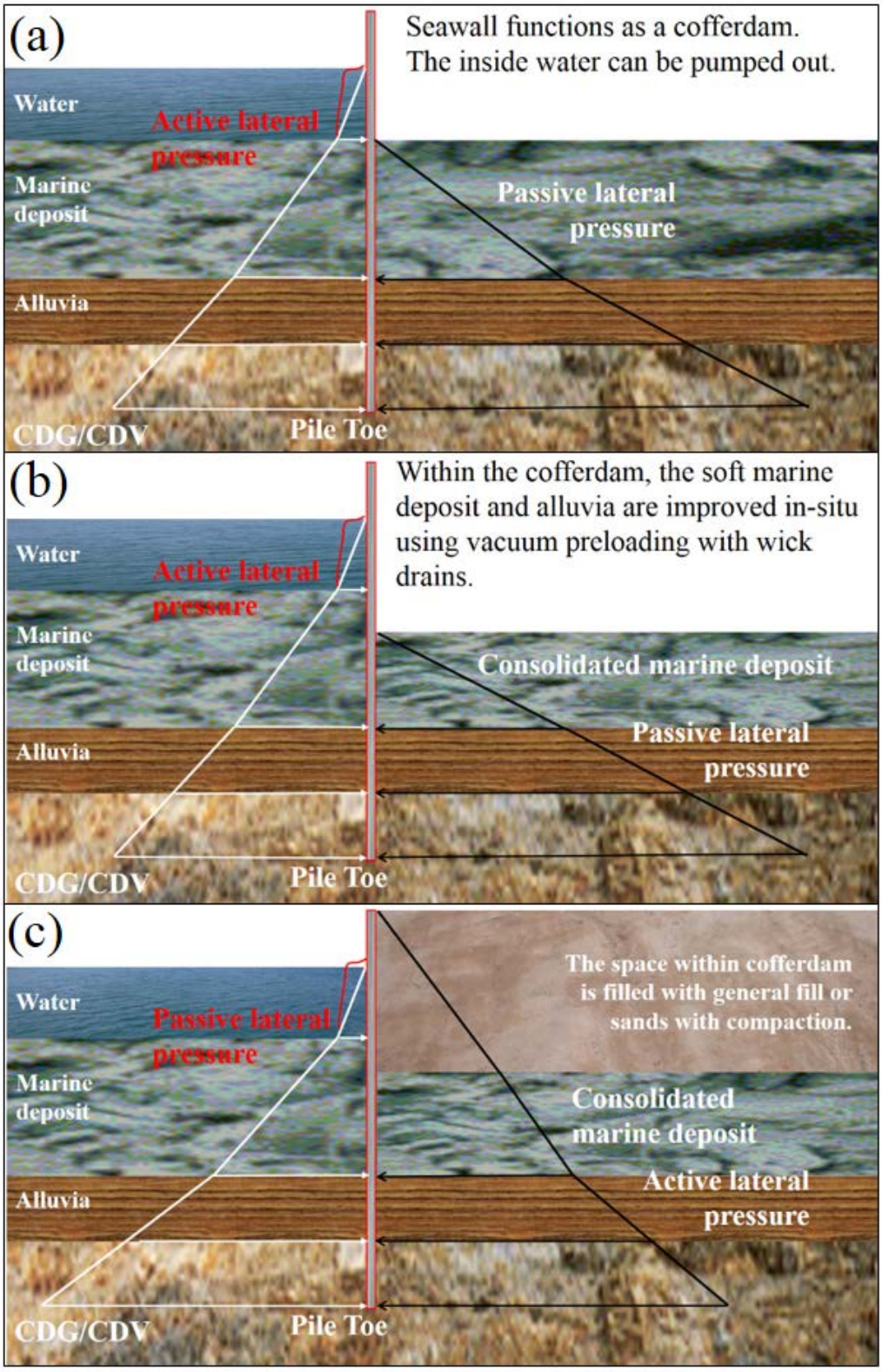

Figure 14: Geotechnical cross-section model for calculation and checking of displacement and stability of the vertical connected pipe walls

(a) Model for the cofferdam during pumping seawater out of the sealed space; (b) Model for cofferdam during treatment of soft marine mud with the cofferdam; (e) Model for the seawall during filling of the soil and after completion of the land reclamation works

The original completion date is the end of 2016, which has to be postponed to the end of 2017 or beyond (News, 2015). It may be due to many factors including the unexpected large deformation and movement of the no dredge seawall. The seawall comprises big steel circular caissons with a diameter of about 30 m. These were dropped into the sea 3 to 4 m apart and joined by a flexible steel wall. Each caisson weighs about 450 tons empty and as the mud is dug out from the middle it drives itself down until it reaches a hard stratum. Because of the huge weights and pressures and thick marine mud involved, the caissons can distort and sometimes tip and move. The sea wall is not expected to fail but it may not keep the correct shape. These unexpected issues have made another concern in local geotechnical community on the applicability of no dredge seawall and reclamation in Hong Kong.

5.3 Applicability

This project has demonstrated that no dredge seawall and reclamation are acceptable and suitable in Hong Kong. But, the large steel circular caisson seawall is too flexible to provide lateral constrains to the large lateral deformation of the soft soils under heavy weight loading of reclamation fills. So, excessive lateral-seaward displacement could occur in such steel caisson seawall. It has to be replaced by another no dredge seawall technology. The above GJPRCP technology can constructed RC seawall with high structural rigidity to retain the soft soils and to constrain their lateral deformation due to the fill weight. So, it can offer the method needed for design and construction of stable and rigid no dredge seawall. Subsequently, the no dredge land reclamation can be realized effectively and economically via the cost-effective and robust treatment of thick soft marine mud associated with the matured vacuum pre-loading with wick drains.

6 CONCLUSION

The GJPRCP technology has the following basic steps. (1) construction of precast reinforced concrete pile according to the site conditions; (2) Jetting of the pile into seabed using pressurized seawater; (3) grouting the I-beam and the tube for fixing the two connected piles and the thin soils on the side wall and the pile toe; (4) In-situ casting of the pile cap. Jetting for driving precast RC piles into soil ground has many advantages. It has no harm to the environment. It is robust and eliminates the quality uncertainty issues. It minimizes noise and vibration. It needs little grout for the thin soil at the pile-soil sides and toe. The tip grouting not only increases the tip resistance but also provides a proof test for adequate tip soil conditions according to design. Because it uses seawater to liquefy ground soils and RC pile own weight to sink itself into deep ground, it can use much less energy and become very cost-effective.

In particular, if boulders in alluvia and residual soils and/or corestones in the CDG or CDV soils are encountered, several methods can be used to overcome the obstacle. They include 1) to relocate the position of the pile nearby; 2) break the boulder or corestone with a hammer on the RC pile or steel bar; 3) supply highly pressurized water to break or shift the solid obstacle; 4) pre-probing such boulder or corestone with steel pipe jetting at the pile position; 5) using the corestones as the pile toe foundation and grout them together if they are very large and abundant.

The GJPRCP technology can offer the method needed for the design and construction of no dredge seawall and reclamation in Hong Kong. The seawall would be robust since it is formed by structurally connected precast RC piles. The settlement of the reclaimed land would be little since the thick marine mud deposit can be treated via matured vacuum pre-loading with wick drains and the fill soils can be compacted with high quality.

ACKNOWLEDGEMENTS

The author acknowledges the financial support the National Science Foundation of China (Project No. 41372336). The author thanks Dr. G.G. Xu and Mr. F.R. He for their site photographs.

REFERENCES

CEO. 2002a. *Port Works Design Manual: Part 3 - Guide to Design of Reclamation*. P.127. Civil Engineering Office (CEO), CEDD, The Government of the Hong Kong Special Administrative Region.

CEO. 2002b. *Port Works Design Manual: Part 4 - Guide to Design of Seawalls and Breakwaters*. p.168. Civil Engineering Office (CEO), CEDD, The Government of the Hong Kong Special Administrative Region.

CEO. 2004. *Port Works Design Manual: Part 2 - Guide to Design of Piers and Dolphins*. p.124. Civil Engineering Office (CEO), CEDD, The Government of the Hong Kong Special Administrative Region

GEO. 1984. *Geotechnical Manual for Slopes. 2nd Edition*. p.305. Geotechnical Engineering Office (GEO), CED, Government of Hong Kong.

GEO. 1988. *Guide to Rock and Soil Description: Geoguide 3*. p.168. Geotechnical Engineering Office (GEO), CED, Government of Hong Kong.

GEO. 1994. *Guide to Retaining Wall Design: Geoguide 1. Second Edition*. p.268. Geotechnical Engineering Office (GEO), CED, Government of Hong Kong.

Hameed, R.A., Gunaratne, M., Putcha, S., Kuo, C. and Johnson, S. 2000. Lateral load behavior of jetted piles, *Geotechnical Testing Journal, ASTM*, 23 (3): 358-368.

Li, S., Yue, Z.Q., Tham, L.G., Lee, C.F. and Yan, S.W. 2005a. Slope failure in under-consolidated soft soils during the development of a port in Tianjin, China. Part 1, field investigation, *Canadian Geotechnical Journal*. 42(1): 147-165.

Li, S., Yue, Z.Q., Tham, L.G., Lee, C.F. and Yan, S.W. 2005b. Slope failure in under-consolidated soft soils during the development of a port in Tianjin, China. Part 2, analytical study, *Canadian Geotechnical Journal*. 42(1): 166-183.

Lumb, P., and Holt, J.K. 1968. The undrained shear strength of a soft marine clay from Hong Kong. *Géotechnique*, 18(1): 25-36.

McVay, M. C., Bloomquist, D., Thiyyakkandi, S. 2014. *Field Testing of Jet-Grouted Piles and Drilled Shafts, Final Report*, FDOT Contract No.: BDK75-977-41, UF Contract No.: 91977, http://ntl.bts.gov/lib/51000/51200/51213/FDOT-BDK75-977-41-rpt.pdf.

News, 2015. HK$7 billion HKBCF artificial island is moving, http://news.cleartheair.org.hk/?p=8389, Sep 21, 2015 by Editor.

Shestopal, A.O. 1959. Jetting of Pipes, Piles, and Sheet Piles, Hydroproject, Institute, Moscow, U.S.S.R. (in Russian). Tsinker, G.P. 1977. Performance of jetted anchor piles with widening, *Journal of Geotechnical Engineering Division, ASCE*, 103(GT3): 213-226.

Tsinker, G.P. 1988. Pile jetting, *Journal of Geotechnical Engineering, ASCE*, 114 (3): 326-334.

Xu G.H., Yue Z.Q., He, F.R. 2004. Grouted jetted precast concrete pile technology for coastal infrastructure development, *Proceedings of the Int. Conf. On Coastal Infrastructure Development – Challenges in the 21st Century, Hong Kong*, Nov. 22 to 24, 2004, pp50. Full paper CD ROM No. 5C-3 (five pages).

Xu G.H., Yue Z.Q., Liu D.F., He F.R. 2006, Grouted jetted precast concrete sheet piles: Method, experiments and applications, *Canadian Geotechnical Journal*, 43(12): 1358-1373.

Yue Z.Q., Selvadurai, A.P.S. 1994a. On the asymmetric indentation of a consolidating poroelastic halfspace, *Applied Mathematical Modelling*, 18: 170-185.

Yue Z.Q., Selvadurai, A.P.S., Law, K.T. 1994b. Excess pore pressure in a poroelastic seabed saturated with a compressible fluid, *Canadian Geotechnical Journal*, 31: 989-1003.

Design and Construction Considerations for Reclamations and the Use of Vibro-Floatation to Accelerate Settlement

A. D. Mackay
ALYSJ joint venture, Doha, Qatar
N. R. Wightman
Aquaterra Consultants Limited

ABSTRACT

This paper provides an overview of the processes effecting reclamations in the Hong Kong Special Administrative Region (HKSAR). A summary of the main offshore topographic features, water flows and geological conditions is provided, highlighting suitable design and construction considerations. A historical summary of lessons learnt is given for past reclamations, commencing from the 1850s to 1995, during which about 3000 Hectares of land was created mainly by end tipping of available fill, progressing to dredged solutions removing the underlying unstable ground to the more recent use of non-dredged ground improvement. An emphasis is given on the use of vibro-floatation to accelerate settlement based on case studies for the 940 Hectare Chek Lap Airport and the 250 Hectare Penny's Bay, Phase 1 and 2, reclamations using vibro-compaction within the sand reclamation, and the more recent 120 Hectare reclamation for the Hong Kong Boundary Crossing Facilities, using vibro-replacement within the underlying ground. Over time construction techniques have progressed to limit instability and mitigate environmental concerns by avoiding dredged reclamation techniques and limit silt dispersal. Considerations are given for the vibro-floatation, which has been successfully used to accelerate settlement both within the reclamation fill and the underlying ground.

1 INTRODUCTION

The HKSAR has a scarcity of land available for development, leading to the use of reclamations throughout its history. During the recent decades reclamations have become larger scale with unique construction and environmental challenges, such as avoiding silt dispersal, placement onto unstable ground and the providing protection against natural elements in the more exposed locations.

A major design and construction consideration is the risk of instability, influenced by offshore topography, typically deepening from north west to south east and increased distance from the Pearl River delta, with ground, typically comprising variable thicknesses of weak, superficial deposits.

The knowledge of reclamation design and construction techniques has progressed with lessons learnt from each project construction. This was originally carried out through end-tipping then, following instability that typically occurred, use of sand blankets and geotextile separators for ground improvement. More recently stone columns, deep cement mixing and / or vertical drain installations with surcharging have been used for ground improvement.

During the recent decade the HKSAR government has enacted a foreshore ordinance requiring stringent environmental impact assessments to be carried out for reclamations, which have resulted in dredging restrictions and a general reduction in reclamations. Although this restricted development during the late 2000s, there has been recent increased pressure to gain land leading to large scale reclamations, which will require construction using non-dredged reclamation techniques.

2 OFFSHORE PROCESSES EFFECTING RECLAMATIONS

2.1 Topography and currents

With the demand for land, reclamations have tended to be located progressively further offshore, with greater exposure to prevailing winds, wave action and off-shore currents. In general more active, erosive conditions are present along the eastern and southern coastlines, influenced by incoming south-easterly winds; more sheltered conditions are present along the Pearl River estuary, to the west, with influences from estuarine waters, micro-tides and a greater volume of suspended fine grained sediment (Weng et al, 1992). See Figure 1 for the locations.

Figure 1: HKSAR coastline locations

The sea bed level generally decreases to the east and south to a maximum depth of 30 metres below sea level to the south east. Local, abrupt decreases in sea-bed level occur along constricted channels

closer to the shorelines, often formed by erosion from increased water flow with associated deposition of coarser grained sands, gravels and cobbles. Finer grained deposition, present in more passive environments, occurs further offshore. The main offshore channels and general HKSAR topography is shown in Figure 2.

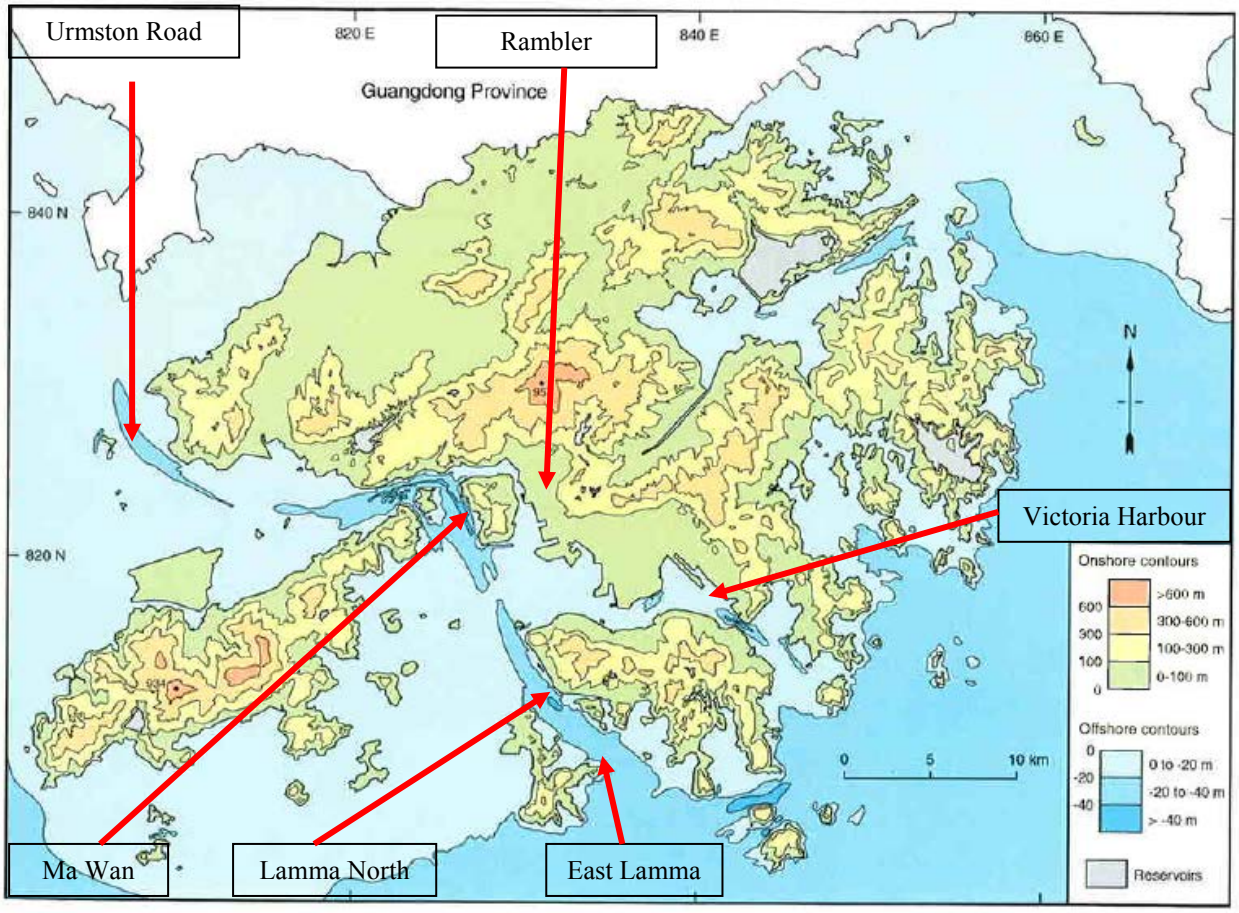

Figure 2: HKSAR sea bed channels and sea bed topography (Fyfe et al, 2000)

The offshore currents are influenced by seasonal, tidal, oceanic and Pearl River delta flows. Due to the continuous water flow along the Pearl River delta tidal influences are minor, up to 2m (Li et al, 1987). Along the southern and western fringes oceanic tidal ranges influence the current flow directions; varying from high spring tide ranges during solstices, June and December, decreasing to low spring tides during equinoxes, April and September (Morton, 1979). The flow directions, influenced by the oceanic currents and wind patterns during winter and summer, are shown in Figures 3 and 4 (Watts, 1973), these are reversed, flowing up the Pearl River estuary, during flood tide conditions.

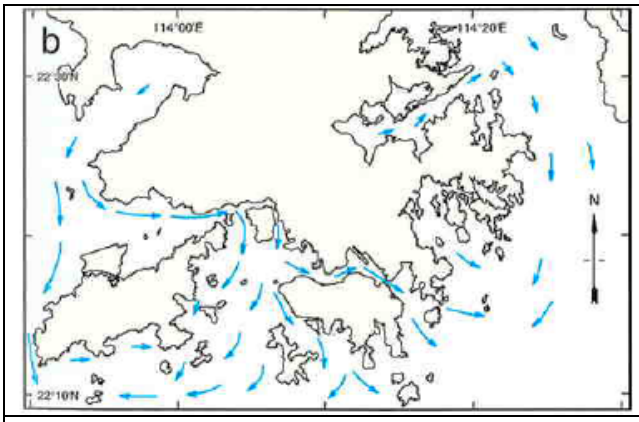

Figure 3: Flow directions, Ebb Winter

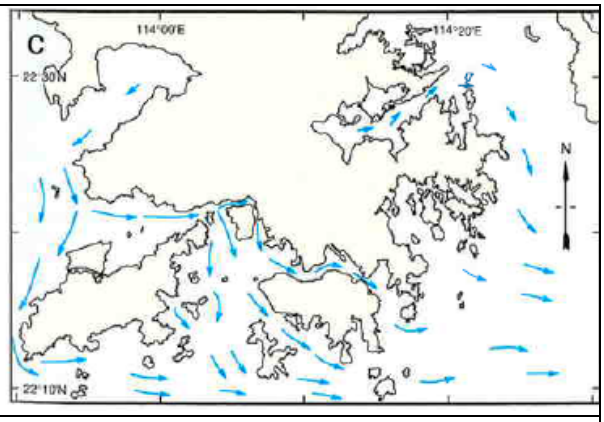

Figure 4: Flow directions, Ebb Summer

The flow velocities are generally weak ranging from 0.1 to 2.2 ms-1, increasing along constricted offshore channels with average flow velocities from 0.5ms-1 for East Lamma, Victoria Harbour and Rambler Channels; 0.6ms-1 for Urmstorm Road Channel and 0.8ms-1 for Ma Wan Channel; channel locations are shown in Figure 2.

2.2 Ground conditions and environmental considerations

Over the HKSAR history, offshore locations have used for contaminated and non-contaminated waste disposal and borrow areas for reclamation fill. These uses have further limited available locations to place reclamations. Offshore borrow areas still exist, however given the minimum volume remaining and scale of future reclamations, extraction may not be economically practical. See Figure 5 for the disposal and borrow areas and Figure 6 for the volume of reclamation fill extraction.

The offshore ground conditions typically comprise relatively weak superficial deposits overlying more competent rock weathered to varying degrees. The superficial deposits comprise marine deposits, deposited in the current marine environment, overlying alluvium, deposited in water borne environments exposed when the sea levels were reduced (Fyfe et al, 2000).

The Marine deposits were placed recently, up to a maximum 10,000 years ago, during the Pleistocene geological period, following the most recent period of glaciation. This reduced the current sea level by about 120 to 130m, allowing terrestrial, alluvial, deposition typically by stream courses flowing over the present sea-bed.

As the sea level rose from its lowest level, 10,000 years ago to present, soft marine silt and clay deposition was placed in horizontal layers. These deposits are represented by the Hang Hau Formation, with the Tsueng Kwan O member located further to the west. Other members of the Hang Hau formation were deposited locally, just over 10,000 years ago, and comprise sand or silt beds (Fyfe et al, 2000). Due to the uneven terrain which the deposition took place the thickness is variable.

The Alluvial deposits comprise the "Chek Lap Kok" formation deposited during the most recent glaciation period over 10,000 years ago. Other more localized formations include the "Tung Chung" formation, having unique deposition within the depressions associated in the karst topography in the vicinity of Tung Chung, and the Sham Wat and Waglan Formations deposited during the previous glacial periods, about 120,000 and 80,000 years ago. Due to the increased age and stress history, resulting from significant changes in sea level, the alluvial deposits have an increased strength. As the deposition took place along stream courses, the deposits are typically linear and, due to the variable and erosive nature of the deposition, comprise lenses and laminae of silts and sands; sub-aerial deposition has often formed a weathered crust, which if left in place prevents penetration into the weaker material beneath. (Fyfe et al, 1995 and GEO, 2007).

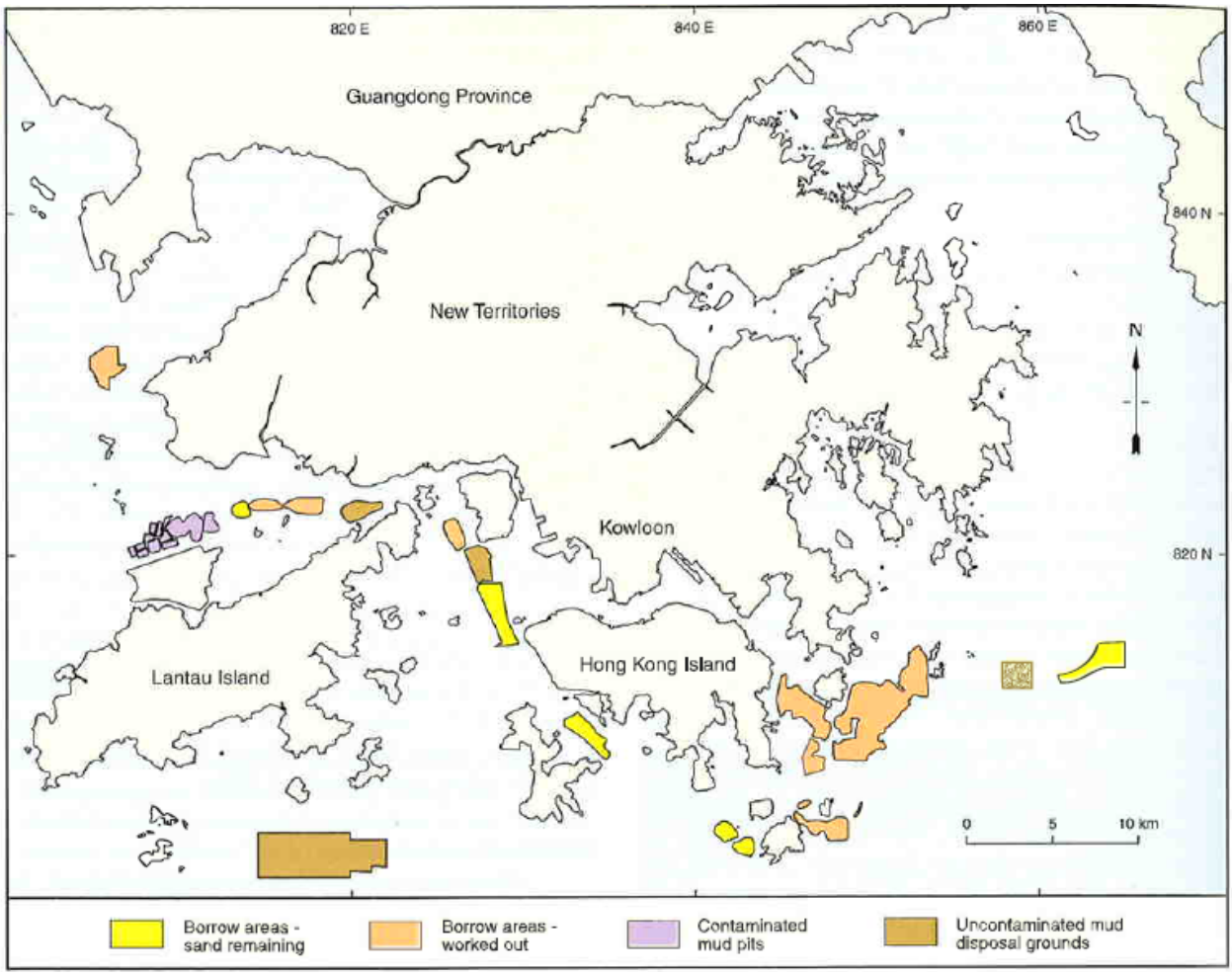

Figure 5: Offshore waste disposal and borrow area locations (Fyfe et al, 2000)

2.3 Geotechnical parameters

The geotechnical parameters of the superficial deposits vary depending upon formation and location. Given the relatively stable environment of the marine deposit formation the parameters are relatively weak and consistent. Due to the variable topography and more granular constituents towards the lower deposition levels the physical properties increase in variability accordingly.

The alluvium was placed in a variable deposition environment with a variable stress history, increasing the strength. Due to the variable constituents, ranging from coarse sand to fine silt with local, preferential drainage paths there is a large variation in geotechnical parameters, particularly compressibility, permeability and settlement characteristics, derived from the coefficient of compressibility and consolidation rate (GEO, 2007 and Mackay, 2016).

2.4 Design and construction considerations for arbitrary locations

A wealth of information is available to assess the offshore ground conditions and topography effected reclamations in the HKSAR. Based on the information available a summary of the thickness, topography, and design and construction considerations for different offshore locations based on available ground investigation data is summarized in Table 2.

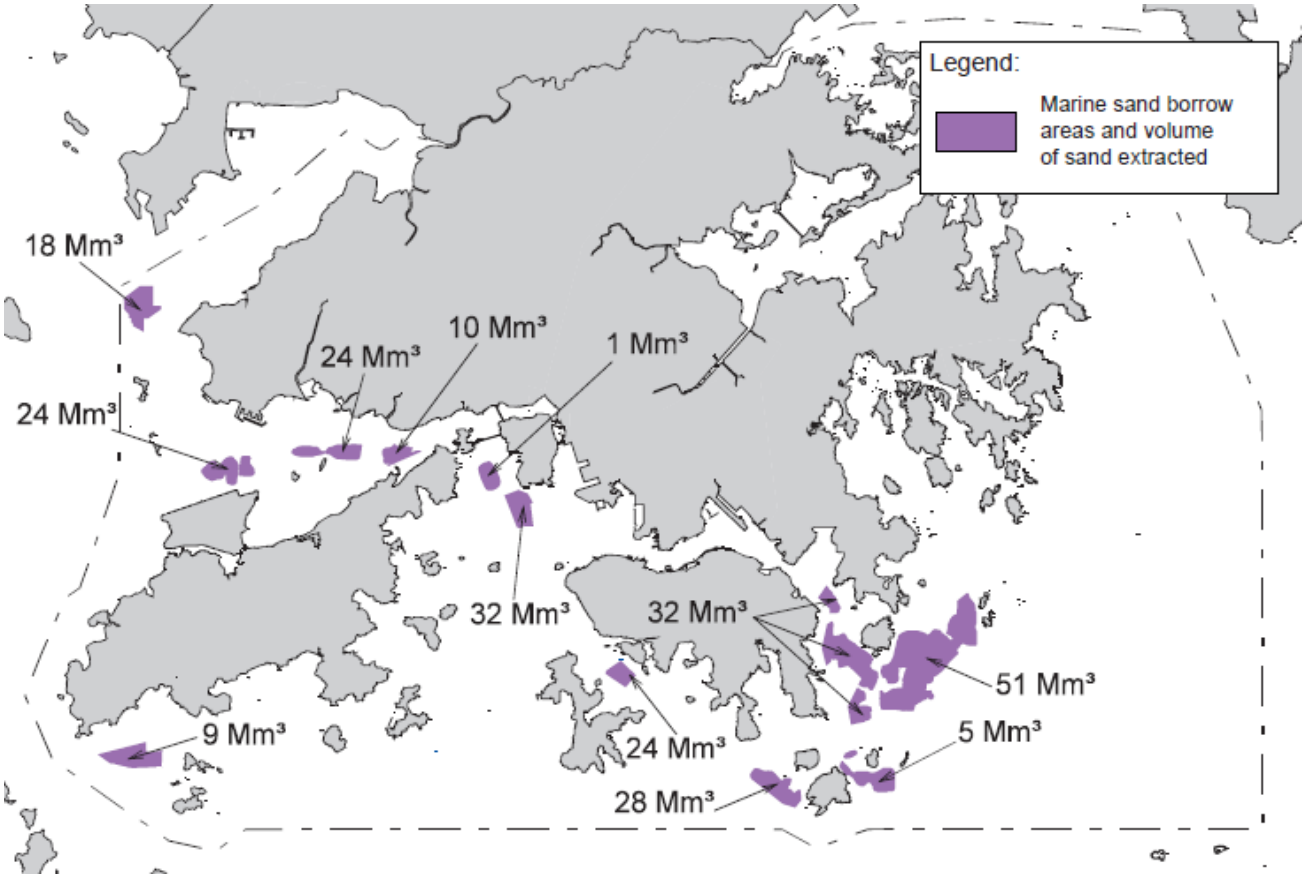

Figure 6: Offshore borrow area volumes used, up to 2005 (CEDD, 2005)

Table 2: Ground conditions, for arbitrary locations (Mackay, 2009 and 2010)

Location	Sea bed depth	Ground Conditions	Design and Construction Considerations.
Deep Bay	1 – 8	12 - 20m Marine Deposits (MD) and 20m Alluvium (All)	
Sha Chau	5 – 10	0 - 5m fill, 6 – 15m MD, 20m All	This area is located over the East Sha Chau Contaminated Mud Disposal Ground complicating the potential construction.
Lantau North West	5 - 10	8m MD, 10m All	
Soko Islands	5 - 20	23 - 26m MD over 6m All	The site has been previously used for borrow material
South Cheung Chau	8 - 16	0 - 10m fill, 14m MD, 20m All	The area is a gazzeted disposal site with highly variable fill thicknesses.
Lamma South.	15 - 20	2m fill, 10m MD, 20m All	Potential for localized fill to have been deposited en-route to the South Cheung Chau disposal site.
East Tung Lung Chau,	25 - 30	12m MD, 20m All	The MD comprises a relatively minor thickness of mud (1.5m). Locally variable seabed level.
Eastern Waters,	25	16 – 19m MD, 22m All	Locally the topography rises to 5.5m at the Victor Rock underwater pinnacle. Approximately 9m thickness of the MD comprises sand.
SE Offshore	20 - 25	17 to 22m MD, 20 - 25m All	MD comprises approximately 10m thickness of sand.
Lamma North	15 – 20	15 to 25m MD, 9m ED, 30m All	The All is granular consolidation is expected to be rapid. Due to the sheltered location stone columns can be installed.

For the locations at Deep Bay Sha Chau Lantau North West the alluvium is generally granular, allowing rapid consolidation and, due to the sheltered location, stone column ground improvement techniques can be adopted. Soko Islands, South Cheung Chau, Lamma South, East Tung Lung Chau, Eastern Waters, SE Offshore and Lamma North are exposed to typhoons and monsoonal swells, dredging is needed to form the seawalls, following formation of the southern and eastern boundaries

3 RECLAMATION HISTORY

Following land auctions in 1841, reclamations were placed along coastal strips of Hong Kong Island and Tsim Sha Tsui. A significant reclamation was the initial 1924 Kai Tak Airport which was the first reclamation to use granular fill (Guildford, 1988 & 1997). Reclamation areas progressively increased during the 20th century from 1050 Hectares (Ha) by 1967, to 3050 Ha by 1991 and 6000 Ha by 1995 following completion of the Chek Lap Kok Airport. During 1995, reclamations comprised 2% of HKSAR territory, accommodating 20% of its population. A summary of the more significant reclamation phases and construction techniques adopted are summarized in Table 3.

Table 3: Significant reclamation summary

Reclamation	Date	Reclamation size, ground conditions and construction approaches
Kai Tak Airport	1952.	Soft marine deposits up to 10m thick were encountered and completely removed beneath the runway and seawall (Lumb, 1976 and Grace et al, 1957).
Sha Tin New Town (Figure 7)	1960 - 1970	Formed by end-tipping fill onto soft mud; causing softening beneath the leading edge causing mud wave formation, long term void formation, differential settlement and instability (Lumb, 1976).
Ma On Shan (Figure 8)	1980 – 1990	Fill placed in layers over a geotextile separator placed on the seabed with placement at 1 in 15 at the leading edge of reclamation front. As there were no strengthening of the underlying mud and control difficulties were encountered for fill supply and stockpiling, failures of the underlying soft mud often occurred (Ng et al, 2007).
Tuen Mun New Town	1980s.	A 240 Ha reclamation underlain by marine deposits up to 15m thick. The dredging and fill replacement was limited to areas requiring foundations, including the seawalls. 1.5m thick marine sand blankets were spread over the mud prior to fill placement (Hadley, 1992).
Tsueng Kwan O (Figure 9)	Mid 1980s,	Underlain by marine muds from 5 to 15m thick. Vertical drains were installed into the marine mud and overlying drainage blankets. Marine muds were dredged beneath the seawalls and a geotextile separator placed prior to filling (Ng et al, 2007).
Siu Ho Wan Depot	1991 – 1992	250 Ha reclamation; 2 to 15m thick marine deposits underlain by 3 to 6m thick alluvial layers. Dredging carried out beneath the seawalls and placement of a 2m thick sand blanket beneath the reclamation. Due to instability wick drains and stone-columns installed for ground improvement (de Silva et al, 1998).
Pak Shek Kok (Figure 10)	1990s.	A 117 Ha reclamation underlain by 6 to 12m of marine mud. Vertical drains were installed and drainage blankets with geotextile separators placed prior to filling. Mud waves were created during the fill placement, possibly due to overfilling; subsequent works adopted heavier duty geotextile separators with thicker sand blankets placed in two phases to overcome the instability (Ng et al, 2007).

Figure 7: Reclamation works in Shatin

Figure 8: Reclamation works in Ma On Shan

Figure 9: Reclamation works in Tseung Kwan O

Figure 10: Reclamation works in Pak Shek Kok

4 CASE STUDIES

4.1 Design and construction, Chek Lap Kok Airport reclamation

The Chek Lap Kok (CLK) Airport reclamation was completed 1998 and provided an additional 938 Ha space for the 1248 Hectare Airport. The reclamation required 197Mm3 of fill, with 114Mm3 obtained from levelling the existing Chek Lap Kok and Lam Chau Islands, within the airport footprint, and the Brother Islands located to the east. 76 million m3 of the fill comprised marine sand fill taken from the offshore borrow areas. As there was limited time available to allow settlement and remove all the soft deposits, approximately 70 million m3 of soft ground was dredged from the site, with dredging depth increased beneath the seawalls to improve the foundation stability (Plant et al, 1998).

Six different fill types were used to form the reclamation dependent upon the end use of the area within the reclamation. Geotextiles were between the boundaries of each fill placement to ensure the separation of the materials. Ground improvement techniques were used to accelerate settlement and improve the ground in areas with more sensitive infrastructure usage and in locations with abrupt changes in underlying ground conditions, such as shorelines with abrupt rises in rock exposures towards the original CLK and Lam Chau Island. As fill was readily available to use as surcharge material was frequently used. Dynamic compaction was effective to about 10m below formation level with one location towards the easternmost limits of the reclamation using this technique (Ground Engineering, 1996). The vibro-compaction was effective for compacting sand fill used extensively over the reclamation as a result the technique was adopted at three main locations. Refer to Figure 11 for the ground improvement locations (Pickles et al, 1998).

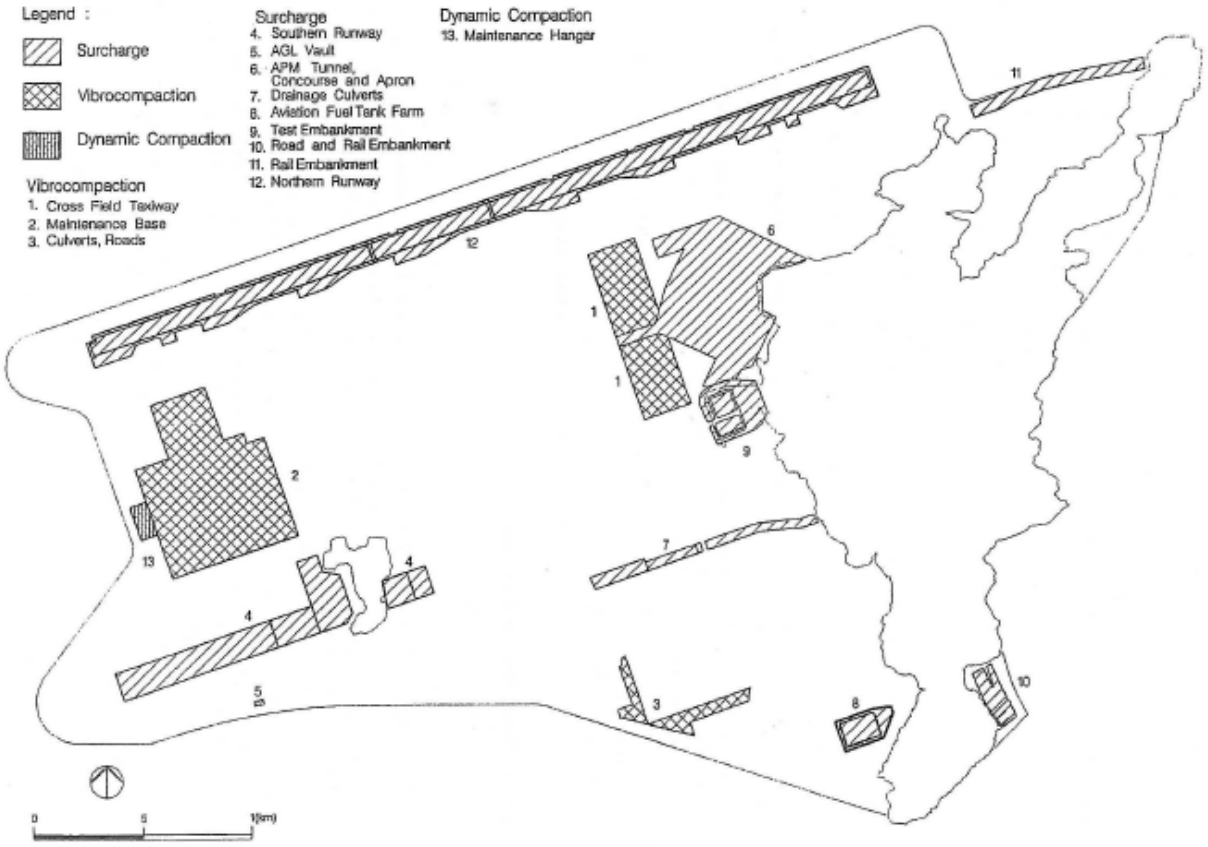

Figure 11: Chek Lap Kok reclamation ground improvement locations

Vibro-compaction was used to improve ground beneath utility and tunnel infrastructures requiring piled support. Placement was by trailer suction hoppers for deep levels with marine vessel access, pipelines for shallow locations were marine vessels could not enter and water cannons for reclamations rising above sea-level (Plant et al, 1998).

All marine sand fill had a low relative density below sea bed level resulting in potentially undesirable settlement following construction. The required increase in relative density was from 65 to 80%, derived from Baldi et al, 1982; Schmertman, 1976 and Robertson et al, 1983 and from past use of this technique for the North Lantau Expressway, West Kowloon Reclamation and West Kowloon Expressway reclamations (Sims, 1994). Trial compactions were carried out to ascertain suitable vibro-compaction methods using light or heavy plant type with spacing between 3.5 to 4.8m. The success in settlement reduction was measured by the increase in relative density, which ranged from 5.8 to 6.8% of the fill thickness for the locations requiring improvement.

4.2 Penny's Bay Phases 1 and 2 reclamations.

The Penny's Bay Phase 1 Reclamation was completed 2005 and is located within the relatively sheltered waters along the southern shoreline of south-east Lantau Island. This reclamation was extended during the Phase 2 reclamation works, completed 2009, providing an additional 60 Hectares of land for the theme park resort. See Figures 12 and 13 for the location, reclamation stages and the works.

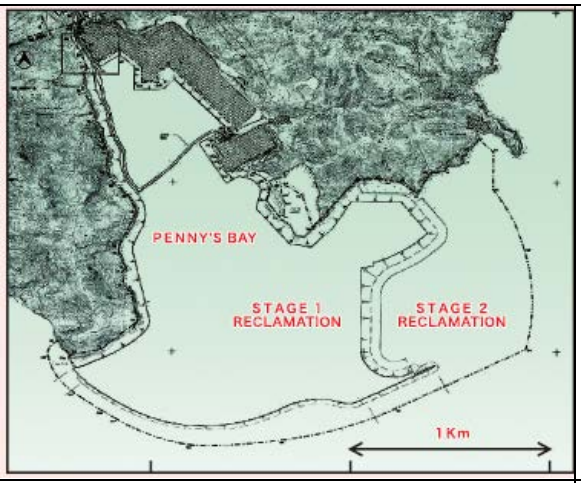

Figure 12: Penny's Bay location

Figure 13: Seawall construction

The superficial deposits underlying the site included up to 30m thickness of Marine Deposits of the Hang Hau formation, over a maximum 20m thickness of Alluvium, Chek Lap Kok formation (Hendy et al, 2002). As the theme park required construction within a rapid time frame the settlement following reclamation placement was minimized; using ground improvement techniques comprising surcharging and vertical drain installation in less sensitive areas, with left in place soft material, and vibro–compaction for the remaining areas used to densify the upper fill levels (Hendy et al, 2003). Although vibro-compaction had been used in many locations throughout HKSAR and Macau (Berner, 1998 and Carter, 1996) the technique had not been used to this scale or its success for reducing long term settlement not been verified.

The optimization of the vibro-compaction method was determined by site trials and ascertained a 2.3 spacing in a triangular pattern to be appropriate. Control of the sand fill, ensuring sand with a limited particle size distribution envelope, was required; with the nearest source satisfying the criteria at East Lamma Channel. The sand fill placement method also needed close control to ensure efficient vibro-compaction. Appropriate methods included hydraulic feed near the placement level avoiding segregation of the fines and ensuring placement in layers. The vibro-compaction technique used on site is presented in Figures 14 and 15.

The design required that the uppermost 15m be compacted with the aim of reducing total and differential settlement over localized soft ground. This was verified by comparing the tip resistance of Cone Penetration Testing (CPT) records before and after vibro-compaction (Sims, 1984). Typically the CPT tip resistance satisfied the specified criteria in dry conditions for fill placed above sea-level. The resistance reduced for fill located below sea level. Typical results of CPT tip resistance prior to vibro-compaction and following compaction, satisfying the specification criteria, are shown in Figure 16 (Hendy et al, 2005).

The process of densification also reduces the void ratio within the material. This was verified by settlement records at both shallow and deeper levels within the fill taken over a 3 month period; these showed that settlement up to 0.4m, or 1.5% of the layer thickness, occurred immediately during vibro-compaction. The results are shown in Figure 17.

Figure 14: Vibro-compaction

Figure 15: Vibro-compaction

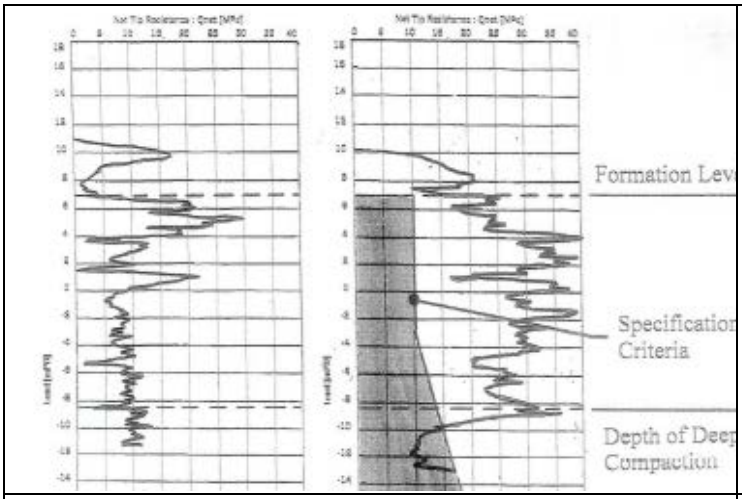

Figure 16: CPT resistance before and after vibro-compaction

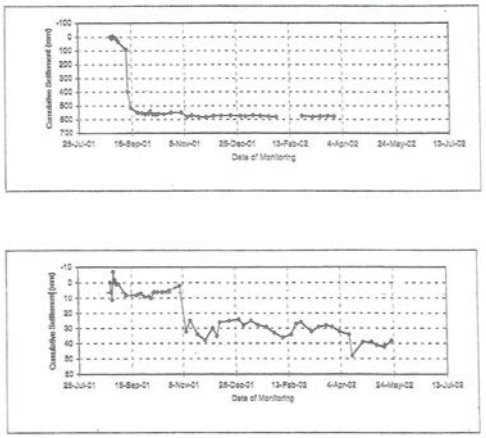

Figure 17: Settlement (3 month period)

4.3 Hong Kong Boundary Crossing Facility reclamation

The Hong Kong Boundary Crossing Facility (HKBCF) reclamation is located east of the CLK Airport. It will provide about 130 Ha to accommodate the facilities and connect with the Hong Link Road to the south east, Tuen Mun to the north and the CLK Airport to the west, see Figure 18 (HyD, 2011). The reclamation is presently approaching completion.

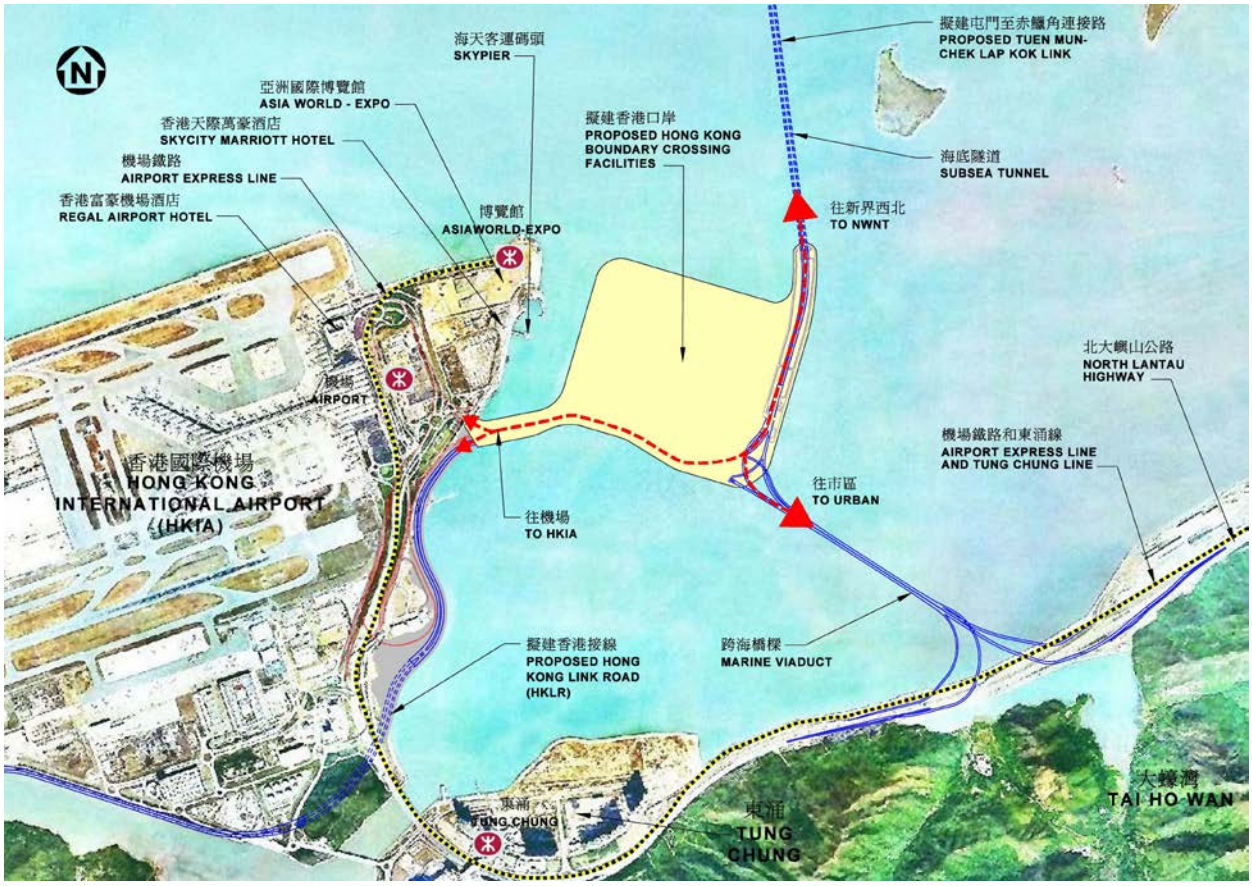

Figure 18: Hong Kong Boundary Crossing Facility location

A non-dredge reclamation solution was adopted for the reclamation to reduce the environmental impact from dredging. As part of this technique the seawalls were formed using an initial circular steel cell installation of between 27 to 31m diameter using sheet piles extending through the soft marine deposits into the underlying alluvium. These were backfilled using inert construction & demolition material or sand. See Figures 19 to 21 for the steel cell locations within the seawall (HyD, 2011).

Figure 19: Outline of the steel cells installation formed as part of the seawall construction (April, 2014)

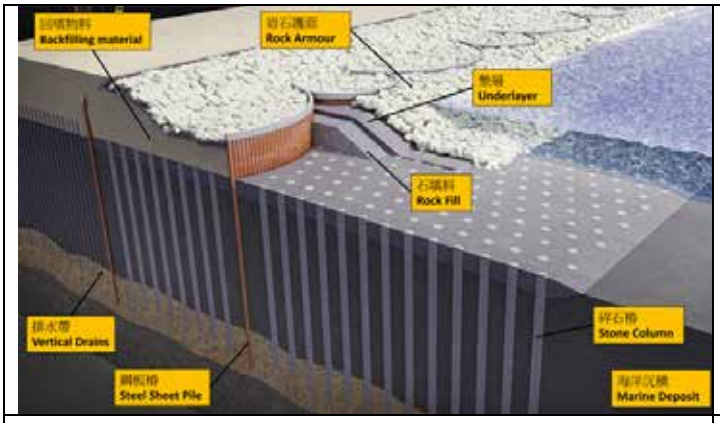

Figure 20: Stone column and steel cell installation

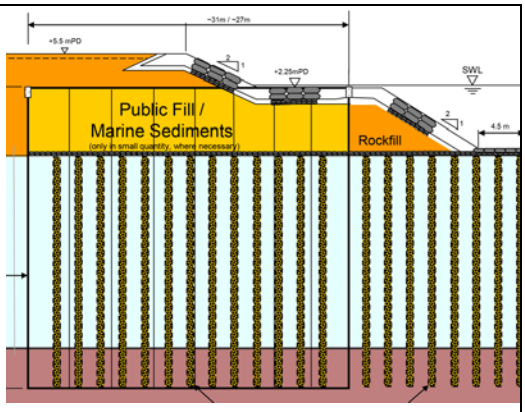

Figure 21: Stone column installation

Following the steel cell installation a 2 m fill blanket was placed on the seabed to allow wick drain installation for 10m into the soft marine deposits. After placing the main reclamation to formatiuon level of +5.5mPD the marine deposits were allowed to consolidate to 80% of the total anticipated value. Tapered stone columns were then installed using vibro-replacement techniques over a 70m wide footprint. The vibro-replacement technique involved replacement of the weak ground by advancement of the vibro-flot and replacement by gravel through a tremie pipe as the vibro-flot was progressively removed. See Figure 22 for the vibro-replacement technique below surface and Figure 23 for its installation offshore (Degen, 2014).

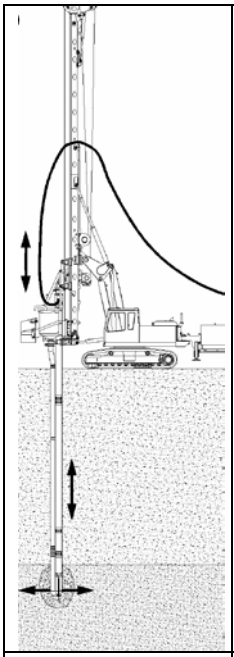

Figure 22:Vibro-replacement

Figure 23: Vibro-replacement from offshore barges at the HKBCF site location

After the vibro-replacement stone columns were installed a surcharge was placed and further 50% consolidation allowed. Refer to Figure 24 for the wick drain and stone column installation. The required strength gain through the wick drain and ultimately stone column consolidation was 15kPa as shown in

Figure 25. The strength gain was verified using shear vane and Cone Penetration Tests (CPTs) prior to the reclamation and following the wick drain and stone column consolidation. (Degen, 2014).

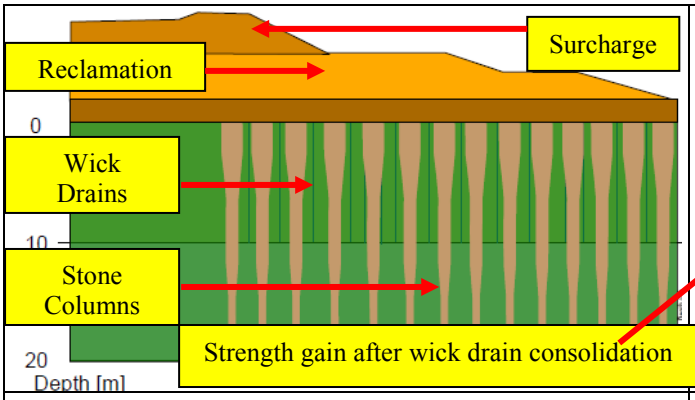

Figure 24:Wick drain and stone column installation

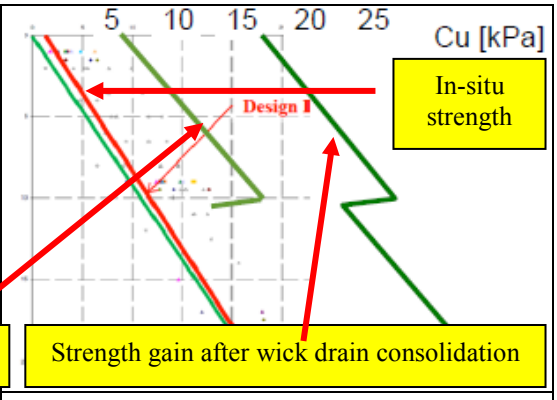

Figure 25: Strength gain through the consolidation stages

5 CONCLUSIONS

The HKSAR has had a history of reclamation instability. This has occurred even though there has been increased knowledge of reclamation techniques, progressing from end-tipping, were instability was a frequent occurrence, to the addition of sand blankets and geotextile separators to drained reclamations, using vertical drain installation in combination with surcharging. More recently the instability has often been exacerbated by the need to form reclamations further offshore, onto more complicated ground conditions, to a larger scale and within accelerated time frames. In all cases the instability resulted from a poor understanding of the ground conditions. More recently the HKSAR government has enacted the foreshore ordinance requiring more stringent environmental impact assessments and resulting in a reduction in reclamations using dredging techniques in the HKSAR. Of the options available vibro-compaction techniques has proven to be suitable for improvement of selected reclamation sand fill. Given the technique can extend to 35m depth and can improve material reducing to silt size, its further use to underlying superficial deposits needs consideration.

ACKNOWLEDGEMENTS

The contents of this paper do not necessarily reflect the views and policies of these supporting organizations, nor does the mention of trade names and commercial products constitute endorsement or recommendation for use.

REFERENCES

Baldi G., Bellotti R, Ghionna V., Jamiolkowski M. & Pasqualini E. 1982. Design parameters for sands from CPT. *Proceedings (Proc.) of the 2nd European. Symposium (Symp.) on Penetration Testing, ESOPT 11, Amsterdam*, May, Vol. 2, pp. 427-432.

Berner, P. 1998. Ground Improvement at Chek Lap Kok: Review of Vibrocompaction at Hong Kong's New Airport, *Transactions, Hong Kong Institution of Engineers (HKIE)*, 5(1), pp 1-5.

Brand, E.W., Massey, J.B. & Whiteside, P.G.D. 1994. Environmental aspects of sand dredging and mud disposal in Hong Kong. *Proc. 1st International (Int.) Congress (Cong.) on Environmental 256 Geotechnics, Edmonton, Alberta*, pp 1-10.

Carter, M. 1996. A settlement Prediction Method Developed for Macau International Airport. *Transactions*, *HKIE*; 3 (1), pp35-40.

Civil Engineering Development Department (CEDD). 2005. *Fill Management: Marine Fill*: http://www.cedd.gov.hk/eng/services/fillmanagement/fm_mf.htm [last accessed: 18 March 2007].

De Silva, S, Sekula, J., & Endicott, L.J. 1998. LAR Depot Construction on Reclamation at Siu Ho Wan. *HKIE Geotechnical (Geo) Division 17th Annual Seminar (Ann Sem), Geotechnical Aspects of the Airport Core Projects*, 29 May, 2013: 111-118.

Degen, W, 2014. Offshore Stone Columns. *Association of Geotechnical and Environmental Specialists (AGS), Reclamation Sem*., 29 November, 2014: No. 7.

Fyfe, J.A., Shaw, R., Campbell, S.D.G., Lai, K.W., & Kirk, P.A. 2000. *The Quaternary Geology of Hong Kong. Hong Kong Geological Survey*, Geotechnical Engineering Office, The Government of Hong Kong Special Administrative Region.

Fyfe, J. A. & Shaw, R. 1995. *Coastal Infrastructure Development in Hong Kong, A Review*. Geotechnical Engineering Office, The Government of Hong Kong Special Administrative Region

GEO. 2007, *Engineering Geological Practice in Hong Kong*, *Publication 1/2007*. Geotechnical Engineering Office, The Government of Hong Kong Special Administrative Region.

Grace, H. & Henry, J.K.M. 1957. The Planning and Design of the New Hong Kong Airport. *Proc. Institution of Civil Engineers*, 32: 275 – 325.

Ground Engineering. 1996. *Geotechnical Aspects of Hong Kong's New Airport. Special Supplement* December 1996, EMAP Publications, London.

Guildford, C. M. 1988. Marine Fill in Hong Kong: A 35 year resume. In P.G.D. Whiteside & N. Wragge – Morley (ed) Marine Sand and Gravel Resources in Hong Kong. *Proc of the Seminar in Hong Kong*, *4 December 1987, Geological Society of Hong Kong*, pp 11 – 22.

Guildford, C. M. 1997. A look back: Civil Engineering in Hong Kong 1841 – 1941. *Asia Engineer, Hong Kong Institution of Engineers*, July 1997: 10-13.

Hadley, D. 1992. Construction and Performance of a drained reclamation in Tuen Mun. *Hong Kong Engineers*:19 – 24

Hendy, M. S & Muir, I.C. 2003. Penny's Bay Reclamation, Stage 1, Effective Reduction of Creep in Sand Fill. *HKIE, Geo Div 23rd Ann Sem, Case Histories in Geotechnical Engineering in Hong Kong,* 9 May, 2003: 123 - 130.

Hendy, M. S & Brown, C.J. 2001. Hong Kong Disneyland Penny's Bay Reclamation – Stage 1 Site Characterisation. *Proceedings of the 14th South East Asian Geotechnical Conf*, *HK*, December, 2001.

Ho, K.S & Chan, Y.C. 1994. Ground Improvement Methods for Marine Mud. *Ground Improvement Methods, 19th May 1994*. *HKIE, Geot. Div*.: 85 - 102.

Highways Department (HyD), 2011. The Hong Kong Zhuhai Macau Bridge web site http://www.hzmb.hk/eng/about_overview_03.html

Li, S. & Wei, H. 1987. The study of deltas during the last decade in China. In: FW Wezel & JL Rau (ed) Progress in Quaternary Geology of east and south east Asia. *Proceedings of the CCOP symposium, Bangkok, Thailand*, 27-30 October, 1986, CCOP Technical Publication No. 18., pp 37 – 46.

Lumb, P. 1976. Land reclamation in Hong Kong, compiled in *a Memorial Collection of Selected Papers and Memoirs of Professor Peter Lumb*: 649 – 663.

Mackay, A.D. 2009. Seawall Geotechnical Design and Construction Considerations for Hong Kong Reclamations. *Civil Engineering. Towards a Better Environment*, *Portugal*; pp C67-74.

Mackay, A.D. 2010. Engineering Site Selection Considerations for Reclamation Seawalls in the Hong Kong Special Administrative Region, *International Association of Engineering Geologists (IAEG)*, *Auckland, New Zealand*: 4311-4320.

Mackay, A.D., 2016. The Acceleration of Settlement for non-dredged Reclamations using Ground Improvement Techniques: *HKIE, Geot. Div. 36th Ann. Sem*., *3 June 2016. Reclamation: Challenges and Beyond*.

Morton, B. 1979. The Ecology of the Hong Kong Sea Shore. In B. Morton (ed), *the Future of the Hong Kong Seashore*. Oxford University Press, Hong Kong, pp 99-123.

Ng, F.H.Y & De Silva, S. 2007. Geotechnical Practice of Reclamations in Hong Kong. *HKIE, Geot. Div. Ann. Sem., 2007, Geotechnical Advancements in Hong Kong since the 1970s*, pp 69-83.

Pickles. A.R & Plant G.W. 1998. Settlement of the Airport Reclamation and Implications for Airport Operations. *HKIE, Geo Div. 17th Ann Sem, Geotechnical Aspects of the Airport Core Projects*, *29 May, 1998, Geotechnical Aspects of the Airport Core Program*: 109-123.

Plant, G.W. Covil, C.S & Hughes, R.A. 1998. *Site Preparation for the New Hong Kong International Airport*. Thomas Telford Publishers.

Robertson P. K., and Campanella R. G. 1983. Interpretation of cone penetration tests. Part I: Sand". *Canadian Geotechnical Journal*, Vo!. 20, 1983.

Schmertman 1. H. 1976. *Predicting the qc!N ratio*. Engineering and Industrial Station, Department of Civil Engineering, University of Florida, GainesviIle. Final Report D-636.

Sims M. 1994. Vibroflotation and its application in Hong Kong, *Ground Improvement Methods, 19th May 1994. HKIE, Geot. Div*, pp 133 - 144.

Watts, J.C.D. 1973. Further observations on the hydrology of the Hong Kong Territotrial Waters. *Hong Kong Fisheries Bulletin No. 3*, pp 9-35.

Weng Y. & Deng, Z. 1992. Improvement and development of the Pearl River Estuary. *Proceedings of the International Conference on the Pearl River Esturary in the Surrounding Area of Macau*, 19-23 October, 1992: 21 - 31.

Ground Investigation and Laboratory Test Considerations for Un-dredged Reclamations

A. D. Mackay
ALYSJ JV, Doha, Qatar
Ada Chan
Leighton Asia, India and Offshore (LAIO)

ABSTRACT

Due to recent demands to form reclamations using non-dredging techniques, placement on relatively weak un-dredged Superficial Deposits (Marine Deposits and Alluvium) is required. The reclamation stability and settlement is determined using appropriate site investigation (SI) techniques to provide ground models which are updated throughout the reclamation project design, construction and operation phases. This paper provides a brief overview of the ground investigation (GI) sampling and laboratory test techniques for offshore Superficial Deposits highlighting requirements to ensure appropriate geotechnical parameters are determined. A review of selected Consolidated Undrained (CU) Triaxial laboratory tests with pore water pressure measurement, commonly used to provide effective shear strength parameters for reclamation stability, is given. The specimens selected had variable inter-bedded structures with different particle sizes, ranging from clay to sand size, affecting the results. A summary of considerations which need attention to ensure high quality and representative parameters are obtained and it is recommended that the failure during CU triaxial testing be taken as the maximum stress ratio of σ_1'/σ_3'. The appropriate level of logging detail is required to assess the accuracy of the geotechnical parameters obtained.

1 INTRODUCTION

Un-dredged reclamations have risks from instability and un-predictable scales and rates of settlement prior to development. These are influenced by the thicknesses and variability of the geotechnical properties of the underlying superficial deposits, which cover the sea-bed beneath the Hong Kong Special Administrative Region (HKSAR) waters.

Recent increases in the scale of reclamation and placement further offshore has put pressure on retrieving representative high quality, "undisturbed" samples and carrying out laboratory testing as part of routine GIs. The findings of the sampling and testing; complementing past case histories, in-situ and borehole tests and back analyses data, carried out during later stages of the reclamation project cycle; should ensure the variability is properly understood and representative geotechnical parameters are determined.

Given the variability of the superficial deposits an overview of the offshore sampling techniques and appropriate quality of the sample retrieved for use in laboratory testing is given. As the CU Triaxial test with pore water pressure (pwp) measurement can be used for stability and settlement assessment, a review of the results taken from random test specimens of Marine Deposits and Alluvium is provided. The influence of the sample quality on the "small scale" variability of the test specimen and the time taken for the permeation of back pressure throughout the specimen is considered. It is highlighted that the variable constituents for both marine deposits and in particular Alluvium within the sample and specimen, require detailed logging to verify the accuracy of the geotechnical parameters.

2 OFFSHORE GROUND INVESTIGATION

2.1 General

Offshore exploratory stations need a stable platform to place exploration equipment and are advanced through an extension from the platform to the sea bed. Platforms can be provided from scaffold erection from the land, if close enough to the shore, or from a floating craft jacked-up on spud legs, typically limited to depths of 12m to sea-bed level. Equipment design is needed for the investigation techniques adopted for the anticipated ground conditions and the environmental factors, such as the depth to sea bed level, wave action, tidal fluctuations and currents, Blacker et al (1985). Further consideration is needed for the anchor holding properties and the positions and fluctuating water levels from tides, waves and swells, Mackay et al (2016) with consideration for compensator systems, Smyth et al (1985). Refer to Plate 1 for an example of an offshore GI platform, GEO (1987).

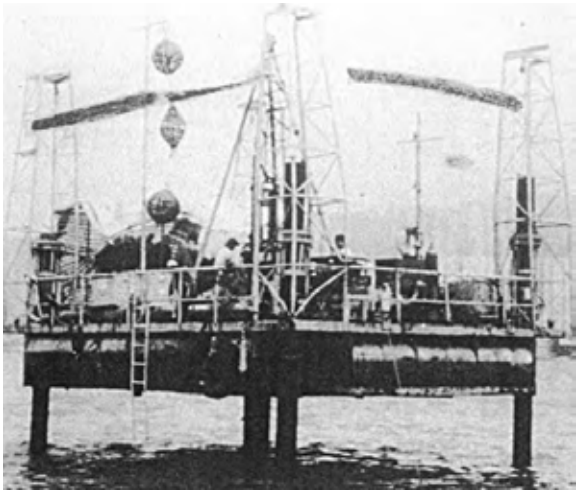

Plate 1: Offshore drilling rig

Plate 2: large diameter piston sample

Plate 3: Vibro-core

2.2 Exploratory station advancement, sampling and appropriate laboratory testing

Offshore ground conditions in the HKSAR typically comprise soft to very soft Marine Deposits over firm to stiff alluvial deposits. In particular the Alluvium is interbedded with granular soils and occasionally contains boulders, cobbles and gravels, GEO (1987 & 2007). The Alluvium and to a limited extent the Marine Deposits overlie weathered rock. A GI for non-dredged reclamations on superficial deposits requires appropriate sampling and field testing during the borehole advancement limiting disturbance and change in ground water content as far as practical. Typically Piston Samplers can be used to retrieve soft to very soft cohesive marine deposits and more robust U100 samplers less sensitive stiff to very stiff alluvium (Whyte, 1984); Thin walled Delft or Swedish Foil Samplers can be used for continuous sampling (Fung et al, 1984). Piston samples with an increased diameter of 254mm were used during 2000 for the Container Terminal (CT) 9 reclamation, Tsing Yi, and 2003 for the Wan Chai Reclamation and the Wan Chai Development, Phase 2, 2003 (See Plate 2). These samples had the advantage of less overall disturbance and improved representation of the ground conditions, particularly sand laminations and fabric, Pyle et al (2007).

Vibrocores are advanced by initial self-weight through the upper-most layers and by a motorized penetrator thereafter. These comprise steel tubes with a PVC liner fitted with a basket in the removable cutter shoe to contain the sample during retrieval; penetration can extend to 6m below sea-bed level through soft ground. This sampling technique provides a rapid retrieval of poor quality samples and has become popular for reclamation GIs during recent decades with 600 samples taken for the CT9 reclamation (2000) and 2400 samples retrieved for the Penny's Bay Stage 1 Reclamation (2003). Refer to Plate 3 for the use of a higher quality vibro-core unit, Pyle et al (2007).

The sample disturbance is affected by the displacement of the ground during the sampler penetration; this can be reduced by increasing the tapering of the sampler cutter shoe. The ground displacement is

determined by the Cutter Area Ratio (AR), defined as the volume of the displaced material in proportion to the sample volume. The ranges are from 10% for piston samples; 30% for the more robust U100 sampler; and 100% for the Split Barrel Standard Penetration Tests (SPTs). The Sample Class used to determine appropriate laboratory testing after sample retrieval is given in Table 1, BS 5930 (1999).

Table 1: Sample quality

Ground composition	Sampling Procedure	Class
Granular soils (sands, silty sands and sandy silts)	Piston sampler / compressed air sampler	2/3
	U100 sampler (with core catcher)	4
	SPT with split barrel sampler	4
Very soft to soft cohesive soils (sandy clays, silty clays or clays)	Piston sampler	1
	Thin walled sampler	1/2
	U100 sampler	2/3
	Delft Continuous Sampler	2/3
Firm to very stiff Cohesive Soils	Triple Core Barrel with retractable shoe	1/2
	U100 sampler	2/3

Class 1 samples are suitable for all standard soil laboratory tests, such as classification, moisture content, density, strength, deformation and consolidation. Lower class samples can be used for less sensitive tests ranging from classification, moisture content and density (Class 2); classification and moisture content (Class 3); and classification only, Class 4, BS 5930 (1999). Weathered rock sampling procedures are adopted if boulders, cobbles and gravels are encountered.

Examples of the disturbance from samples taken using the SPT split sampler are shown for Marine Deposits in Plates 4 and 5 and Alluvium in Plates 6 and 7, copied from Fletcher (2004). Disturbances may include an increased density for granular soils, distortion of the fabric for cohesive soils, and sample breakage and changes in moisture content. Despite the limitations on the type of laboratory test the samples provided data on the variability of the superficial deposits.

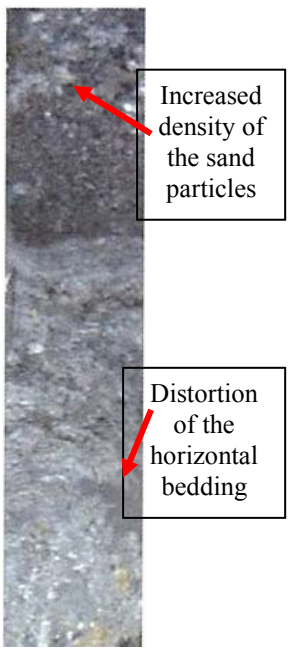

Plate 4: Marine deposits (Sand)

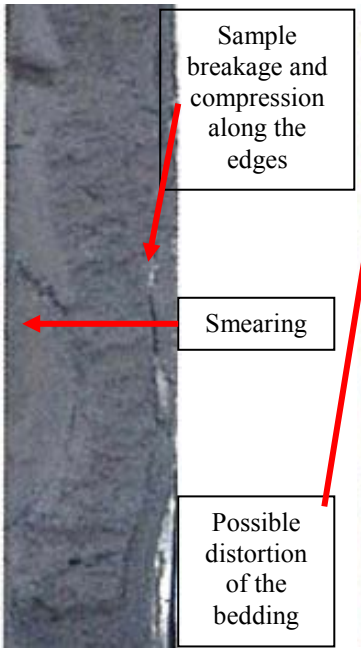

Plate 5: Marine deposits (Silty clay)

Plate 6: Alluvium (Dessicated crust)

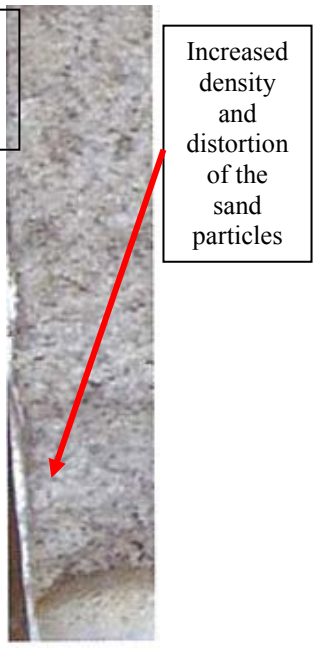

Plate 7: Alluvium (Coarse sand)

3 LABORATORY TESTING

3.1 General considerations for laboratory testing for reclamations

As the geotechnical properties of the Marine Deposits and Alluvium depend upon the soil fabric, it is vital that geological characteristics are recorded in detail during sample extrusion and the laboratory test specimen preparation, the influence of the fabric on the laboratory test result needs consideration. In the HKSAR "the examination of samples of soil is one of the most important aspects of a GI" and "all undisturbed samples should be re-examined each time a specimen is taken for testing." Samples without a scheduled laboratory test should be "extruded; split down the centre for examination and described and photographed", GEO (1987). The roles and tasks for key individuals, responsible for the laboratory test scheduling and supervision and the detail for the soil description, including the origin; verification of the field description, in particular fabric, and other geological effects affecting the test are set out in HKAS (2009), BA (2010), GEO (1987), GEO (2001) and Chan et al (2015).

Standard classification tests, including particle size distribution (psd) and Atterberg Limits, can be carried out on samples of Class 4 or better. These tests are cheap, rapid and provide complementary data for more detailed and sensitive shear strength and deformation testing. The tests can be carried out after other tests and detailed sample examination have been completed and used for indirect estimation of other parameters such as undrained shear strength, compression and permeability, Wroth et al (1978) & Mackay (1994).

3.2 Permeability

This is defined as the ability of a soil to allow fluid to pass through and is related to the void content, pore shape and pore connectivity, Smith (2006). The normally consolidated Marine Deposits and over-consolidated Alluvium are both deposited in water borne environments with the consistent particle size and shape within successive deposition layers allowing a reasonable correlation between permeability (cms^{-1}) and empirical formulae, such as the Hazen equation, referenced $C *(D_{10})^2$, for each representative layer. The equation is C an empirical coefficient from zero to 1.5, averaging one and D_{10} is the grain size (mm) passing the 10^{th} percentile on the psd grading curve, Smith (2006).

For undisturbed samples, the permeability can vary across partings, laminae and fabric within a test specimen; suitable permeability estimates are therefore needed to determine differences between layers (laminae). Estimates from the psd test can provide cross checks for direct test results determined in-situ, which cover a greater volume of undisturbed ground potentially providing more representative results, GEO (1987). Suitable permeability estimates are required to indirectly determine the magnitude and rate of consolidation which are also dependent upon the length of drainage and compressibility.

3.3 Magnitude and rate of settlement

The magnitude and rate of settlement can be assessed from One-dimensional Consolidation and Isotropic Compression laboratory tests, GEO (2001) and Rowe Cell laboratory tests, Premchitt et al (1996), Head (1992) and Rowe et al (1966). As horizontal layers with variable permeability are typically present in superficial deposits the differences between the horizontal (C_h) and vertical rate of consolidation (C_v) can differ significantly within a test specimen. Due to the limited size of the specimen used for the one-dimensional oedometer tests this may not represent the horizontal layers and rate of in-situ consolidation accordingly. These tests should not be used for superficial deposits, GEO (2001).

The Rowe tests can be carried out on test specimens of 76, 150 and 250mm diameter. It has the advantage of better control of the drainage from the test specimen; through the centre, sides, top or base; flexible or rigid strain application by adjusting the type of platen used; measurement of pwp, water expulsion volume and back pressure application; and constant rate or step increase in loading. In addition to the potential use of larger specimen sizes provides a better representation of the in-situ conditions. The flexibility of the test set up provides a more accurate representation of the conditions present during reclamation, with similarities to in-situ drainage through more permeable layers located towards the upper or lower levels of the consolidating layer or use of a band drain installations, represented by drainage through the specimen centre. The equipment and test set up is shown in Plate 8 and Figure 1.

Plate 8: Rowe test equipment

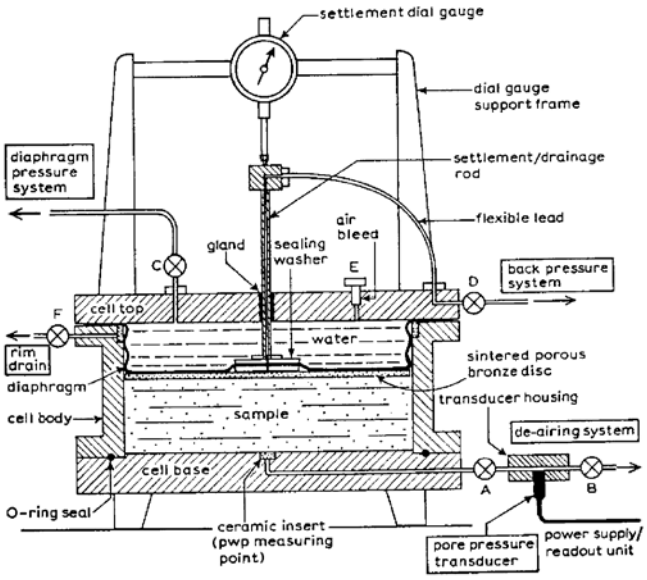

Figure 1: Rowe test set up

Despite the accuracy of the Rowe consolidation test results, limitations include the height to diameter ratio, reducing representative variability in the horizontal layers, and the time and cost needed for testing. Examples of tests on 254mm diameter samples from the CT 9 and Wan Chai Stage 2 Reclamation GIs (2000 and 2003) took several weeks to complete with increased expense, limiting their use only to larger scale reclamations, Pyle et al (2007).

Magnitudes and rates of consolidation can be obtained from Isotropic Compression laboratory tests carried out on test specimens with an increased height to diameter ratio of 2:1, providing better representation of the horizontal laminae within the test specimen. The test is carried out by varying effective stress application within a triaxial cell. The test limitations are drainage through the top, however tests specimens with low permeability can be accelerated through drainage along the sides, through filter paper, and from the base. Assuming the soil has isotropic properties comparisons can be made between the void ratio and coefficients of consolidation, however for tests using different drainage conditions, particularly side drains and variations in stiffness and permeability within the specimen, there are difficulties in calculating the coefficient of consolidation, GEO (2001).

3.4 Shear strength

Shear strength tests can be used to assess the stability of the underlying superficial deposits. Rapid imposed loading during reclamation provides limited periods for the increased pore water pressure to reach equilibrium with the surrounding ground and dissipate. The stability in this condition is assessed using the undrained shear strength parameter determined by the Quick Undrained (QU) triaxial test. The aim of any un-dredged reclamation is ensure loading is imposed gradually allowing sufficient time for the pore water pressure to reach equilibrium and dissipate. The effective shear strength parameters needed to assess these conditions are determined by the CU triaxial tests with pwp measurement.

4 CONSOLIDATED UNDRAINED TRIAXIAL TESTING FOR SUPERFICIAL DEPOSITS

4.1 The test

Based on GEO, 2001, the main test stages of the CU triaxial test with pwp measurement are saturation, all voids in the test specimen are saturated; consolidation, reaches the scheduled state of effective stress;

and compression - shear failure through a consistent axial strain from the consolidation rate. The test apparatus is shown in Plate 9 and main components in Figure 2.

Plate 9: Triaxial test equipment

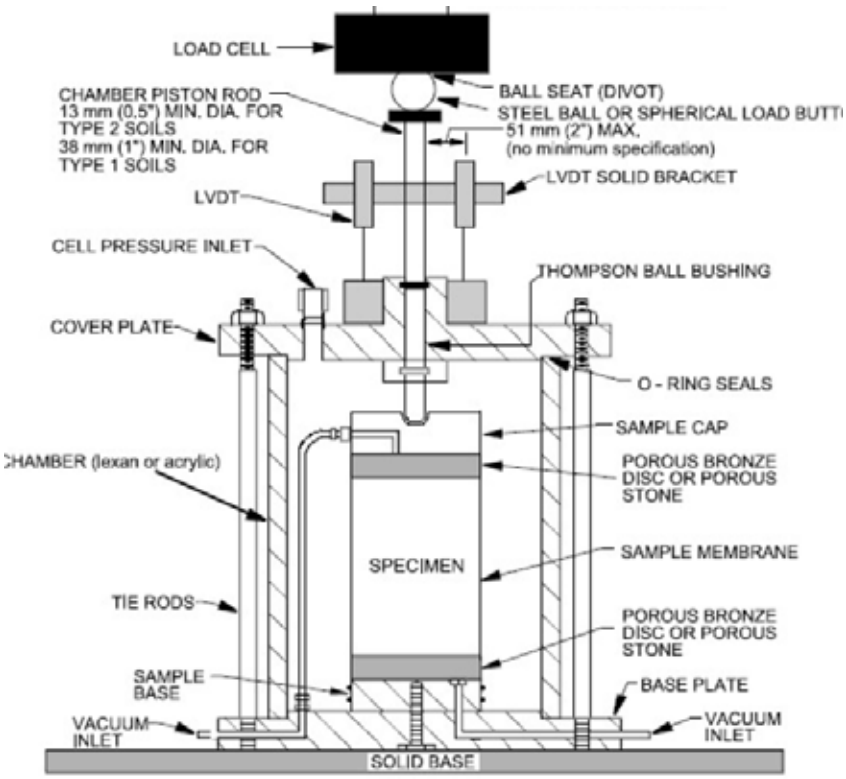

Figure 2: Triaxial test set up

The saturation and pwp measurements are applied and measured through porous stone placed on top and at the base of the specimen respectively; sufficient time is needed to ensure that the pwp is equally distributed throughout the specimen. As sub-horizontal laminae are typically present in superficial deposits with potential orders of magnitude difference in permeability and thicknesses less than the specimen height (particularly in Alluvium), considerable time may be needed for the pwp to permeate the specimen and reach equilibrium when applied from the top of the specimen. During saturation initial permeation in the more granular layers occurs with an increased pwp can result in volume change. In dense soils the pressure increase may force the soil particles apart (swelling) reducing strength by decreasing the inter-particle friction. Loose soils, may have a volume reduction (compression), with an increase in strength. Filter paper side drains may be used to accelerate the test period in soft clays with low permeability, typical of marine deposits, however membrane corrections are required, GEO (2001).

Consolidation is carried out by scheduling an effective stress, estimated from the in-situ effective stress conditions were the sample was taken. For the Marine Deposits, which are normally consolidated, the in-situ stress is potentially the maximum stress which the test samples was subjected. For Alluvium these have been subjected to a past stress history and when exposed to terrestrial weathering may be cemented from past duricrust formation, Mackay et al (2016). The confining stress should therefore be increased sufficiently to exceed the over-consolidation ratio or the strength of the cementing component. During consolidation the back pressure should not fall below the final saturation pressure and care taken to ensure the volume increase is not excessive and / or localized. The use of side drains in soft lower permeability layers may allow a decrease in the drainage path between horizontal layers with different permeability accelerating the pwp equalization, however difficulties may occur interpreting the results and calculating the coefficient of consolidation, GEO (2001). The provision of side drains may represent drainage paths between layers represented by the installation of a more permeable medium, such as wick drains, allowing increased vertical drainage flow.

Compression is continued until a failure stress condition is reached, which can be either the maximum effective principal stress ratio of the applied axial pressure to the confining pressure ($\sigma_1'/\ \sigma_3'$); the deviator stress ($\sigma_1'- \sigma_3'$) or shear continuing at a constant pore pressure and shear stress application. The appropriate failure criteria is given by Bishop et al (1976); for the normally consolidated cohesive Marine Deposits, the maximum deviator stress and constant pore pressure should be similar.

Multi stage tests are not recommended due to the potential for significant errors in the shear strength assessment from excessive strain to failure, GEO (2001). The subsequent test stages may also follow the failure plane formed during the previous stage.

4.2 Review of CU triaxial tests with pore water pressure measurements

4.2.1 General

Selected CU triaxial tests with pwp measurements on specimens were reviewed from a piston sample of Alluvium, from 19 to 20m below ground level (bgl) taken from a borehole used to investigate the West Kowloon reclamation. The geological characteristics of the selected specimens were compared with other specimens taken from the same borehole, including a Mazier (M101) sample of Alluvium, from 21 to 22.1 m bgl, and a disturbed U76 sample (typically not used for strength testing) of Marine Deposits taken from 17.3 to 17.8 m (m bgl). Plates 10 to 13 present the specimens taken from each sample, cut along the centre after test completion. The geological sample description, GEO (1992) is provided and key geological features influencing the test result annotated.

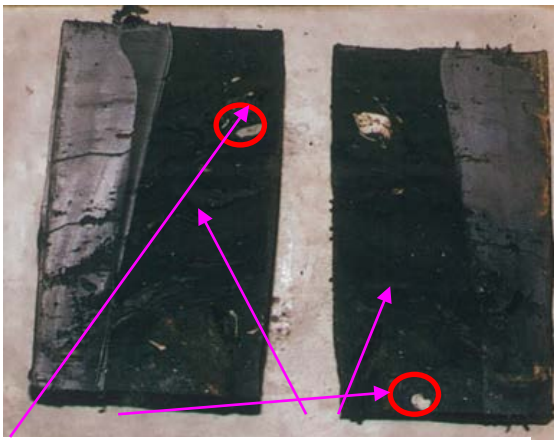

Plate10: U76, specimen – 17.6–17.8m bgl (Marine Deposit); grey, slightly sandy, clayey silt

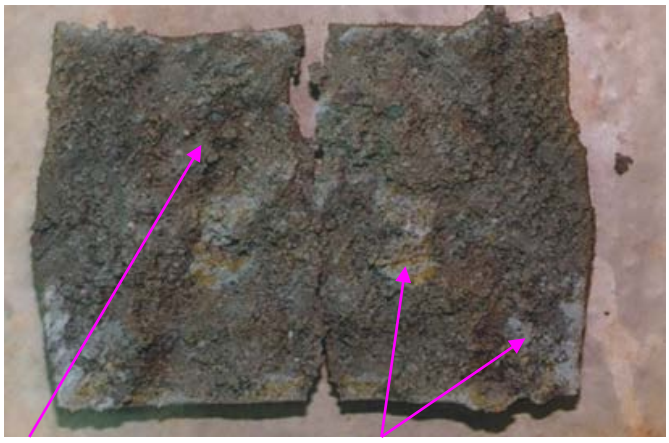

Plate 11: Piston, specimen – 19.55 – 19.7m bgl (Alluvium); light grey, silty, very gravelly sand

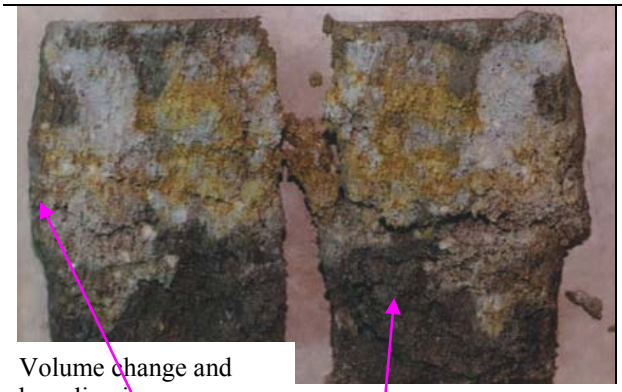

Plate 12: Piston, specimen – 19.7–19.85m bgl (Alluvium); light grey, silty, very gravelly sand

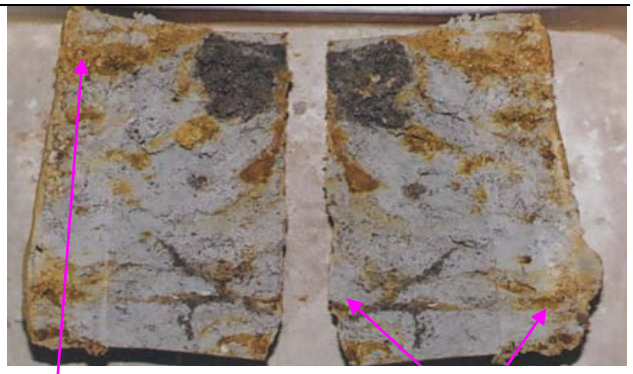

Plate 13: M101, specimen – 21–22.1m bgl (Alluvium); brown slightly sandy clayey silt

4.2.2 Geological features influencing the CU test results

Geological fabric influencing the failure characteristics shown in Plates 3 to 6 is summarized in Table 2.

Table 2: Geological fabric influencing failure within the alluvium

Sample / deposit	Specimen (m bgl)	Geological Fabric influencing failure	Failure characteristics
U76 / Marine	17.6–17.8	Consistent grain size with fine laminae and large shell fragment constituents.	No distinct failure; sample possibly compressed during retrieval.
Piston / Alluvial	19.55–19.7	Random inclusions of lighter grey coarser grained constituents.	Through coarser grained inclusions from the uppermost to lowest specimen levels
	19.7–19.85	sub-horizontal light grey and orange coarse grained constituents	Sub-horizontal “barreling” within coarse grained layer influencing the failure
Mazier / Alluvial	21–22.1	Stronger orange-brown duricrust within coarser grained sub-horizontal light grey layers	Sub-horizontal “barreling” within a coarse grained layer towards the lower levels.

As summarized in Table 2, for the alluvium the failure locations appear to be influenced by the presence of coarser grained layers or duricrust providing an increased bonding strength between particles. The variability, or otherwise, of the horizontal layers is fundamental in assessing the strength, however the geological description provided in the logs and specimen descriptions prior to testing are typically based on disturbed jar samples, which is insufficient to provide description for the geological fabric and potential influences on the test specification.

4.2.3 Review of the CU test results

The test specimens taken from the Piston Sample, 20 to 21m bgl, for CU triaxial testing were saturated by raising the cell pressure to the pwp in increments of 5kPa before reaching a pwp of about 200kPa; approximately equal to the in-situ effective water pressure. Consolidation took place by increasing the confining pressure to 400kPa with 128 and 1605 minutes needed for the upper and lower specimens to reach 100% consolidation. This suggested relative interconnection of the more permeable layers in the upper specimen. Following consolidation the axial strain rate for both test specimens was set at 0.047mm / minute and compression continued until reaching the deviator stress, σ_1’- σ_3’. A summary of the failure criteria, percentage and failure stage is summarized in Table 3.

Alluvium has experienced a past stress history, for the specimens tested peak failure occurred upon reaching the maximum stress ratio, at axial strains of 4 to 5.5%, which occurred a short period after the maximum pwp was exceeded. This allowed dissipation to occur prior to failure overcoming the pre-

existing intergranular stress. The failures presented in Plates 4 and 5 occurred after the maximum deviator stress was reached at strains between 19 to 21%, representing residual failure conditions occurred. The maximum σ_1'/σ_3' ratio and deviator stress are therefore considered to be representative of the peak failure condition, overcoming the past stress history from over-consolidation, and the maximum deviator stress represents the residual failure condition.

Table 3: Depth (metres below ground level, mbgl),

Specimen (m bgl)	Failure Criteria	Failure value (kPa)	Strain (% axial length)	s' (kPa)	t' (kPa)
19.55–19.7	Pwp	349kPa	4.1	171	100
	σ_1'/σ_3'	3.94 (ratio)	4.95	180	107
	$\sigma_1'-\sigma_3'$	303kPa	20.79	269	151
19.7–19.85	Pwp	317.6kPa	2.16	196	113
	σ_1'/σ_3'	4.38 (ratio)	5.4	292	184
	$\sigma_1'-\sigma_3'$	667.5kPa	18.96	555	334

4.2.4 Considerations

The CU triaxial test is relatively cheap and rapid and has been traditionally used to determine geotechnical parameters in the HKSAR. Laboratory testing is a vital part of a site investigation process if appropriate geotechnical parameters are to be used for reclamation input. Superficial Deposits have inherent variability which needs recognition when interpreting geotechnical parameters from the results. Particular attention for testing superficial deposits from both the responsible person for test scheduling the laboratory test supervisor are:

- Strain rate – applied at a relatively slow rate to avoid rupture of sensitive, fine grained layers;
- Side drains – at lower stress test levels for superficial deposits their effect on the strength is minimal, they would accelerate pwp distribution between low permeability horizontal layers;
- Geological detail – the fabric needs describing for the sample and specimen prior to testing, and of the specimen after testing;
- Test schedules - appropriate stresses need consideration to estimate over-consolidation ratios;
- Volume – Changes can be localized and needs recording to assess how failure occurs;
- Disturbance – appropriate recording is needed to verify if the result is accurate

Detailed descriptions are recorded during laboratory testing which is often not included in the GI log. Greater interaction is required between the laboratories and the GI contractor.

5 CONCLUSIONS

Un-dredged reclamations placed on superficial deposits are costly and need sufficient time for successful completion. There are numerous uncertainties that exist from the variability of the underlying ground, which requires a high quality, planned site investigation, continuing through all reclamation project stages. Some of these include instability and excessive settlement which require accurate assessment of the geotechnical parameters, which can assessed form CU triaxial testing, as part of the SI phases. The SI needs comparison and integration with other stages and SI methods, such as a review of past similar projects with similar ground conditions and construction techniques, detailed site inspections, GI in-situ testing and sampling with accurate descriptions. For laboratory tests comparisons are needed with geotechnical parameters determined from indirect test results to verify accuracy. Appropriate judgement of suitable parameters based on the use of risk assessment rather than prescriptive adoption of parameters and stability assessments are needed.

ACKNOWLEDGEMENTS

The contents of this paper do not necessarily reflect the views and policies of these supporting organizations, nor does the mention of trade names and commercial products constitute endorsement or recommendation for use.

REFERENCES

Bishop, A.W. & Henkel, D.J. 1976. The Measurement of Soil Properties in the Triaxial Test. *Edward Arnold, London*: 227.

Blacker, P. & Seaman, J.W., 1985. A review of Current Nearshore and Offshore Site Investigation Practice in Waters around Hong Kong. *Conference (Conf.) Proceedings (Prroc.) on Geological Aspects of Site Investigation, Hong Kong.* Published by the Geological Society of HK, Bulletin No. 2, ed. Ian McFeat Smith.

British Standard (BS) 1377, 1990. *Methods of Testing for Soils for Civil Engineering Purposes.* BS Institute (BSI), London, 406 p.

British Standards (BS) 5930:1999 + A2:2010 (2010). *Code of Practice for Site Investigation.* BSI. London, 147p.

Building Authority (BA), 2010. *Code of Practice for Site Supervision*. *HKSAR Government.*

Chan, A.W.K., Mackay, A.D. & Wightman, N.R. 2015. Considerations for Consolidated Undrained Triaxial Testing of Saprolites for Design. *The Hong Kong Institution of Engineers (HKIE), Geotechnical Division (Geot. Div.), 35th Annual Seminar (Ann. Sem.), 22 May, 2015*, *Soil Structure Interaction: from Modelling to Observations in Hong Kong since the 1970s*: 151-160

Chen, Y.J. & Kulhawy, F.H., 1993. Undrained strength interrelationships CIUC, UU, & UC tests. *Journal Geotech Engineering, American Soc. of Civil Engineers,* Vol. 119, no. 11: 1732-1750.

Fletcher, C.J.N. 2004. *The Geology of Site Investigation Boreholes from Hong Kong*. Association of Geotechnical and Environmental Specialists.

Geotechnical Engineering Office (GEO); 1987. *Guide to Site Investigation (Geoguide 2).* Geotechnical Control Office (GCO), HKSAR Government: 362 p.

GEO, 1992. *Guide to Rock and Soil Descriptions (Geoguide 3).* GCO, HKSAR Government, 189 p.

GEO, 2001. *Model Specification for Soil Testing*. GEO, Civil Engineering Development Department (CEDD), HKSAR Government.

GEO, 2007. *Engineering Geology Practice in Hong Kong*. GEO, CEDD, HKSAR Government.

Head K.H., 1992. *Manual of soil laboratory testing, Volume 3: Effective stress tests, second edition*, John Wiley & Sons, New York.

Hong Kong Accreditation service (HKAS). 2009. *Hong Kong Laboratory Accreditation Scheme (HOKLAS), 003 (9th Edition)*. Technical Criteria for Laboratory Accreditation. HKAS

Mackay, A.D., 1994. *Comparison of Reported Characteristic Test Data for London Clay with Published Correlations*. MSc dissertation. University of Birmingham, UK, Foundation Engineering.

Mackay, A.D & Wightman, N.R. 2016. Design and Construction Considerations for Reclamations and the use of Vibro-Compaction to Accelerate Fill Settlement. *HKIE, Geot. Div. 36th Ann. Sem., 3 June 2016. Reclamation: Challenges and Beyond.*

Premchitt, J., Ho, K.S., & Evans, N.C., 1996. *Conventional and CRS Rowe Cell Consolidation Test on Some Hong Kong Clays, GEO Report 55*. Civil Engineering Department, HKSAR.

Pyle, S.M., Brock-Hollinshead A., Y.Y. Ho., Koo, Y.C. & Collar, F. 2007. A Review of Site Investigation Techniques Introduced to Hong Kong in the Last 30 Years. *The HKIE, Geot. Div., 27th Ann. Sem., 15 May, 2007, Geotechnical Advancements in Hong Kong since the 1970s:* 23-31.

Rowe, P.W. & Barden, L., 1966. A New Consolidation Cell. *Geotechnique,* Volume 16, No.2, pp 162-170.

Smith, I., 2006. *Elements of Soil Mechanics.* J Wiley. Jul 12, 2006 - Technology & Engineering – pp 552.

Smyth, D.V. & McSweeney, T.V., 1985. Power Swivel Improves Offshore Drilling Quality. *Contractor (Hong Kong).* June 1985: 13-15.

Whyte, I.L., 1984. The Quality of U 100 Sampling. *Proc. 20th Regional Meeting of the Geological Society Engineering Group*, *Guildford, United Kingdom*: 419 – 423.

Wroth, C.P. & Wood, D.M. 1978. The Correlation of Index Properties with Some Basic Engineering Properties of Soils. *Canadian Geotechnical Journal,* Volume 15, No. 2: 137-145.

A Structured Anisotropic Creep Model for Hong Kong Marine Deposits

S.W. Lee & Y.S. Lee
Golder Associates (HK) Limited, Hong Kong
N. Sivasithamparam
Norwegian Geotechnical Institute, Norway
W.W.L. Cheang
Plaxis AsiaPac, Singapore

ABSTRACT

Creep-SCLAY1S is a constitutive model developed to capture the behaviours of soft, normally consolidated/lightly over-consolidated clays encompassing anisotropy, structure (bonding) and rate-dependence (creep). Input parameters can be obtained or derived from the results of standard laboratory tests. This paper briefly describes the main features of Creep-SCLAY1S and its input parameters. The model has been used to simulate a well-documented test embankment in Chek Lap Kok in 1981–1983. Numerical modelling of surcharging and PVD-accelerated settlement in one-dimensional manner is presented. Predictions are compared to the measured subsurface settlements and excess pore pressures in Upper Marine Clay and Lower Marine Clay. Creep-SCLAY1S predicts well the subsurface settlements. An omission of the destructuration and creep features will under predict the settlement at the top of clay by 0.87m, of which 60% is due to destructuration and 40% creep. Prediction of excess pore pressures in the latter part of consolidation of rest period is less satisfactory.

1 INTRODUCTION

Natural clays exhibit behaviours such as fabric anisotropy, effect of interparticle bonding and rate-dependence (e.g. creep). Combination of the fabric and bonding is called the structure. Destructuration occurs when the interparticle bonding is destroyed by irrecoverable strain caused by creep and an increase in loading.

Figure 1 shows the compression curves of natural and reconstituted samples in oedometer tests. A reconstituted sample with no bonding would follow the intrinsic compression line (ICL) with gradient λ^*_i. A natural sample with initial bonding would yield at a higher value of effective stress, and its compression curve would then converge with ICL as the bonding is gradually destroyed. The natural sample has a post yield λ^* greater than λ^*_i, because destructuration causes additional irrecoverable volumetric strain. At Point A on the natural compression curve the volumetric or vertical strain ε comprises (i) a small elastic recoverable component, (ii) a hardening component that would be experienced by the soil in an unbonded state, and (iii) a component due to bond degradation, see Figure 2 (Gens & Nova 1993) from the perspective of conventional elasto-plastic theory. At Point B the elastic component dominates, and at Point C the degradation component is negligible because the bonding has largely been destroyed at this stage.

Sivasithamparam et al. (2015) have developed a constitutive model Creep-SCLAY1S to model anisotropy, destructuration and creep. This model has been used to back analyse a well-documented test embankment in Chek Lap Kok in 1981–83 to assess the contributions of destructuration and creep to the measured settlements and excess pore pressures in the foundation clays.

2 CREEP-SCLAY1S

A brief description of the model is given here and the mathematical formulation is referred to Sivasithamparam et al. (2015). The model adopts an inclined yield surface and a rotational component of hardening to represent the evolution of fabric anisotropy during irrecoverable straining, see Figure 3. The effect of bonding is introduced by an intrinsic (reconstituted) yield surface and a natural (normal

consolidation) yield surface. An increase in volumetric strain is associated with the expansion of intrinsic yield surface due to hardening and the shrinkage of natural yield surface due to bond degradation (Gens & Nova 1993). The model incorporates three hardening laws – (i) change in size of the intrinsic yield surface due to irrecoverable creep volumetric strain (ε_v^c), (ii) change in inclination of the yield surface with ε_v^c and creep deviatoric strains (ε_d^c), and (iii) degradation of bonding with ε_v^c and ε_d^c. Creep is based on an idea of visco-plastic multiplier, using a modified creep index μ^* which can be easily derived from standard oedometer tests.

Table 1 summarizes the input parameters of the model. Appendix A shows how the parameters are derived from standard laboratory tests and field tests.

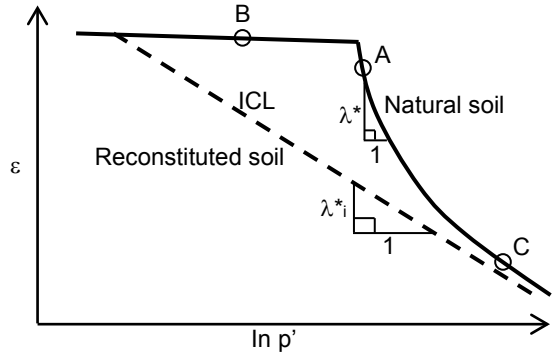

Figure 1: Natural & reconstituted compression curves

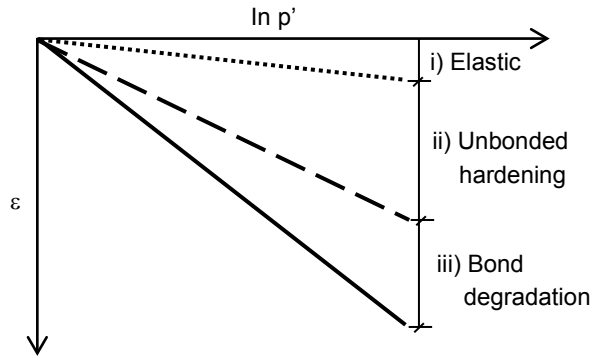

Figure 2: Components of volumetric strain

Table 1: Input parameters for Creep-SCLAY1S

Compressibility and strength		Anisotropy	
κ^*	Slope of swelling/recompression line in ε (vertical strain) – ln p' (mean effective stress) space	α_0	Initial inclination of yield surface
ν'	Poisson's ratio	ω	Absolute effectiveness of rotational hardening
λ^*_i	Slope of post yield compression line in ε – ln p' space for reconstituted soil	ω_d	Relative effectiveness of rotational hardening
M	Stress ratio of critical state line (CSL)		

Destructuration		Creep	
χ_0	Initial bonding	μ^*_i	Modified creep index of reconstituted sample
ξ	Absolute rate of destructuration		
ξ_d	Relative rate of destructuration		

Note:
When the structure (bonding) feature is switched off, i.e. $\chi_0 = 0$, intrinsic λ^*_i and μ^*_i derived from test on reconstituted sample become λ^* and μ^* derived from test on natural sample

3 CHEK LAP KOK TEST EMBANKMENT IN 1981–83

Foott et al. (1987) and Zhu (1999) provided details of the test embankments including the measured subsurface settlements and excess pore water pressures (epwp) in the foundation clays. Figure 4 shows the layout plan of the site, and the NW quadrant is of interest. Figure 5 shows that the ground conditions are Upper Marine Clay (UMC) underlain by Upper Alluvial Crust (UAC), Lower Marine Clay (LMC) and Lower Alluvium (LA). Figure 6 shows the filling history of the test embankment. Prefabricated vertical drains (PVD) of Alidrain brand had been installed in the NW quadrant at a triangular spacing of 1.5m to a level of

approximately -21mPD. An instrumentation cluster comprised a Sondex settlement system and pneumatic/hydraulic piezometers. Figure 7 shows the elevations of the instruments installed in the middle of the PVD triangular grids. Monitoring data was available for approximately 1,000 days.

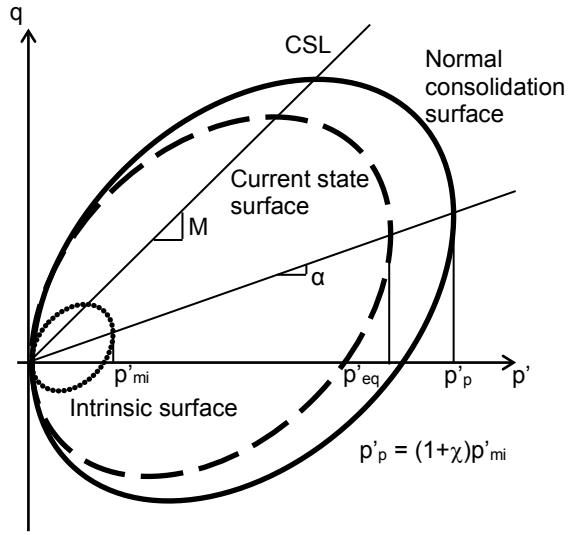

Figure 3: Yield surfaces at different stress states

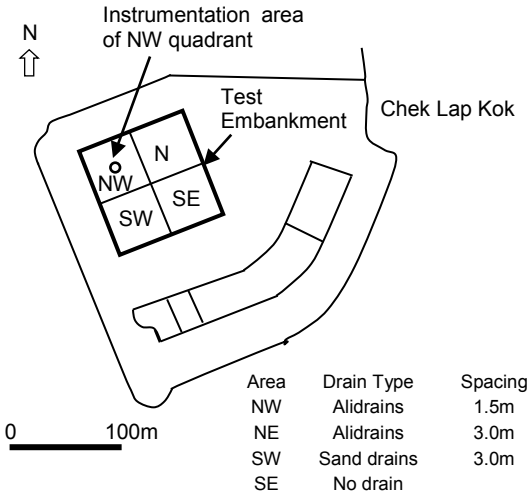

Figure 4: Site layout plan

Extensive field and laboratory soil tests had been carried out for the whole site (Koutsoftas et al. 1987). Undisturbed soft and stiff cohesive samples were respectively obtained using stationary piston samplers and thin walled tube samplers by pushing. The UMC was soft to very soft marine clay with pockets of shells, the UAC comprised interbedded layers of very stiff clay and dense sand, the LMC was medium to stiff clay interbedded with sand lenses, and the LA comprised very dense sand with occasional clay pockets. Table 2 summarizes the range of measured soil properties (Zhu 1999).

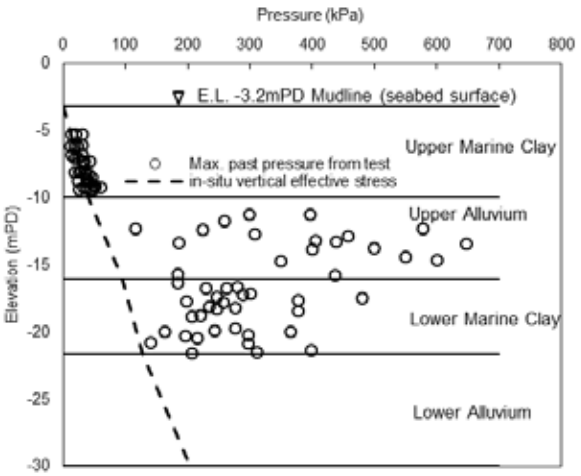

Figure 5: Ground conditions

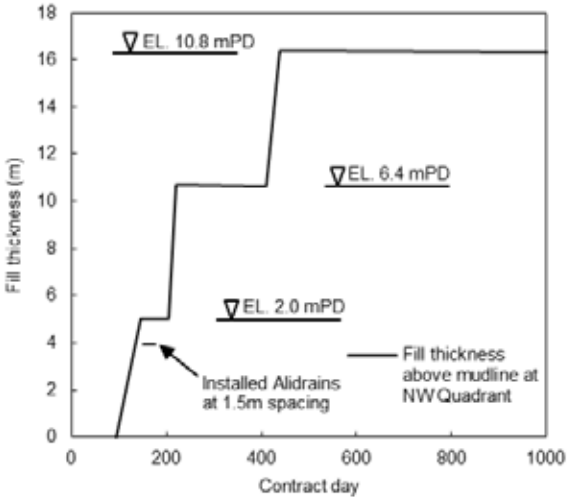

Figure 6: Filling history

Table 2: Range of measured soil properties for the whole site.

Parameters	UMC	UAC	LMC	LA
Plasticity index (%)	40 – 65	20 – 35	25 – 40	31
Bulk density, ρ_b (Mg/m^3)	1.45	1.95	1.85	2.01
Compression ratio, CR	0.3 – 0.5 (0.36$^{\#}$)	0.1 – 0.2 (0.15)	0.2 – 0.35 (0.23)	0.132
Recompression ratio, RR	0.02 – 0.03 (0.025)	0.015 – 0.035 (0.025)	0.02 – 0.05 (0.035)	0.019
Coefficient of secondary compression, $C_{\alpha\varepsilon}$	> 0.015 (0.0175)	0.008	0.017 – 0.03 (0.024)	0.0053
Vertical permeability, k_v (m/s)	2E-9 – 5E-9 (2.2E-9)	1.8E-8	2E-9 – 3E-10 (2.5E-10)	1E-8
Horizontal permeability, k_h (m/s)	3E-9 – 5E-9 (4E-9)	3.6E-8	4E-9 – 8E-10 (6E-10)	2E-8
Over consolidation ratio, OCR	1.5 – 2	2 – 11	1.2 – 4	-
Effective cohesion, c'	0	-	0	-
Effective friction angle, ϕ'	28°	-	28°	-

Notes:
1. Value in bracket represents average; $^{\#}$ Choa et al. (1990)
2. $\lambda^* = CR/\ln 10$ for oedometer test on natural soil sample

4 NUMERICAL MODELLING

Numerical modelling has been carried out using PLAXIS 2D V2012. Creep-SCLAY1S has been implemented in PLAXIS as a user-defined soil model. An axisymmetric unit cell models one-dimensional (1D) loading beneath the middle of the test embankment. Figure 8 shows the axisymmetric unit cell divided into PVD, smear and original soil zones to model horizontal drainage towards the PVD. The model has 1,899 nos of 15-noded elements. Table 3 summarizes the radial zones and their input permeability values.

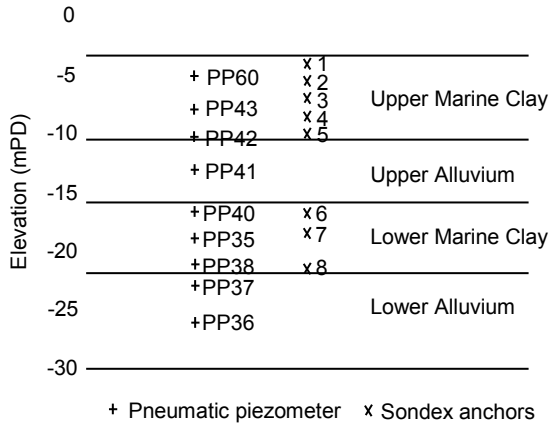

Figure 7: Locations of installed instruments

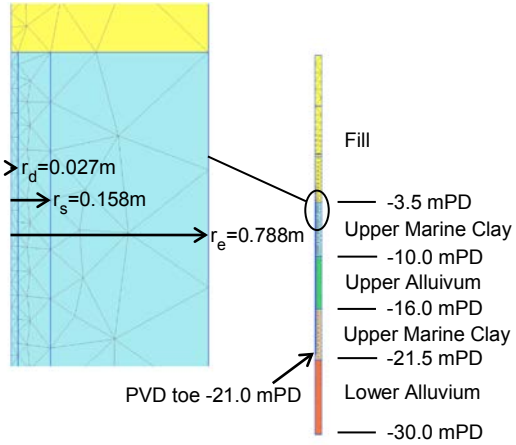

Figure 8: Axisymmetric unit cell model

Table 3: Radii of PVD, smear and original soil zones and input permeability values.

Zone	Radius	Derivation	Input permeability, k
PVD	r_d = 27.45mm	$r_d = (t+w)/4 + t/10$ (Long & Covo 1994) Drain width, w = 100mm, thickness, t = 7mm	$k_d = q_w/(\pi r_d^2)$ q_w = discharge capacity of drain Initial q_w (q_{w0}) is taken as 100m^3/year q_w decreases with time as per the curve of discharge capacity ratio in Figure 9 (Chai & Miura 1999)
Smear	r_s = 157.5mm	r_s/r_m = 2.5 r_m = radius of mandrel = 63mm	k_h/k_{sh} = 3; k_v/k_{sv} = 3 k_h, k_v = undisturbed original soil horizontal and vertical permeability in Table 2 k_{sh}, k_{sv} = smear zone horizontal and vertical permeability
Original soils	r_e = 787.5mm	r_e = 0.5*(1.05×drain spacing)	k_h and k_v of undisturbed original soils in Table 2

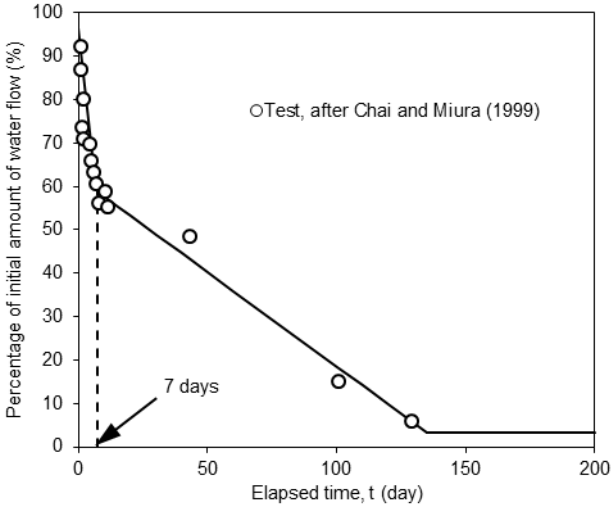

Figure 9: Discharge capacity of PVD reducing with time

Table 4 summarizes the input parameters for the foundation clays modelled using Creep-SCLAY1S with drainage type Undrained (A), with reference to the measured soil properties in Table 2 and derivation of the parameters in Appendix A.

Table 4: Input parameters for Creep-SCLAY1S modelling foundation clays.

Soil	γ (kN/m^3)	e_{ini}	M_c	λ^*_i	κ^*	ν'	POP (kPa)	K_0	C_k
UMC	14.5	1.60	1.11	0.106	0.011	0.2	15	0.64	1.35
UAC	19.5	0.85	1.20	0.043	0.011	0.2	300	1.08	0.43
LMC	18.5	1.15	1.11	0.066	0.015	0.2	150	0.75	0.80
LA	20.1	0.55	1.20	0.038	0.008	0.2	250	0.75	0.28

Notes:

1. ϕ' for UMC and LMC = 28°; ϕ' for UAC and LA = 30° (Zhu 1999)
2. λ^*/λ^*_i is taken as 1.5; Lo Presti et al. (2003) and Low (2004) reported λ^*/λ^*_i ratios 1.5 to 2.0
3. POP is pre-overburden pressure = pre-consolidation pressure minus initial effective vertical stress
4. $K_0 = 0.51(OCR)^{0.42}$ for initial stress equilibrium (Zhu 1999)
5. C_k controls change in soil permeability due to change in void ratio, $\log(k/k_0) = -\Delta e/C_k$

Table 4: Input parameters for Creep-SCLAY1S modelling foundation clays (continued).

Soil	α_0	ω	ω_d	χ_0	ξ	ξ_d	μ^*_i
UMC	0.426	27	0.65	3	9	0.2	5.07E-3
UAC	0.458	67	0.76	3	9	0.2	2.33E-3
LMC	0.426	43	0.65	3	9	0.2	4.93E-3
LA	0.458	77	0.76	3	9	0.2	1.53E-3

Notes:

1. Sensitivity (S_t) of Hong Kong marine clays is 3 to 5 with an average 4 (Cheung & Yeung, 2009); $\chi_0 = S_t - 1$
2. μ^*/μ^*_i is taken as 1.5

The Fill layer has been modelled using Mohr Coulomb with a unit weight γ of 19 kN/m3, Young's modulus E of 20MPa, Poisson's ratio ν' of 0.3, ϕ' of 32° and drainage type Drained. The modelled groundwater level is +1.5mPD. Consolidation analysis has been run with updated mesh and updated pore pressure to consider the submergence effect and the reduced clay thickness due to ongoing clay compression. In consolidation, the left and right drainage boundaries are closed due to symmetry and the top and bottom boundaries are open. Table 5 summarizes the modelled construction phases, as per the real construction program.

Table 5: Modelled construction phases.

Phase	Activity	Increment in days in PLAXIS	Contract day
0	Initial equilibrium	0	130
1	Fill to +2mPD	22	152
2	Rest period	9	161
3	Install PVD	18	179
4	Rest period	34	213
5	Fill to +6.4mPD	14	227
6	Rest period	185	412
7	Fill to +10.8mPD	26	438
8	Rest period	672	1110

Notes:

1. Thickness of fill placed has considered the on-going compression at the top of UMC
2. Actual filling only started on Contract day 130

Four analyses have been carried out to assess the effects of destructuration and creep on the predicted subsurface settlements and epwp in the UMC and LMC, see Table 6.

Table 6: Features modelled in four analyses.

Analysis	Anisotropy	Destructuration	Creep
A1	Yes	Yes	Yes
A2	Yes	No	Yes
A3	Yes	Yes	No
A4	Yes	No	No

5 NUMERICAL RESULTS

Figure 10 shows the predicted subsurface settlements in the UMC and LMC from all analyses. The data points and the lines represent the measurements and the predictions respectively. Analysis A1 modelling both destructuration and creep predicts well the subsurface settlements. A2 without destructuration and A3 without creep under predict the subsurface settlements, predicting 0.51m and 0.33m less settlement respectively at the top of UMC. A4 without both destructuration and creep significantly under predicts the settlement at the top of UMC by 0.87m. This demonstrates the importance of incorporating both destructuration and creep in predicting soft clay settlements.

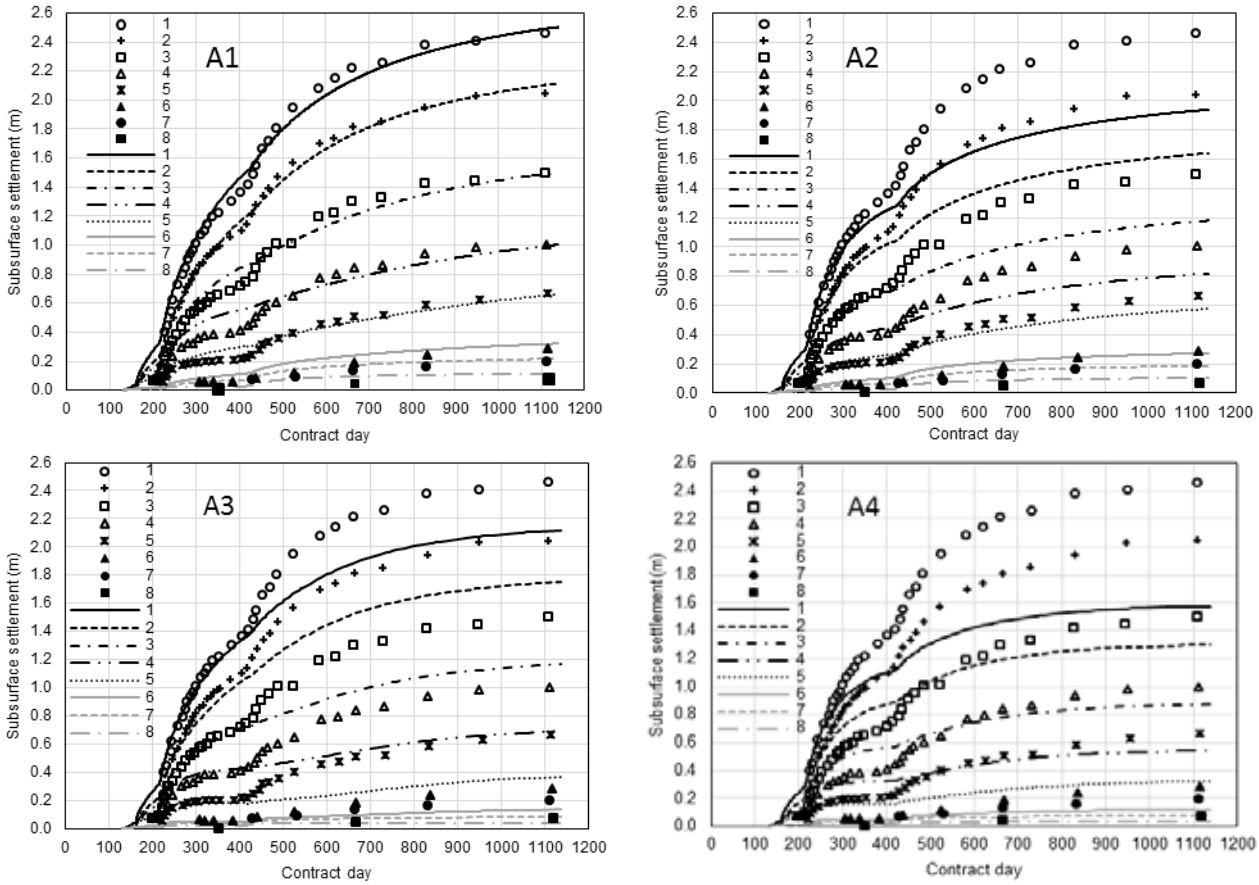

Figure 10: Predicted subsurface settlements in UMC (Point 1-5) and LMC (Point 6-8)

Figure 11 shows the predicted epwp in the UMC from all analyses. Analysis A1 predicts reasonably well the generation and dissipation of epwp, except from Day 900 onward when the measured epwp ceased dissipating. A2 without destructuration under predicts the maximum epwp by 38kPa. A3 without creep predicts reasonably well epwp, being slightly less than the A1 prediction by 10kPa. A4 without both destructuration and creep shows a more significant under prediction of epwp.

Figure 12 shows the predicted epwp in the LMC from all analyses. The slow dissipation of epwp from Day 438 onward cannot be predicted by all analyses. This could be due to (i) inadequacy of the soil constitutive model or/and (ii) inappropriate input of soil/PVD permeability or flow boundary conditions. A4 shows that excluding both destructuration and creep significantly under predicts the epwp from Day 650 onward.

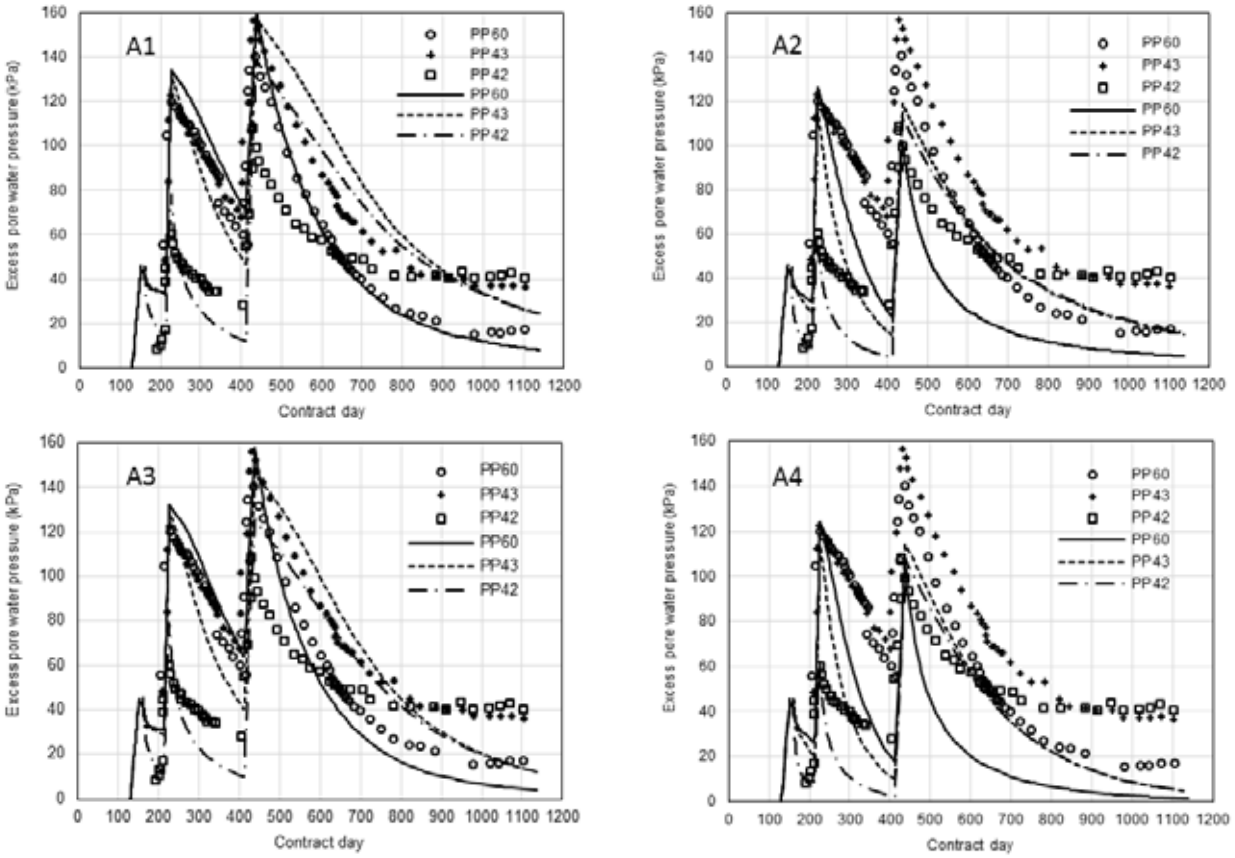

Figure 11: Predicted epwp in UMC

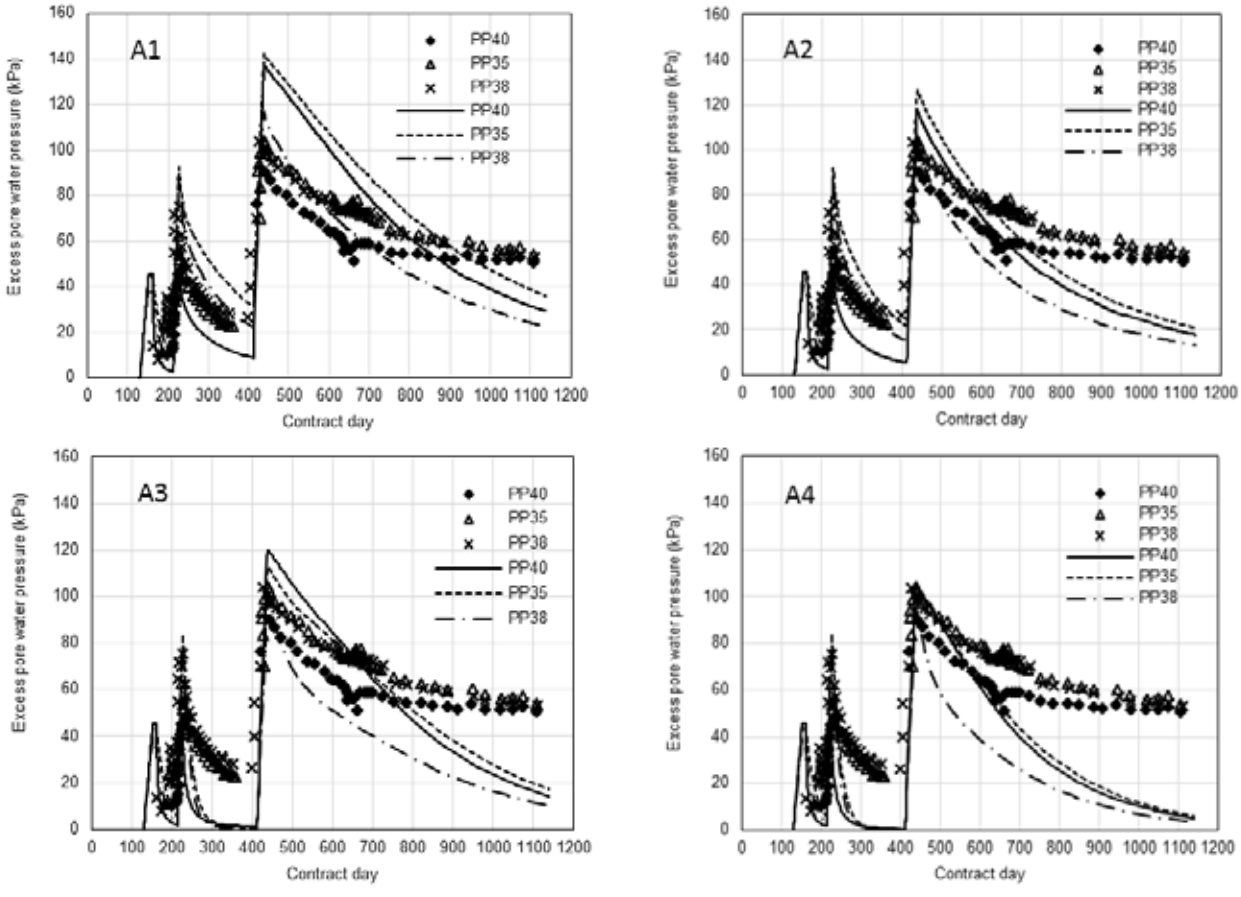

Figure 12: Predicted epwp in LMC

6 DISCUSSION AND CONCLUSIONS

In practice, soil samples are subject to disturbance during sampling in the field and sample preparation in the laboratory, resulting in a partial/total destroy of bonding. An issue with oedometer test is too large increments in loading that misses the yield point of natural soil sample and hence the high post yield λ^* value. All these factors result in the measured λ^* value being close to the intrinsic value λ^*_i, see Figure 1. In this scenario, the effect of bonding and its subsequent degradation should be exclusively considered in modelling. The destructuration feature in Creep-SCLAY1S allows the specification of bonding through a sensitivity (S_t) parameter and the subsequent degradation of bonding with irrecoverable strain, i.e. it mimics the compression curve of natural soil in Figure 1.

Care should be exercised when using an elevated value of λ^* to indirectly allow for additional volumetric strains caused by destructuration (Koskinen et al. 2002). The is because (i) destructuration proceeds at different rates with different stress paths, and (ii) when loading is increased to many time higher than the yield stress, destructuration proceeds until λ^* reduces to λ^*_i.

Creep rate is dependent on the OCR of clay, and hence it is important to establish a correct initial OCR in initial stress equilibrium. Construction induced stress path will change the relative position of Current State Surface (CSS) and Normal Consolidation Surface (NCS) in Figure 3, hence changing the OCR. Creep-SCLAY1S tracks the change in OCR due to both stress change and time increase, which is important in estimating creep settlement during construction and in long term.

The back-analysis of Chek Lap Kok test embankment reveals that the features of destructuration and creep need to be included in order to better predict the measured subsurface settlements in the foundation clays. Without them, the settlement at the top of UMC was under predicted by 0.87m (60% due to destructuration and 40% creep). Even the advanced Creep-SCLAY1S model cannot predict the slower dissipation of epwp in the latter part of consolidation of rest period. This could be due to the inadequacy of the soil model or/and the inappropriate input soil/PVD permeability or flow boundary conditions.

APPENDIX A

Compressibility and strength		Anisotropy	
κ^*	$\kappa^* = C_S/\{\ln 10\,(1 + e_0)\}$ C_S is swelling index from oedometer test e_0 is initial void ratio	α_0	$\alpha_0 = 1/3(\eta_{K0}^2 + 3\eta_{K0} - M^2)$ $\eta_{K0} = \{3(1 - K_0^{nc})\}/(1 + 2K_0^{nc})$ $K_0^{nc} = 1 - \sin\phi'$
λ^*_i	$\lambda^*_i = C_C/\{\ln 10\,(1 + e_0)\}$ C_C is compression index from oedometer test on reconstituted soil	ω	$\omega = (1/\lambda^*)\ln\{(10M^2 - 2\alpha_0\omega_d)/(M^2 - 2\alpha_0\omega_d)\}$
M	$M_c = 6\sin\phi'/3 - \sin\phi'$ in triaxial compression $M_e = 6\sin\phi'/3 + \sin\phi'$ in triaxial extension	ω_d	$\omega_d = 3/8\{(4M^2 - 4\eta_{K0}^2 - 3\eta_{K0})/(\eta_{K0}^2 - M^2 + 2\eta_{K0})\}$
Destructuration		Creep	
χ_0	$\chi_0 = S_t - 1$ S_t is sensitivity, e.g. ratio of peak to remoulded strength from field Vane test	μ^*_i	$\mu^*_i = C_\alpha/\{\ln 10(1+e_0)\}$ C_α is secondary compression index from oedometer test on reconstituted soil
ξ	$\xi \approx 9$; Gras et al. (2015)		
ξ_d	$\xi \approx 0.2$; Gras et al. (2015)		

Note: When the structure (bonding) feature is switched off, i.e. $\chi_0 = 0$, intrinsic λ^*_i and μ^*_i derived from test on reconstituted sample become λ^* and μ^* derived from test on natural sample

REFERENCES

Chai, J.C. & Miura, N. 1999. Investigation of factors affecting vertical drain behaviour. *J. Geotechnical and Geoenvironmental Engineering, ASCE*, 125(3): 216-226.

Cheung, C. & Yeung, A.T. 2009. Statistical analyses of geotechnical engineering properties of Hong Kong marine clays. *2nd Int. Conf. New Developments in Soil Mechanics and Geotechnical Engineering*. *North Cyprus*, 534-561.

Choa, V., Wong, K.S. & Low, B.K. 1990. *New airport at Chek Lap Kok – Geotechnical review and assessment*. Consulting Report to Maunsell Pte Ltd, Singapore.

Foott, R., Koutsoftas, D.C. & Handfelt, L.D. 1987. Test fill at Chek Lap Kok, Hong Kong. *J. Geotechnical Engineering, ASCE*, 113(2): 106-126.

Gens, A. & Nova, R. 1993. Conceptual bases for a constitutive model for bonded soils and weak rocks. In Anagnostopoulos et al. (eds.), *Geotechnical Engineering of Hard Soils – Soft Rocks*, Balkema, 485-494.

Gras, J.P., Sivasithamparam, N., Dijkstra, J. & Karstunen, M. 2015. Permissible range of model parameters for natural fine grained materials. Submitted to *Acta Geotechnica*.

Koskinen, M., Karstunen, M. & Wheeler, S.J. 2002. Modelling destructuration and anisotropy of a natural soft clay. In Mestat (ed.), *5th European Conference Numerical Methods in Geotechnical Engineering*, 11-19.

Koutsoftas, D.C., Foott, R. & Handfelt, L.D. 1987. Geotechnical investigation offshore Hong Kong. *J. Geotechnical Engineering, ASCE*, 113(2): 87-105.

Lo Presti, D.C.F., Jamiolkowski, M. & Pepe, M. 2003. Geotechnical characterization of the subsoil of Pisa Tower. In Tan et al. (eds.), *Characterization and Engineering Properties of Natural Soils*, Balkema, Vol. 2: 909-946.

Long, R. & Covo, A. 1994. Equivalent diameter of vertical drains with an oblong cross section. *J. Geotechnical Engineering, ASCE*, 120(9): 1625-1629.

Low, H.E. 2004. *Compressibility and undrained behaviour of natural Singapore marine clay: effect of soil structure*. MEng thesis, National University of Singapore.

Sivasithamparam, N., Karstunen, M. & Bonnier, P. 2015. Modelling creep behaviour of anisotropic soft soils. *Computers and Geotechnics*, 69: 46-57.

Zhu, J.G. 1999. *Experimental study and elastic visco-plastic modelling of the time-dependent stress-strain behaviour of Hong Kong marine deposits*. PhD thesis, The Hong Kong Polytechnic University.

A Special Problem with Ground Investigation Works in Reclaimed Areas in Hong Kong - Buried Unexploded Bombs

H. C. Chan, H. S. Leung & Y. L. Cheung
Geotechnical Engineering Office, Civil Engineering and Development Department,
Hong Kong SAR, China

ABSTRACT

From time to time unexploded bombs left over from World War II are encountered in different locations in Hong Kong and they pose serious safety hazards to the general public. In reclaimed areas the hazards are more severe as the unexploded bombs are usually buried under the reclamation fill and may not be detected easily. In these cases, to mitigate the risks of loss of lives, injuries and damages by hitting and inadvertently setting off an unexploded bomb during drilling for the purpose of ground investigation, special safety procedures have been developed. A possible added safety procedure using TDR is also being developed. The TDR technique has been trialed in a number of cases in office, depot and field environments. Encouraging results have been obtained which show that the technique could probably be used for monitoring of drilling progress and detection of buried metallic objects encountered by the casing and drilling/sampling head. Another interesting observation is that the TDR technique can also work on a single conductor.

1 INTRODUCTION

Ground investigation (GI) works involving drillholes were to be carried out in a reclaimed area in Hong Kong, to provide information on the ground conditions and soil properties to support the design of excavation works. During the planning of the GI works the land owner advised that there could be unexploded bombs left in the ground since World World II, but the types, quantities and locations of the unexploded bombs were unknown. Unlike most cases on non-reclaimed land, the unexploded bombs are expected to be buried at considerable depths under fill (i.e. reclamation fill) and may not be detected easily. Subsequently a joint site meeting was carried out between the land owner, the design engineer and the GI contractor. At first the possibility of locating the unexploded bombs by geophysical survey was considered. However, due to the large amounts of underground utilities (e.g. water pipes, electrical ducts, drainage pipes, etc) existing on site, geophysical methods were considered not very appropriate.

To avoid the hazard of hitting and inadvertently setting off an unexploded bomb during drilling, special safety procedures have been developed. A possible added safety procedure using TDR (Time Domain Reflectometry) is also being developed and some encouraging results have been obtained.

2 RISK ASSESSMENT AND MITIGATION

2.1 Introduction

Unexploded bombs are discovered in different areas in Hong Kong from time to time, and a good summary of the discoveries can be obtained from the Explosive Ordnance Disposal Bureau. Possible bomb types include air bombs, mortar bombs, grenades, torpedoes, and mines. Many of the bombs are found lie near the ground

surface, but some are buried. In reclaimed areas, most of the bombs are expected to be buried under the reclamation fill, and some have been discovered during excavation or dredging operations (Gallagher 2014, CEDD webpage at http://www.cedd.gov.hk/ eng/services/fillmanagement/doc/guidance_note.pdf). The buried bombs pose a special risk to GI works including drilling and digging of trial pits. Prominent examples (obtained from Explosive Ordnance Disposal Bureau and other sources) include the following:

1. During the reclamation for Disneyland Park, Penny's Bay in the period from June 2000 to November 2002, 488 bombs were encountered and dealt with.
2. When a cargo ship was mooring off Tsing Yi Island on 6 July 1995, a 500-pound bomb was accidentally lifted from the seabed by the ship's anchor.
3. During the reclamation of an area outside Victoria Park in March 2015, a 400-pound Japanese mortar bomb buried at 15m depth, containing 110 pound of TNT was found. The bomb's steel shell was about 1 inch (i.e. 25mm) thick and it had a large potential area of destruction.

To avoid the hazard of hitting and inadvertently setting off an unexploded bomb, the site workers could be pre-warned and advised to use extra precaution while digging manually. However, for drilling, special safety procedures need to be developed as the drilling and sampling equipment often encounter hard objects such as boulders, concrete pieces, abandoned buried utilities which could not be found on records, etc. A bomb could be mistaken to be one of these hard objects and accidents could occur if the GI operations are continued as normal. The following sections present risk assessments of the drilling operation and propose special safety procedures for drilling. In Section 3 a possible added safety procedure using TDR is presented.

2.2 Risks arising from rotary core drilling, field testing and soil sampling

Rotary drilling rigs (Chan & Lau, 1986) and portable soil sampling systems (Chan et al 2001) of different power outputs are commonly employed in field testing and sampling. Before drilling is started, a "surface geophysical" detection equipment such as electro-magnetic pipe locator is often adopted to locate any utilities nearby and an inspection pit is manually dug at the location of the hole. Field testing typically includes standard penetration test (SPT), vane shear test, constant/falling head permeability test and cone penetration test. Soil sampling typically includes triple-tube soil sampling, SPT sampling, U-100 sampling and piston sampling.

Special risks arise in the conduction of the above ground investigation activities when potential buried bombs are present. The bombs buried at considerable depth (i.e. > 5m) may not be detected before the commencement of drilling. The driller may notice the presence of buried bomb from decreased advance rate when the drill bit touches the bomb shell, however, the driller could mistake the metallic object to be a boulder. If the driller increases the feed force on the drill bit to break through the "boulder", damage or explosion of the bomb may result. Similarly, the workers can hardly be aware of the presence of buried bomb during dynamic probing tests.

Bomb explosion leads to a blowout through the drillhole and may injure the workers. The vibration can also damage nearby facilities. In the worst scenario, a bomb at shallower depth can blow up the works areas during explosion. On the other hand, partial damage to the bomb's shell and explosive causes a precarious situation and may hinder further works. The original drillhole alignment may also be affected due to a bomb explosion.

The special risks are summarized in Table 1.

2.3 *Suggested special safety precaution measures for drilling*

Some special safety precaution measures have been developed for a GI works order in a reclaimed area in Hong Kong, by a term GI Contractor of GEO, CEDD, with input from a geotechnical Consultant. The precaution measures are summarized as follows:

1. Although the chance is very low, but if we are going to encounter unexploded ordnance, it will be at the time when the drill rig is operating.
2. Unexploded ordnance will normally not be left in in-situ saprolite, so once we have drilled through the fill layer/superficial deposits, the risk of encountering unexploded ordinance may reduce.
3. 3m deep inspection pit shall be excavated at each drill hole location to eliminate the risk of encountering unexploded ordnance at shallow depth.

4. At greater depth, the likely consequence of drilling works encounter unexploded ordnance is mainly shattering of the drill rigs. Therefore, the drill rig operator and the assistant shall step back slightly and stay away from the rig during the drilling operation. Only essential personnel should stay in the vicinity of the drill rig.
5. Special attention should be paid when hard material is encountered, especially when the drilling is within Fill or Marine Deposit layers, the drill hole should be terminated when necessary.

Table 1: Special risks when potential buried bombs are present

Activities	Hazards due to bomb explosion	Likelihood	Severity
Inspection pit excavation	· Life losses and injuries	Low	High
	· Damage to properties	Low	High
Drilling, SPT test/sampling or U-100 sampling	· Life losses and injuries	Medium	High/Medium
	· Damage to the bombs	Medium	Low
	· Disruption to drillhole alignment	High	Low
Other tests/sampling	· Life losses and injuries	Low	High/Medium
	· Damage to the bombs	Low	Low
	· Disruption to drillhole alignment	Low	Low

Among the different testing and sampling activities, more attention should be paid to SPT or U-100 sampling/testing as they are more likely to set off unexploded ordnance if encountered. The ground condition should be closely kept in view to make timely adjustment on site regarding SPT or U-100 sampling/testing. It is advisable to curtail these activities in fill with hard fragments, if practicable.

3 POSSIBLE ADDED MONITORING PROCEDURE USING TDR TO ENSURE SAFETY

3.1 Background and theory

Time domain reflectometry (TDR) has been widely used in the power transmission industry as a non-destructive method for detecting anomalies along coaxial cables (O'Connor & Dowding, 1999; Siddiqui et al, 2000). The technique involves sending an electrical pulse by a TDR equipment (commonly called a cable fault finder, which consists of a pulse generator and an oscilloscope) along a pair of parallel conductors surrounded by a dielectric material. The velocity of propagation of the pulse depends on the arrangement and electrical properties of the conductors and the dielectric constant of the surrounding material. As the pulse travels along the conductors, reflections are created where the conductors change in electrical properties or cross-section, or where the surrounding material changes. The oscilloscope shows the time of travel of the reflections from the location where the changes occur to a reference position in the TDR equipment. In Hong Kong, TDR has been widely used as a non-destructive method for quality control of soil nailing works (Cheung 2006), in which the soil nail and a copper wire form a pair of parallel conductors.

During hole drilling, SPT testing and soil sampling are often carried out, in which case the casing and the drill rod/sampler form a coaxial conductor. Therefore the TDR technique could be applied. Where the outer and inner conductors are in contact with a metallic object such as a buried bomb or piece of metal, by applying TDR measurement, the presence of such a metallic object could be detected.

Furthermore, a fairly common conception is that TDR works on parallel conductors only, however, it can be shown that pulse travel velocity and reflections can also be detected in a single conductor. In the latter case the reflected signals are usually weaker and are more prompt to be affected by a larger surrounding environment. The authors consider that the cause of this phenomenon is that the return path of the pulse and reflections is more uncertain and depends on the surrounding environment.

3.2 Initial trial results

A number of initial trials in the office, depot and field environments have been carried out and are summarized in Table 2. In each trial the times to the first major reflection and further reflections if seen were recorded. Since the lengths of the conductors used were known, the velocity of pulse propagation was calculated by dividing the length travelled by the time of the reflection. For example, in Trial No. 9, an HW casing of length 1.08m was set up in a depot (Figure 1). A coring barrel attached with a drill rod, of total length 1.19m, was placed inside the casing and served as the inner conductor of a coaxial conductor, with the casing acting as the outer conductor. The two poles of a TDR equipment were then connected to the outer and inner conductors, and the display unit showed the reflections of the pulse as measured by the oscilloscope (Figure 2). The horizontal axis of the display represented time and the vertical axis voltage. Further descriptions of the working of the TDR equipment can be found in Cheung (2006). In Figure 2, the dashed vertical line on the left marked the time of the pulse when leaving the poles of the TDR equipment, while the solid line on the right marked the time of the first major reflection. From Figure 2, the time of travel of the pulse from the poles of the TDR equipment to the location of the first reflection and back to the poles is about 10 ns. Hence the velocity v of the pulse is given by

$$v = \text{distance travelled} / \text{time of travel} = 1.08 \times 2 / 10 = 0.216 \text{ m/ns} \quad (1)$$

The above deduced value of v is a reasonable value for electrical pulse propagation along parallel metallic conductors in air. The pulse propagation velocities deduced in the Trials Nos. 1, 2, 5, 8, 9 and 10 also fall into reasonable ranges. However, for cases where the conductors are longer than about 20m, it was difficult to interpret the reflections which are mostly weak in magnitude. Therefore, so far the TDR method has been shown to be applicable to the common ground investigation setup for hole drilling only at shallow depths, say, less than 10m. This limitation may be due to the limited power output of the TDR equipment used, rather than the nature of TDR.

Figure 1: HW casing with length 1.08m

Another remarkable result is from Trial No. 8, in which a steel channel was placed under the casing and barrel of Trial No. 9. In the resulting display shown in Figure 3, it can be seen that the time of travel to the first reflection is also about 10 ns, but a closer inspection shows that the reflected wave form was substantially different from Figure 2. Therefore, in this case, the presence of metal at the bottom ends of the inner and outer conductors can appreciably change the reflected wave form (enclosed in red circles in the figures).

Another remarkable case was Trial No. 10 in which an SW casing 2.15m in length was placed inside an inspection pit. Connecting the positive pole of the TDR equipment to the casing top, with the negative pole unconnected, produced a display shown in Figure 4. Reflections are observed and the time to the major reflection is about 30 ns. Thus there is a potential to apply the TDR technique to a single conductor such as a casing.

Furthermore, in Trial No. 4, the inverted reflection noted was probably caused by inadvertent touching of the Triple-tuble sampler with the HW casing.

Table 2: Summary of initial trials

Trial No.	Date	Conductors/length	Environment	Remarks
1	9.11.2015	2 piston samplers/ 1.096m	Office	Noticeable reflection
2	10.11.2015	SPT Sampler inside HW casing/ 1.645m	Depot	Noticeable reflection when positive pole is connected with casing
3	10.11.2015	PW casing, HW casing, Triple-tuble sampler/ 36.15m	Field	Noticeable multiple reflections
4	10.11.2015	PW casing, HW casing, Triple-tuble sampler/ 38.29m	Field	Inverted reflection noted
5	13.11.2016	HW casing, piezometer with connecting steel rod/ 9.10m	Field	Noticeable reflection when positive pole is connected with casing
6	20.1.2016	PW casing/ 21m	Field	Weak reflections noted
7	20.1.2016	PW casing, piezometer with connecting steel rod/ 21m	Field	Weak reflections noted
8	17.3.2016	HW casing, sampling barrel with connecting steel rod, steel channel at bottom/ 1.08m	Depot	Noticeable reflection
9	17.3.2016	HW casing, sampling barrel with connecting steel rod/ 1.08m	Depot	Noticeable reflection
10	1.4.2016	SW casing/ 2.15m	Field	Noticeable reflection

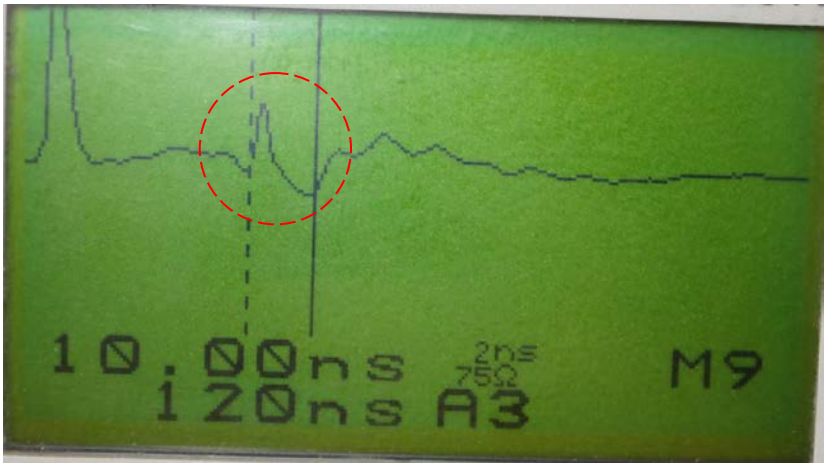

Figure 2: Barrel and rod inside HW casing

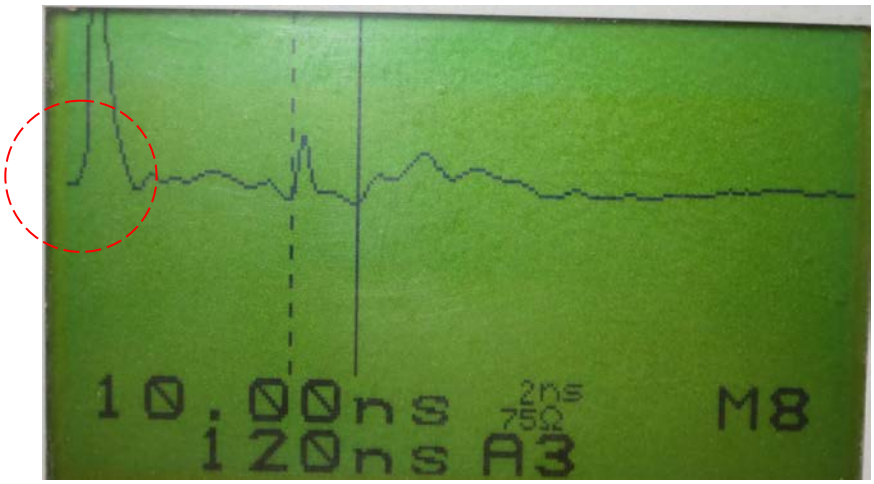

Figure 3: Barrel and rod inside HW casing, with channel at bottom

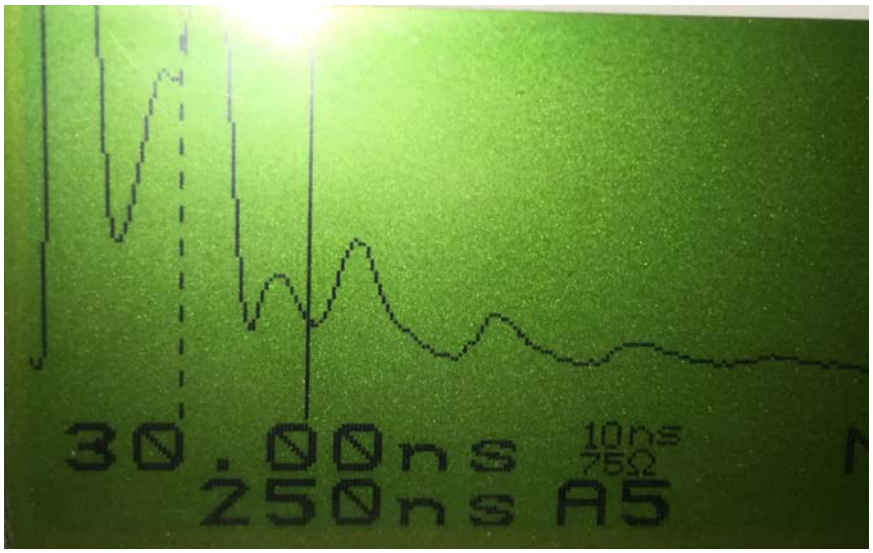

Figure 4: SW casing inside inspection pit

3.3 Discussion and possible further improvements

The TDR technique has been trialed in a number of cases in office, depot and field environments. Encouraging results have been obtained which show that the technique could probably be used for monitoring of drilling progress and detection of buried metallic objects encountered by the casing and drilling/sampling head. Presently noticeable reflections for only relatively short (say, less than 10m) conductors can be obtained. However, this is probably due to the limited power output of the TDR equipment used in the trials, rather than the nature of TDR. Another interesting observation is that the TDR technique can also work on a single conductor, in addition to parallel conductors.

The TDR technique can be conveniently applied to the existing drilling setups without any modification, and measurements can be done fairly quickly. It can potentially be used to monitor drilling progress and detection of buried metallic objects, including bombs, under the casing or drilling head/sampler. The particular TDR equipment being used in this study is also commonly used for soil nail length testing, and is found to be able to give meaningful reflections for conductors (i.e. casings or drilling heads/samplers) less than about 10m in length. Regarding bomb detection, the most dangerous buried depth is expected to be several meters, as bomb explosion creating a crater 3m deep has been reported (Gallagher 2014). At several

meters depth, a buried bomb normally cannot be detected by manual digging, and geophysical methods may also have limitations in its detection. Should the bomb be accidentally set off by drilling, the whole works area and nearby areas could be blown up, resulting in serious loss of lives, injuries and property damages. In a site where unknown buried bombs are suspected, drilling should be carried out with more caution than normal, and the TDR technique could be used to assist detection of any bombs encountered.

For further improvements, more trials can be carried out with more powerful TDR equipment. More detailed studies of the reflected waveforms should be carried out so that the TDR technique can be used for monitoring of drilling progress and detection of buried metallic objects. More trials should also be carried out on single conductors (e.g. a casing), which could render the technique more useful.

4 CONCLUSIONS

In reclaimed areas serious hazards may arise during ground investigation activities where unknown unexploded bombs are present. The unexploded bombs are usually buried under the reclamation fill and may not be detected easily. In these cases, to mitigate the risks of loss of lives, injuries and damages by hitting and inadvertently setting off an unexploded bomb during drilling, special safety procedures have been developed. A possible added safety procedure using TDR is also being developed. The TDR technique has been trialed in a number of cases in office, depot and field environments. Encouraging results have been obtained which show that the technique could probably be used for monitoring of drilling progress and detection of buried metallic objects encountered by the casing and drilling/sampling head. Another interesting observation is that the TDR technique can also work on a single conductor. Further possible improvements to the TDR technique have also been suggested.

ACKNOWLEDGEMENTS

This paper is published with the permissions of the Head of the Geotechnical Engineering Office and the Director of Civil Engineering and Development, The Hong Kong SAR Government.

REFERENCES

Chan, M.H.C., Leung, B.N., Pang, P.L.R. & Pyle, S.M. 2001."Development of a portable triple-tube sampler for slope investigations", *Proceedings of the Fourteenth Southeast Asian Geotechnical Conference*, *Hong Kong*, vol. 1, pp 715-718.

Chan, M.P. & Lau, S.H. 1986. Drilling in Hong Kong. *Contractor (Hong Kong)*, May 1986: 11-14.

Gallagher, S. 2014. Let's not rely on luck when it comes to unexploded bombs. South China Morning Post. Available at http://www.scmp.com/news/hong-kong/article/1604055/.

Cheung, W.M. 2006. *Use of Time Domain Reflectometry to Determine the Length of Steel Soil Nails with Pre-Installed Wires*. GEO Report No. 198. Geotechnical Engineering Office, Hong Kong, 37 p.

GEO. 1987, *Guide to Site Investigation (Geoguide 2),* Geotechnical Engineering Office, Hong Kong.

O'Connor, K.M. & Dowding, C.H. 1999. *GeoMeasurements by Pulsing TDR Cables and Probes*. CRC Press, 394 p.

Siddiqui, S.I., Drnevich, V.P., & Deschamps, R.J. 2000. Time domain reflectometry for use in geotechnical engineering. *Geotechnical Testing Journal*, ASTM, vol. 23, No. 1.

Geotechnics of Quaternary Marine Deposits in Hong Kong

N. R. Wightman
Aquaterra Consultants Limited, Hong Kong

ABSTRACT

The size of reclamations in Hong Kong's has steadily increased since the early 1900's to supplement the limited supply of buildable land. The engineering considerations have also become more complex as the marine soils are encountered in deeper and thicker sequences. including the underlying residual soils and saprolites. With both current and future reclamations being located in areas of substantial clay thickness (over 30m thick), sequence logging is essential. Early descriptions of offshore geology were grouped into marine mud and alluvial sand / clay strata, which was later modified when distinct secondary layers were encountered too upper alluvial and lower alluvial strata. With multiple layers being encountered in much thicker sequences and with distinct changes in soil properties, this paper highlights the quaternary sequence in detail based on research from HKU. The geotechnics of the sequences and the engineering behaviour of these thicker marine quaternary clays is governed by their properties particularly their sensitivity to disturbance and the presence of dissolved gases produced through long term thermogenic processes. The focus is on accurate observations and geological modelling, modifying ground investigation procedures to obtain correct data and obtaining meaningful geotechnical parameters for design is vitally important prior to reclaiming land.

1 INTRODUCTION

1.1 Historical land record

It has long been established that Hong Kong's limited supply of buildable land can be increased by reclamation processes from the current shoreline. The size of reclamations since early 1900's has steadily increased in the Victoria Harbour area from being near the original shorelines to almost mid harbour. Consequently the seabed soils and deeper quaternary strata are encountered in thicker sequences such as at West Kowloon, Hung Hom and Central reclamations. The underlying residual soils and saprolites are also encountered as thicker strata.

In more recent decades, large reclamations or constructions have been constructed outside the immediate harbour area for breakwaters, railways, airport, amusement parks and other commercial uses. Locations are to the west of Hong Kong include areas such as Tai O, Penny's Bay, and Tsing Yi and to the East at Tsueng Kwan O. The offshore 'island' type constructions as at Chek Lap Kok and the future artificial islands between Hong Kong and Lantau tend to cover extensive areas. Each location encounters similar geological conditions and geotechnic concerns.

1.2 Previous studies

Case studies have now shown that often dredging of the clays was not carried out due to the disposal volumes and disposal concerns. Other literature has shown that sub-dividing the quaternary deposits is possible into a layered sequence relating to the glacial / interglacial cycles when the sea level fluctuated by over 100m. This is especially pertinent in the areas to the west of Hong Kong, centred around the Pearl River Estuary, which has a historical record of geology which extends beyond the Holocene period into the earlier quaternary

period. These are represented by very thick layers of clay which were laid down in marine environments between the ice ages (i.e. periods of high sea level) and includes granular deposits from the glacial periods. The nature and behaviour of the Quaternary deposits in Hong Kong has typically been with oversimplified with descriptions for offshore soils being described as either marine mud, alluvium and saprolite following the main geological stratigraphic descriptions. While it suited earlier geologists and geotechnical engineers to group the encountered thin layers of soils into some main geological groupings, projects are now encountering much thicker sequences of offshore deposits than those represented by this simple descriptive model.

This paper introduces a more detailed model for describing and categorising the quaternary deposits to meet geological and engineering standards that are demanded by today's designs. The range of geotechnical properties is wide with one clay display high sensitivity properties which causes high loss of strength when disturbed. Dissolved gases derived from thermogenic disintegration of shell matter is also encountered. It is important to understand the unusual nature of these deep marine soils. They require special attention and study to understand their true variation of properties and often extreme engineering behaviour. It is vitally important to obtain quality geological information and improved modelling with related geotechnics prior to undertaking any engineering designs for reclamations.

2 EXAMINING THE QUATERNARY GEOLOGY

2.1 Quaternary geology

The quaternary period extended for 1.8 million years up to the last ice age about 12,000 years ago. The Pleistocene quaternary sequences lie directly below the soft Holocene marine muds. It is important to realise that the quaternary strata in Hong Kong for the last 0.5 million years has been directly influenced by the past glacial cycles and the falling and rising of the corresponding sea levels (Yim *et al*, 2004). The multiple layering of clay and sand deposits that formed the Chek Lap Kok (CLK) formation (Fyfe *et al*, 2000) is seen though out the coastal waters of Hong Kong. The CLK formation is thinner near shore and within the Victoria Harbour area but much thicker sequences with more layers have been encountered to the west in Tai O and north of Lantau Island.

There is a direct relationship to alluvial sands being deposited during depressed sea levels during periods of glaciation and marine clay being deposits during warmer calmer inter glacial periods when the sea level recovered (Yim & Choy, 2004). It is important to distinguish each stratum in order to accurately model the marine geology. This model, shown in Figure 1, describes soils in relation to their suggested geological history as defined by the sequencing produced from the glacial cycles. This model firstly aids the observations from sampling by allowing the sequence to be correctly labelled and secondly allows the parameters derived to be grouped correctly together to create a more accurate set of design inputs.

2.2 The Quaternary glacial cycles

The Quaternary glaciation cycles have been described as lasting 0.5 million years with five distinct cycles, Figure 1, evident similar to other location about the globe and which affected Hong Kong marine geology. The sand strata were deposited when the seabed was exposed during periods of low sea levels (as low as -120m below sea level) and marine clay was deposited during periods of higher sea levels, Figure 1.

Some minor glacial cycles also occurred, which only affected the ground at lower depths with vegetation growth subsequently buried with returning sea levels. The main glacial cycles (Bahr *et al*, 2005) separated the terrestrial sand or granular deposits from the marine clay deposits. All the marine clay layers have plant remains or humus as well as having supported marine life with shell matter left behind but for the earlier clay layers the shell matter has disintegrated through thermogenic processes, Figure 3.

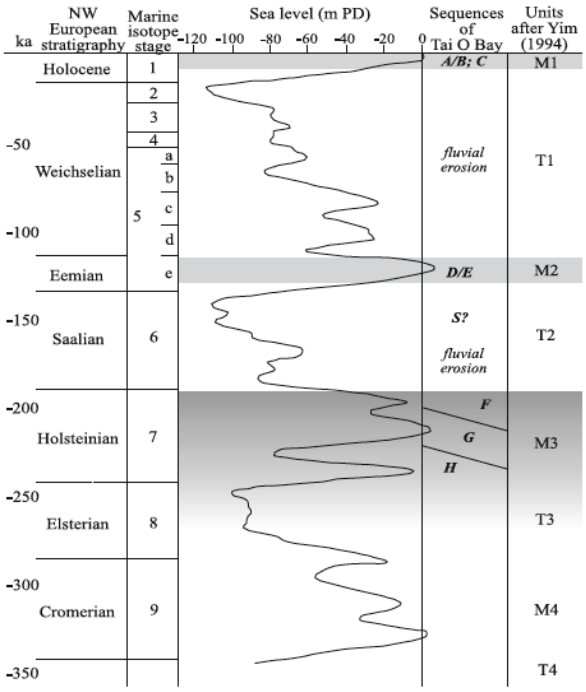

Figure 1: Sea level relationship to quaternary stratagraphical units at Tai O. (Bahr *et al*, 2005)

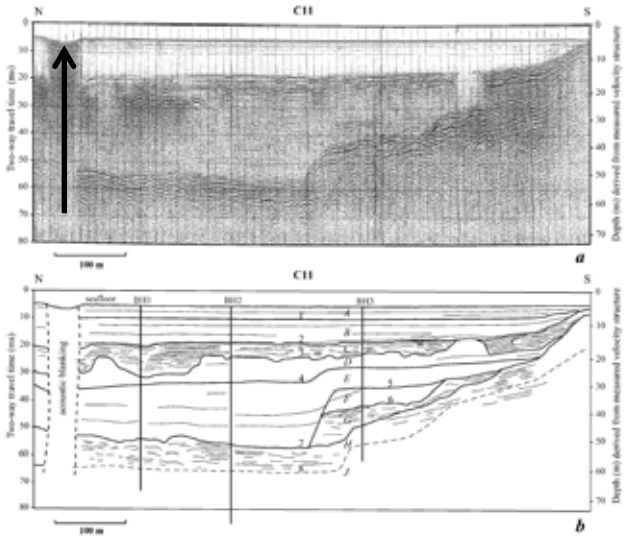

Figure 2: Acoustic masking at the north indicating biogenic gas release from deeper M3 clay. (Bahr *et al*, 2005)

2.3 Thermogenic processes and marine gas

Marine gas in Hong Kong was investigated and reported as occurring in the marine muds, (Premchitt, 1992). Gases from marine layers deep below the seabed have been identified as a plume of bubbles during siesmic surveys, Figure 2, (Bahr *et al*, 2005). Methods to sample and test for gases using monitoring devices and BAT gas sampling equipment was also carried out at Hung Hom (Wightman & Mackay, 2008) which recorded seven gases dissolved in the ground water (O_2, CO, CO_2, H_2S, N, O_2 and CH_4) often reaching saturation levels which causes excess gas to be held in gaseous bubble form.

The main gases of importance were the carbon dioxide and methane content due to being at saturation levels and higher concentrations. The marine clay contains biodegradable material (vegetation, shells and minerals) that promotes microbial activity forming 'holes' in the clay by disintegration of this matter as well as promoting gas formation through thermogenic processes to fill the voids so formed depending on depth. It is known that pyrite from decomposing rock causes acid conditions in clays which eventually dissolve shells fragments hence the older clay layers do not have shell matter present. The by-product of shells (carbonate) dissolving is carbon dioxide. Later thermogenic process of sulphate reduction also creates methane but only once all the carbonate has been depleted. Both carbon dioxide and methane are dissolved and stored in the pore water of the clay due to the net increase in the unit weight of the pore water (up to about 1.06 times pure water). The gases may remain in dissolved form until released by some disturbance such as tidal or reclamation influences.

Gas generation may slowly continue and gases will be released once the pore water becomes over saturated resulting in gas masking on seismic logs. The affect of reclamation is to consolidate the underlying clays but the gradual displacement of the pore water but in this case including the dissolved gases. At Hung Hom the reclamation produced water migration up to a sand layer, which liquefied when encountered. This was the first time in Hong Kong that such an event caused complete tunnel flood inundation. The set of circumstances or the presence of gas, which lead to the liquefaction were not pre-conceived and a normal ground investigation had been carried out. The 'new' data from a more developed ground investigation later showed gas levels were measureable at the surface and from using BAT sampling of groundwater. The interesting fact was that the gas was proven not to be from gas main leakages or decomposition of sewage but emanating from within the deeper Quaternary geology sequence of marine clays.

GASES (Dissolved gas / ions)	Sea Level SEABED	AFFECT OF RECLAMATION FILL OLD SEABED
[Depth <2m] O_2 CO_2	**AEROBIC ZONE** by aerobic reduction only due to dissolved oxygen present. $C_{106}H_{263}O_{110}N_{16}P_1 + 138O_2 \rightarrow 106CO_2 + 16NO_3 + HPO_4^{2-} + 122H_2O + 18H^+ + energy$ After Drever (1982)	**Biogenic zone now possible** **ANAEROBIC SULPHATE REDUCING ZONE**
SO_4^{2-} HS^- HCO_3^- CO_2	**ANAEROBIC SULPHATE REDUCING ZONE** As oxygen becomes depleted, biogenic breakdown of organic material to bicarbonates & sulphides starts. High levels of dissolved sulphate inhibits methane being produced. $2[CH_2O] + SO_4^{2-} \rightarrow 2HCO_3 + HS^- + H^-$ After Nageswaran (1983) or $SO_4^{2-} + 2[CH_2O] + 2H^+ \rightarrow 2CO_2 + H_2S + 2H_2O$ After Canfield (1993)	**ANAEROBIC CARBONATE REDUCING ZONE now possible** Thermogenic breakdown of complex organic / inorganic compounds i.e. shells, to produce methane gas.
CH_4 H_2 CO_2	**ANAEROBIC CARBONATE REDUCING ZONE** Thermogenic breakdown of complex organic / inorganic compounds i.e. shells. Methane first produced by biological reduction of carbon dioxide by biologically produced hydrogen. $CO_2 + 4H_2 \rightarrow CH_4 + 2H_2O$ After Nageswaran (1983)	**Anaerobic carbonate and anaerobic sulphate reducing zone possibly move upwards.** **ANAEROBIC SULPHATE REDUCING ZONE** (Carbon limited)
CH_4 SO_4^{2-} HS^- HCO_3^- CO_2	**ANAEROBIC SULPHATE REDUCING ZONE** (Carbon limited) Thermogenic anaerobic oxidation of methane through sulphate reduction. Pyrite (FeS_2) is also formed under anoxic conditions which readily oxidises to acid. $CH_4 + SO_4^{2-} \rightarrow HCO_3^- + HS^- + H_2O$ After Muralidhar *et al* (2006) or $2[CH_2O] \rightarrow CO_2 + CH_4$ After Stumm & Morgan (1995)	**NO CHANGE** in overall environment

Figure 3: Processes of gas production with depth for both pre and post reclamation conditions.

2.4 Detailed geological modelling of Quaternary deposits

Previous geological models described one layer of alluvial clay, Figure 4, and this was later revised to upper and lower marine clay and alluvium. The lower marine clay can have sub-aerial discolouration plus the marine shell matter has disintegrated, giving the appearance of a non-marine clay layer, which is then identified as being alluvial clay along with the alluvial sandy layers, which occur between the clay strata.

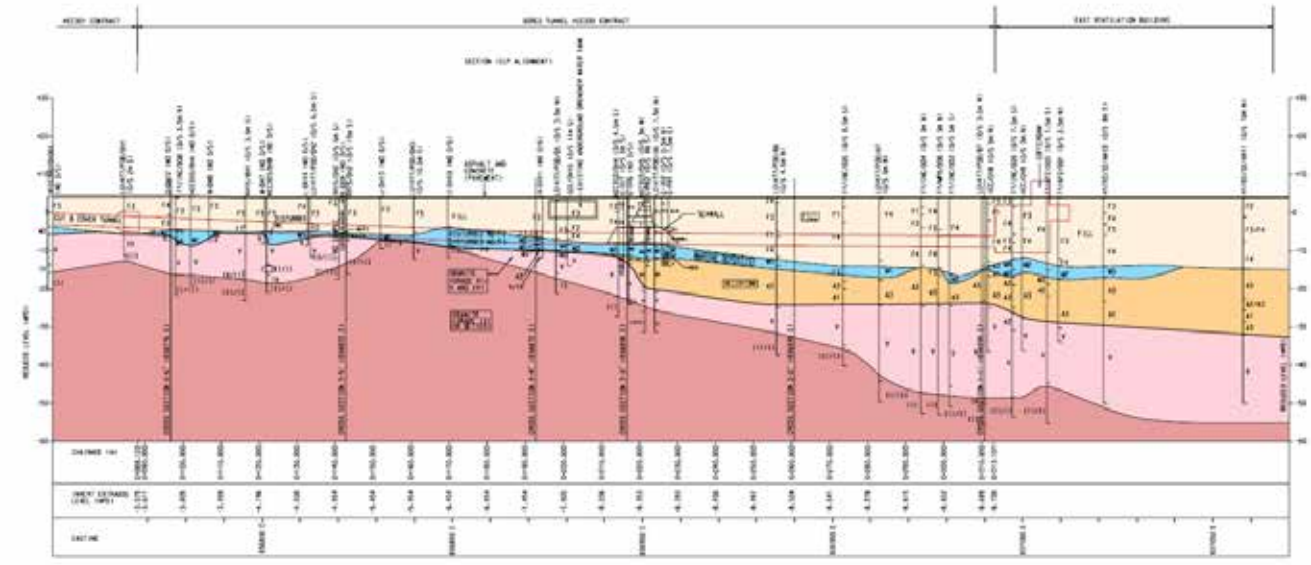

Figure 4: Geological profile of Hung Hom Bay reclamation showing alluvial clay A1 at depth.

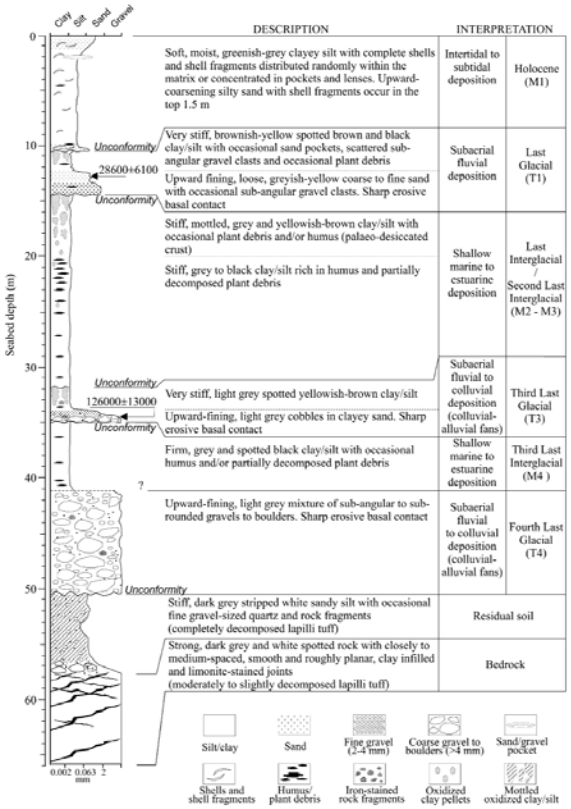

Figure 5: Tai O Bay stratigraphical & lithological description and interpretations (W.W-S Yim *et al*, 2008).

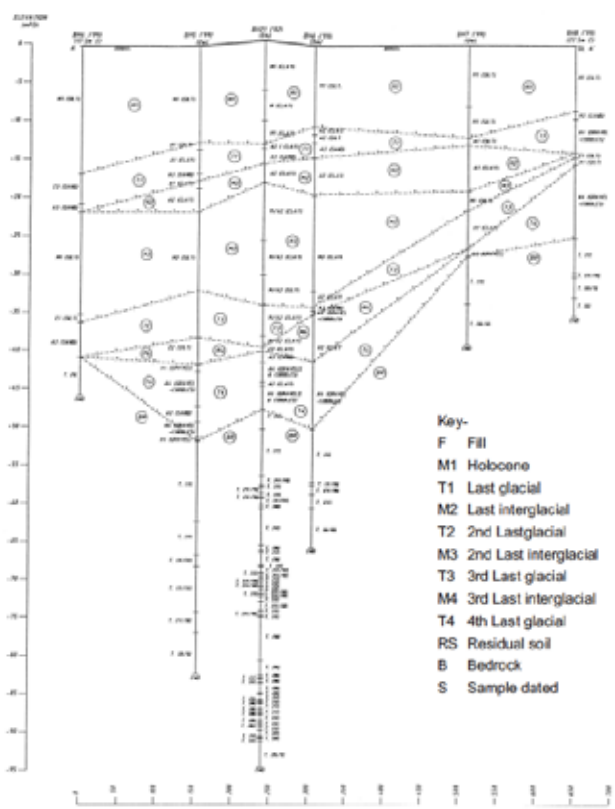

Figure 6: Geological logging at Tai O with glacial cycle units being used to identify distinctly different layers. (Wightman & De Silva, 2008).

Thinly bedded marine and alluvial layers were often combined for ease of modelling particularly as sampling was widely spaced missing geological detail from the profile. With the presences of substantially thicker clays in the waters to the west of Hong Kong, the thickness of clay are in the order of tens of metres, the logging of boreholes needs to be revised to explain the distinct occurrence of the now thicker sand and clay strata and separate out layers with distinctly different geotechnical behaviour. It should be noted that much greater thickness of weathered rock strata occurs in offshore locations due being protected from erosion by the overlying deposited soils. This also has great implications on geological modelling and design aspects of very large reclamations. For instance, residual soil and Grade V completely decomposed granite (CDG) has been recorded as being over 40m thick. Residual soil is also often described as alluvial clay although the soil rests just above the CDG and has no indications of having been transported.

To obtain a complete geological stratigraphic record without gaps, a geological borehole with continuous sampling is required (Wightman & De Silva, 2008) and (Fletcher *et al*, 2000). The importance of continuous logs allows for changes in the type of strata to be observed particularly the tops of the main clay layers which were exposed as seabed and which show discolouration from dark grey to orangey grey after being sub-aerially exposed prior to the next main strata being deposited. Not all sequence strata are found at some locations due to erosion of the surfaces or whole layers. The true thickness of soil layers can be recorded from continuous logs and thinner soil layers will also be logged without being missed by a wide sampling regime. Once these geological borehole samples have been examined, the interpreted geological model will be of benefit in producing the soil properties required for reclamation designs, Figures 5 & 6 and Table 1.

2.5 Offshore soil geotechnics

The offshore geotechnics varies considerably with depth. Each stratum has a set of parameters and change between sand and clay layers being quite pronounced. The sands are granular by nature and dense particle contacts means the soil is dilatant when sheared. Figures 7, 8 and 9 show a typical broad range of results for clay M3 at about 30 to 40m below sea level.

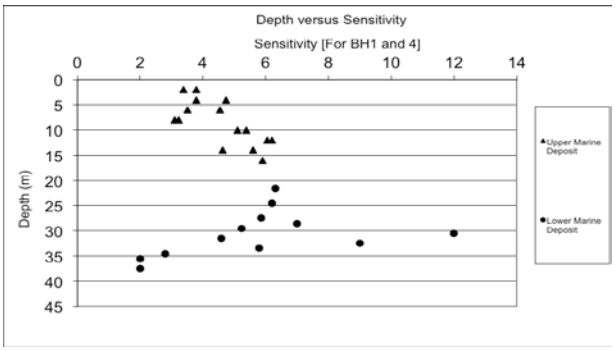

Figure 7: Sensitivity of marine clay M3 is very high at 12.

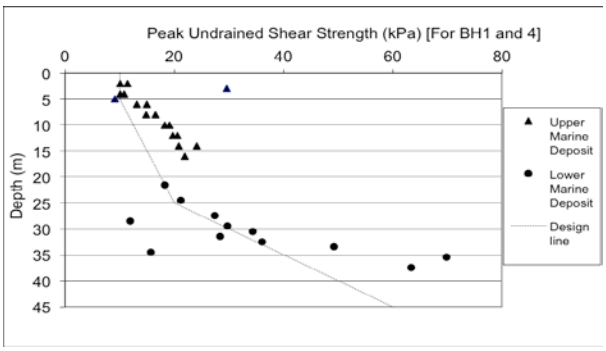

Figure 8: Peak strength is low at 30m depth in M3 clay.

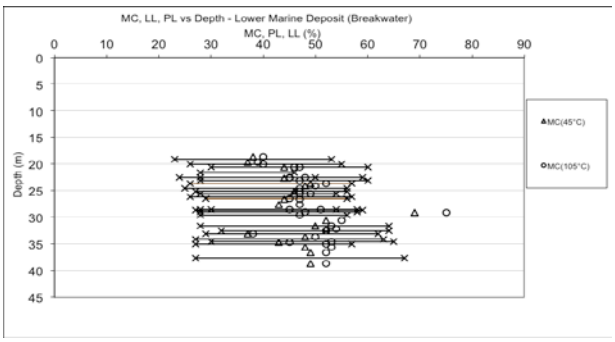

Figure 9: Marine clay (M3) at about 30m depth has very high moisture content greater than liquid limit.

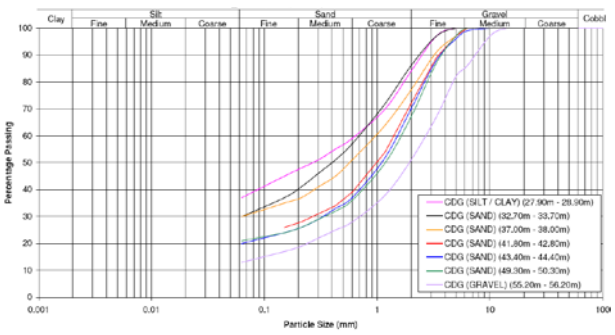

Figure 10: Decreasing coarseness of CDG from depths 55.2 m to 27.9 m from a sand / gravelly soil to silt/clay soil. (Wightman, 2009)

The clay layers have distinct strength and stiffness differences continuously downward. Each clay layer set of properties must be grouped individually and the sub aerially exposed weathered clay (up to 2m thick) will be stronger than the rest of the layer and can form a sub division of the stratum.

Table 1: Schematic log from drillhole HY-93-32-AH14 from within the reclaimed Hung Hom Bay with further interpretation relating to the Quaternary glacial cycle soil deposits.

Depth (m) (GL=4.07mPD)	Schematic Log of drillhole No. HY-93-32-AH14	Log Description (1994)*	Quaternary Geology Interpretation	Quaternary Geology after Yim, W.W.-S. *et al* (2008)]
0m 20		RECLAMATION 1994 Coarse gravel and boulders. Medium dense yellowish brown silty medium to coarse SAND with gravel. Rubble.(concrete and brick) [FILL]	FILL	F [M1 - Top of Holocene Dredged]
  23		Firm, black to grey very sandy silty CLAY. [ALLUVIUM]	Marine CLAY	M1 Holocene (base)
  24.5		Very dense light yellow fine SAND. [ALLUVIUM]	Alluvial SAND Terrestrial deposit	T1 (Last Glacial)
  26		Medium dense grey silty medium SAND [ALLUVIUM]	Alluvial SAND Terrestrial deposit	T1 (Last Glacial)
  29		Stiff brownish grey slightly sandy silty CLAY [ALLUVIUM]	Marine CLAY Sub-aerially exposed	M2 (Last interglacial)
  31		Stiff greenish grey and black silty CLAY with occasional organic clay. [ALLUVIUM]	Marine CLAY Estuarine Deposits	M2 (Last interglacial)
  32.5		Stiff, grey sandy silty CLAY [ALLUVIUM]	Marine CLAY Estuarine Deposits	M3/4 (3rd / 4th last interglacial)
  53.9		Extremely weak, reddish brown to red mottled with white, completely decomposed fine to medium GRANITE.	Residual Soil Grade V Granite Grade IV Granite	RS
		[MDG /SDG]	Grade III / Grade II Granite [MDG /SDG]	B Bedrock

*Footnote: Non-continuous sampling sequence may lead to lack of data on thin layers.

Marine clay (M3) has shown particular adverse properties with shear vane peak and residual values giving a clay sensitivity of up to 12, Figure 7. This represents a clay strength loss to one twelfth the peak strength value on disturbance and means the clay almost liquefies due to the very high water content of the clay, Figure 9, sometime above the liquid limit value obtained (Wightman & De Silva, 2008). Even though high values such as this appear to be spurious in nature, in actual fact they occur from the affects of gas generation in the clay. The properties of this clay were formed over a long period of time and during periods of loading and unloading from glacial and sea level changes. It is important to note that the gases generated in the clay dissolve into the groundwater and can continue to do so until saturation is achieved. As water containing dissolved gas is denser that pure seawater, the water containing gases remains in situ until disturbed by reclamation loading or pressure reduction. The borehole record at Kai Tak for instance shows RS and CDG over 40m thick, Figure 10, with changing composition and properties throughout with weaker more clayey RS

and CDG in the upper levels to more granular and stronger CDG in the lower layer (Wightman, 2009). It is advised to carefully distinguish between weathered rock strata and alluvial deposits, which needs to be recognised as a source of logging error. Some geotechnical parameters are given in Table 2 for Quaternary marine soils and soils relationships with depth.

Table 2: Absolute ages of the Quaternary marine and terrestrial units for borehole BH21 at Tai O breakwater (Wightman & De Silva, 2008) with stratigraphical units, formation names and typical soil parameters

Stratigraphical Unit [Log Name / unit]	Age (ka)	Geological Period	Depth (m)	Borehole BH21 log	mc	L_L	ρ_d	φ'
(after Yim & Choy, 2004)		Present Day	0.00	*Seabed*	%	%	Mg/m^3	Deg
M1 - [Upper Marine	<8.1	Holocene	13.00	Very soft to soft, dark grey silty CLAY with occasional shells	28-83	33-71	0.9-1.6	29 [c_u=10 to 15kPa]
T1 - [Upper Marine - & Estuarine]	8.1-70	Pleistocene: Last Glacial	15.60	Stiff / medium dense, brownish yellow & black SILT and CLAY with sand pockets with some fine gravels of rock fragments	23-27	47-48	1.2-1.9	25-33.7
M2 - [Upper Alluvium]	90-140	Last Inter-glacial	18.10	Firm to stiff, light grey dappled yellow or spotted yellowish brown, slightly silty CLAY.	16-34	21-75	1.3-2.0	25
T2 - [Upper Alluvium]	150-180	2nd Last Glacial	-	*Not encountered in BH21 but present elsewhere in Tai O Bay.*	21-41	21-74	1.3-1.4	16-34.6
M3 - (Lower Marine)	190-240	2nd Last Inter-glacial	30.10	Firm to stiff, grey to black, slightly silty CLAY	40-70	43-73	1.0-1.3	25 [c_u=18 to 38kPa]
T3 - (Lower Marine)	250-300	3rd Last Glacial	39.60	Stiff, brownish yellow silty CLAY. Yellowish brown mottled grey, silty, SAND. Light grey, sub-angular COBBLE sized strong Tuff and siltstone.	-	-	-	-
M4 - [Lower Alluvium]	310-340	3rd Last Inter-glacial	40.10	Firm, grey mottled yellowish-brown, slightly sandy silty CLAY with occasional decayed plant debris. Firm, dark greenish grey, slightly sandy clayey SILT with decayed plant debris	27-48	30-56	1.0-1.6	24 [c_u=40 - 50kPa]
T4 – [Lower Alluvium]	350-370	4th Last Glacial	47.75	Light grey, sub-angular, GRAVEL and COBBLES of moderately weak and moderately strong rock and occasional quartz w sand / boulders.	-	-	-	-
M5	380-420	4th Last Inter-glacial	-	Not in BH21	-	-	-	-
T5	>440	5th Last Glacial	-	Not in BH21	-	-	-	-
Bedrock –Tuff (G-V)	140 Ma	Jurassic	-	Extremely weak, light grey, spotted white and grey, completely decomposed, coarse ash crystal TUFF. (Firm to stiff, silty sandy CLAY)	-	-	-	-

2.6 Effects of marine gas on geotechnics

The effect of marine gases exsolving slowly has been recorded by geophysics using marine seismic methods. The trace of gases from marine layers deep below the seabed have been identified as a plume of bubbles

exsolving from groundwater, Figure 2, that has become over saturated and begins to release excess gases (Bahr *et al*, 2005). This is a slow but continuous process and only occurs if water pressure reduction through tidal rise and fall. The bubbles may remain trapped in the soil and may re-dissolve back into the groundwater if the water pressure increases. These affects were clearly identified in Lake Nyos in Cameroon, Africa with dissolved high concentrations of carbon dioxide close to saturation, Figure 11, are being vented by self propelled water stream to the surface of the lake continuously for over 10 years, Figures 12 & Plate 1, to prevent mass instantaneous exsolving of the gases (Halbwachs *et al*, 1999 and 2004).

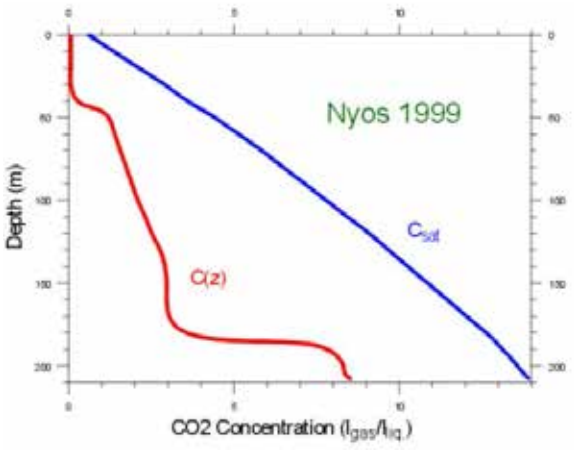

Figure 11: Gas saturation curve of CO2 with depth. (Halbwachs *et al*, 1999).

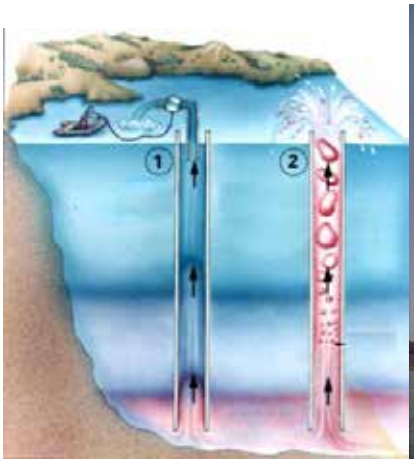

Figure 12: Degassing of Lake Nyos using a fixed pipe. (Halbwachs *et al.* 2004)

Plate 1: 20 m high water fountain caused by CO_2 continuously exsolving.

Other effects of exsolving gases occur through very rapid exsolving from saturated sands layers causing gas driven liquefaction of the ground towards atmospheric conditions (Wightman & Tattersall, 2009). Similarly during excavation of a cofferdam to recover the tunnelling operation, a TAM was jettisoned from the side wall drilling tube under great pressure from liquefaction caused by the disturbance of gas saturated ground water in a sand stratum, causing the second rescue cofferdam to flood.

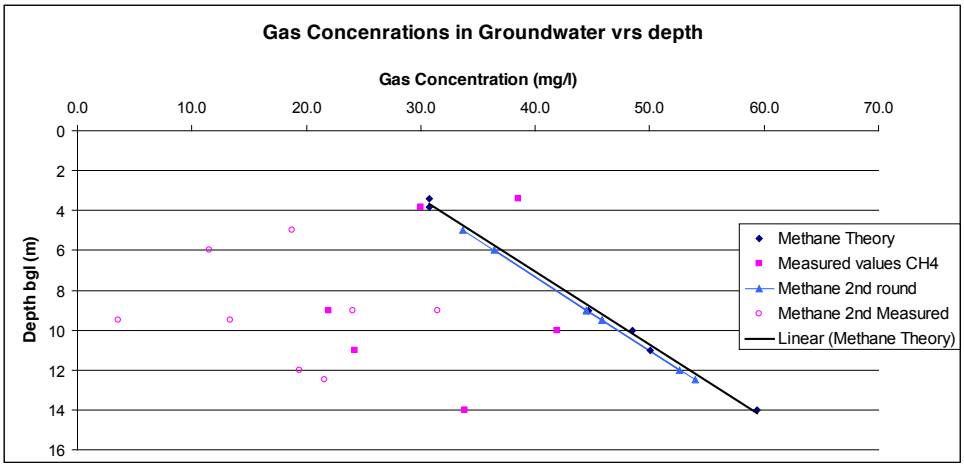

Figure 13: Gas concentrations versus depth with gas saturation limit indicated for methane at Hung Hom Bay reclamation (Wightman & Mackay, 2008).

The forces imposed by exsolving gases should not be underestimated nor is the safety aspect of methane or hydrogen sulphide gas releases. The presence of these naturally occurring gases can cause unusual and unexpected types of ground behaviour that without the gases being present would normally result in a stable construction environment. Once gas is released, the Boyle's Law of gasses is obeyed with volume of gas noted increasing inversely proportional to the pressure reduction. The effect creates an increasingly disturbing force on soils, with strength reduction or losing all strength by the soil or failing by rapid gas charged liquefaction should conditions allow this to happen. In Hong Kong, the measurements at Hung Hom Bay show that the gases in the groundwater have already reach saturation levels, Figure 13, hence the large amount of gas that was monitored (Wightman & Tattersall, 2009).

2.7 Ground investigation additional requirements

In order to design a ground investigation to retrieve the required level of details and geotechnical design parameters, the following tests, sampling or surveys may be required.

a) The use of marine seismic survey to detect the presence of gas masking and often deeper releasing of gas causing a vertical gas plume (Bahr et al, 2005), which indicates deep marine clay gas storage and or production. Release of gases from clay interstices is slow and affected by tidal fluctuations or directly by reclamation activities, (Wightman & De Silva, 2008) and (Wightman & Tattersall, 2009);

b) Continuous mazier sampling of ground for observations to accurately distinguish the presence of multiple layers of alluvium and marine clays (geological borehole samples have mazier tubes split rather than extruded. (Fletcher et al, 2000);

c) Sampling groundwater from boreholes using the BAT vacuum sampling tube, Plate 2, to obtain samples of groundwater containing dissolved gases to check for gas saturation levels. The escaped gas in the head space of the vacuum tube is included in the water saturation calculation, (Wightman & Mackay, 2008);

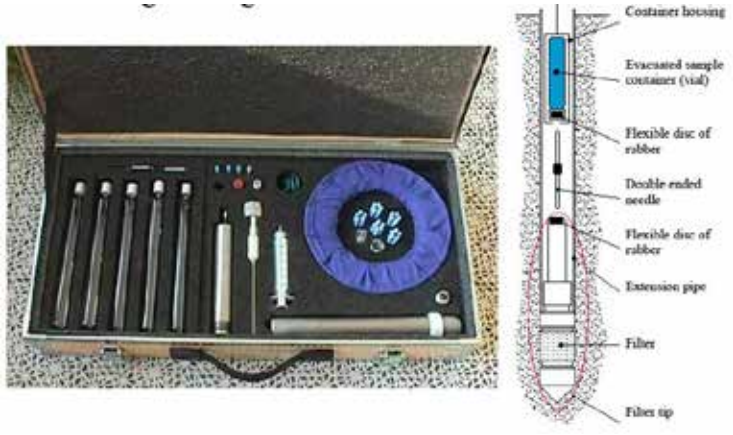

Plate 2: GeoN groundwater gas sampler

Plate 3: Gel-Push triple tube sampler coats the sample in a gel for frictionless recovery of samples.

d) Careful and slow extraction of highly sensitive clay or cohension less sand samples to enhance recovery, (Wightman & De Silva, 2008), (De Silva et al, 2010a & b) and (Wightman et al, 2001);

e) Use of drilling muds to improve recovery conditions for weak soils (Wightman et al, 2001);

f) Use of thermoluminesces scanner on closed undisturbed mazier tubes prior to opening for inspection by cutting tube and not extuding sample, (Yim et al, 2008);

g) Use of gel-push samples, Plate 3, for ultra low disturbance during sampling to obtain quality samples for triaxial or other testing, (De Silva et al, 2010a & 2010b);

h) Surface gas testing measurements using hand held detector during pipe pile welding to check for methane and possibility of flashovers during the welding process, (Wightman & Mackay, 2008); and

i) Decomposed rock can become very thick off shore and ground investigations results from Kai Tak (over 40m thick) show even the completely decomposed granite changes in particle size and geotechnical

parameters from a soft residual soil to those just prior to being described as highly decomposed. Multiple layers need to be considered during the investigation and the design due to the many tens of metres of the strata investigated, (Wightman, 2009).

In summary, ground investigations do need further elements added to obtained more detail and to check for more onerous conditions. The logging of split mazier samples are often opened and laid out together so that variations of stratigraphy are more easily seen. The geological logging needs to include the quaternary sequences as described above to fit in with the deposition over the duration of the glacial cycles.

2.8 Effects on designs

The Tai O breakwater design (Wightman & De Silva, 2008), disclosed specific site conditions relating to the design and considerations of the ground behaviour. The site was underlain by 33m of stratigraphical units M2 and M3 clay with the lower clay showing signs of very high sensitivity (Fig. 7 & 9). Of the design options considered including complete dredging of the bay at the location of the breakwater, installation of wick drains or stone columns and deep mixing, the option that was constructed was a reinforced mattress to spread the load from the breakwater over a wider area (Tsang *et al*, 2004), to create a stable foundation over the weak clay layer. The construction stage timing was important to ensure stability but long-term effects were to expect about 0.5m of settlement over 50 years. This long-term settlement affect was considered acceptable compared to the more costly options or the onerous construction difficulties faced by installing ground improvements. It also avoids disturbing the deep but highly sensitive clay layer (M3).

Each reclamation site needs a very careful set of possible scenarios in terms of ensuring both short and long term stability effects have considered with the presence of sensitive clay and gasses potentially disturbing the soil. It is suggested that by careful separation of data, the geotechnics of each quaternary layers can be grouped to give a true representation of parameters and allow weaker layers to be considered as a separate soil in geotechnical design models.

3 CONCLUSIONS

Offshore Quaternary deposits require careful sampling, logging and accurate identification to produce realistic geological models to be made. The CLK clay and sand sequence labelling needs to be avoided from grouping all soils above weathered rock into large bands of mixed soils. It is suggested that the geological model needs to be improved by accurately identifying all sub units of the Quaternary sequence (related to glacial cycles). It is important to understand the unusual nature of these deep marine soils. They require special attention and study to understand their true variation of properties and displaying often extreme engineering behaviour.

Ground investigations are often designed using standard procedures and it is further suggested that ground investigations for deep reclamations are designed to consider the more obscure soil such as recovering clay of high sensitively, monitoring for the presence of gases and direct vacuum sampling of groundwater to determine the saturation level of dissolved gases.

With more focus on geological boreholes a continuous log will help to denote the quaternary geological sequence caused by previous glaciation cycle. The grouping of soil properties and parameters for each soil unit will allow better understanding of the ground conditions and potential behaviour of the ground to aid future reclamation designs. It is therefore vitally important to obtain quality geological information with improved logging and modelling with related geotechnics prior to undertaking any engineering designs for reclamations

REFERENCES

Bahr, A., Wong, H.K., Yim, W.W.-S., Huang, G., Lüdmann, Chan, L.S. and Ridley Thomas, W.N. 2005. Stratigraphy of Quaternary inner-shelf sediments in Tai O Bay, Hong Kong, based on ground-truthed seismic profiles. *Geo-Marine Letters 25*: 20-33.

Canfield, D.E. 1993. Organic matter oxidation in marine systems. Interactions of C, N, P, and S biogeochemical cycles and global change. *NATO-ASI Series 14*.

Drever, J.I. 1982. *The Geochemistry of Natural Waters*, Prentice-Hall, Inc., Englewoods Cliffs, N.J., pp. 388.

Fyfe, J.A., Shaw, R., Campbell, S.D.G., Lai, K.W. & Kirk, P.A. (2000). *The Quaternary geology of Hong Kong. Hong Kong Geological Survey*. GEO, HKSAR.

Fletcher, C.J.N., Wightman, N.R., & Goodwin, C.R. 2000. Karst - related deposits beneath Tung Chung New Town, Hong Kong: implications for deep foundations. *Proc. of Conference on Engineering Geology HK 2000*, Institution of Mining and Metallurgy, Hong Kong Branch: 139-150.

Halbwachs, M. 1999. Monitoring the Safety level of the Lake during the Degassing Process. Paper from internet site: http://richon.club.fr/richon/Webcam_nyos/Nyos_webcam.

Muralidhar K., Mazumdar, A., Karusuddauah, S.M., Borole, D.V. & Rao, B.R. 2006. Evidences of methane-derived authigenic carbonates from the sediments of the Krishna-Godavari Basin, eastern continental margin of India. *Current Science*, Vol. 91, No.3, pp 318-323.

Nageswaran, S. 1983. *Effect of gas bubbles on the sea bed behaviour*. PhD Thesis, St. Catherine's College, Oxford.University.

Premchitt, J., Rad, N.S., To, P., Shaw, R. and James, J.W.C. 1992. A study of gas in marine sediments in Hong Kong. *Continental Shelf Research 12/10*: 1251-1264.

Silva, S.D., Wightman, N.R. & Kamruzzaman, M. 2010a. Geotechnical ground investigation of the Padma main bridge". *Proc. of IABSE-JSCE Joint Conference on Advances in Bridge Engineering II*, *8-10 August 2010, Dhaka, Bangladesh*: 427-436.

Silva, S.D., Wightman, N. & Kamruzzaman, M. 2010b. Geotechnical ground investigation of the Padma main bridge. *Proc of Bangladesh Geotechnical Conference 2010*: *Natural Hazards and Countermeasures in Geotechnical Engineering, ISSMGE, 4-5 November 2010, Dhaka, Bangladesh*: 181-188. [Updated paper].

Stumm, W. & Morgan, J.J. (1995). *Aquatic Chemistry. Aquatic Chemistry: Chemical Equilibria and Rates in Natural Waters*, 3rd Edition, Wiley: p1040.

Tsang, K.K.H., McArthur, A., & Gormley, A. 2004. Tai O, A new development to preserve nature and history. *Proc. of Inter. Conference on Coastal Infrastructure Development*, *November 2004, Hong Kong*.

Wightman, N.R. (2009). Destabilisation of natural slopes relating to soil density loss – strength reduction, *Proc of 29th Annual Seminar, HKIE Geotechnical Division, 17 April 2009, Hong Kong*: 85-90.

Wightman, N.R. & De Silva, S. 2008. Design and construction of a breakwater using a geosynthetic raft at Tai O Bay, Hong Kong. *Proc. HKIE Geotechnical Division 28th Annual Seminar*, 2 May 2008: 269-274.

Wightman, N.R., Hitchcock, B.K., Burbidge, H.T., Frappin, P. & Goodwin, C.R. 2001. Advances in site investigation practice for deep foundations, Tung Chung New Town, Lantau Island, Hong Kong. *Proceedings of the International Conference on Insitu Measurement of Soil Properties and Case Histories*: *IN-SITU 2001, Bali, Indonesia*: 511-519.

Wightman, N.R. & Mackay, A, 2008. Gas ground investigation for tunnelling works at Hung Hom Freight Depot, Hong Kong. *Proc. of International Conference World Tunnel Congress & 34th General Assembly*, *ITA-AITES, 19-24 September 2008, Agra, India*: 98-109.

Wightman, N.R. & Tattersall, J.W. 2009. Tunnel failure mechanism by exsolving gas: a proposed model. *Proc. of International Conference 17th ICSMGE EGYPT 2009*, *Bibliotheca Alexandrina, Alexandria, Egypt*. 5-9 October 2009, pp 2520-2523.

Yim, W.W.S. 2001. Stratigraphy of Quaternary Offshore Sand and Gravel Deposits in the Hong Kong SAR, China. *Quaternary International,* 82 (2001): 101-116.

Yim, W.W.S. and Choy, A.M.S.F. 2004. A circa 0.5-million year geological model for geotechnical engineering in Hong Kong. *Proc. 24th Annual Seminar on Recent Advances in Geotechnical Engineering*, *Geotechnical Division, The Hong Kong Institution of Engineers*: 123-137.

Yim, W.W.S, Hilgers, A., Huang, G & Radtke, U. 2008. Stratigraphy and optically stimulated luminescence dating of subaerially exposed Quaternary deposits from two shallow bays in Hong Kong, China. *Quaternary International* 183: 23-39.

Ground Treatment by Cutter Soil Mixing (CSM) and its Application at Tuen Mun – Chek Lap Kok Link Northern Connection Sub-sea Tunnel Section

Raymond Wong, Derek Yung, Alex Chan & Ricky Pang
Bachy Soletanche Group Limited, Hong Kong

ABSTRACT

The Contract HY/2012/08 involves the design and construction of a dual two-lane sub-sea tunnel of approximately 5km long between Tuen Mun Area and the future Hong Kong Boundary Crossing Facilities (HKBCF) on Lantau Island. The main contractor Dragages-Bouygues Joint Venture (DBJV) adopts two tunnel boring machines (TBM) of 14m and 17.6m diameter for the tunneling works. DBJV had designed the break-in plug using soil improvement technique at the location ahead of the launching shaft and employed Bachy Soletanche Group Ltd. (BSGL) to carry out the work. The strength requirement (UCS) of the plug was minimum 3MPa in the reclaimed sand and 1.5MPa in Marine Deposit and Alluvium layers. The permeability of the treated ground was required to achieve $1x10^{-6}$m/s. BSGL had proposed to use an innovative technique Cutter Soil Mixing (CSM) and completed on schedule the ground treatment work of the break in plug for this project. It was the first time to use CSM technique in Hong Kong. This paper presents the process design considerations and the application of CSM technique at the project site; some technical issues and return of experience are also discussed.

1 INTRODUCTION

Deep cement mixing uses a wide range of techniques to inject binder agents to mix with the soil and form columns, for example, to reinforce the ground for subsequent construction. The type and amount of binder will determine the hydraulic and mechanical characteristics of the soil. Deep cement mixing generally comprises three stages: premixing of the soil, injection of the binding agent and incorporation of the soil/binder mix. The inclusions produces no, or very little, spoil. The structures produced by soil mixing can be columns, or panels or continuous trenches. The technique works with a wide range of soils and is particularly efficient in loose soil which are free from coarse elements.

CSM (or namely GEOMIX® under Soletanche's patent) is a deep cement mixing process which uses Hydrofraise technology. Basics of this process are shown in figure 1: During the downward excavation under action of two counter-rotating cutting wheels, natural soil is bulked, mixed/premixed with a specific injected fluid and then displaced towards the top of the cutting head. As the machine is withdrawn upward again, rotation of wheel is reversed to displace the mix from above the cutting head to below it, during this phase a binding agent is injected and mixed with the soil. Depending on soil conditions and type of construction, the excavation fluid and the binding agent can be similar or different.

Specific instructions for treatment such as injected volumes and mixing factors are adapted according to natural soil characteristics (e.g. type of soil, sieve analysis, permeability, water table level, water content). These instructions are controlled and recoded through a monitoring system installed on the machine. Geomix has been used worldwide in various geotechnical applications such as retaining walls, cut-off walls, mitigation of liquefaction hazards and soil improvements. This paper presents its first use in Hong Kong as the soil improvement technique to form the TBM break-in plug in the newly reclaimed land.

Figure 1: Construction process in Geomix technique with CSM equipment *[1]*

2 PROJECT SITE CONFIGURATION

The break-in plug is located immediately outside the diaphragm wall launching shaft, and is composed of 3 main elements: (i) CSM treatment (plan area about 32m x 45m) from ground level to 4m below TBM; (ii) 2.0m diameter jet grouted column as supports for CSM on bearing soil stratum; (iii) A row of 1.6m diameter overlapped jet grouted columns as the seal of the interface between the CSM and the diaphragm wall. The bird view of the project site is shown on plate 1 and the schematic arrangements of the plug are shown on figure 2.

Plate 1: Bird view of project site

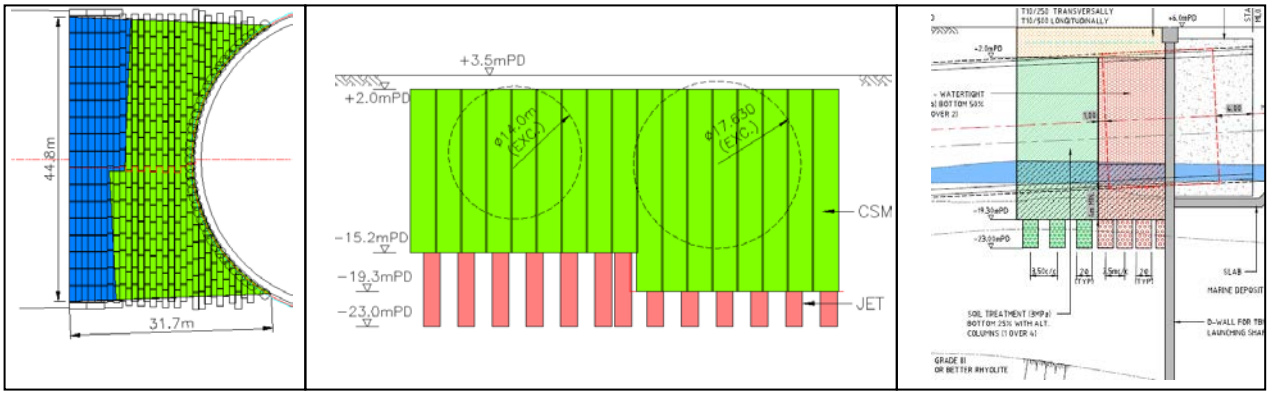

Figure 2: Schematic arrangement of the TBM break-in plug

3 DESIGN ASPECTS

As a ground improvement process, design encompasses two distinct aspects:

(i) The designer of the main contractor carried out the functional design which described the way in which the treated soil and the untreated soil interact to produce the required overall behavior;

(ii) The specialist subcontractor carried out process design which described the means by which the required performance characteristics are obtained from the treated soil by selecting and modifying the process control parameters.

The designer of DBJV specified the treatment zone, location, dimensions, depths, the required uniaxial compressive strength (UCS) at 28days from the cored samples shall be minimum 3MPa in the reclaimed sand and 1.5MPa in Marine Deposit and Alluvium layers. Also the permeability of the treated ground was required to achieve $1x10^{-6}$m/s.

BSGL selected the CSM/Geomix as the soil mixing technique, and based on the designer's requirement and the site conditions determined the initial working parameters. BSGL carried out trial panel and trial jet grout columns and verified and/or adjusted the initial working parameters to be the final production parameters.

Table 1: Summary table of the final working parameters in the project site.

CSM working parameters	
mixing down:	bentonite slurry
mixing up:	cement grout
$1m^3$ batch of cement grout was made of : 1015 kg OPC cement 680 Litres water 1 Litres retarder Plastiment-VZ to get W/C of 0.67, density of 1.69+/- 0.02, rheology of 2 to 3 extra hours	

The execution parameters for the deep cement mixing by CSM are set to reach the target specifications with respect to two major factors: ground conditions and binder.

By representing at least 50% of the final mixture, particle size distribution curves from sieve analysis and water content are key parameters driving both strength gain and hydraulic conductivity.However, additional factors such as organic matter and presence of contaminants, if any, must be taken into account as they disturb the cement hardening process.

The second major factor is the binder type and binder dosage. Former laboratory and field studies have clearly demonstrated that nature of hydraulic binder (clinker, blast furnace slag, pozzolans, lime, etc.) has an important influence strength of the mixture. Once binder blend has been selected for the project, binder dosage needs to be established in accordance with the target specifications and the soil conditions.

At execution stage, binder dosage is finally adjusted depending on the construction procedure.

For example, based on the specified minimum UCS at 28 days and the factor of 1.7 to account for the variability of 30% and confident level of 95% in a log-normal distribution of the UCS, we determine the target cement/water ratio of the final cement-soil mixed product which composes of the in-situ water content (depending on soil properties) and the additional quantities of water and cement from the binder dosage (depending on flow rate and lifting speed of the mixing tool).

4 DEEP CEMENT MIXING PROCESS

Based on the functional requirements (permeability and structural) of the two portions of the break-in plug, the panel layout of CSM was designed as shown in figure 3. In portion 1, there were 284 panels overlapping longitudinally and transversely. In portion 2, there were 117 panels overlapping longitudinally only. For efficient excavation without unfavorable deviation, it is important to enable the cutting head working in the ground of balanced soil stiffness. Therefore, the panel construction sequence was planned as four-cycled pattern, namely primary, secondary, tertiary and quaternary panels.

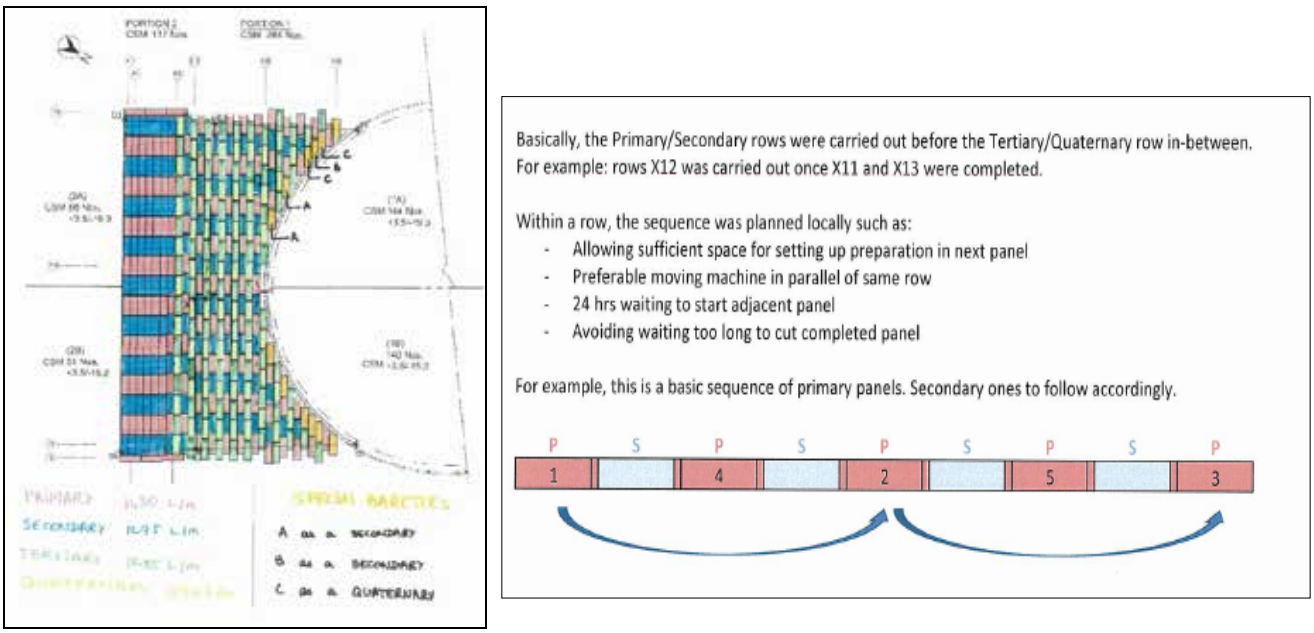

Figure 3: Panel layout of CSM plug and the principle of panel sequence

The basic machine for CSM is assembled by counter-rotating cutter head system equipped with 2 counter-rotating drums for a 2800mm x 1000mm section, powered by high torque hydraulic motors inside the wheels, the 25m Kelly bar and the Liebherr LRB 255 carrier with 30m long mast, see plate 2. Real-time monitoring of the actual parameters (e.g. depth, rate, motor torques, flow rate, injected fluid volume, deviation in both directions, ground and compensation pressure, etc) was used and the display on the cabinet is shown on plate 3.

Plate 2: Schematic set up of batching plant for CSM

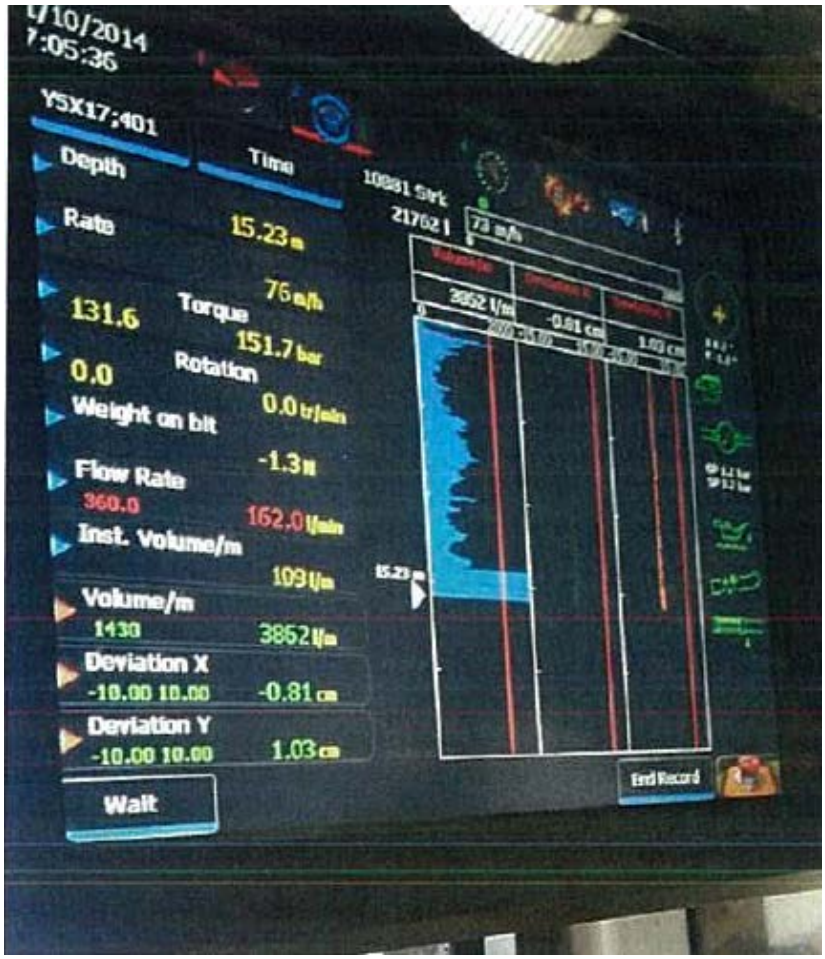

Plate 3: Screen of Real-time monitoring of CSM parameters

5 OBSTRUCTIONS ENCOUNTERED IN TRIAL PANELS AND MODIFIED DESIGN

The expected ground condition for the CSM was a layer of reclaimed sand overlaying on the Marine Deposits and followed by Alluvium and CDG. However, a layer of hard rock in the reclaimed depth was found during the predrilling process done just before the commencement of the trial panels. During the trial panel, instruction was given to try excavating through the hard rock. However, due to the obstruction of the hard rock, the Kelly bar shook and the cutter jammed many times in ground during the mixdown phrase. After pulling out the cutter head, damage was reported as the scraper being bended by rocks stuck in the cutter plates. In the second trial, the cutter was jammed again and could not be withdrawn until the surrounding material was removed by a diaphragm wall grab. See Plate 4 for the hard rocks at the cutter plates found in trial panels.

After these two trials, it was evident that the CSM was not able to excavate through the unexpected hard blocks. The design of the plug had to be modified to stop the CSM on the hard block layer found during mixdown of each panel and to extend the jet grout columns upto the bottom of CSM. As a result, the quantities of jet grouted columns was increased significantly, additional resources were mobilized to meet the deadline of the TBM break-in operation. Figure 4 shows the as-built 3-D plot of the plug composed of CSM and jet grout and the key data of the changes due to the unexpected obstructions. Thanks to the excellent effort of the team, the ground treatment of the plug was completed and TBM passed through the break-in plug on schedule.

Plate 4: Hard rocks blocked at cutter plates found in trial panels

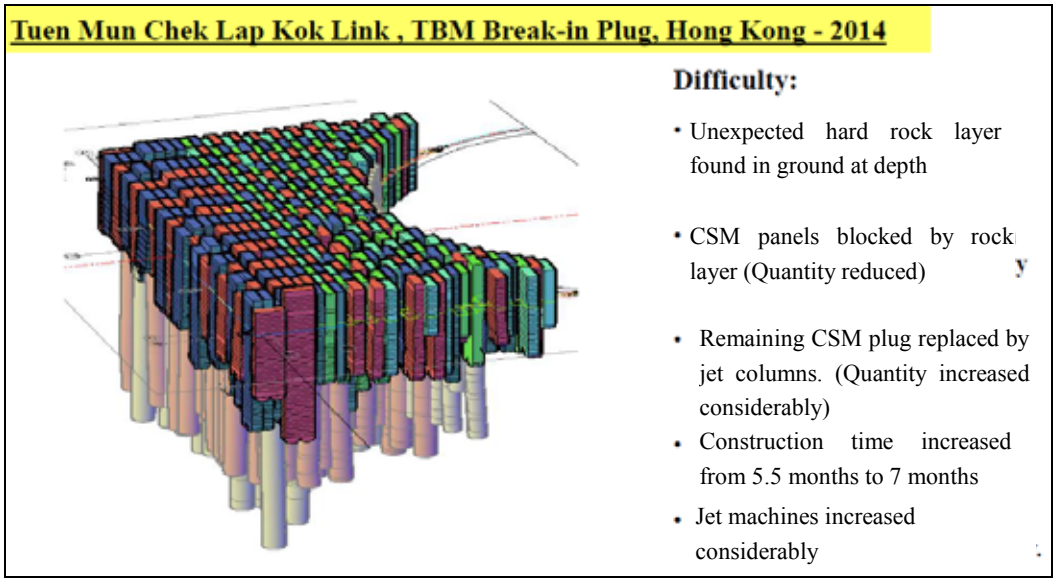

Figure 4: As-built 3-D plot of the plug composed of CSM and jet grout and the key data of the changes due to the unexpected obstructions

6 QUALITY CONTROL

Apart from the real-time monitoring, the finished CSM were also cored and tested for UCS strength. In the coreholes, permeability tests and televiewer tests were performed. Both the UCS (see figure 5) and permeability test results were satisfactory. Moreover, the homogeneity of the treated soil were also shown by the core sample and the televiewers (see plate 5 and plate 6).

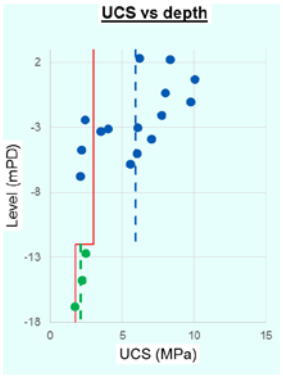

Figure 5: UCS results

Plate 5: Cored samples

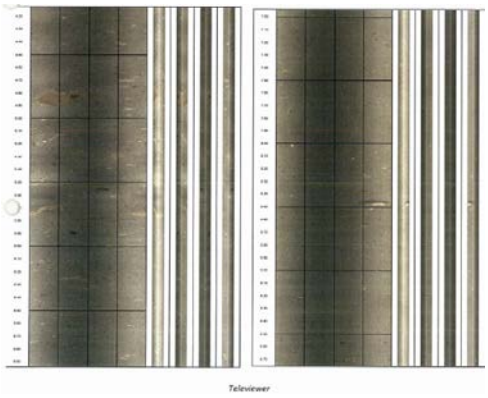

Plate 6: Televiewer report

After proving the quality of the break-in plug, the TBM started its operation on schedule and passed through the break-in plug safely in good condition. DBJV appreciated BSGL's effort and took pictures on the CSM/ jet grouted plug during the regular inspection outside the TBM cutter head (see plate 7)

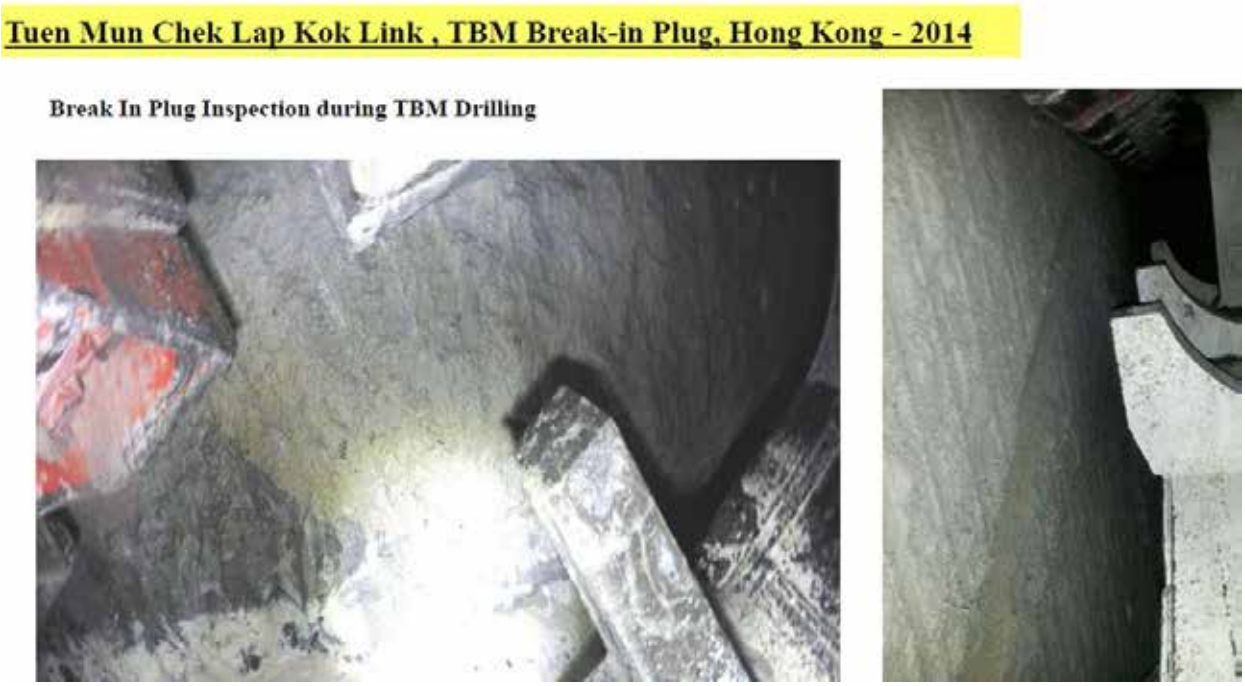

Plate 7: Surface of break-in plug outside TBM cutter head

7 CONCLUSIONS

The first CSM application in Hong Kong was clearly a success. Despite the modification of works due to unexpected soil conditions, all technical requirements were met and final TBM operation was achieved without any issues. Compared to jet-grouting, CSM is highly cost effective as it requires much less resources such as cement and water. When combined with jet-grouting to ensure continuity with existing structures, CSM can advantageously be added to the range of techniques applicable in soft soil and reclaimed areas in Hong Kong for ground improvement as well as cut-off walls and retaining walls.

REFERENCES

Benhamou L. and Mathieu F., 2012. Geomix Caissons against liquefaction. *ISSMGE-TC211 International Symposium on Ground Improvement IS-GI, Burssels* May 2012.

BS EN14679: 2005 *Execution of special geotechnical works – Deeping mixing, Annex B: Aspect of design.* BSI

Mathieu F. et al. 2012. Deep soil mixing with Geomix method: Influence of dispersion in UCS values on design calculations. *Grouting and Deep Mixing 2012, Proceedings of the fourth International Conference on Grouting and Deep Mixing*, *New Orleans*, pp. 334-342.

Soletanche Bachy (2011): Technical Guide

Design and Performance of a Drained Reclamation in Malaysia

Y.C. Lam
Minconsult Sdn Bhd, Malaysia
S.W. Lee
Golder Associates (HK) Limited, Hong Kong, formerly Geotechnical Consulting Group (Asia) Ltd.

ABSTRACT

A drained (non-dredged) reclamation of about 70 hectares for a 2100 MW (3x700MW) coal-fired power plant was constructed in the southern tip of Peninsula Malaysia in 2003–2004. The inter-tidal site was formerly a fish farm and characterized by mangrove and mudflat. The reclamation was built on 25m thick soft Holocene clay underlain by Pleistocene alluvium, involving hydraulic filling, prefabricated vertical drains and surcharging. The filling and surcharging were carried out in six stages with intervening rest periods, to allow for strength gain in the soft marine clay. A gentle slope of 1V:10H formed the leading edge of the reclamation. This paper presents the ground conditions, soil properties, design methodologies, instrumentation and field performance of the reclamation. The challenges encountered and the monitoring data presented provide a well-documented case history for future reclamation works in similar ground conditions.

1 INTRODUCTION

A 2100 MW coal-fired power plant was the first private coal-fired plant in Malaysia and was the biggest coal-fired Independent Power Producer in South-East Asia. The project site was reclaimed from a 70 hectare swampy coastal land in the southern tip of peninsular Malaysia (Barry et al. 2004, Lam et al. 2015), see Figure 1. The US$2 billion project was built on a fast-track schedule and was completed on schedule within 48 months from its commencement date of March 2003. The reclamation involved hydraulic sand filling, installation of prefabricated vertical drains (PVD) and surcharging, see Figures 2 and 3. The site was subdivided into four areas – Power Island (27 ha), coal storage yard (28 ha), switchyard (9 ha), and a construction laydown area (6 ha), see Figure 4.

Figure 1: Site location

Figure 2: Hydraulic filling

Figure 3: PVD installation

The construction of the proposed coal storage yard had to achieve the performance objectives of

(i) a minimum sandfill thickness of 15.4m;
(ii) target settlement to be achieved at the guaranteed final acceptance date, which is at least 90% of primary settlement under the 15.4 m high sandfill;
(iii) a finished platform level of RL +4m MLSD;
(iv) primary settlement not increasing by more than 150 mm at 12 months after the final acceptance date;
(v) differential settlement not exceeding 125mm over 50 m distance along the centerline of stacker reclaimer at 12 months after the final acceptance date; and
(vi) the foundation clay underlying the finished platform to have adequate bearing capacity to support 14m high coal stacks stockpiled at an angle of 40º with a unit weight of 9.5 kN/m^3.

This paper focuses on the design and field performance of the coal storage yard reclamation.

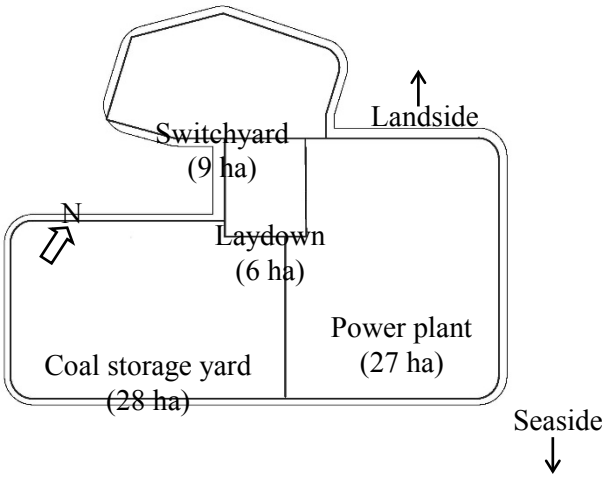

Figure 4: Four areas of reclamation

Figure 5: Initial mangrove and mudflat

2 GROUND CONDITIONS

The coastal area was characterized by mangrove and mudflat, see Figure 5. The site was formerly used for fish farming. The average prevailing ground level was at RL +0.75m MLSD, and the groundwater level was typically 1m – 2m above and below the ground level. The geological succession comprised 20m – 25m of soft to very soft marine clay (Holocene) overlying older alluvium (Pleistocene) and residual soils. The alluvium and residual soils were firm to stiff clayey silt/silty clay, and consolidation settlement was considered not significant in these layers. Comprehensive field and laboratory tests were carried out to obtain soil parameters for detailed design of the reclamation.

The marine clay (MC) was classified as having high to extremely high plasticity. The clay content was 30% – 60%, the activity 1 – 2, and the specific gravity 2.45 – 2.55. Figures 6, 7 and 8 show the Atterberg limits, compressibility and consolidation parameters, and over-consolidation ratios (OCR) of the MC, respectively. A slight over-consolidation (OCR >1) of the MC near the ground level could have been caused by (i) loading imposed by the bunds for fish farming, and (ii) seasonal drying near the ground surface. Table 1 summarizes the properties of the MC.

Table 1: MC properties

Properties	Lower bound	Upper bound	Average
Liquid limit (LL), %	81	119	96
Water content (WC), %	58	88	71
Plastic limit (PL), %	21	40	34
Compression index (C_c)	0.81	1.28	1.01
Initial void ratio (e_0)	1.96	2.55	2.20
Compression ratio ($C_c/1+e_0$)	0.19	0.42	0.31
Coefficient of vertical consolidation (c_v), m^2/yr	0.58	4.50	1.58
Pre-overburden pressure (POP), kPa	4	35	14
OCR	Varying from 2.5 at top to 1.0 at 20m deep		

Note: POP = pre-consolidation pressure (p_c) minus initial effective vertical stress (σ'_{v0})

SPT-N values in the top 20m of the MC were generally 0 blow/300mm. Figure 9 shows the undrained shear strength (c_u) measured by the in situ penetration Vane tests in the MC. A scatter in the c_u data points is evident, and a moderately conservative design line $c_u/\sigma'_{v0} = 0.3$ was selected. The sensitivity of MC was 2 – 7, with an average of 3. Figure 10 shows the results of a piezocone (CPTU) test in the coal storage yard. The MC layer is delineated by the measured low cone resistance q_c values and high pore pressures.

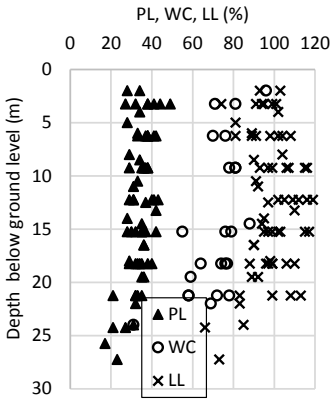

Figure 6: Atterberg limits

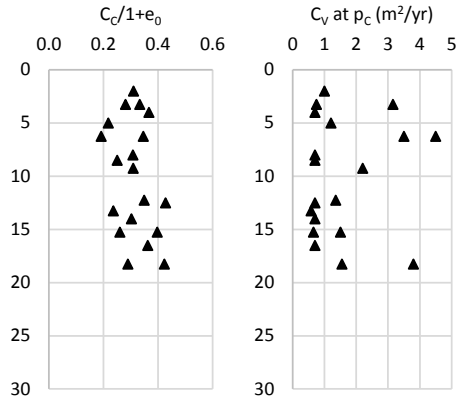

Figure 7: Compressibility and consolidation

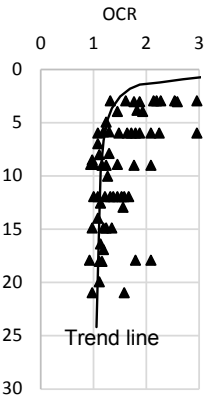

Figure 8: OCR

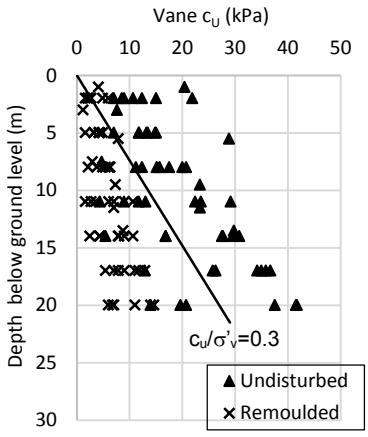

Figure 9: Vane c_u

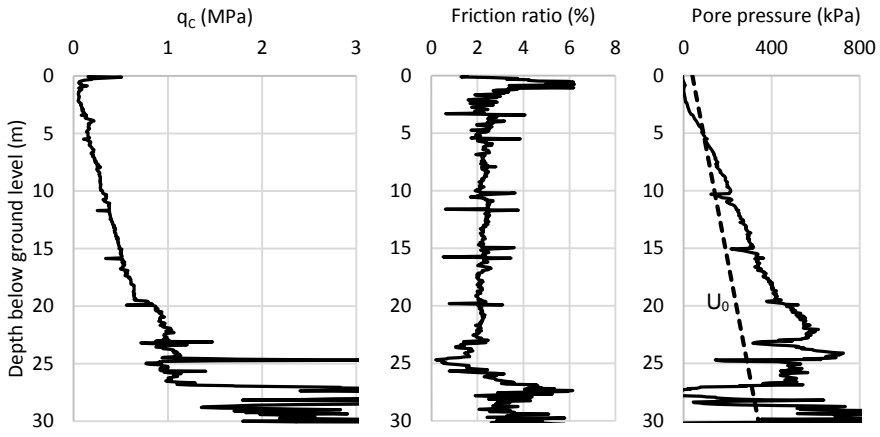

Figure 10: CPTU results

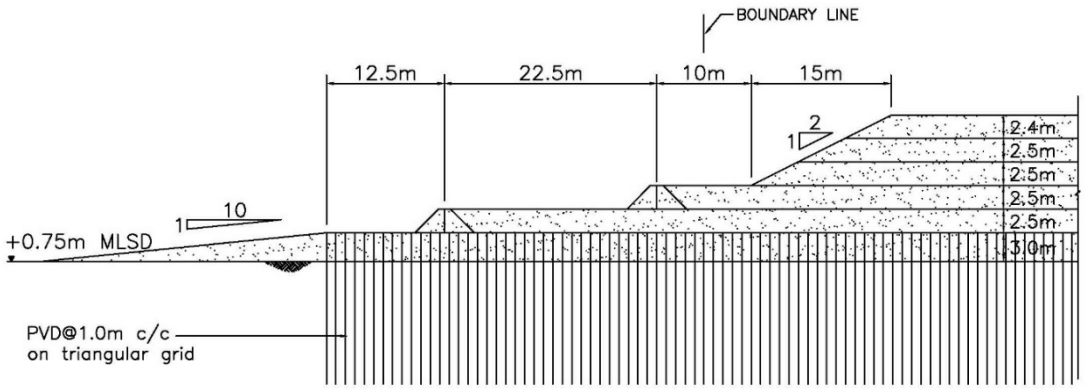

Figure 11: Typical cross-section of reclamation

3 DESIGN FOR RECLAMATION

Design for the drained (non-dredged) reclamation adopted the conventional soil mechanics theories, VDrainSt spreadsheet calculation (Bo et al. 2003), Slope/W Version 5 program and PLAXIS Version 8.2 numerical modelling. A brief description on the design is given here. Figure 11 shows a typical cross-section of the reclamation at the coal storage yard. A gentle slope 1V:10H forms the leading edge of the reclamation. The PVDs were installed at triangular grid spacing of 1.0m c/c through the full depth of MC. Figure 12 shows examples of PLAXIS and Slope/W models. Table 2 summarizes the features of each calculation method.

Table 2: Features of each calculation method

Methods	Features
Soil mechanics theories	• Equation to calculate ultimate primary settlement $S_{ult} = (C_r/1+e_0)*H*\log(\sigma'_c/\sigma'_{v0}) + (C_c/1+e_0)*H*\log([\sigma'_{v0}+\Delta\sigma']/\sigma'_c)$, where C_r =swelling index, H = clay thickness, σ'_c = pre-consolidation pressure, $\Delta\sigma'$ = increase in effective vertical stress • Barron's (1948), Carillo's (1942) and Hansbo's (1979) equations to calculate degree of consolidation (U) accelerated by PVD, i.e. radial & vertical drainages
VDrainSt	• An algorithm embedded within Microsoft Excel to calculate settlement with time for staged reclamation construction with consolidation accelerated by PVD. It takes into account i) staged sandfill loading; ii) reduced loading due to sandfill settlement below GWT, i.e. submergence effect; iii) delayed PVD installation subsequent to first placement of sandfill; and iv) variation of soil stress history (e.g. OCR) with depth • Combine vertical and horizontal drainage using Carillo's equation • Consider smear effect
Slope/W	• Limit equilibrium analysis using the Morgenstern and Price method to predict factors of safety of reclamation slope at different construction stages • Input c_u values for MD at different construction stages had considered the strength gain with time as a function of the achieved degree of consolidation (U) calculated using Barron/Carillo/Hansbo equations and/or VDrainSt
PLAXIS	• Consolidation analysis with updated mesh and updated pore water pressures to consider the effects of large deformation and submergence • Model PVD in 2D plane strain using Bergado & Long's (1994) method to convert radial flow to plane strain flow • Model staged placements of sandfill, rest periods, and surcharge removal • Adopt Soft Soil constitutive model for marine clay, and Mohr Coulomb model for sandfill. In Soft Soil, the effective stress input parameters were calibrated so as to match the design c_u/σ'_v profile established from field Vane tests • Predict generation and dissipation of excess pore water pressures (epwp) with time, settlements, and FOS of reclamation slope at different construction stages using the Phi-c' reduction method

The S_{ult} and U calculated by soil mechanics theories provide a sanity check to those predicted by the computer programs. The VDrainSt predicted settlement-time behaviour and the Slope/W predicted FOS of reclamation slope provide sanity checks to those predicted by PLAXIS. Table 3 shows the design sequence of staged construction in the coal storage yard. The minimum FOS adopted for the reclamation slope is 1.15.

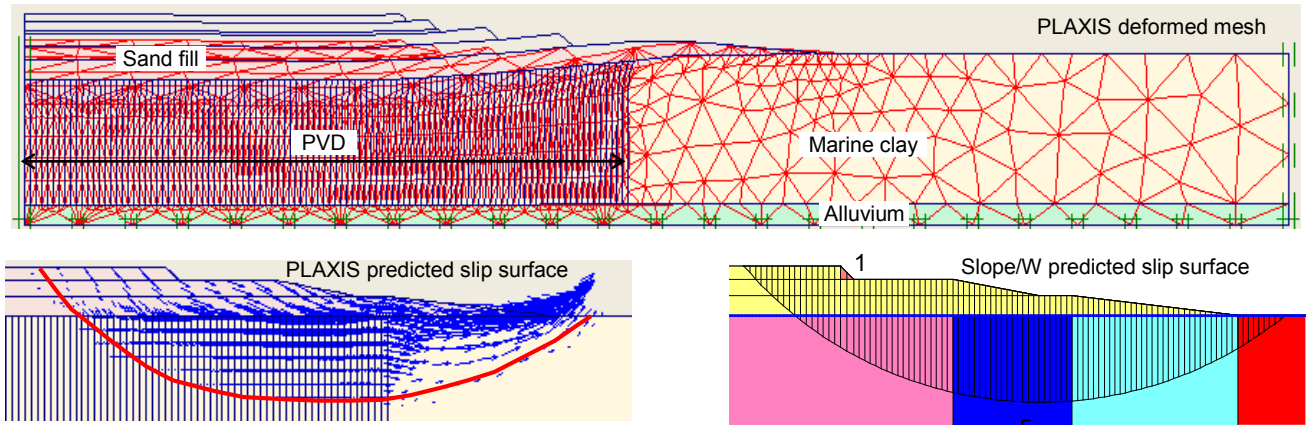

Figure 12: PLAXIS and Slope/W models

Table 3: Design sequence of staged construction in coal storage yard

Lift No.	Sandfill cumulative thickness (m)	Construction Sequence	Incremental days	Cumulative days
1	3.0	Place hydraulic sandfill	18	18
	3.0	Install PVD at 1m spacing on triangular grid	10	28
	3.0	Rest period [a]	52	80
2	5.5	Place hydraulic sandfill	20	100
	5.5	Rest period [a]	5	105
3	8.0	Place hydraulic sandfill	10	115
	8.0	Rest period [a]	35	150
4	10.5	Place dry sandfill	15	165
	10.5	Rest period [a]	5	170
5	13.0	Place dry sandfill	15	185
	13.0	Rest period [a]	16	201
6	15.4	Place dry sandfill	15	216
	15.4	Rest period	94	310
7	RL +4m MLSD	Remove surcharge to finished platform level [b]	7	317

Notes:
(a) Indicative time period only. Actual rest period will depend on the actual strength gain verified by interim field tests to ensure the stability of reclamation slope
(b) Removal of surcharge should be verified by measured settlement data (i.e. Asaoka's (1978) plot to determine 90% primary settlement) and degree of consolidation achieved in the field

Before removing the surcharge, the degree of consolidation achieved in the MD should be at least 90% estimated using Asaoka's plot. After removing the surcharge, it was targeted to achieve an OCR of greater than 1.2 in the MC to minimize its long-term secondary compression settlement.

4 FIELD PERFORMANCE

Clusters of instrumentation were installed at a spacing of 100m×100m on square grids. Each cluster comprised a settlement marker, movement marker, magnetic extensometer, inclinometer, observation well, and pneumatic piezometer. Due to the hydraulic filling activities and large settlements in the order of 4m – 5m, a large number of the instruments were blocked or malfunctioned during construction, in particular the pneumatic piezometers. Due to the malfunction of the pneumatic piezometers, it was decided to use Asaoka's plot and verification of strength (c_u) gain in the MD by interim field Vane tests to determine the degree of consolidation achieved prior to surcharge removal. This paper only presents the selected instruments with comprehensive monitoring data in the coal storage yard, see Figure 13 for their locations.

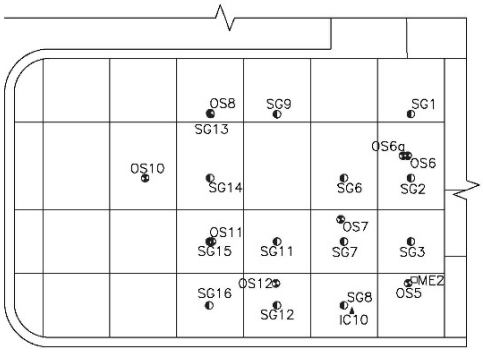

Figure 13: Instrument locations

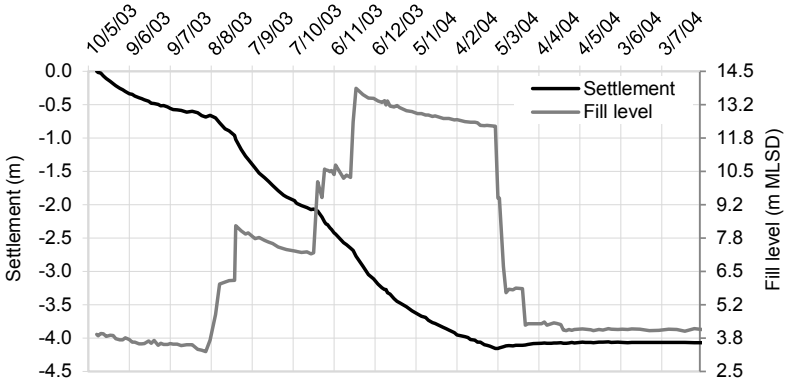

Figure 14: Settlements recorded at SG7

Figure 14 shows the measured settlements at the top of marine clay (MC) at settlement marker SG07. From 7-Aug-2003 to 22-Nov-2003, the sandfill level was gradually raised from RL +3.8m to RL +13.8m MLSD, and the settlements correspondingly increased from 0.7 to 4.15m. Commencement of removal of surcharge on 3-Mar-2004 by 8m caused a rebound (upward displacement) by 98mm. Figure 15 shows the rebounds measured at other settlement markers upon removal of the surcharge to the finished platform level of RL +4m MLSD. The maximum rebounds were 45mm – 98mm, after which the settlements increased slightly in a gradual manner, i.e. switching from swelling to consolidation process.

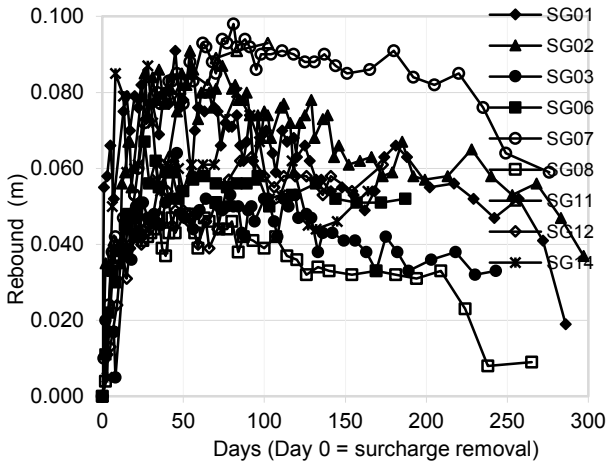

Figure 15: Rebounds due to surcharge removal

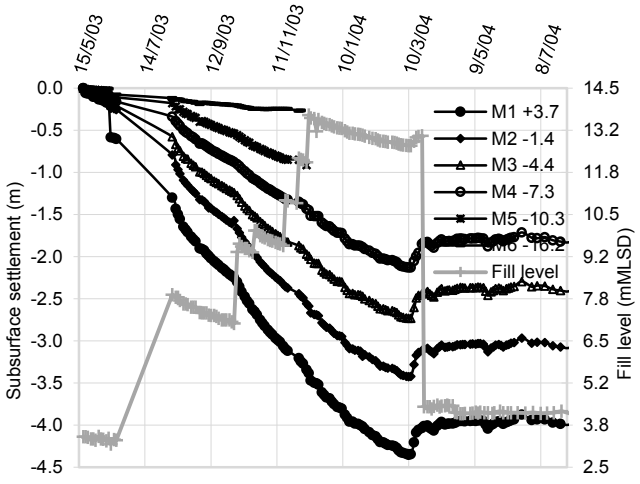

Figure 16: Subsurface settlements at ME02

Figure 16 shows the measured subsurface settlements in the MC layer at extensometer ME02. An increase in the sandfill thickness caused an increase in the subsurface settlements. Upon the removal of surcharge, magnets M1 to M4 at RL -7.3m MLSD showed rebounds by 340mm – 380mm.

Figure 17 shows the measured subsurface horizontal displacements towards the seaside at inclinometer IC10. It is noted that IC10 was installed late and the first reading was only available on 15-Oct-2003, i.e. the measured horizontal displacements did not include early displacements. Figure 18 plots the maximum horizontal displacements at RL -8.2m MLSD level against time. Following the last placement of sandfill to RL +10.35m MLSD on 18-Nov-2003, the horizontal displacements increased in a gradual manner with a decreasing rate with time. During the surcharge removal between 3rd and 23-Mar-2004, the horizontal displacements reversed in direction towards the landside by about 50mm.

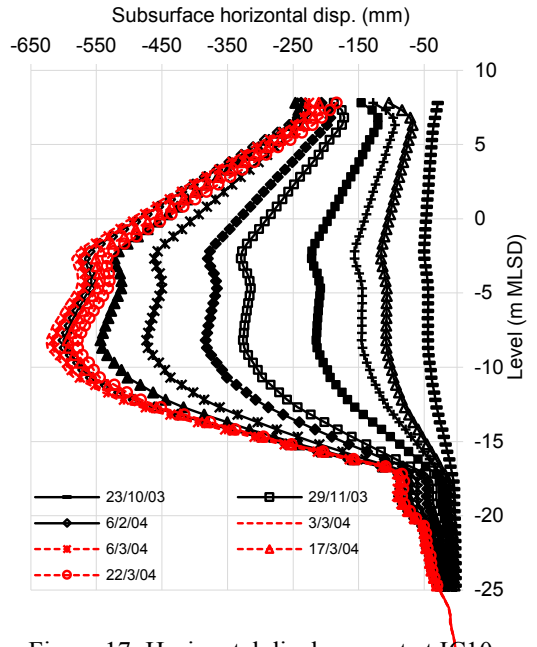

Figure 17: Horizontal displacement at IC10

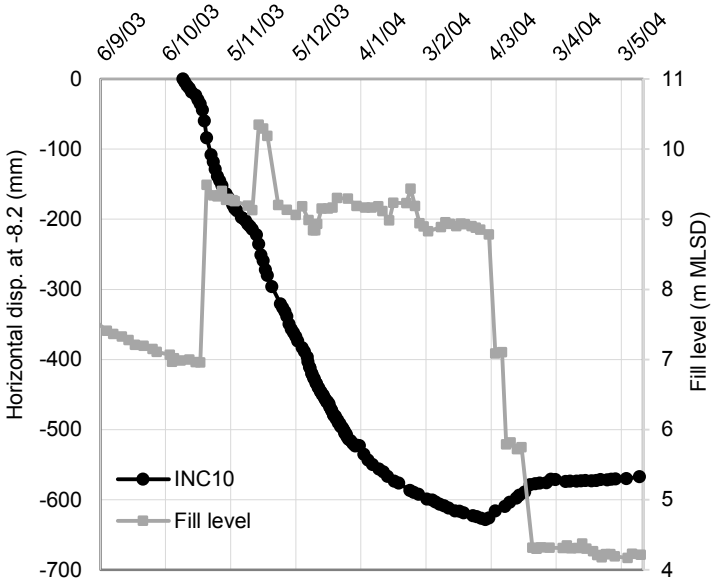

Figure 18: Horizontal displacement at RL -8.2 m MLSD

Figure 19 shows the measured water levels within the sandfill by observational wells. The water levels were relatively high at RL +4m to RL +5.5m MLSD in Aug-2003, gradually decreasing to RL +1.5m MLSD at end of 2004. The high water level in the sandfill was believed to be caused by hydraulic filling, large volume of water discharged from the PVDs and high rainfall intensity in the area (total rainfall of 2,371 mm in 2003).

Asaoka's (1978) graphical plots were carried out to estimate the final settlement (hence 90% primary settlement) and the operational coefficient of horizontal consolidation (c_h) in the field. Figure 20 shows an example of Asaoka's plot. Considering the high water level in the hydraulic sandfill (i.e. a lower effective surcharge load), the degrees of consolidation determined from Asaoka's plot had been adjusted to consider that in long-term the water level would return to the initial groundwater level. The operational c_h was back-analyzed using Magnan & Deroy's (1980) equation in Table 4.

Table 4: Magnan & Deroy's (1980) c_h equation

$c_h = \{-1/8\Delta t\}\{d_e^2 F(n) \ln\beta_1\}$	where Δt = time increment in Asaoka's plot; d_e = 1.05*PVD spacing on triangular grid; $F(n) \approx \ln(n) - 0.75$; $n = d_e/d_w$; d_w = equivalent PVD diameter = 2(drain width + thickness)/π; β_1 = slope of Asaoka's plot

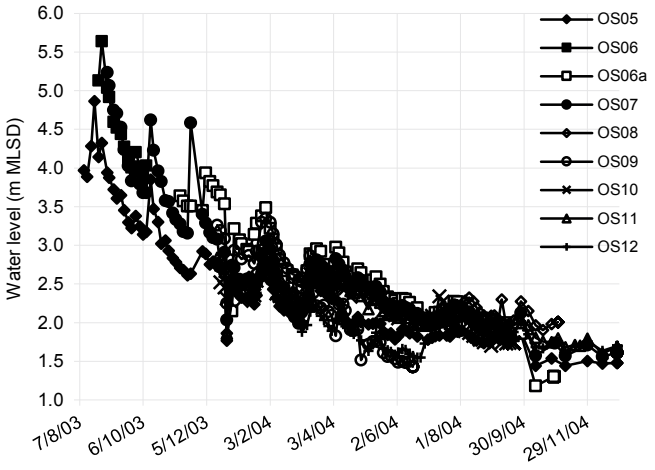

Figure 19: Water levels within sandfill

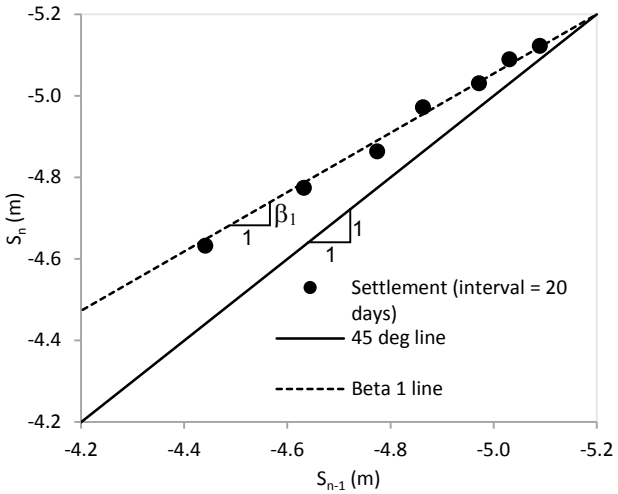

Figure 20: Asaoka's plot for SG09 (Δt = 20 days)

It is noted that the Magnan & Deroy equation does not specifically considered the smear effect caused by PVD installation. Hence, the back-analyzed c_h represents a lumped value in which the smear effect is reflected in the measured settlements via parameter β_1. The back-analyzed c_h values were 1.4 – 2.6 m^2/yr, compared to the c_h of 1.0 m^2/yr, which was conservatively adopted in the original design.

Figure 21 compares the predicted settlements by PLAXIS and the monitored readings at markers SG13, SG14, SG15 and SG16. A good agreement is obtained between the predictions and the field measurements. Table 5 summarizes the challenges faced by the instrumentation during the construction of reclamation.

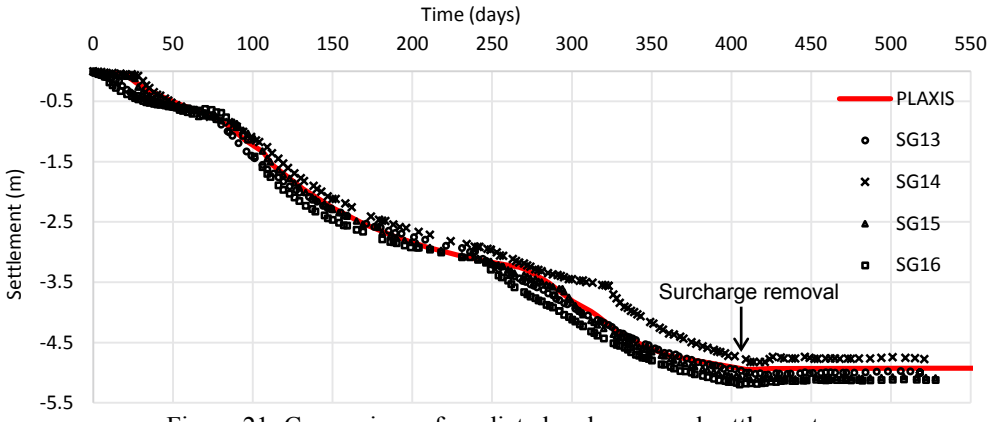

Figure 21: Comparison of predicted and measured settlements

5 SUMMARY

In the course of reclamation construction interim back-analyses of the monitoring data had been carried out, and it was revealed that the field performance of the reclamation generally conformed to the design predictions. The reclaimed land with ground improvement for the four different areas were successfully handed over to the client by the guaranteed final acceptance dates. The monitoring data presented in this paper and the challenges faced by the instrumentation serve as a well-documented case history for future drained (non-dredged) reclamation projects in similar ground conditions. Figure 22 shows an aerial photo of the power plant in operation. Figure 23 shows a trailing suction hopper derdger used to construct the reclamation.

Table 5: Challenges faced by instrumentation.

Instruments	Challenges	Proposed solutions
Settlement plate	• Plate installed at original ground level was displaced by first stage of hydraulic filling	• Plate installed on original ground level to be bedded onto a 100 mm layer of sand
Magnetic extensometer	• Blockage of access tube due to large settlement in marine clay causing buckling of tube	• A pure bentonite grout (instead of cement-bentonite grout) for grouting annulus around access tube to reduce downdrag on the tube
Inclinometer	• Blockage of access tube due to large settlement in marine clay causing buckling of tube	• Telescopic couplings to reduce downdrag and to accommodate some buckling at tube joints
Pneumatic piezometer	• Pneumatic tubing was displaced during hydraulic filling causing distress to the tubing	• Use a permanent steel tube to protect the pneumatic tubing full height above the tip

Figure 22: Completed 3x700 MW Power Plant on reclaimed land

Figure 23: Trailing suction hopper dredger “Inai Kenanga”, owned by IMW Malaysia

ACKNOWLEDGEMENTS

The data for this work had been collected by IMW Dredging Sdn Bhd who was the appointed EPC contractor. It would not have been possible to prepare this paper without the valuable source data. The authors wish to thank Malakoff Corporation Berhad for permission to publish this paper and bring this important project to a wider audience. The supports of Rentak Jitu Project Management Sdn Bhd and Zelan Construction are acknowledged.

REFERENCES

Asaoka, A. 1978. Observational procedure of settlement prediction. *Soils and Foundation*s, 18(4): 87-101.

Barron, R.A. 1948. Consolidation of fine-grained soils by drain wells. *Trans. ASCE*, 113: 718-742.

Barry, T., Krishnan, S. & van der Bend, L. 2004. Reclamation for a power plant in Johor, Malaysia. *Proc. 15th Southeast Asian Geotechnical Conf.*, *Bangkok*, 557-532.

Bergado, D.T. & Long, P.V. 1994. Numerical analysis of embankment on subsiding ground improved by vertical drains. *Proc. Int. Conf. on Soil Mech. and Found. Eng.*, *New Delhi*, 1361-1366.

Bo, M.W., Chu, J., Low, B.K. & Choa, V. 2003. *Soil improvement – prefabricated vertical drain techniques*. CENGAGE Learning, Singapore, ISBN 981-243-044-X.

Carillo, N. 1942. Simple two- and three-dimensional cases in the theory of consolidation of soils. *J. of Mathematics and Physics*, 21(1): 1-5.

Hansbo, S. 1979. Consolidation of clay by band shaped prefabricated drains. *Ground Engineering*, 12(5): 16-25.

Lam, Y.C., Ganendra, D. & Prasad, K. 2015. Land reclamation & soil improvement works for a coal-fired power plant in Malaysia. *Proc. 15th Asian Regional Conf. on Soil Mech. & Geotech. Eng.*, *Fukuoka*, 1767-1772.

Magnan, J.P. & Deroy, J.M. 1980. Analyse graphique des tassements observes sous les ouvrages. *Bulletin de liaison Laboratories des Ponts et Chaussees*, 109: 45-52.

Use of Vacuum Consolidation in Australia

R.B. Kelly
SMEC Australia & NZ

ABSTRACT

Vacuum consolidation has been used to improve soft ground for the Ballina Bypass section of the Pacific Highway upgrade and in reclamation works for the Port of Brisbane. In both projects the key constraints were deep deposits of soft clay, insufficient time for conventional staged construction and a need to prevent embankment failures dumping sediment into a sensitive marine environment. The Menard system of vacuum consolidation was used for both projects. Data from the Ballina project are presented in detail and compared with the Port of Brisbane. The beneficial effects of vacuum consolidation on embankment stability were demonstrated at Ballina where fill was placed rapidly to 8.5m thickness. The vertical alignment of the motorway was increased in height during this period and additional surcharging was required to achieve the design post construction settlement criteria. A further 5.5m of surcharge fill was placed after the vacuum system was switched off to achieve 6.5m of settlement. By the end of construction it was assessed that the design post construction settlement would be achieved. This case history demonstrates the ability of vacuum consolidation to maintain embankment stability under high fills and the adaptability of the system to changing conditions.

1 INTRODUCTION

Vacuum consolidation has been used to improve soft ground for the Ballina Bypass section of the Pacific Highway upgrade and in reclamation works for the Port of Brisbane. In both projects the key constraints were deep deposits of soft clay, insufficient time for conventional staged construction using prefabricated vertical drains and a need to prevent embankment failures dumping sediment into a sensitive marine environment. Rigid inclusions could have been used at both sites but were un-economic due to the deep deposits of soft clay and vacuum consolidation was assessed to be the most cost effective solution.

The Menard system of vacuum consolidation was adopted for both projects. The systems were designed using conventional consolidation theory where the design vacuum pressure was treated as an equivalent surcharge. A conventional system was constructed at Ballina whereas at the Port of Brisbane, a cut off wall through a hydraulically placed sand fill layer at ground surface level and extending through a subsurface sand layer within the soft clay (Indraratna et al, 2011) was constructed around the perimeter of the site to provide a vacuum seal.

The beneficial effects of vacuum consolidation on embankment stability were demonstrated at both sites where fill was placed rapidly and kept stable. At Ballina, the vacuum was applied for about 9 months and 4.5m of settlement occurred during this time. The system was allowed to consolidate for another 10 months and settlement reached 5m. The vertical alignment of the motorway was increased in height during this period and additional surcharging was required to achieve the design post construction settlement criteria. By this time the vacuum system had been decommissioned but the vacuum consolidation had improved the strength of the soft clay to a degree where the system could be converted into a surcharge and wick drain system using the existing vacuum drains. A further 5.5m of surcharge fill was placed to achieve 6.5m of settlement.

The performance at the Ballina site is reported in this paper in detail due to the change in operation from vacuum to non-vacuum loading. Incomplete case histories for the Ballina site have previously been reported by Kelly et al (2008) as well as Kelly and Wong (2009), from which much of the information presented in this paper is drawn. The performance at Ballina and the Port of Brisbane are compared where applicable.

This case history demonstrates the ability of vacuum consolidation to maintain embankment stability under high fills and the adaptability of the system to changing conditions.

2 GEOLOGY

The regional geology of the floodplain comprises extensive and often thick deposits of Quaternary Holocene alluvium overlying rock (Bishop, 2004). Quaternary soil deposition involved infilling of remnant levee-bank structures and incised palaeo-channels up to 40m depth. The geology at the site of the vacuum consolidation trial comprises a uniform deposit of soft to firm silty clay overlying residual soil and bedrock. The depth of the silty clay varies from near zero at Cutting 1 to 25m at the northern end of the site, near borehole BH832 adjacent to Emigrant Creek. A geological long section is shown in Figure 1.

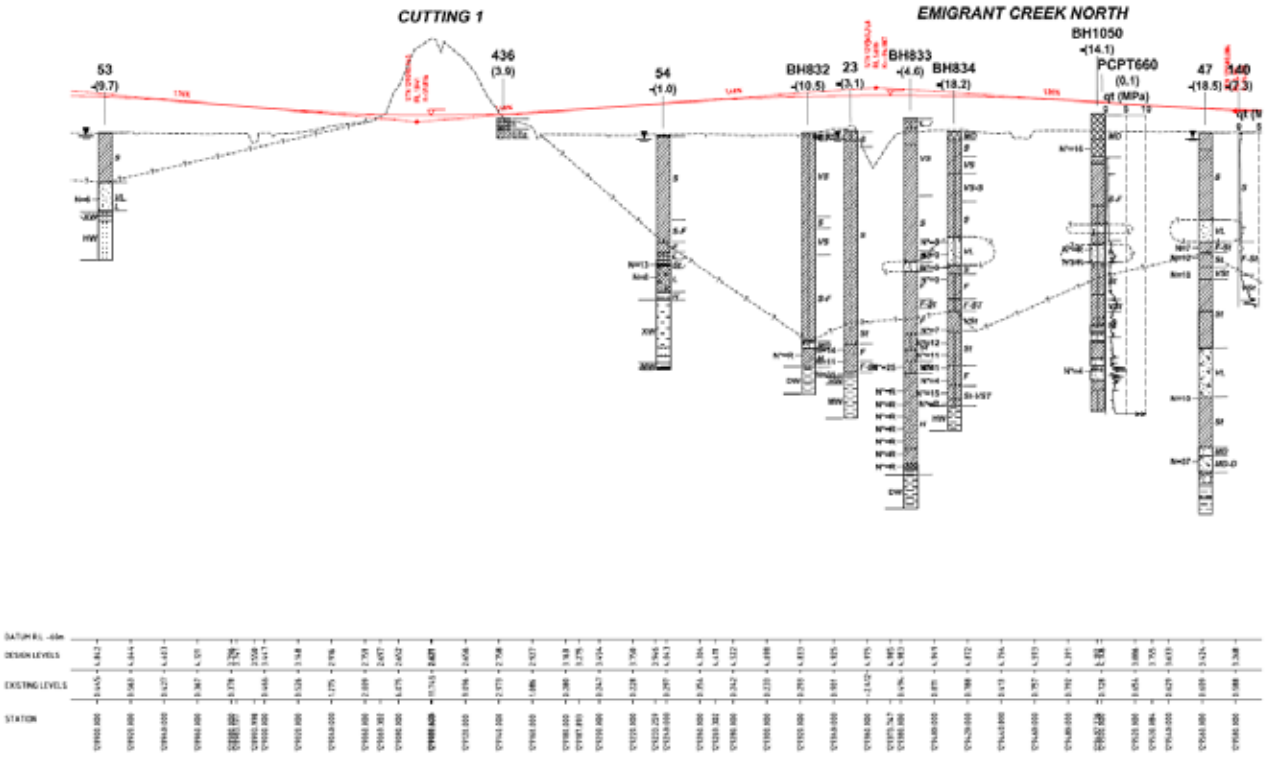

Figure 1: Geological long section

The Port of Brisbane is in the process of reclaiming 235Ha of land at the mouth of the Brisbane River at Fisherman Island. The area also acts a repository for dredged mud from the approach channel to the port. The soil profile comprises highly compressible clay to 30m thickness with an undrained strength around 15kPa near the top of the unit. The dredged mud has a much lower undrained shear strength depending on when it was placed and the duration that a 2m to 3m thick sand capping material had been in place (Indraratna et al, 2011).

The geotechnical model for Ballina is shown in Figure 2. Overconsolidation ratios (OCR) drop below 1.0 in Figure 2. This is not considered to be correct and the actual OCR was thought to be about 1.3 at depth.

3 VACUUM SYSTEM

The Vacuum Consolidation system is described by Masse et al (2001). A schematic drawing of the vacuum system used is shown in Figure 3. The system comprises disconnected vertical and horizontal drains where the hydraulic connectivity occurs through the sand layer, and a 1mm thick HDPE membrane sealing the system. The horizontal drains are 50mm in diameter, the vertical drains are 34mm in diameter and are installed using a wick drain rig with a 110mm square base plate.

Construction of the system began with placement of a coarse sand layer to act as a working platform for plant as well as the drainage layer. The vertical drains were installed at 1.2m square spacing at both Ballina and the Port of Brisbane, then the horizontal drains and then the instrumentation. The outlet connections for the horizontal drains and some of the instrumentation are connected to a manifold that becomes welded into the membrane. The cut off trench was excavated around the perimeter of the vacuum area and a layer of fine grained sand placed on top of the coarse grained sand to protect the membrane. The membrane was installed and sealed around the manifold as well as any instruments protruding through the membrane. The cut off trench was filled with water to seal the system from leaks. The vacuum pumps were turned on and the joins between the membrane sheets checked for leaks. Leaks were often detected by the sound they make. Any leaks that are found are sealed at this time. The vacuum suction developed in the sand beneath the membrane and was also transmitted down the vertical pipes. Figure 3 indicates that the vacuum pressure can be considered an isotropic stress increment in addition to the initial anisotropic stress state in the soil. After the vacuum pressure was fully developed, fill was placed on top of the membrane. A layer of fine grained sand was first placed in order to protect the membrane from punctures. General fill was then placed on top of the sand layer. The target vacuum pressure at both Ballina and the Port of Brisbane was 70kPa. The 70kPa pressure was adopted as a balance between what was considered achievable in construction and to maximize the benefit of vacuum consolidation. The vacuum pressure was considered equivalent to a surcharge pressure for the purpose of design calculations and conventional analysis was used to assess the surcharge/vacuum requirements to achieve operational stage settlement criteria.

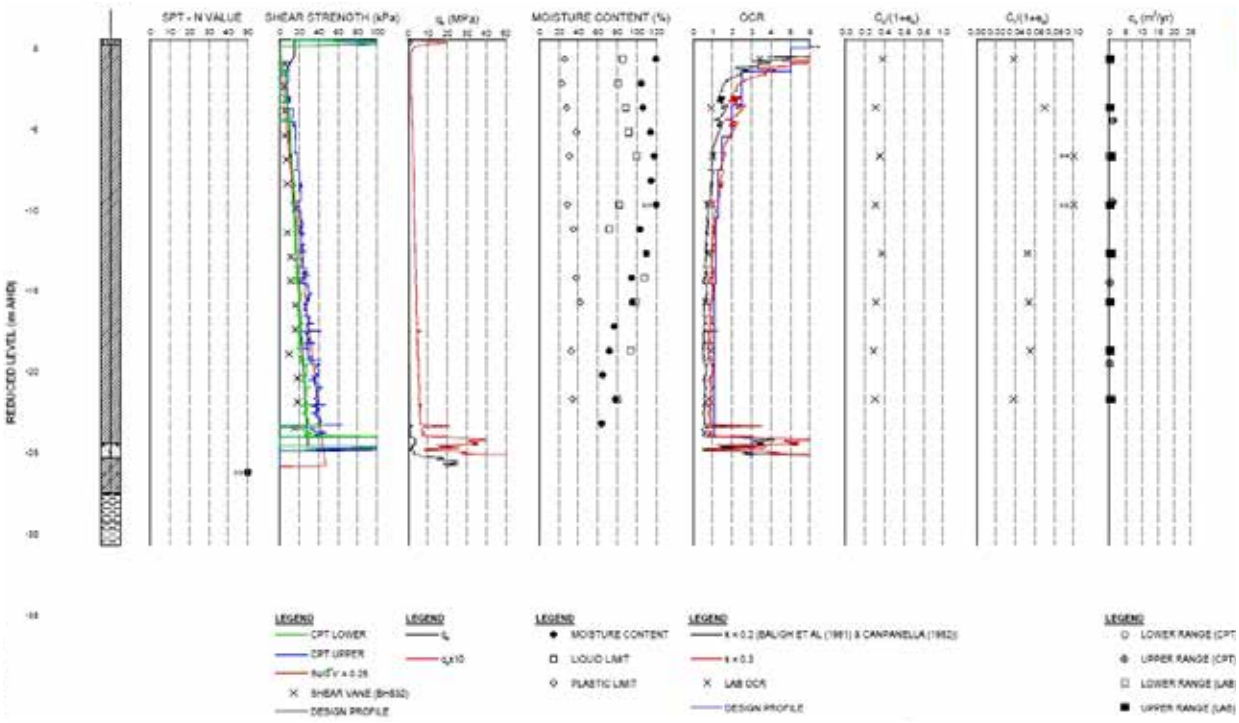

Figure 2: Geotechnical model at Ballina

The vacuum consolidation system is said to have two technical advantages over conventional wick drain consolidation systems. The first advantage is that transmission of the suction pressure down the pipes

develops an isotropic component of pressure that is transferred to the soil during consolidation. The isotropic loading pushes the stress path for a soil element away from the failure criterion and has the effect of enhancing stability of the embankment. This allows more fill to be placed in a given period of time than would be possible in a conventional wick drain system and substantially reduces the total construction time because staged construction may not be required. When the vacuum is turned off there will also be a component of isotropic unloading. The second advantage is that the suction pressure acts as an equivalent surcharge to fill and less fill needs to be placed to develop a desired total surcharge pressure. To gain the full benefit from this action, the vacuum pumps need to be left running until the desired degree of consolidation is developed in the soil.

The vacuum system also has two potential disadvantages. Firstly, if sand layers are present within the clay these may allow the suction pressure to dissipate. A cut off trench can be installed around the perimeter of the system through the sand layers to seal the system but this adds to the cost. Secondly, the extracted ground water may need treatment prior to release into the environment. At Ballina, the ground water was acidic and contained naturally occurring heavy metals. The water was collected in sedimentation ponds and treated with a compound called Electrobind™ by the company Virotech. Ground water treatment adds to the cost and also the need for treatment ponds adds to the area of land required for the work.

Cost comparisons with other ground treatment options for the Ballina Bypass indicated that the Menard vacuum system becomes cost effective when the thickness of soft clay is in excess of 13m to 15m, for the conditions encountered at Ballina.

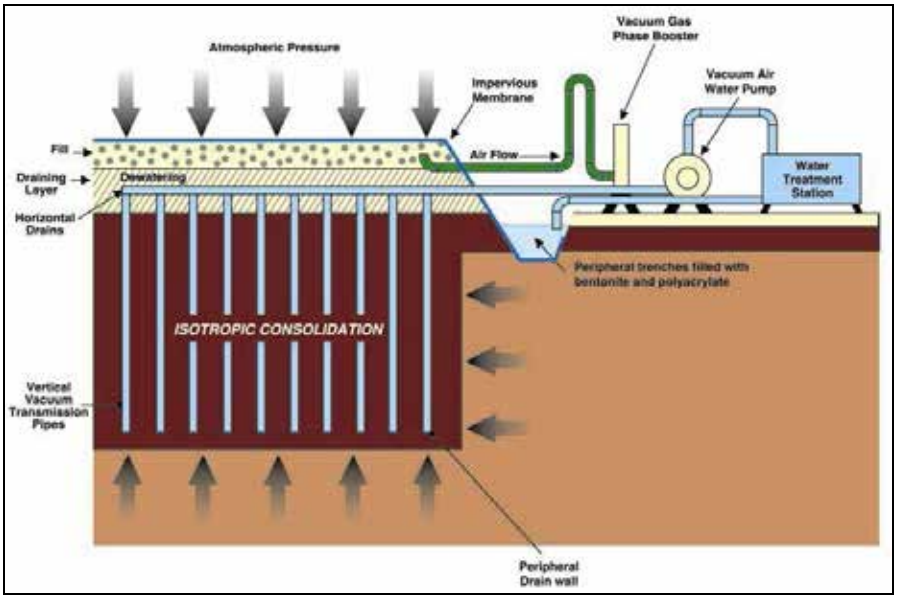

Figure 3: Vacuum consolidation system (Masse et al, 2001)

4 CONSTRUCTION STAGING

The construction staging at Ballina is summarised in Table 1.

Table 1 Construction staging

Construction Stage	Start date	Finish date
Placement of 1.5m thick sand drainage layer	8 Nov 2006	24 Nov 2006
Install temporary settlement plates	17 Nov 2006	23 Nov 2006
Install vertical and horizontal transmission pipes	13 Dec 2006	21 Dec 2006
Install inclinometers, extensometers and vibrating wire piezometers	11 Jan 2007	7 Feb 2007
Top up fill to 2m thickness	15 Jan 2007	2 Feb 2007

Lay vacuum membrane	2 Feb 2007	7 Feb 2007
Place 0.3m sand protection layer over membrane	7 Feb 2007	11 Feb 2007
Install permanent monuments and settlement plates	11 Feb 2007	11 Feb 2007
Start vacuum pumps	2 Mar 2007	-
Place additional fill to maximum 8.5m thickness	19 Mar 2007	6 July 2007
Consolidation under vacuum	6 July 2007	3 Dec 2007
Switch off vacuum	3 Dec 2007	-
Consolidation without vacuum	3 Dec 2007	11 Dec 2008
Additional Filling (the equivalent of 5.5m at 21kN/m^3)	11 Dec 2008	4 Sep 2009
Consolidation without vacuum	4 Feb 2009	9 Mar 2010

There was an extended delay between placing the membrane and starting the vacuum pumps to allow for water treatment ponds to be constructed adjacent to the vacuum area. Settlement during this period caused a build up of water pressures beneath the membrane which forced the membrane to bulge outwards. The membrane was cut in several locations to relieve the water pressure and then resealed prior to starting the vacuum pumps.

5 MONITORING DATA

The location of the instrumentation is shown in Figure 4. Settlement plates (SP), permanent monuments (M), magnetic extensometers (E), inclinometers (I), vibrating wire piezometers (P), vacuum pressure gauges, standpipes (SPP) and load cells (L) attached to the tensile fabric were used. One vibrating wire piezometer (P3e) was installed inside one of the vertical transmission pipes to a depth of 19.4m below original ground surface level. The remaining piezometers were installed approximately at the centre of the square vertical drain spacing pattern, and therefore record the maximum pore pressures in the clay. Settlement plates SP1 and SP2 are located in an area where prefabricated vertical drains were installed. The remaining settlement plates were installed in the area treated by vacuum consolidation.

The original groundwater level recorded in the standpipes was about 0.2m below ground level.

The time-settlement plot for the twelve settlement plates is shown in Figure 5. The magnitude of settlement recorded by the plates reflects the thickness of soft clay at each location. The vacuum pumps were turned on at day 2/3/2007 and turned off at day 3/12/2007. Near settlement plates SP11 and SP12, the settlement in the first day of operation was 45mm and the settlement averaged 22mm / day over the 18 days when the vacuum was operating prior to additional filling. The settlement was 4.4m when the vacuum pumps were turned off and 5.0m prior to placement of additional filling. The rate of settlement decreased once the vacuum pumps had been turned off from 6mm / day to 1.2mm / day. After the additional 5.5m of fill was placed, settlement was allowed to occur until a maximum settlement of 6.46m was reached at settlement plate SP12.

Inferred excess pore pressures measured by the vibrating wire piezometers are shown in Figure 6 along with data from the vacuum gauges installed beneath the membrane. The inferred excess pore pressures include the effects of settlement but not of changes to static groundwater levels. The pressure at the vacuum pumps was about -98kPa, which is nearly the maximum suction that can be generated. This pressure was consistently maintained throughout the vacuum period, with isolated exceptions when fuel ran out. The suction pressure measured by the vacuum gauges beneath the membrane was a maximum of -80kPa and reduced to -65kPa by the end of the vacuum period. Some leakage through the soil or beneath the membrane may have been responsible for the reduction in pressure. The inferred excess pore pressure measured by piezometer installed in the drainage pipe was a near perfect match to the suctions measured beneath the membrane indicating that the full vacuum pressure was being transmitted down the vertical transmission pipes. The pressure measured by piezometers 2a and 3a also became negative indicating that the full surcharge and vacuum pressures had been transmitted to the soil at the depth of these piezometers. The pressures measured by piezometers 2b, 2c, 3b, 3c and 3d all appeared to reflect the surcharge loading only with minimal contribution from the vacuum pressure. This is inferred to indicate that the permeability of the soil was sufficiently low that the suction pressure front had not extended from the vertical transmission pipe to the location of the piezometers.

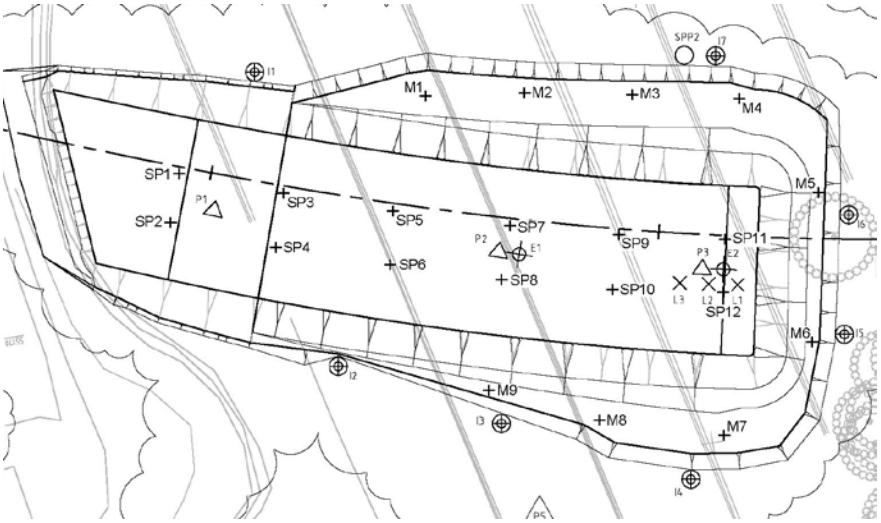

Figure 4: Layout of instrumentation (M = monuments, I = inclinometers, SP = settlement plates, P = vibrating wire piezometers, SPP = standpipe piezometers, E = extensometers)

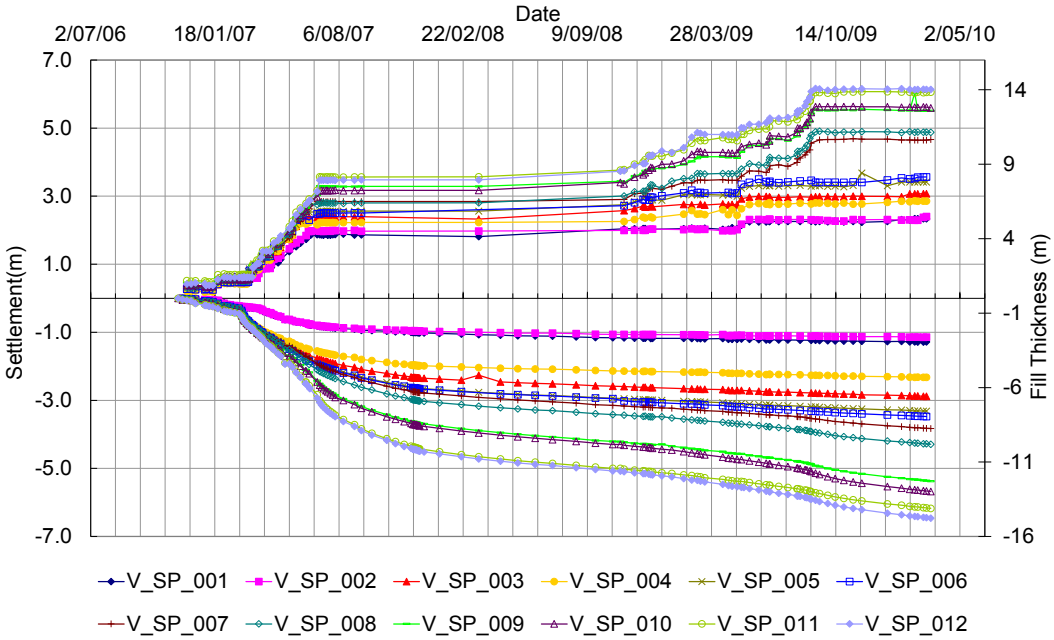

Figure 5: Settlement plate data

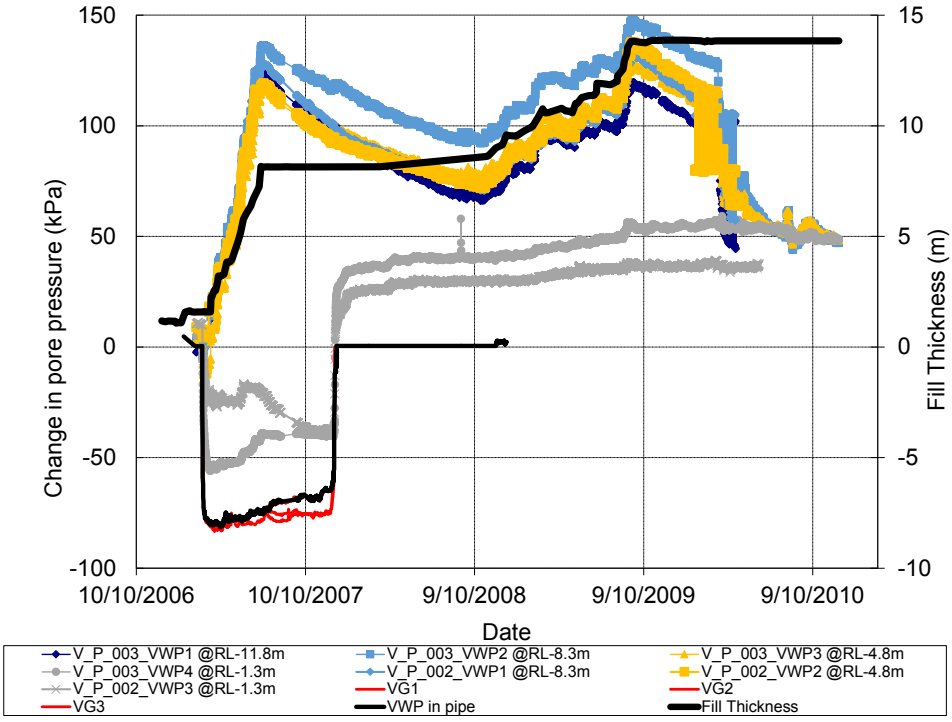

Figure 6: Excess pore pressures

Lateral deformations recorded by Inclinometer I3 are shown in Figure 7 and deformations recorded by Inclinometer I6 are shown in Figure 8. The data in Figure 7 shows that the soil moved outwards prior to the vacuum pumps being turned on, then the soil moved inwards on commencement of pumping until the additional fill was placed when the soil moved outward again. The data in Figure 8 shows that a shear plane had formed at about 13m depth between the embankment and Emigrant Creek. The shear plane appeared about the time the fill had been placed to 8.5m thickness.

Assessment of the embankment stability, and by implication the rate of surcharge filling, was performed using the method described by Tavenas and Leroueil (1980). The maximum lateral deformations recorded by the inclinometers are compared with the settlement at the centre-line of the embankment. Impending instability is indicated by the ratio of lateral displacement increment to settlement increment approaching unity. Tavenas and Leroueil (1980) suggest that a ratio of 0.15 to 0.2 indicates a low risk of instability. Maximum lateral displacements are plotted against settlement in Figure 9. Inclinometer I1 lies adjacent to the PVD area while the other inclinometers ring the vacuum area. Around the vacuum area, when the vacuum was in operation, the ratio of lateral displacement to settlement did not exceed 0.13 when the surcharge fill was less than 5.3m thick and increased to 0.3 once the fill thickness reached 7m. The ratio was greatest in the areas where the berm widths were least. As the width of the berms increased the ratio decreased. However, the data indicates that the embankment was stable in all areas, which implies that stability berms may not be required. During the consolidation period the ratio reduced. Once the vacuum pumps were turned off, around 4.4m settlement at occurred at I5 and I6; and the ratio increased again to about 0.35. This shows that the embankment had relaxed and moved outward more rapidly for a period of time after the pumps were turned off. When the additional surcharge was placed after decommissioning of the vacuum system, the ratio increased to a maximum of 0.66, which remained below the trigger level for action which was a ratio of 0.7.

In contrast, the ratio in the standard surcharge area approached one after a fill thickness of only 2.5m had been placed. A hold point preventing further filling in the standard surcharge area was invoked until the ratio dropped below 0.6. Subsequent filling to 4.1m increased the ratio to one again and a second hold point was applied. Stability berms would have allowed a faster rate of filling in this area. This comparison shows clearly the beneficial effects of vacuum consolidation. More fill can be placed more rapidly on top of the vacuum consolidation area than can be placed using standard surcharge filling methods.

A similar comparison between PVD treated areas and vacuum treated areas at the Port of Brisbane showed similar results.

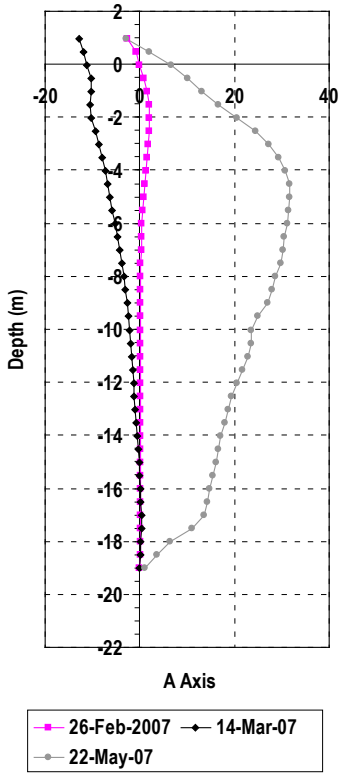

Figure 7: Inclinometer I3

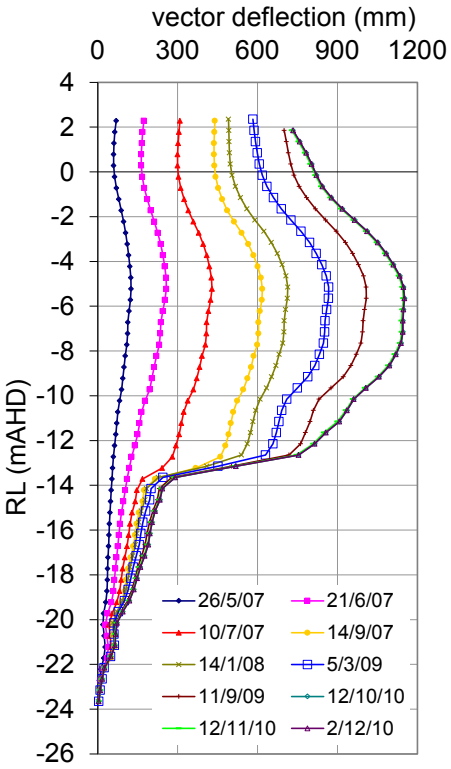

Figure 8: Inclinometer I6

6 POST VACUUM INVESTIGATIONS

A number of boreholes and piezocone tests were performed through the embankment after the vacuum pumps had been turned off and the suction pressures dissipated but prior to the placement of additional fill. U75 tube samples were taken and moisture content and oedometer tests performed. The results of these tests from samples taken near settlement plates SP11 and SP12 are compared with similar data taken from samples obtained prior to embankment construction in Figures 10 and 11. Compression ratios ($C_c/(1+e_0)$) are compared in Figure 10 and show that the compression ratios measured after the vacuum had ceased were about two-thirds the value of the data taken before embankment construction on average. This is an indication that the large deformations had de-structured the soil to some extent. Design assumed a bi-linear void ratio-log effective stress relationship. In principle, use of a non-linear void ratio – effective stress relationship would have allowed this behavior to be modelled but this was not attempted. Moisture contents are compared in Figure 11. The moisture contents measured after vacuum consolidation are less than those measured pre-vacuum consolidation from ground level to about 12m depth. This is to be expected in soil that has been consolidated. In contrast, the moisture content measured post-VC was similar or greater than those measured pre-vacuum consolidation below about 12m depth. It is not clear why this is the case, although it is possible that the two values at about 15m and 17m depth may have been affected by the shear plane that had formed beneath the embankment.

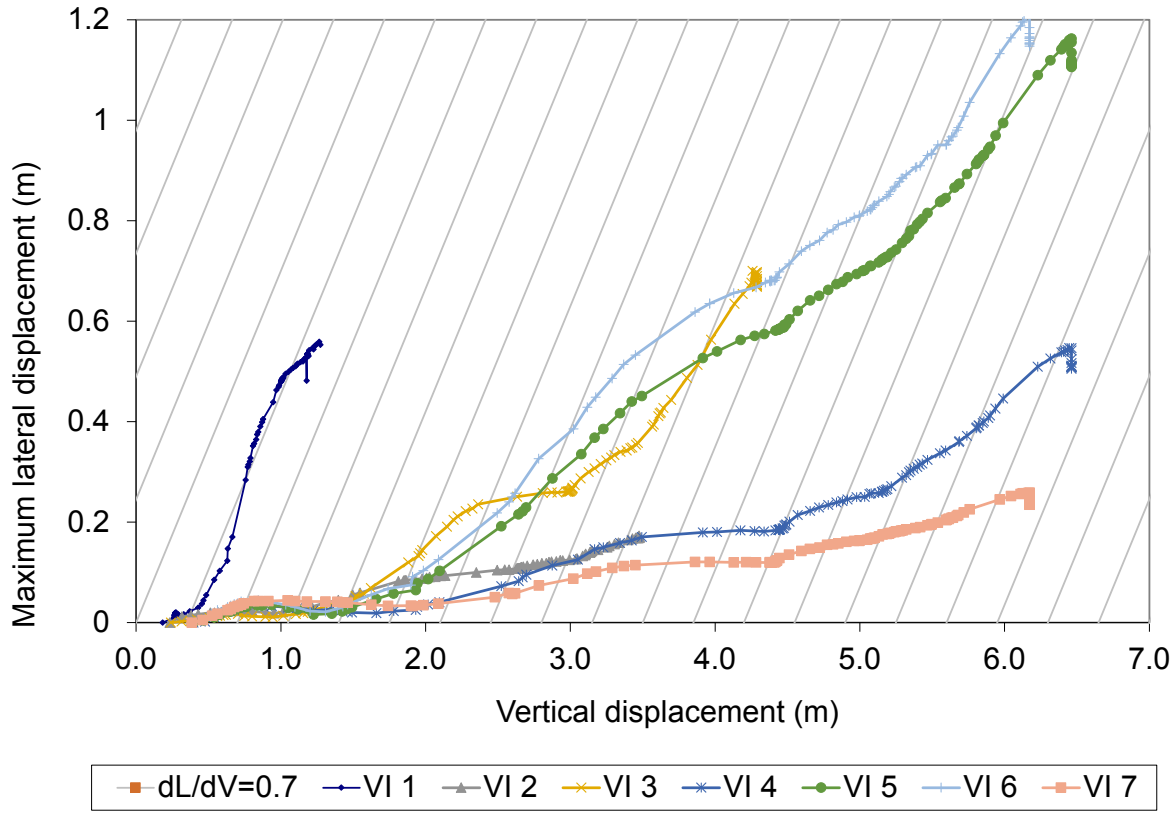

Figure 9: Inferred embankment stability plot

Data from piezocone tests performed pre and post vacuum consolidation are presented in Figures 12 and 13. These tests were performed after approximately 4.5m of settlement at settlement plates SP11 and SP12 and 3.0m settlement at SP7 and SP8. From 0m to these settlements, the figures show traces associated with fill materials. Below these levels the cone tip resistance is significantly greater than the value pre-VC within a 2m to 4m zone. This reflects the excess pore pressure data which showed that full suction pressure was transmitted to these soils. Below this level the increase in excess pore pressure is smaller, indicating that the degree of consolidation of these layers was less than the upper layers. This is again consistent with the excess pore pressure data.

There is an anomaly shown in Figure 12 between 9m and 12m depth where the cone tip resistances pre and post vacuum consolidation were similar. This may again be a manifestation of the shear plane that developed during construction. The magnitude of the shear strain at this location may have been sufficiently large to develop post-peak shear strength in the soils.

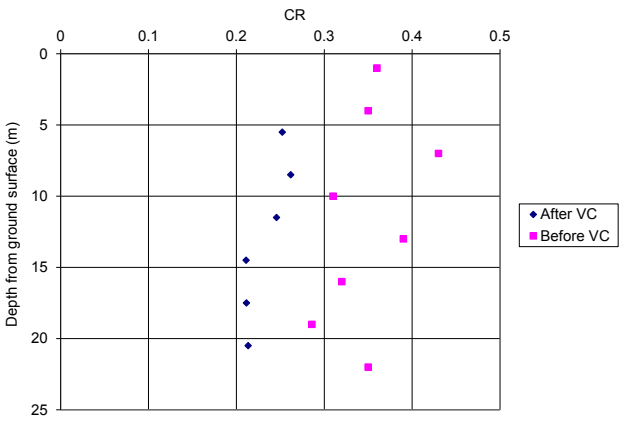

Figure 10: Compression ratio

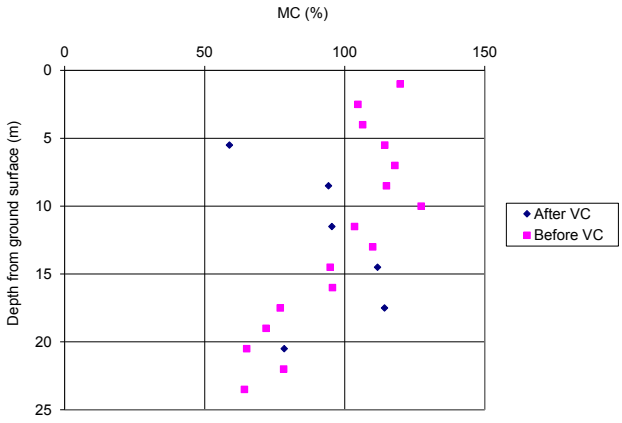

Figure 11:Moisture content

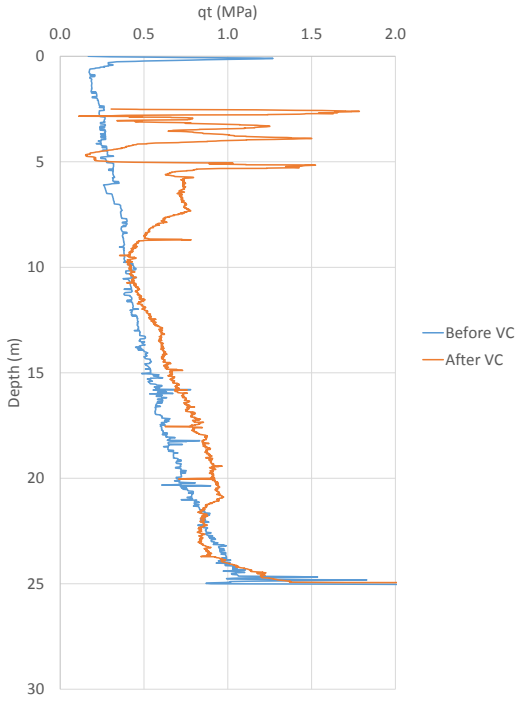

Figure 12: Data near SP11 and SP12

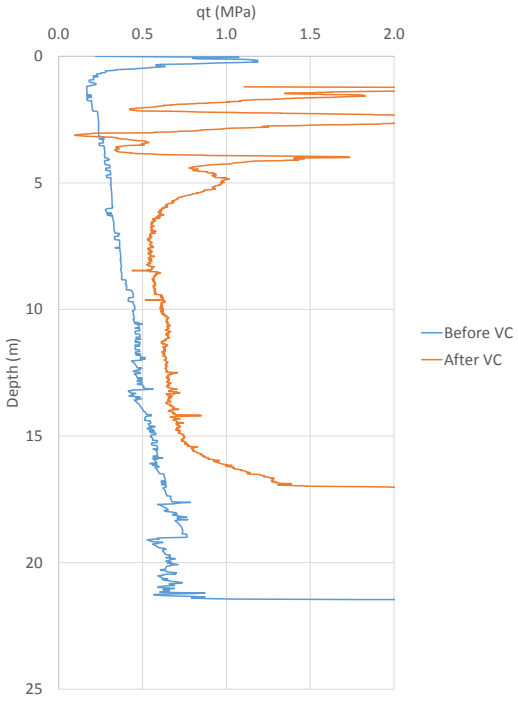

Figure 13: Data near SP7 and SP8

7 BACK ANALYSES AFTER THE ADDITIONAL SURCHARGING

Back analyses performed at the end of the vacuum period were unable to reconcile pore pressure and settlement data when the material parameters derived from the original site investigation were adopted. The compression parameters had to be increased by 30%, the overconsolidation reduced to nearly 1.0 at depth and the permeability was reduced by a factor of about 2 to match the data. Results of one-dimensional settlement calculations performed after 14m of fill had been placed are compared with settlement plate data in Figure 14. The back analyses performed at this time were able to match the settlement data reasonably well. Similarly the total pressures measured by the vibrating wire piezometers were reasonably well matched by the analyses in Figure 15.

At the time, such a large increase in compression parameters and reductions in overconsolidation ratio was considered to be unrealistic. However, more recent research standard investigations performed about 500m south of the vacuum site (Pineda et al, 2016) have shown that the magnitude of the parameters required to fit

the monitoring data was realistic. This result clearly emphasized the need to obtain high quality soil samples for laboratory testing in order to accurately predict the performance of the vacuum system.

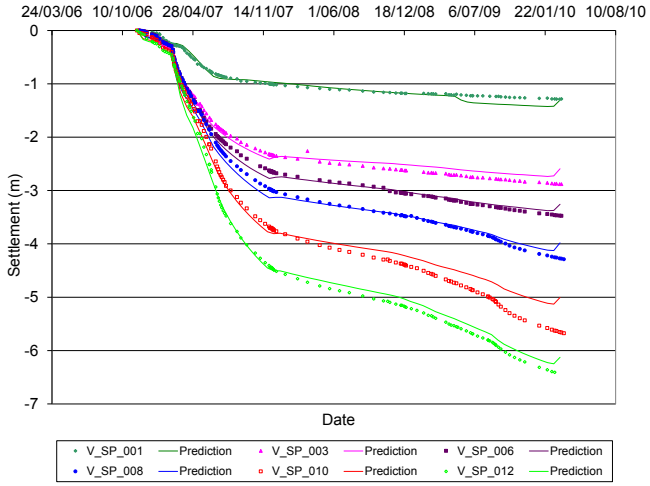

Figure 14: Back analysis of settlement

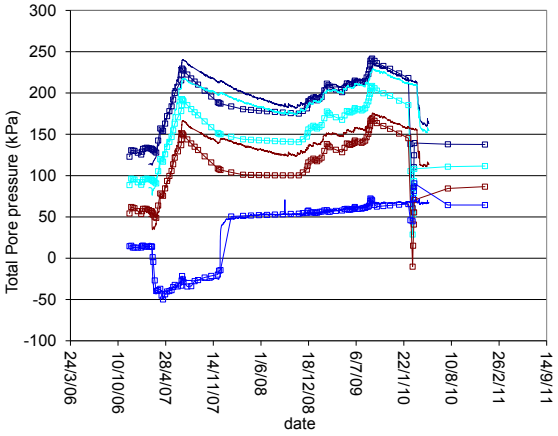

Figure 15: Back analysis of pressure

8 CONCLUSIONS

The vacuum consolidation system was successfully implemented. The vacuum system allowed the surcharge fill to be placed more rapidly than possibly using conventional staged construction techniques and this sped up the construction process. A shear plane formed in the soft soil during construction but the vacuum system prevented failure. Post construction site investigations showed improvement in the ground in general, except for where the shear plane formed. Back analyses were able to match the measurements by increasing the compression parameters, reducing the overconsolidation ratio and reducing the permeability of the soil. This demonstrates the importance of high quality site investigations.

ACKNOWLEDGEMENTS

The author acknowledges the Roads and Maritime Services of New South Wales for use of the data.

REFERENCES

Bishop D. T. (2004). "A proposed geological model and geotechnical properties of a NSW estuarine valley: A case study", *8th Australian and New Zealand Geotechnical Conference*

Kelly, R., Small, J., and Wong, P. (2008) Construction of an Embankment Using Vacuum Consolidation and Surcharge Fill. *GeoCongress 2008:* pp. 578-585.

Kelly, R.B. and Wong, P.K. (2009) An embankment constructed using vacuum consolidation, *J. Australian Geomechanics Society*, 44(2), 55-64

Indraratna, B, Rujikiatkamjorn, C., Ameratunga, J. and Boyle, P. (2011), Performance and prediction of vacuum combined surcharge consolidation at Port of Brisbane, *J. Geot and Geoenv Eng., ASCE*, 137(11), 1009-1018

Masse, F., Spaulding, C.A., Wong. I. C. and Varaksin, S. (2001), "Vacuum Consolidation: A Review of 12 years of Successful Development", *Geo-Odyssey ASCE Virginia Tech*.

Pineda J.A., Suwal, L., Kelly R.B., Bates L. & Sloan, S. W. (2015) Characterization of the Ballina clay. *Geotechnique published online* DOI: http://dx.doi.org/10.1680/jgeot.15.P.181

Tavenas, F. and Lerouiel, S. (1980), "The behaviour of embankments on clay foundations", *Can. Geotech. J.*, Vol. 17, 236-260

Gaining Access over Extremely Soft Deposits using a Geogrid Stabilised Granular Layer

G. Murtaza
Tensar International Limited, Malaysia

ABSTRACT

Extremely soft soils are typically encountered in dredged fills or sludge lagoons. The depth of such deposits could be up to several meters. Theses soils pose challenges for civil engineers and require special attention. Gaining safe access for pedestrians and vehicles on to such deposits is one of the key challenges, as even walking on such soils is impossible in most cases. Conventional methods are expensive and time consuming. Stiff geogrids when incorporated in to an unbound aggregate layer form a mechanically stabilised layer (MSL) that offers safe access on to such deposits and creates a permanent capping layer for subsequent operations and developments. Crucial to the success of this technique is the correct construction methodology. A number of case studies demonstrate successful application of a mechanically stabilised layer (MSL) to gain access over extremely soft soils.

1 INTRODUCTION

Reclamation over the soft soils has been an important source of land supply in many countries particularly having shortage of usable land. About 7,000 square kilometers of entire country of Netherlands (one sixth of total area) have been reclaimed from the marshes, swamps, lakes and sea. South Korea, Singapore, Hong Kong, Japan and Bahrain are some of the countries who have added several square miles to their lands. Increased demand for housing, industrial, commercial and infrastructural developments are some of the factors resulting land reclamation activities.

Design and construction of reclamation works requires special attention due to the presence of commonly extremely soft soils which are not simple to deal with. When it comes to reclamation works, there are several challenges for civil engineers including, but not limited to, gaining safe access on to the site, health and safety issues, pressure to reduce construction costs, tight construction schedules and complying with the environmental requirements. Traditional methods of design and construction of reclamation works commonly fail to solve most of these issues. Therefore, innovative design and construction techniques need to be considered when dealing with reclamation works.

Geogrids have many applications in civil engineering. Access on weak grounds, paved/unpaved roads, working platforms and hard-standings, grade separation structures (reinforced soil walls and slopes), railway structures, heavy duty pavements for container yards and airfield are some of the examples where geogrids have established their superiority over the traditional methods resulting in economical, safe, environmentally friendly and speedy solutions. This paper discusses the use of geogrids to form a mechanically stabilised granular layer which offers innovative solution to civil and geotechnical engineers for many of their problems related with extremely soft soils.

2 USE OF GEOGRIDS

2.1 Background

The use of geogrids for ground stabilisation applications (weak grounds) could be traced back to late 1970's when heavy duty extruded nets (originally used for agriculture, horticulture and packaging) were deployed for coastal reclamation in Japan (Figure 1).

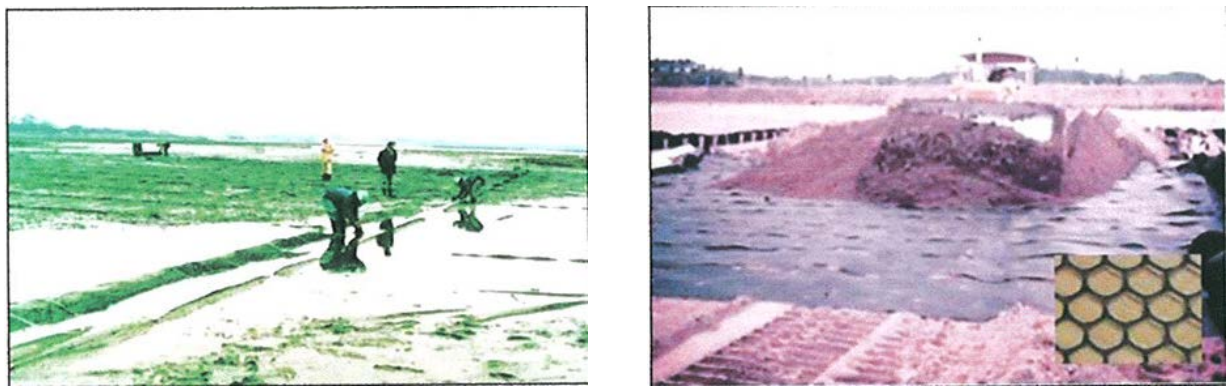

Figure 1: Coastal reclamation using an extruded mesh in Japan in the 1970's

This arose the need for further investigation. An early research carried out by Dr G.W.E Milligan at Oxford University Engineering Department in 1980 on the use of mesh products to improve the performance of granular fill on soft grounds concluded that fill stabilised with stiff mesh indicated improved performance particularly at high loads, whereasd less stiff mesh was found to be less effective (Figure 2). Therefore, for optimum performance the mesh should be very stiff and the fill particles should interlock fully with the mesh structure.

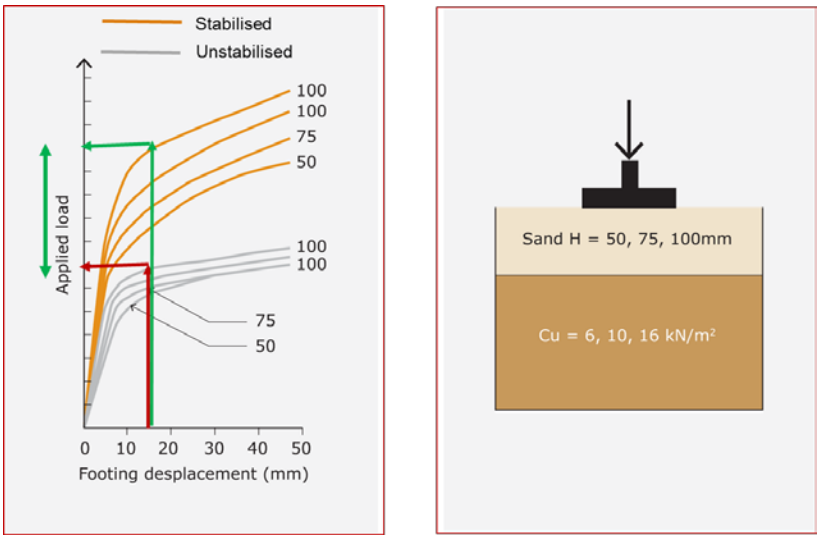

Figure 2: Research at Oxford University in 1980

A new manufacturing process was developed to introduce greater stiffness in to the geogrid. In 1982, biaxial geogrids with much superior stiffness modulus than standard meshes were produced as a result of

punching and stretching polymer sheets orthogonally. Figure 3 below shows application of stiff monolithic geogrids for ground stabilisation on a highway project in early 1980's.

Figure 3: Ground stabilisation on a highway using monolithic geogrids (early 1980's)

Further research to improve the performance of these geogrids lead to the development of new generation hexagonal geogrids. Figure 4 below shows application of hexagonal geogrid over extremely weak foundation soils for two different projects.

Figure 4: Two examples of ground stabilisation using hexagonal geogrids over extremely soft soils

2.2 Geogrid Stabilised Layer

In the European Organization for Technical Approvals (EOTA) Report TR041, stabilization has been defined as "the beneficial consequence on the serviceability of an unbound granular layer via the inhibition of the movement of the particles of that layer under applied load. This is the result of the mechanical effect of confinement on an aggregate layer, resulting from the mechanism of interlock provided by a stiff geogrid structure." The aggregate interlock provided by a stiff geogrid effectively stiffens the aggregate and enables any imposed loads to be distributed over a wider area than would be the case without a geogrid.

Stiff geogrids can form a composite, known as mechanically stabilized layer (MSL) when they are incorporated in to unbound aggregate layers. The benefits of mechanically stabilised layers have been quantified by various research works carried out both under static loads as well as dynamic wheel loads. Over

the extremely weak grounds, application of these mechanically stabilised aggregate layers not only offers safe human and machinery access on to such soils but also results in increased bearing capacity of the aggregate layers under heavy loads and reduction in layer thickness.

2.3 Performance parameters of stabilising geogrids

For biaxial geogrid, the stiffness of geogrid is organized along the rib directions (machine and cross-machine direction). See the polar diagram of tensile stiffness at low strain for a biaxial geogrid in Figure 5. Biaxial geogrids are more effective in spreading the wheel loads in rib direction than in diagonal direction.

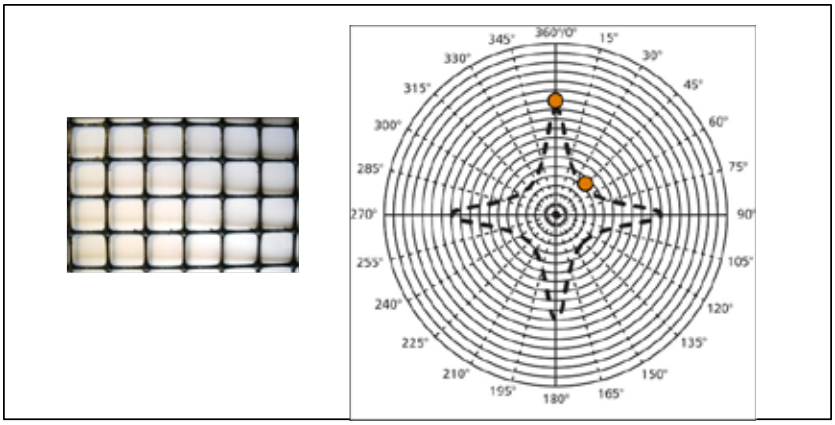

Figure 5: Polar diagram showing the stiffness footprint of a biaxial geogrid

A hexagonal shape geogrid resulted in an improved performance due to its ability to spread the applied loads in all directions more effectively than biaxial geogrid. The hexagonal structure provides a near circular stiffness response which matches the radial wheel load distribution (Figure 6). This uniform and balanced response is important for optimizing stabilisation performance.

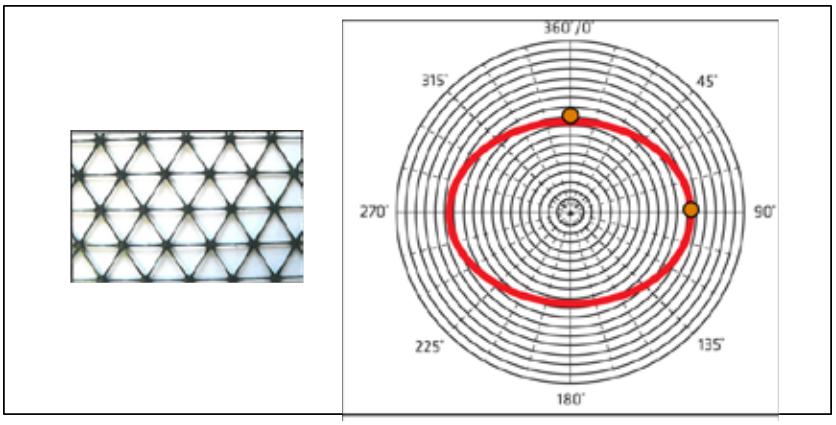

Figure 6: Polar diagram showing the stiffness footprint of a hexagonal geogrid

Research at Nottingham Pavement Research Facility concluded that radial stiffness at low strain and associated radial stiffness ratio are very good indicators of expected trafficking performance of a mechanically stabiliser layer.

As the stabilising geogrids work by the mechanism of interlock, it is also important that the stabilising geogrids have appropriate hexagonal pitch to offer effective interlock to the aggregate and also have high

junction efficiency. The configuration of the geogrid ribs and the integral junctions provide lateral restraint to the aggregate particles as they partially penetrate the geogrid apertures.

3 CASE STUDIES

This section describes 3 case studies where geogrids were incorporated into the granular fill to form a mechanically stabilised layer to get access on the extremely weak existing soils.

3.1 Port of Gisborne Log Yard New Zealand 1995

The Port of Gisborne Logging Yard has been constructed over reclaimed land. The reclamation fill comprised approximately a 4m depth of variable materials including organic matter, timber and hardcore (broken bricks, concrete, stone etc) all over a shelf of unconsolidated muddy sandstone, known locally as papa soil. Occasional infilled channels up to 10m deep were encountered. The subgrade for the log yard consisted of soft areas with a CBR of less than 1% (Figure 7). The client experienced considerable problems with trucks and loaders sinking up to their axles.

Figure 7: Poor ground conditions on site (CBR < 1%)

Loadings on the yard included a 70 tonne axle loading Wagener unloading approximately seventy to ninety, 14 tonne tandem axle trucks per day. The fully laden trucks were up to 46 tonnes capacity (Figure 8).

The original design required a pavement depth of 700mm to take the loads from the log handler. An alternative solution was to provide a mechanically stabilised layer (MSL) incorporating a layer of geogrid. This enabled a reduction in pavement depth from 700mm to 350mm (Figure 9). Stabilising geogrid were laid on the subgrade and covered with 150mm to 200mm of quarry scalping. This was topped with 100mm of AP40 base course and 50mm of AP20 surfacing. After ten years of heavy duty use, the installation performed satisfactorily as shown in Figure 8. As the construction materials in the project area were very expensive, a considerable savings were made as well.

Figure 8: Log handling Wagener operating on new construction

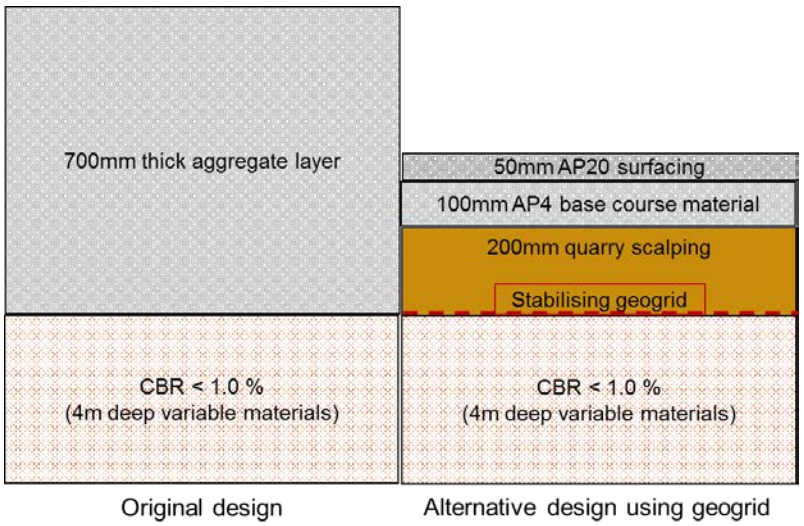

Figure 9: Comparing original design with stabilised design

3.2 Sludge Lagoon at Dowley Gap Sewage Treatment Works (STW), Bingley West Yorkshire 2001

Environmental and general health and safety issues led to the requirement for capping the disused sludge lagoon at Dowley Gap Sewage Treatment Works in Bingley, West Yorkshire (Figure 10). The original proposal was to employ lime stabilisation and band drain techniques. The extremely soft consistency of the sludge meant that access to install the cap was very difficult. Additionally, the client wanted to provide long-term safe access for pedestrians and light vehicles with the potential to be used as an open amenity area.

Figure 10: Sludge lagoon at Dowley Gap STW required capping

The sludge lagoon, measuring 14,000m2 in plan had been in use since World War II but disused since the late1990's. Tests showed that the 7m deep lagoon contained sludge that had failed to consolidate with time and had no significant shear strength. It could not therefore support any significant loadings in its current state.

It was proposed to install multiple layers of geogrid to facilitate installation of the capping using local granular fill (Figure 11). Very careful placement of fill materials by the contractor, combined with a leachate drainage and gas venting system and an impermeable cover, a mechanically stabilised layer with multiple layers of stabilising geogrid was installed. This resulted in capping of the sludge lagoon with significant cost and time savings compared with lime stabilisation and band drain techniques which were considered originally.

Initially a layer of a stabilising geogrid was placed directly on top of the sludge, facilitating access for site personnel. The first fill layer was then raked into a consistent 300mm thick layer, without compaction, before placing the second layer of stabilising geocomposite geogrid (geogrid factory-bonded to a geotextile filter). Another 300mm of fill, incorporating the leachate drainage system was then placed followed by the final layer of geogrid. Once the overall fill thickness had reached 1m, it was possible for medium-sized construction plant to gain access on top of the lagoon (Figure 12).

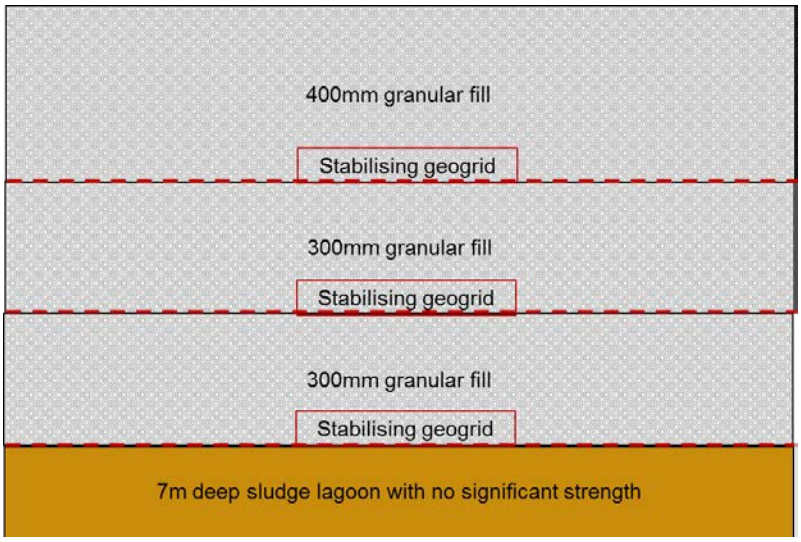

Figure 11: Mechanically stabilised layer with multi-layers of geogrid

The project is an example of one of the most extreme uses of geogrids to date. Crucial to the success of this approach was the ability to place a thin layer of fill over as wide an area as possible without overstressing the underlying soil at any particular location. Too thick a layer at any point would have led to mobilisation of a rotational type failure mechanism and the fill and underlying geogrids sinking into the sludge. Fill was placed using a combination of back-actor equipment, cranes with concrete skips and, towards the centre of the lagoon, even wheelbarrows.

Figure 12: Sludge lagoon at the end of capping operation

3.3 Heitenen Harbour, Kotka Finland, 2005

A dredged material disposal lagoon with deposits up to 8m deep having shear strength of only 0.7–1.0 kPa needed capping for environmental reasons and also to permit the creation of a freeport car parking storage area. About 180,000 m2 of very soft ground had to be covered to create a firm standing area. As the existing grounds were too soft to even support human access, therefore the original proposal required frozen ground (feels very solid and does not collapse under foot) before construction could start. This required long waiting period before the ground freezes to solid due to drop in temperature during winter season. This was impracticable and inefficient as the original proposal did not include a consideration of the critical installation stage and required frozen ground during construction.

A mechanically stabilised layer (MSL) incorporating stiff stabilising geogrids within granular fill was used to provide increased load spread and bearing capacity over the deposits to create a layer which was structurally safe (Figure 13). Additionally the construction of stabilised aggregate layer could take place in all temperature conditions and did not require the deposits to be in a frozen state. The base geogrid layer was factory bonded to a geotextile and supplied as a geocomposite which provided stabilisation function as well as separation function between the aggregate and the highly mobile fine deposits. A trial area proved the effectiveness of the system and the full project construction followed on immediately. The hard standing area performed well even after subjected to various in-service loadings in the years following construction.

4 CONCLUSIONS

Extremely soft soils are typically encountered in dredged fills or sludge lagoons and gaining access to such deposit is extremely challenging. The traditional methods of construction over such deposits are time consuming, expensive and are not environmentally friendly. Application of mechanically stabilised layer (MSL) incorporating stabilising geogrids within aggregate layer is an innovative method to solve soft ground problems. Secant stiffness, secant stiffness ratio, junction efficiency and hexagonal pitch are key performance

related parameters of stabilising geogrids. The benefits of mechanically stabilised layer include safe access to extremely soft soils, improvement in bearing capacity and reduction in construction material.

Figure 13: Extremely soft deposits at Heitenen Harbour, Kotka Finland

REFERENCES

European Organisation for Technical Approvals. 2012. *Non-reinforcing hexagonal geogrid for the stabilisation of unbound granular layers by way of interlock with the aggregate.* KIWA

Hall, C.D. 2010. A new geogrid type for ground stabilisation in International Congress on Environmental Geotechnics, *Geosynthetics and New Materials. New Delhi,* 8-12 November 2010

Practical Design of Vibro Stone Columns

W. Sondermann & V. R. Raju
Keller Group plc
J. Daramalinggam
Keller AsiaPacific Ltd
M. Yohannes
Keller (M) Sdn Bhd

ABSTRACT

Vibro stone columns have been used to improve weak ground since the 1950s. The stiff and highly frictional granular elements of stone columns increase the stiffness and shear resistance of weak ground, and the highly permeable nature of the columns accelerates consolidation settlements so as residual settlements are limited to within tolerable value. For stone column design, a variety of design methods have been used over the years ranging from simple hand calculations to complex 3-D numerical models. Important considerations include type of structures to be supported, in-situ soil properties, stone column material parameters, area replacement ratio, stress concentrations and consolidation times. Like all other geotechnical designs, stone column design requires both stability and serviceability checks**.** This paper presents several practical design methods and highlights some of the strengths and weaknesses of each approach. It is crucial that for simpler models, the assumptions that underlie the model and model limitations are well understood by the designer. Complex models are often assumed to be more accurate, but also contain many approximations and assumptions which must be kept in mind. Importantly all design methods, simple or complex, must be verified by post treatment testing and calibrated by field measurements. It is also worth noting that at present, even complex 3-D numerical models do not fully account for installation effects that accompany Vibro stone column installation, which is an area for further research.

1 INTRODUCTION

Vibro stone columns (VSC) are compacted granular columns, installed in weak ground with the aid of a depth vibrator, sometimes called a "poker". In the case of the dry bottom-feed method, the depth vibrator penetrates to design depth using its own weight, a 'pull down' force and compressed air. Once the required depth is reached the depth vibrator is extracted gradually, accompanied by an up-down motion, allowing stone to flow in to the void that has been created. The up-down motion and centrifugal force of the depth vibrator allows formation of a compacted, granular column. The column formed is larger than the initial hole created by the penetration process. The construction of stone columns with a depth vibrator ensures properly formed compacted stone columns to the required diameter and depth as well as densification the surrounding soil in between the columns. The installation process is shown in Figure 1, and is often termed Vibro replacement (VR).

The Vibro replacement technique provides an economical and flexible solution, which easily adapts to varying ground conditions. Since 1950s, Vibro replacement been used widely due to its versatility. Many infrastructure projects such as major highways, expressways and railways, have been built on stone column improved ground. Other structures typically supported by stone columns include airport runways and taxiways, power plants, storage tanks, mine stockyards, reclamations, earth embankments, factories and buildings.

2 IMPROVEMENT AND LOAD CARRYING MECHANISM

Compared to rigid concrete or steel piles, the load carrying mechanism of VSCs is different. Instead of shaft friction and end bearing resistances, the VSC transmit loading to the ground primarily by bulging and mobilizing the soil lateral stresses. Usually VSCs are designed as a group of columns acting together, rather than as individual columns working in isolation. Typical column diameters range from 0.6 m to 1.1 m, and typical

column grids are triangular or rectangular, with center-to-center spacings ranging from 1.5 m to 2.5 m. When the columns are placed at a reasonable spacing, they influence each other and act as a group. When a uniform loading is applied on the treated ground, particularly where a granular platform is present, arching occurs and the columns act as a group, with some stress still being borne by the in-situ soil (Kirsch and Kirsch, 2010).

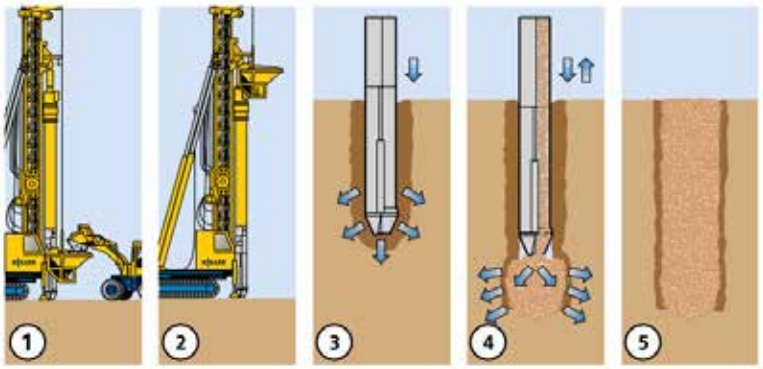

Figure 1: Schematic diagram showing typical installation process of Vibro Stone Columns by the dry bottom-feed method.

2.1 Improvement in stiffness to limit settlements

The primary improvement that is obtained from VSCs is with regard to compressibility. Due to their reinforcing effect, a larger portion of the load gets concentrated on the stiffer VSC elements while reduced stresses are imposed on the surrounding soil. As a result a uniform reduced settlement is achieved as compared to the case of otherwise unimproved condition. The ratio by which the settlement is reduced is a good gauge of the effectiveness of the treatment.

2.2 Improvement in shear strength to increase bearing capacity and slope stability

The presence of highly frictional elements in the weak ground enhances the load carrying capacity of the original, unimproved ground. The fact that the columns are stiffer than the existing ground mean that stresses concentrate on them, resulting in further improvement to the shearing resistance of the ground. This improvement enables soft ground to sustain higher loadings, and also enables slopes and embankments to be safely supported on soft soils at a reduced the risk of external instability or slip failure.

2.3 Improved drainage/permeability to increase rate of consolidation

The presence of VSC increases the permeability of the ground. The large diameter and high permeability of column materials means that they act as large vertical drains, thereby accelerating consolidation.

2.4 Liquefaction mitigation

Vibro stone columns concentrate shear stress induced by earthquake action onto stiffer columns (and hence reducing the shearing stresses on the soil) and can quickly and effectively dissipate the earthquake induced pore water pressures in the surrounding soil. This is particularly true for relatively liquefaction prone soils. In addition, the installation process results in compaction of liquefiable soils, further reducing the risk of liquefaction.

3 FACTORS AFFECTING THE PERFORMANCE OF VSC

3.1 Variations in soil conditions

Weak soils ranging from fine sands to clays can be economically improved using VSCs. In the case of silty sands, once the fines content is greater than 15 to 20%, stone columns are preferred over Vibro compaction as in such soils, the particles cannot be efficiently rearranged into a denser state by vibration energy. Contrary to older practice in the 1970s and 1980s, ultra-soft to soft mining slimes and marine clays have been treated effectively with stone columns (Raju and Hoffmann (1996) and Raju (1997)). Figure 2 shows the applicability of Vibro replacement for different soil conditions.

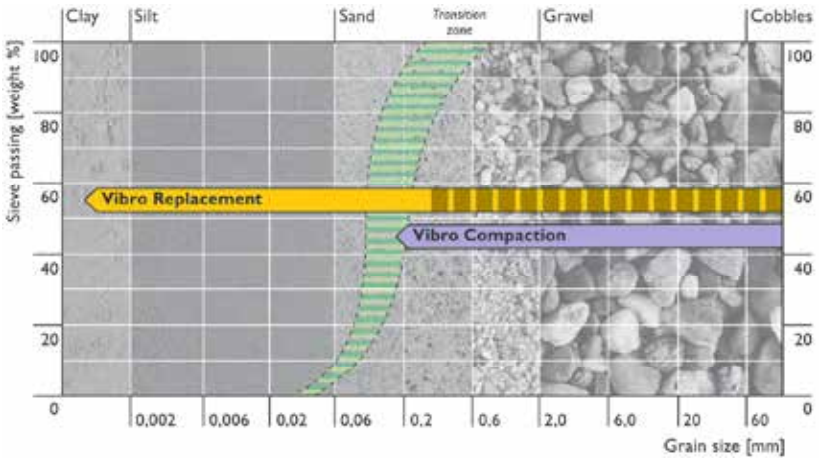

Figure 2: Soil grading and suitability for improvement by Vibro replacement

Intermediate layers of highly plastic organic and peat layers having thickness of more than twice the stone column diameter can only be improved marginally. In such cases bulging checks and secondary consolidation settlement checks may be warranted (Kirsch and Kirsch, 2010).

3.2 Construction methods

It is worth nothing that some methods of installing stone columns (e.g. using casings and top vibrators) result in a lower degree of compaction, and hence lower stiffness and friction angle.

A proper drainage layer composed of free draining, granular material must be provided. This layer has to be of adequate thickness and minimum contamination. As this layer serves as a load transfer platform, good compaction is essential.

3.3 Installation effects

Installation effects of stone column in sandy or sandy silt soils results in local densification. This phenomenon leads to enhanced performance of the ground and an increased settlement reduction factor (Kirsch, 2006). In the case of cohesive soils susceptible to remoulding, the installation process initially results in build-up of pore pressure in the saturated soil and increase in horizontal stress. However, soon after loading is initiated and reconsolidation takes place, the soil in the remoulded zone quickly recovers and gains its stiffness. This boost in the soil stiffness also increases the confinement offered to the stone columns by the cohesive soil. More details on the installation effects and its assessment by field measurements and numerical methods can be found in Kirsch (2006) and Carvajal *et al.* (2013).

3.4 Post-installation activities

In some instances, controlled filling rates and adequate rest period are important for the proper performance of VSCs installed in weak cohesive soils. This allows the soil to gain some strength and avert any instability. The condition of the drainage layer has also to be checked and contaminants removed.

As a good means of checking the performance of improved ground, instrumentation is required to monitor the load-settlement behavior of structures supported on stone columns. Where necessary, piezometers, settlement cells, pressure cells, inclinometers, rod settlement gauges, and settlement markers can be used to assess the performance with respect to time and loading.

4 AN OVERVIEW OF DESIGN METHODS

Single column approach

Some approaches assume single Stone column as a pile, in that usually only the head is loaded and the column is considered to act (and fail) independently of other surrounding columns. The different failure mechanisms, as shown in Figure 3, include bulging of long columns, shearing of short columns, punching or sinking of short floating columns and bulging of columns in deeper, softer layer.

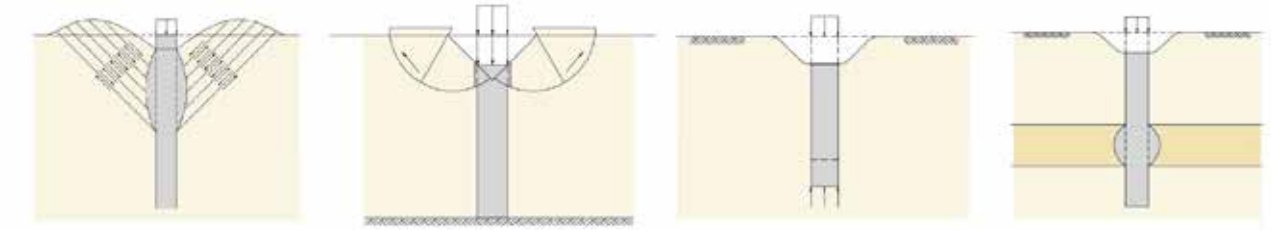

Figure 3: Different failure mechanisms of a single stone column (after Kirsch and Kirsch, 2010)

In practice, columns are rarely if ever designed to function as single columns. Columns are designed in groups. Multiplying the capacity of an isolated column by the number of columns in the group to obtain group bearing capacity is far too conservative.

Group columns approach

Most other design approaches consider group column acting together, since most applications require improvement of a significant area. The failure mechanism of column groups is significantly different than that of single columns. The mechanism of interaction is also different between the action under rigid rafts and under flexible load transfer platforms (Figure 4).

Comprehensive experimental studies on group action of columns were done by Muir Wood *et al.* (2000). Based on this study, the difference between single and group actions were found to be significant in terms of load sharing and interaction. The importance of area replacement ratio was also noted.

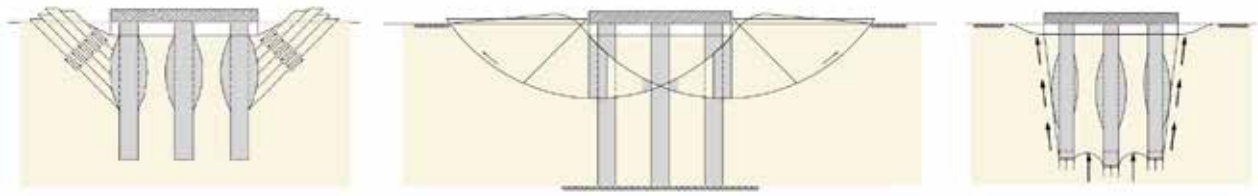

Figure 4: Different failure mechanisms of a group of stone columns (after Kirsch and Kirsch, 2010)

Unit cell idealization

The unit cell method is the most common simplification for VSC design methods. In the case of a large grid of stone columns, a unit cell comprising a single column with surrounding soil can be idealized as representative of the whole treatment (Figure 5). The unit cell has an equivalent diameter (d_e) and represents a treatment with

a certain area replacement ratio (A_c/A). As shown in the diagram, the load share of the columns is higher due to their stiffness. The ratio of the stress on the columns (σ_{sc}) to that of the surrounding soil (σ_s) is called the stress concentration (n).

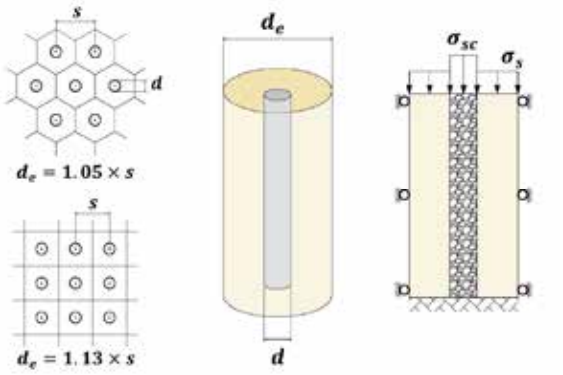

Figure 5: Unit cell method of idealization for simplified design of VSC

The unit cell approach assumes strain compatibility, i.e. vertical strains across any horizontal plane are equal. This means that the soil and column experience the same vertical deformation. Such a model considers a predominantly oedometric stress state, and under normal circumstances of loading, the stone column yields at a constant volume. This assumption is reasonable for columns in a large grid with uniform loading. More generally however, columns experience a triaxial stress state, particularly at the edges of the treatment zone (Barksdale and Bachus, 1983).

A usual approach of considering the improvement in shear strength of improved ground is by homogenization. Here, the composite ground is considered to have equivalent shear strength parameters. The equivalent shear strength parameters (or composite parameters) of the improved ground are either computed based on an area ratio or more realistically a stress ratio. A weighted average of parameters solely based on area is considered conservative, as it does not take into account the reinforcing effect (stiffness) of the stone columns.

Most of the approaches consider the stress ratio method to compute the equivalent shear strength parameters (eg. Barksdale and Bachus (1983), Priebe (1995)). The stress concentration ratio (n) increases with time as the soil consolidates (Barksdale and Bachus, 1983). It is to be noted that, the stress concentration does not only depend on the area ratio, but also on the ratio of Young's modulus (E_{sc}/E_s), angle of shearing resistance of the column and length of the columns.

4.1 Design for settlement

For the case of settlement reduction, most design approaches consider the unit cell concept. In such a case, an infinitely large area improved by a uniform grid of stone columns having the same diameter, is considered under an even load. Under such an oedometric condition, the settlement improvement factor (β) can be defined as the ratio of settlements of unimproved ground (s_o) to that of improved ground (s_i), i.e. $\beta = s_o / s_i$. Figure 6 compares improvement factors calculated by various methods.

Priebe (1995)

Priebe first developed the semi-empirical approach for Vibro replacement design in the 1970s, which was extended and published in 1995. This approach for stone column design has been widely used.

The underlying assumptions of this approach include considering the stone columns as resting on a rigid, competent bearing strata and that the column material is incompressible, in order to come up with a basic improvement factor called n_0. This basic improvement factor also assumes that the soil and column bulk densities are neglected. This inherently implies that a loaded column would deform by expanding uniformly from head to toe, since there is no increase in lateral support of the soil with depth. The basic improvement

factor is then revised in two steps, taking into account column compressibility and increase in lateral support with depth. This gives the improvement factor used in actual design calculations called n_2. Subsequently, additional settlements from the non-rigid base are calculated.

Priebe (1995) assumes that because the soil is displaced laterally during stone column installation, the initial resistance corresponds to that of "liquid" stress state (i.e. K = 1.0). This is reasonable assumption, given that cavity expansion usually means that the earth pressure coefficient is greater than one.

This approach is easy to use and gives good prediction of settlements albeit its simplified assumptions. Having the friction angle of the column material, preferred area replacement ratio and the soil's Poisson's ratio, one can estimate the settlement reduction rather quickly. Importantly, the Priebe method has be used extensively over the year, with input parameters in various soil conditions well-calibrated to measured settlements (e.g. Wehr and Herle, 2006)

Goughnour and Bayuk (1979)

Goughnour and Bayuk (1979) continued the approach of Hughes *et al.* (1975) in preferring an incremental solution to determine the settlement of stone column improved ground. This approach also considers a unit cell approach, with the assumptions that no shear stress develops at column top and toe, frictionless unit cell perimeters and strain compatibility between columns and soil. The unit cell is divided into equal slices, and computation of vertical deformation is done top to bottom. For each slice, two computations are made for the vertical deformation; one for elastic and one for elasto-plastic condition, and the maximum is taken to be as the governing case.

This approach is not typically employed for practical design since it is laborious and requires a number of iterations. A computer program or a spreadsheet is required to evaluate the iterative procedure. Goughnour and Bayuk (1979) method also requires more input data for the computations, such as compression index and initial void ratio of the soil.

Van Impe and Madhav (1992)

The settlement prediction approach proposed by Van Impe and Madhav (1992) takes into consideration the dilatancy angle (ψ) of the granular stone column material. The method implies that the dense granular matrix of the stone column has to undergo dilatory deformation; while the soil has to develop larger confining stress to resist the column's tendency for dilation. Such an interaction results in a favourable effect on the settlement reduction factor.

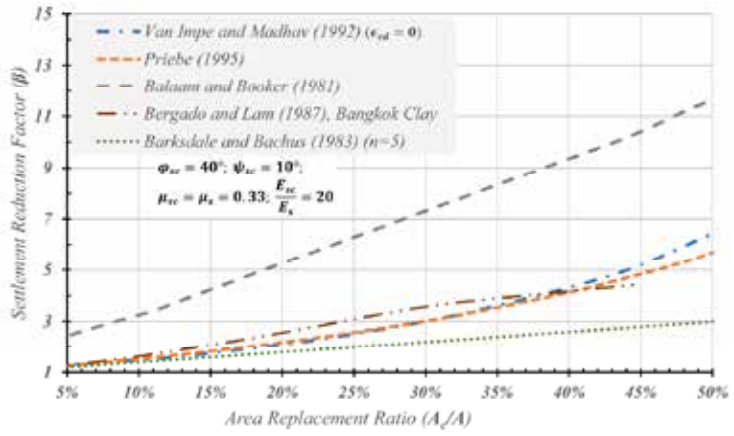

Figure 6: Comparison of the improvement factor (β) calculated by different methods

4.2 Design for shearing resistance

One of the benefits of stone columns is to enhance the load carrying capacity of weak soils. They also enable ground below slopes to withstand slip failure. Hughes and Withers (1974) observed that for large area of stone column treatment, bearing capacity is not a concern for the most part (except near the edges). Most bearing capacity relations are either associated with bulging failure (of single columns) or general shear failure (of group columns). For slope stabilization the available design approaches include (*i*) weighted average shear strength method (Bergado *et al.*, 1994), (*ii*) composite ground method with modified stress concentration (Priebe, 2003), (*iii*) trench wall method with stress concentration (Barksdale and Bachus, 1983), and (*iv*) Average of area-ratio and stress-ratio method (Kirsch and Sondermann, 2003).

Barksdale and Bachus (1983)

Basic assumptions of this approach include that the full strength of both the stone and soil is mobilized. Quick loading conditions are also assumed to prevail, which means that the soil is in undrained state. The ultimate bearing pressure and ultimate lateral stress outside the failure surface are assumed to be principal stresses. Based on this, the stress equilibrium is worked out to give the ultimate bearing capacity of the improved ground. It is worthwhile noting that this approach assumes a planar failure surface and does not consider the possibility of local bulging failure of single columns. Bearing capacity evaluation using the Barksdale and Bachus (1983) method is a preferred method due to its simplicity; nonetheless it is suggested that the stress concentration factor (n) can be computed using Priebe's basic improvement factor (β) (Kirsch and Kirsch, 2010).

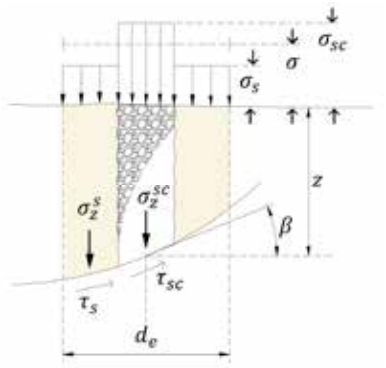

Figure 7: Unit cell idealization and notations for slope stability problems (modified after Barksdale and Bachus, 1983)

For slope stability analysis, stress concentration is considered in the unit cell approach (Figure 7). This implies that the stress concentration is vital for stability problems, since higher loads on the column are required to mobilize its full frictional resistance. Barksdale and Bachus (1983) extend the unit cell to the whole slope and recommend doing stability analysis based on what is commonly called the "Profile method" (Barksdale and Bachus, 1983, Bergado *et al.,* 1994).

Priebe (1995, 2003)

Further to design for settlement, Priebe (1995) gives shear strength parameters (cohesion and friction angle) of composite ground that are computed from stress ratio. Priebe (1995) recommends correcting the basic improvement factor (n_0) to allow for column compressibility. This gives a reduced improvement factor (n_1) and corresponding composite shear parameters (ϕ_1 and c_1). Priebe (1995) also gives an option to consider the effect of overburden on improvement. This results in higher improvement factor (n_2) and higher composite parameters (ϕ_2 and c_2 corresponding to n_2). When computing the composite shear strength parameters Priebe (1995) gives the option to reduce the share of load on the columns (m' rather than m). This is recommended in order not to overestimate the shear parameters when stress ratio method is applied.

Priebe (1995) has given elaborate procedure for estimation of bearing capacity of shallow foundations on stone columns. However, it is seldom used due to the numerous steps involved. In the case of stability below slopes, Priebe (1995) recommended that shear strength parameters computed from m_1' be used, i.e. load share of columns reduced and not including effect of overburden. This approach has been used extensively (i.e. composite ground with parameters ϕ_1 and c_1), together with controlled construction of the fill/loading.

Later, Priebe (2003) suggests that safety can be evaluated by the slice method taking the slip circle and the stone column as a 2D system and applying stress concentration to amplify the load on the columns while reducing the load on the soil (i.e. adjusted loads method). Conversely, for a simpler solution he recommends a reduction in the improvement with depth to account for the unloading of columns below slopes (i.e. corrected shear values method). The Priebe (2003) method with corrected shear values is very useful for slope stability problems, even though it is a lengthy exercise requiring vertical and horizontal subdivisions of the ground. A common slope stability program can be used to evaluate the safety of the composite ground afterwards.

Bergado et al. (1994)

Based on field studies made on Bangkok Clay (Bergado and Lam, 1987), Bergado *et al.* (1994) propose the average shear strength method to evaluate the composite ground parameters. This approach is seldom applied, but when applied it is used for slope stability problems. It includes evaluation of equivalent cohesion and unit weight based on area ratio method; whereas the composite angle of friction is evaluated by considering the load share as well.

4.3 Design for drainage

Stone columns accelerate the consolidation process of compressible soils because of the high permeability of the columns; but at the same time the stiffness effect of the columns also plays a role in reducing the consolidation settlements. For the first case where only drainage prevails with little to no reinforcement, the solution is similar to that of vertical drains (e.g. Barron, 1948; Hansbo, 1981). The coupled effect of radial consolidation and reinforcement has been studied with the aid of numerical modelling (Balaam and Booker, 1981) or closed form solutions (Han and Ye, 2002; Castro and Sagaseta, 2009). However, during column installation, disturbance of the soil surrounding the column and contamination of the column material that is in contact with the soil can take place. This results in degraded consolidation rate (Barksdale and Bachus, 1983). This effect (called smear effect) should be considered in the general solution of design for drainage.

Balaam and Booker (1981)

Balaam and Booker (1981) consider the vertical and lateral deformation of stone columns, and seek to provide solutions for an elastic soil–column system. The idealization for this approach includes a unit cell that is loaded by a smooth and rigid raft and linear-elastic material properties for the soil and column. They defined dimensionless parameters that affect the solution and checked the results by modifying few parameters at a time.

They demonstrated that at initial conditions the load on the soil is more than that of the columns. This is because the soil behaves in undrained conditions, resulting in a high incompressible constrained modulus. But with time the load share of the columns increase as consolidation takes place. In this approach the time dependent behaviour was evaluated considering Barron's (1948) assumption, where the column is taken as a perfect drain. Moreover, since the effects of smear are not considered, this method does not depict consolidation precisely.

Practical use of this method involves the reduction of the effective diameter of the column, in order to match measured field results. The actual column diameter is typically reduced by 10-15% to give the effective diameter.

Han and Ye (2002)

In an extension of an earlier paper (Han and Ye, 2001), the authors set out by assuming that the soil around the column is fully saturated. A unit cell with circular influence area, loading application via a rigid foundation base

and a constant load throughout the consolidation process are the grounds based on which the solution was proposed.

This approach assumes linear elastic behaviour for both the soil and the column, but accounts for a variable modular ratio. Smear effect is considered in this approach. Since the variation of pore pressure and vertical stress is uniform over the radial distance of a unit cell, the average values of each can be used in the stress equilibrium calculation. At the same time, vertical strain compatibility and perfect lateral constraint (i.e. zero horizontal strain) with respect to time are taken to occur. This leads to faster consolidation rates and high final stress concentrations as pointed out by Castro and Sagaseta (2009).

Han and Ye (2002) method clearly demonstrates how the stress concentration ratio (n) and diameter ratio (d_e/d) affect consolidation rates. However, the short comings of this approach lie in the assumption of elastic material properties and higher equivalent consolidation coefficient. These result in faster calculated consolidation time and higher stress concentration factors over time as compared to other alternatives.

Castro and Sagaseta (2009)

They consider radial equilibrium of stresses/strains into their relationship, in addition to vertical strain compatibilities as considered by Han and Ye (2002). The assumption that the vertical effective stress and pore pressures are taken to be uniform over the radius of the unit cell is still valid in this approach. The approach has an elastic component, which is similar to Balaam and Booker (1981), and a plastic deformation component, which considers the column as a Mohr-Coulomb material with a constant dilatancy angle. For the elastic component, this approach is in good agreement with Balaam and Booker (1981). For the plastic component, all the stress and strain increments from the moment of yielding are obtained using compatibility and equilibrium equations to find a closed form solution. This approach is preferable since it tries to resolve the problem holistically. Elastic and elasto-plastic material properties are included, with the possibility to account for column dilation. The results also match closely with FEM analyses.

Figure 8 shows the comparison of different approaches in terms of elastic settlement rates. From this, it is clear that Han and Ye (2002) approach gives a faster degree of consolidation compared to other approaches. Figure 9 also shows that Han and Ye (2002) shows an infinite improvement with increase in area ratio, while Castro and Sagaseta (2009) capture the attenuation of improvement after some replacement ratio.

It is worth pointing out however, that within the normal range of area replacement ratios and modulus ratios, the Han and Ye (2002) method is sufficiently flexible for practical use, providing input parameters are calibrated from field measurements of consolidation rates.

4.4 Design for liquefaction resistance

Liquefaction susceptibility of soils and its assessment was first developed by Seed and Idriss (1971) based on simplified, semi-empirical approach. Safety factor against liquefaction is the ratio of the Cyclic resistance ratio (*CRR*), which is the soil capacity to resist liquefaction, to the Cyclic shear stress ratio (*CSR*), which is the caused by the design earthquake. When the *CRR* is equal or less than *CSR* it implies that the soil is predisposed to liquefaction in the event of the design earthquake.

The installation of stone columns is a popular method of effective liquefaction mitigation. The improvement with stone columns against liquefaction is as a result of: (*i*) increased density of the in-situ soil, (*ii*) increased resistance to cyclic loading due to reinforcing effect of the columns, (*iii*) accelerated drainage and dissipation of pore pressure.

The Seed and Booker (1977) approach was the first to address the effect of a granular drain to mitigate liquefaction by providing an easily accessible horizontal drainage. Priebe (1998) notes that the resistance offered by Vibro replacement against liquefaction cannot be easily computed. As a result, rather than estimating what resistance is afforded by stone columns to the ground, computations are made to reduce the acting forces (Priebe, 1998). Baez and Martin (1993) proposed an approach similar to Priebe's, in that it tries to compute a reduction in *CSR* and its assumption that the columns deform in pure shear together with the soil. However, this approach predicts the highest CSR reduction compared to the other alternatives. The considerations made by Priebe (1998) and Baez and Martin (1993) were further extended by Goughnour and Pestana (1998), who took into account the flexural response of the stone columns. This means that the improvement offered by the columns is limited due to their slenderness since they act as flexural members. This approach is more conservative

compared to Priebe (1998) and Baez and Martin (1993). The Priebe (1998) approach gives a reduction in *CSR* that is intermediate, it has also been applied widely since its publication.

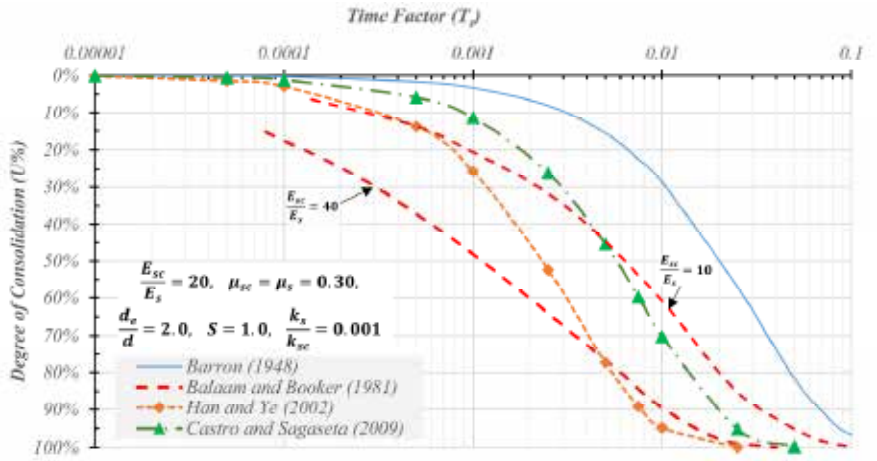

Figure 8: Comparison of elastic rate of settlement between different approaches

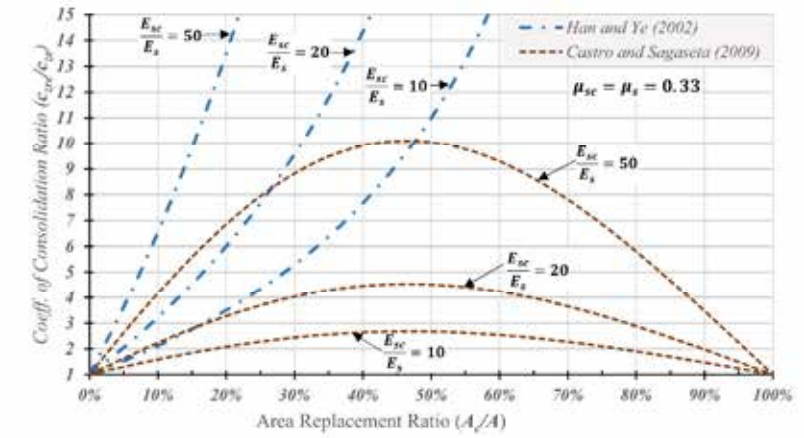

Figure 9: Comparison of equivalent coefficients of consolidation for elastic columns, and effect of modular ratio (modified after Castro and Sagaseta, 2009)

5 FINITE ELEMENT APPROACH

Finite Element (FE), and also Finite Difference models, either in 2D or 3D provide a class of tools that overcome many of the simplifications of the semi-empirical or analytical methods. Modern FE models allow the consideration of the effects of variation in geometry across the problem space, multiple load cases, time effects and variations in soil properties. Balaam *et al.* (1976) presented a pioneer finite-element approach for stone column improved soft clay; they were able to examine the effect of stiffness of the stone columns on deformation. Balaam and Booker (1981) also were able to do extensive studies of group of stone columns supporting a rigid slab, and studied the deformation behaviour. Mitchell and Huber (1985) were the first to introduce an axisymmetric finite-element model with groups of columns and they compared their results with field performance. Kirsch and Sondermann (2003) also used 3D finite element modelling to compare results to field measurements. Kirsch (2006, 2008) further extended the use of finite element modelling to study installation effects and load-settlement response of group columns, and to do a parametric study on floating stone columns.

Most early 2D approaches are axisymmetric models of the unit cell. Simplified 2D plane strain approaches varied from those aimed at giving best estimate of ground deformations (Wehr and Herle, 2006) to those incorporating equivalent conversion of some parameters such as permeability to a plane strain model (Weber *et al.*, 2008). Tan *et al.* (2008) propose two practical simplified methods for modelling stone columns as "gravel trenches", without modification of permeability parameters. It is also possible to model the improved ground with composite parameters (e.g. from Priebe, 1995) keeping in mind that the composite parameters do not accurately account for lateral stiffness or drainage.

More current FE approaches consider 3D modelling to capture the soil and column interaction, and particularly the stress concentration and arching behaviour that occurs (Figure 10). Moreover, the effect of permeability on consolidation related deformations and pore pressures also more accurately modelled. Thus, for flow and liquefaction associated problems, 3D FE analyses is preferred.

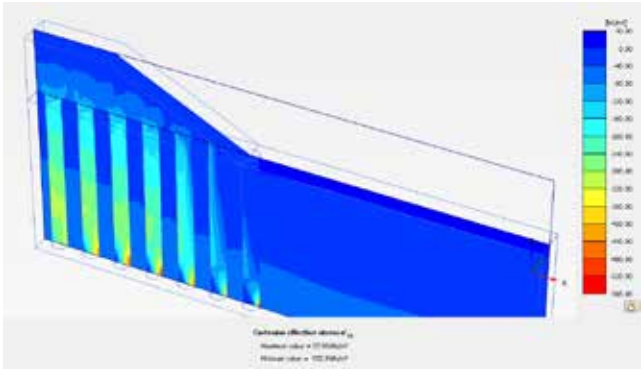

Figure 10: Sample 3D finite element model showing stress concentration in columns

FE analyses have helped to integrate vertical loading, horizontal deformations and consolidation effects; which are otherwise decoupled actions in empirical/analytical design approaches. FE analyses is also useful in that it allows modelling of the ground improvement together with any foundation it supports or abutting elements. Kirsch and Kirsch (2010) recommend that for important projects on very soft to soft cohesive soils, the approach for design should be by employing finite element modelling.

It is however important to realize that even finite element models are simplifications of complex field phenomenon, and designers must be acutely aware of these simplifications. For example installation effects (which result in a reduction and then gain in shear strength of soft clays, or densification of silts and sands) are very difficult to model. Another example is the effect of placing a working platform on soft clays, which disturbs or displaces the clay and alters the original strength profile of the in-situ ground. The designer must ask if the model reasonably captures all the salient features of the field situation. Because even the most complex models contain simplifications, calibration therefore is essential.

6 THE ROLE OF CALIBRATION

The Priebe (1995, 2003) method has been widely used for design of Vibro stone columns. The approach has evolved over the years and has expanded to include design for liquefaction (Priebe, 1998). Due to its wide application, the method has been field calibrated by designers over the years. For example, Yee *et al*. (2015) show the results of a long-term test embankment built on stone columns where the Priebe (1995) and Han and Ye (2002) methods were used to make accurate "Class A" predictions of settlement and rate of consolidation. This demonstrates that any design approach ought to be field calibrated to ensure a safe and economic design.

It is also vital that any finite element or laboratory model be checked against field measurements. Such a calibration would be helpful to justly extrapolate the model to a bigger scale and estimate performance reliably. The role and importance of calibration of finite element approaches has been demonstrated by Kirsch (2008).

7 CLOSING REMARKS

7.1 Summary

In general, Vibro stone columns are typically used to improve ground in order to sustain higher loading with less deformation, to stabilize slopes, to improve bearing capacity, to mitigate liquefaction susceptibility and facilitate consolidation. A stone column improved ground will usually have an improved settlement performance by two to three times, and an increased bearing capacity by two to three times. The safeties against instability in sliding or liquefaction are also meaningfully boosted after improvement.

Where the Vibro stone column design involves difficult ground conditions, numerous external actions or interaction between different elements, 2D or 3D numerical modelling would be best suited to tackle the problem. Examples include structures on soft to very soft soils, problems involving multiple load stages or problems where lateral movements of the columns are expected to be significant.

When designing for Vibro replacement for cases that predominantly require deformation control, the Priebe (1995) approach is a practical and well-proven method. The same approach can be used for estimating safety of stone column improved slopes, provided moderately conservative values of composite parameters can be used. For a more detailed assessment of safety of slopes, the Priebe (2003) method or the method recommended by Kirsch and Sondermann (2003) can be followed. Bearing capacity calculation for shallow foundations over stone columns can be evaluated using Bachus and Barksdale (1983) approach with improvement factor as computed from Priebe (1995). For construction over soft, compressible ground where consolidation is a vital consideration the methods of analysis suggested by Balaam and Booker (1981), Han and Ye (2002) or Castro and Sagaseta (2009) can be applied, but always with appropriately calibrated input parameters. For liquefaction susceptible soils, design of Vibro replacement and subsequent improvement can be assessed by Priebe (1998) method. Where the columns are slender or widely spaced, a more precise estimation of safety is required, flexural effects can be considered utilizing Goughnour and Pestana (1998) approach.

All design approaches have simplifying assumptions. The choice of method have to be decided based on its underlying premises, simplifying assumptions and field calibration of input parameters.

7.2 Areas of further work

With the advancement in computational capabilities and better understanding of geotechnical modelling, 2D/3D numerical modelling of stone columns can be done to predict performance of improved ground. However, better calibration of input parameters, particularly for advanced soil models is still required.

An additional area of further work would be to investigate installation effects more closely. As demonstrated by previous work, installation effects are significant in the performance of stone column improved ground. But these effects are not considered as inherent components of the design approaches. Further detailed studies are required to understand and estimate the effect of installation on performance of stone columns in different types of soils.

REFERENCES

Baez, J. I., & Martin, G. R. 1993. Advances in the design of vibro systems for the improvement of liquefaction resistance. In *Symposium Ground Improvement*, 1-16

Balaam, N. P., & Booker, J. R. 1981. Analysis of rigid rafts supported by granular piles. *International Journal for Numerical and Analytical Methods in Geomechanics*, *5*(4), 379-403.

Balaam, N. P., Booker, J. R., & Poulos, H. G. 1976. *Analysis of granular pile behaviour using finite elements*. University of Sydney, School of Civil Engineering, Civil Engineering Laboratories.

Balaam, N. P., & Poulos, H. G. 1983. The behaviour of foundations supported by clay stabilised by stone columns. In *European Conference on Soil Mechanics and Foundation Engineering, 8th, 1983, Helsinki, Finland*.

Barksdale, R. D., & Bachus, R. C. 1983. *Design and Construction of Stone Columns Volume II, Appendixes*. Washington, DC, USA: Federal Highway Administration.

Barron, R. A. 1948. *The influence of drain wells on the consolidation of fine-grained soils*. Diss., Providence, US Eng. Office.

Bergdao, D. T. & Lam, F. L., 1987. Full scale load test of granular piles with different densities and different proportions of gravel and sand on soft Bangkok clay, *Soils and Foundations*, Vol. 27, No. 1, 86 - 93

Bergado, D. T., Chai, J.C., Alfaro, M.C., Balasubramaniam, A.S. 1994. *Improvement techniques of soft ground in subsiding and lowland environment*. CRC Press.

Carvajal, E., Vukotić, G., Castro, J., & Wehr, W. 2013. Comparison between theoretical procedures and field test results for the evaluation of installation effects of vibro-stone columns. In *Proc. International Conference on Installation Effects in Geotechnical Engineering. Rotterdam. GEO-INSTALL.*

Castro, J., & Sagaseta, C. 2009. Consolidation around stone columns. Influence of column deformation. *International Journal for Numerical and Analytical Methods in Geomechanics*, *33*(7), 851-877.

Goughnour, R. R., & Bayuk, A. A. 1979. Analysis of stone column-soil matrix interaction under vertical load. *Coll. Int. Renforcements des Sols*, 279-285.

Goughnour, R. R., & Pestana, J. M. 1998. *Mechanical behavior of stone columns under seismic loading*.

Han, J., & Ye, S. L. 2001. Simplified method for consolidation rate of stone column reinforced foundations. *Journal of Geotechnical and Geoenvironmental Engineering*, *127*(7), 597-603.

Han, J., & Ye, S. L. 2002. A theoretical solution for consolidation rates of stone column-reinforced foundations accounting for smear and well resistance effects. *The International Journal of Geomechanics*, *2*(2), 135-151.

Hansbo, S. 1981. Consolidation of fine-grained soils by prefabricated drains. *Proc. of 10th ICSMFE, 1981*, *3*, 677-682.

Hughes, J. M. O., & Withers, N. J. 1974. Reinforcing of soft cohesive soils with stone columns. *Ground Engineering*, *7*(3).

Hughes, J. M. O., Withers, N. J., & Greenwood, D. A. 1975. A field trial of the reinforcing effect of a stone column in soil. *Geotechnique*, *25*(1), 31-44.

Kirsch, F. 2006. Vibro stone column installation and its effect on ground improvement. *Numerical Modelling of Construction Processes in Geotechnical Engineering for Urban Environment*, 115-124.

Kirsch, F. 2008. Evaluation of ground improvement by groups of vibro stone columns using field measurements and numerical analysis. In *Proceedings of the 2nd International Workshop on the Geotechnics of Soft Soils, Glasgow* (pp. 241-248).

Kirsch, K., & Kirsch, F. 2010. *Ground improvement by deep vibratory methods*. CRC Press.

Kirsch, F., & Sondermann, W. 2003. Field measurements and numerical analysis of the stress distribution below stone column supported embankments and their stability. In *International Workshop on Geotechnics of Soft Soils-Theory and Practice* (pp. 17-19).

Mitchell, J. K., & Huber, T. R. 1985. Performance of a stone column foundation. *Journal of Geotechnical Engineering*, *111*(2), 205-223.

Muir Wood, D., Hu, W., & Nash, D. F. T. 2000. Group effects in stone column foundations: model tests. *Geotechnique*, *50*(6), 689-698.

Priebe, H. J. 1995. The design of vibro replacement. *Ground engineering*, *28*(10), 31.

Priebe, H. J. 1998. Vibro replacement to prevent earthquake induced liquefaction. *Ground engineering*, *31*(9), 30-33.

Priebe, H.J. 2003. Zur Bemessung von Rüttelstopfverdi chtungen, Anwendung des Verfahrens bei extrem weich en Böden, bei schwimmenden Gründungen und beim Nachwei s der Sicherheit gegen Gelände- oder Böschungsbruch, *Bautechnik 80(6)*, 380 – 384.

Raju, V. R., & Hoffmann, G. 1996. Treatment of tin mine tailings in Kuala Lumpur using vibro replacement. In *Proc. 12th SEAGC*.

Raju, V. R. 1997. The behaviour of very soft cohesive soils improved by vibro replacement. *Ground Improvement Geosystems–densification and reinforcement, Thomas Telford*, 253-259.

Seed, H. B., & Booker, J. R. 1977. Stabilization of potentially liquefiable sand deposits. *Journal of the geotechnical engineering division*, *103*(7), 757-768.

Seed, H. B., & Idriss, I. M. 1971. Simplified procedure for evaluating soil liquefaction potential. *Journal of Soil mechanics & Foundations Div*.

Tan, S. A., Tjahyono, S., & Oo, K. K. 2008. Simplified plane-strain modeling of stone-column reinforced ground. *Journal of Geotechnical and Geoenvironmental Engineering*, *134*(2), 185-194.

Van Impe, W. F., & Madhav, M. R. 1992. Analysis and settlement of dilating stone column reinforced soil. *ÖIAZ*, *137*(3), 114-121.

Weber, T. M., Springman, S. M., Gäb, M., Racansky, V., & Schweiger, H. F. 2008. Numerical modelling of stone columns in soft clay under an embankment. *Geotechnics of soft soils-focus on ground improvement. Taylor & Francis, London*, 305-311.

Wehr, J., & Herle, I. 2006. Exercise on calculation of stone columns–Priebe method and FEM. *Numerical Methods in Geotechnical Engineering*, 773-776.

Yee, Y.W., Prasad, P.V.S.R., Ooi, L.H., Daramalinggam, J., 2015, "Instrumented Low Embankment on Stone Columns for the Ipoh-Padang Besar Double Tracking Project", *Jurutera, January 2015, The Institution of Engineers Malaysia*, 23-25.

Vibro Stone Columns: Proper Construction Practices

V. R. Raju
Keller Group plc
Y.W. Yee
Keller ASEAN
J. Daramalinggam
Keller AsiaPacific Ltd

ABSTRACT

Vibro stone columns have been in use since the 1950s, supporting numerous structures such as road and railway embankments, reclamation slopes, large storage tanks, multi-storey buildings, material stockpiles and airport runways. While well-calibrated geotechnical design is essential for the effective use of Vibro stone columns, proper construction practices are equally important. Construction activities can be broadly divided into two stages: activities during stone column construction (mainly by the specialist contractor) and activities after column construction and handover (mainly by the general contractor). These activities include additional soil investigation, automated monitoring of column construction parameters, acceptance testing, proper construction and maintenance of drainage blankets, controlled construction of the structure, and deflection/ deformation monitoring during construction of the structure. It is also important that throughout the construction process, consistency with design assumptions is maintained and checked. The successful construction of a tall reinforced-soil wall in Selangor, Malaysia and the stabilization of a reclamation slope overlying soft clay in Singapore (using off-shore stone columns) are presented as examples.

1 INTRODUCTION

A Vibro stone column is a compacted granular column made of stone (in contrast with sand) that has been constructed using a depth vibrator. It can be constructed in all types of soils, but is normally used in fine-grained cohesive soil where conventional compaction is less effective. Typical column diameters range from 0.6 m to 1.1 m. Columns are built in either a square or triangular grid pattern, with center-to-center spacings ranging between 1.5 m to 2.5 m.

Figure 1 shows the types of soils that Vibro stone columns are used in, compared to Vibro compaction.

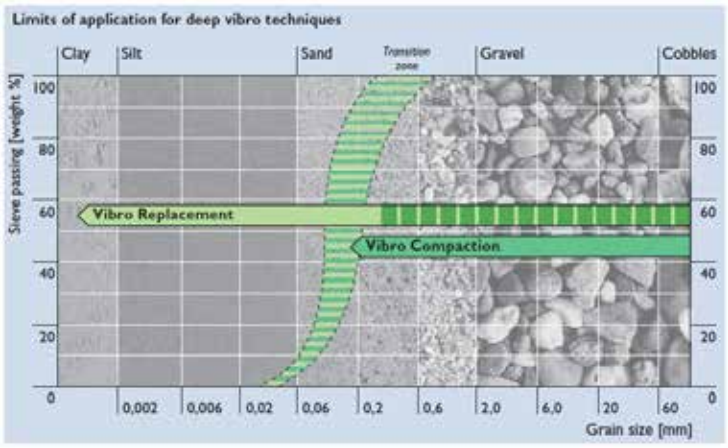

Figure 1: Applicability of deep Vibro techniques

Vibro stone columns have been used to support various structures across the world, since its first use in Germany in 1956 (Raju & Sondermann, 2005). These include road and railway embankments, reclamation slopes, large storage tanks, multi-storey buildings, material stockpiles and airport runways. Table 1 provides a summary of a few projects in Asia over the years. This paper covers proper construction practices for Vibro stone columns. An accompanying paper (Sondermann *et al.*, 2016) provides an overview of practical design considerations.

Table 1: Selected Vibro stone column projects in Asia

Country	Description	Year
Malaysia	Shah Alam Expressway. 600,000 linear meters of stone columns for highway embankments.	1994
Singapore	Seraya Island Tank Farm. 10,000 linear meters of stone columns for 5 tanks	1996
Malaysia	Putrajaya. 67,000 linear meters of stone columns for bridge embankment	1999
Singapore	Oiltanking Tank Farm. 10,000 linear meters of stone columns for tanks, office buildings, pump stations and substation.	2005
India	Hindustan Petroluem. 108,000 linear meters of stone columns for 25 oil storage tanks and ancillary facilities	2010
Malaysia	Vale Iron Ore Facility. 400,000 linear meters of stone columns for iron ore stacks	2013
Malaysia	Alor Pongsu Highway. 40,000 linear meters of stone columns for highway embankments	2013
India	Mundra LNG. 330,000 linear meters of stone columns for 2 LNG tanks and regasification structures	2014
India	Cochin International Airport. 105,000 linear meters of stone columns for aircraft taxiway and parking apron	2015

On land, Vibro stone columns are usually constructed via the wet top-feed method or more commonly the dry bottom-feed method. In the wet top feed method, a stable hole is created in the ground by a combination of vibrations, depth vibrator self-weight and water jets. With the annular space between the vibrator and the surrounding soil maintained by the water jetting, the hole is progressively filled with aggregates and compacted into the soils, and the column is constructed in a top-feed manner. Repeated re-penetration of the depth vibrator into the stone results in a column of well-compacted and interlocked stone, with a high friction angle and stiffness.

An issue with the wet top-feed method is the handling, treatment and disposal of large quantities of water from the flushing process. Such is generally handled with the construction of well-planned silt ponds that recycled the water and disposed back into the waterways when completed. Practically, wet top-feed columns have been successfully constructed to depths of over 20 m.

In the dry bottom-feed method (Figure 2), no water is used to flush or stabilise the hole. Instead, the depth vibrator is driven down by a combination of compressed air, vibrations and a pull-down force from the purpose built rig (or depth vibrator self-weigh in the case of crane hung systems). Stone is fed to the tip of the depth vibrator through a stone tube, and the hole itself is kept open by the vibrator and extension tubes, a process adequately known as the bottom-feed technique. Using purpose-built base machines (Figure 3), the dry bottom-feed method has been used to construct columns over 20 m deep, while with the crane-hung method (Figure 4), columns exceeding 40 m deep have been constructed. Vibro stone columns have been constructed in soils with undrained shear strengths as low as 6 kPa (Raju *et al.*, 2004). For more details of both the wet top-feed method and dry bottom-feed method of construction, please refer to Raju & Sondermann (2005).

A challenge with the crane-hung methods is maintaining adequate verticality of the vibro string during penetration and column construction, for onshore construction but particularly for offshore construction. Here, the design of the vibro string and operator skill are essential in maintaining sufficient verticality.

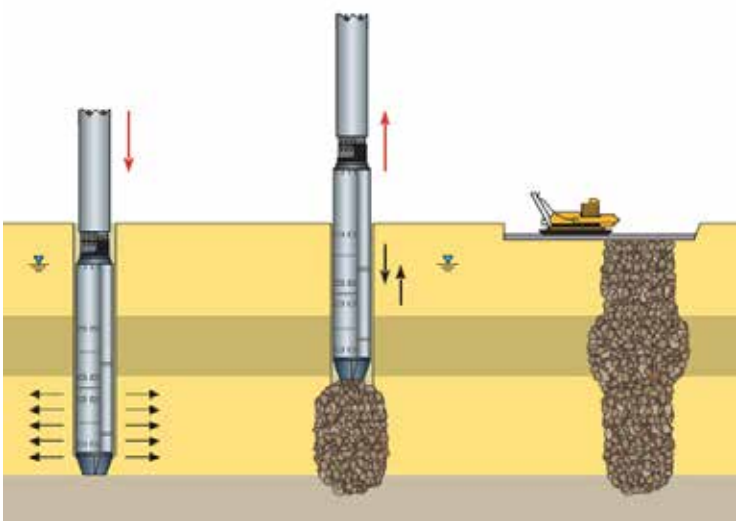

Figure 2: Dry bottom-feed construction process

Figure 3: Dry bottom-feed columns installed for a dockyard, using purpose-built rigs (East Malaysia, 2014)

Figure 4: Dry bottom-feed columns installed using the crane hung method, Malaysia, 2006.

Offshore, Vibro stone columns cane installed using the blanket method, the dry bottom-feed method or the gravel jet bottom-feed method (Leong & Raju, 2007)

Because Vibro stone columns are compacted granular columns, they improve in-situ ground in three ways, namely increased stiffness, increased shearing resistance, increased permeability. In silty or sandy soils, there is the added benefit of compaction of the in-situ soils. As the columns are made of compacted (but unbounded) stone, they exhibit ductile behaviour and retain their reinforcing properties even at relatively large strain. Various design methods exist, that are reviewed elsewhere (Kirsch & Kirsch, 2010)

2 EXISTING CONTRUCTION STANDARDS

The European Standard EN 14731:2005, "Execution of special geotechnical works- Ground treatment by deep vibration", covers ground treatment by deep vibratory compaction and vibrated stone columns, with the use of depth vibrators. It does not cover methods whereby granular columns are installed with an impact or top vibratory driven casing. It provides guidance on site investigation, materials suitable for different types of Vibro

stone column, design considerations, execution and testing. This European Standard is used in Europe and parts of Asia.

The BRE (2000) guide, "Specifying vibro stone columns", provides a framework for specifying ground improvement by Vibro stone columns, and separates the roles of "Vibro Designer" and "Specialist Contractor". In some Design & Construct contracts, these roles will be fulfilled by different parts of the same organisation. BRE (2000) is divided into two parts, the Technical Specification, and Notes for Guidance and Information and is used as a reference document.

The US Department of Transportation, Federal Highway Administration's two-volume "Design and Construction of Stone Columns" (Barksdale & Bachus, 1983a, 1983b) is a comprehensive overview of construction practise and design methods up till 1983. While some of the recommendations are outmoded, others remain useful even today.

3 ACTIVITIES BEFORE AND DURING COLUMN CONSTRUCTION

3.1 Desk study and site investigation

As with all geotechnical studies, it is very useful to do a desk study, where old maps, site investigation reports, design reports and photographs are compared with the present site conditions. Sometimes this study will reveal important changes to the landscape. Old mine tailings ponds may have been in-filled, old rivers diverted and old hills blasted away. All this helps plan the layout of the proposed structure and the site investigation required.

The pre-designed site investigation needs to be planned with the anticipated structure, performance criteria, possible soil conditions and probable foundation solution in mind. The site investigation "tools" (e.g. type of boring rig, SPT equipment, sampling tube, field testing equipment, CPT equipment) should be appropriate to the anticipated soil conditions, and allow some flexibility for the designer to alter the SI plan if needed. It is worth noting that the type of site investigation will differ, depending on whether piling or ground improvement is anticipated. Vibro stone column design is sensitive to the permeability of the in-situ ground, in addition to its undrained shear strength and stiffness. Additional site investigation during construction (usually by CPT) should be specified to confirm design assumptions and to provide additional data in between the original investigation points.

3.2 Testing and approval of materials

It is important to test and approve the materials to be used for the job prior to any significant quantity being delivered to site. For example, aggregate for Vibro stone columns should be tested for particle size distribution. Note that due to the inherent nature of both the top- and bottom-feed methods, different specifications are specified for the aggregates sizes. While these are important for geotechnical performance, poorly sized aggregate can cause blockages of the equipment, resulting in costly delays. During construction, materials that are delivered to site can be periodically tested to ensure they meet specifications.

3.3 Construction drawings and setting out

Setting out of individual column points should be done with an accuracy that matches the intended use. For example, where Vibro stone columns are used to support a strip or pad footing, setting out and positioning of depth vibrator should be done with greater precision. BRE (2000) recommended a positional tolerance of not more than 150 mm for a foundation element such as a strip footing, with a larger tolerance possible for other applications. In large area improvement, an advantage of Vibro stone column is that moderately deviated columns will not significantly affect the performance of the treatment.

3.4 Monitoring of column construction

If construction drawings and setting out is done correctly, column installation proceeds. Critical QA activities are the monitoring, recording and review of column construction parameters. Among other things, EN 14731:2005 specifies the following as part of site records: (a) Depth of penetration at each location, (b) Time required to reach maximum depth and details of times and depths during withdrawal, (c) Vibrator power

consumption during penetration and compaction of granular material or soil for depth vibrators, and (d) Quantity of stone used in each column.

Figure 5: Rig operator's control and display units

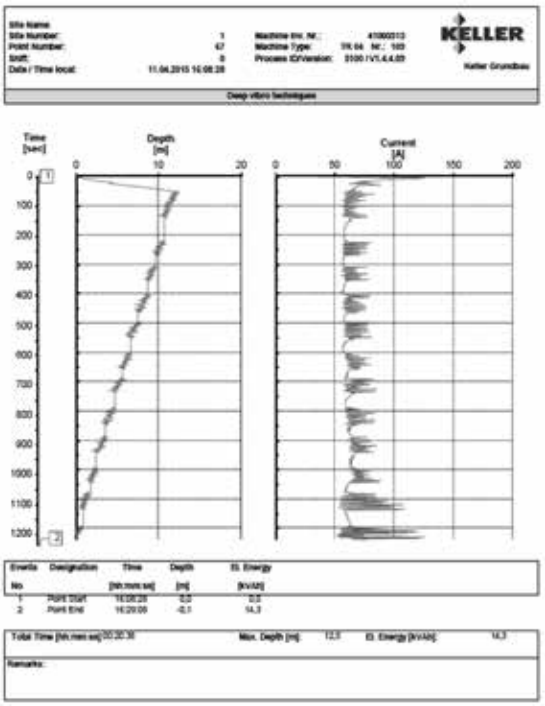

Figure 6: Sample printout of column construction parameters for dry bottom-feed method

A modern automated monitoring system (Figure 5) is able to capture a number of these parameters, display them in real-time to the operator, record and transmit them to the site office or elsewhere. A sample printout for a dry-bottom feed stone column is shown in Figure 6. It is crucial that the column construction parameters are reviewed by an experienced engineer on a daily basis so that anomalies (e.g. short columns, incomplete columns) are picked up. The average consumption of stone per column should be monitored to give an estimate of the average column diameter, which is a critical design input. If an obstruction has been encountered that is difficult to remove, a decision not to remove it should be based the predicted impact of the alteration of the treatment scheme. Therefore, such a decision should be taken in consultation with the designer.

3.5 Some comments on offshore installation

If offshore installation in very soft marine clays is required, it is good practise to lay a gravel blanket (1-2 m) over the seabed that will provide some confinement to the column heads during construction. This is similar to the confinement provided by the granular working platform for onshore installation.

4 ACTIVITIES AFTER COLUMN CONSTRUCTION

4.1 Acceptance testing

After careful soil investigation, geotechnical design, construction controls and analysis of construction data, post construction testing is to be carried out and typically these comprise load tests on columns. These are usually regarded as a form of quality control. EN 14679: 2005 describes two basic kinds of load tests. These are (a) large scale load tests (including large plate load tests and zone tests), and (b) individual column plate load tests, with loading plates placed concentrically on individual columns.

Kirsch & Kirsch (2010) recommend that for single column plate load tests, the loaded area is equivalent to the area of the unit cell (or tributary area) of each column. They indicate that where the thickness of soft soil layer is up to 5 times the diameter of the unit cell, the single column test is representative of the performance of an infinite column grid. A typical single-column load test setup, using an excavator as a reaction frame is shown in Figure 7, and a photograph of a kentledge setup is shown in Figure 8.

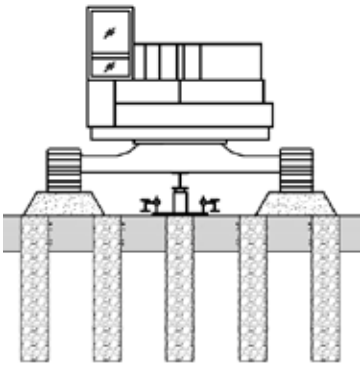

Figure 7: Schematic showing test using excavator as reaction frame

Figure 8: 175-ton kentledge load test on a single column using a 2.3 m x 2.3 m plate (Singapore, 2005)

4.2 Construction of drainage layer or load transfer platform

As stone column improve the ground also by allowing excess pore pressures to dissipate upon loading, the construction of a proper drainage layer is crucial. Often, it is sufficient to construct a granular working platform for the rigs, to be later used as drainage layer (Figure 9).

In other instances, if the working platform is non-granular or becomes severely damaged due to column installation, in it necessary to “trim” the platform away and reinstate a clear granular blanket for drainage purpose.

4.3 Controlled construction of superstructure

It is general good practise that controlled construction of the superstructure is practiced. This will allow time for excess pore pressures to dissipate, allowing the soil to gain strength and preventing excessive differential settlement. This principle may be illustrated in the case of a 19 m high iron-ore stockyard in Malaysia. The key features of this “staged filling” are (a) Clear loading stages and sequences (e.g. Figure 10), (b) Instrumentation and automatic alerts if trigger levels have been reached, (c) Clear instructions on how to proceed if a trigger level has been reached, (d) Regular review by an engineer, and (e) Agreement as to when “uncontrolled” loading and unloading of the stockpiles are allowed.

Figure 9: Granular working platform, which will then serve as drainage layer

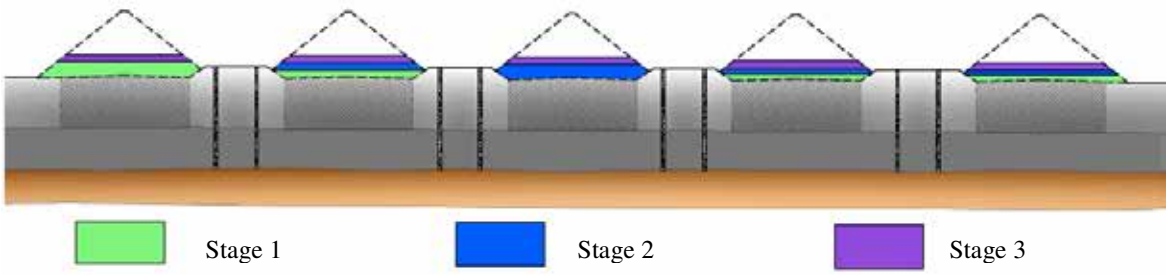

Figure 10: Schematic showing proposed loading sequence at iron-ore stockyard

This approach is akin to the Observational Method. In this instance, the staged filling allowed optimal design of the Vibro stone column scheme, reducing the replacement ratios. If loading and unloading of the iron ore was designed to be uncontrolled from the start, the replacement ratios would have to be much higher in order to ensure adequate factors of safety against slope failure. This would drive construction cost and time up.

A similar principle applies to the construction of earth embankments or reinforced soil walls. In some instances, temporary stabilizing berms (Figure 11) are placed at the toe of the embankment as a part of the design scheme. The design intent of the berm should be made clear to the earthworks contractor, and premature removal of the berm strictly prohibited.

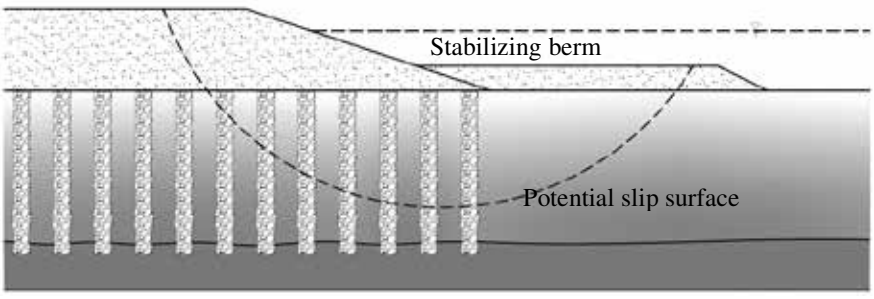

Figure 11: Stabilizing berm

With tight construction schedules, the presence of an adequate number of instruments (inclinometer, piezometers, settlement markers) will help make data-driven decisions about when to build the next stage of

embankment or when to remove a berm, etc., avoiding potentially catastrophic movements. Nowadays, automated monitoring systems are available with graphical user interfaces providing real-time data and alerts, which are accessible to owners, consultants are contractors.

4.4 Monitoring

Long-term monitoring of the structures after completion may be necessary and always recommended. At very least, the structure should be monitored during the defects notification period. This protects both the Owner (from defective workmanship or materials) and the contractor (from unfounded allegations). The type and frequency of the monitoring should be discussed in advance. Contractors should consider a monitoring program, even if not required by the contract, especially if the works have been performed on a Design & Construct basis. This provides valuable feedback regarding design assumptions leading to safer and more economical designs.

Monitoring must include a complete record of nearby construction, maintenance and repair activities that could affect the performance of a structure. For example, a trench dug beside a building could result in differential movement, or a dewatered excavation could result in the lowering of the ground water table and therefore settlements.

5 CASE STUDIES

5.1 Reinforced soil wall, New Pantai Expressway, Malaysia

In 2003, at the location of reinforced soil walls at the Pantai Dalam Interchange, on the New Pantai Expressway in Malaysia, very soft silts to soft sandy silts were encountered to depths varying from 5 m to 12 m. Being on the bank of the Klang river, this was not surprising. Conventionally, the walls would be supported on driven piles. An alternative solution of Vibro stone columns was proposed, to support the reinforced soil walls, up to 13 m in height. Depending on the height of the wall, the replacement ratios varied from 15% to 35%.

As Figure 12 illustrates, first a stable granular working platform had to be created, which would also serve as a drainage blanket for the columns. Columns were installed in the conventional way, with real-time monitoring and post construction review of column construction parameters. Figure 13 shows a completed wall.

Figure 12: Stone columns being installed over soft, water-logged soils from a stable working platform.

Figure 13: Completed reinforced soil wall, nearly 13 m high.

A key feature of this project is the long-term monitoring of the reinforced soil walls as they were being constructed, and beyond (Figure 14). Because the soils were silty in nature and relatively fast draining, the plot shows that nearly all settlements occurred during the construction period.

In fact this characteristic of the Vibro treatment is noticeable in many projects in that most of the settlements occurred during the construction of the embankment and residual settlement of limited amount will come after the full embankment is place. For more details, the reader is referred to Hari Krishna & Yee (2006).

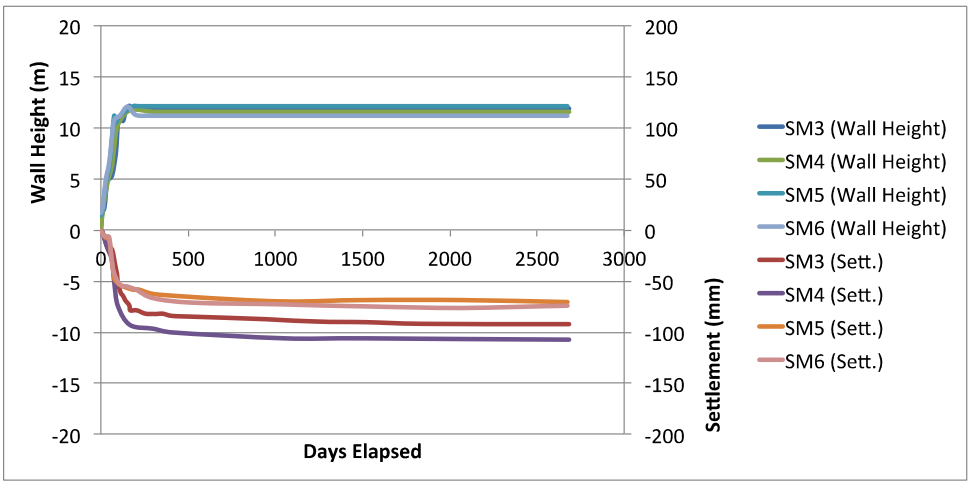

Figure 14: Long-term monitoring of wall settlements

5.2 Reclamation slope, Tekong Island, Singapore

At the Tekong Island reclamation, Singapore, the conventional method of forming the reclamation perimeter bund was to dredge a trench, form a sandkey and bund, and densify the sandfill using Vibro compaction. However, for a 200 m stretch, it was not possible to employ this method due to the presence of an existing stretch of bund (Figure 15). Therefore, offshore stone columns were used to stabilise the soft clay in-situ, for the safe construction of the sandbund (Figure 16). Cone penetration tests showed that the soft clay ("Upper" marine clay) had tip resistances (q_c) of 0.25 MPa, gradually increasing to 1 MPa.

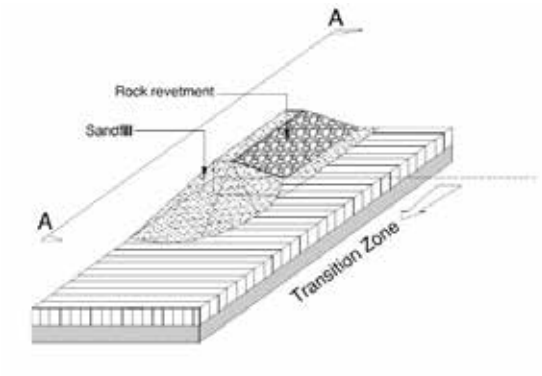

Figure 15: Reclamation bund, showing potential slip-circle

Figure 16: Offshore column installation in progress.

A total of 43,000 linear meters of 1.1 m diameter column were installed to depths of 28 m below sea level. The Consultant's design replacement ratio was 30%. The depth meant that a "gravel jet" system had to be used to deliver the stone to the stone chamber at the top of the vibrator string. Positioning was done using a GPS receiver mounted on the tip of the crane boom. As direct load testing of the columns were impractical in undersea condition, quality assurance was paramount. Stone consumption per column and column construction records were carefully checked. The reclamation bund was successfully constructed over the improved ground. For more details, the reader is referred to Leong & Raju (2007).

6 CONCLUSIONS

Vibro stone columns are legitimately classified as soil improvement techniques as they not only provide reinforcement to the weak soils but also improvement the characteristics of the surrounding soils with time. They have been used extensively in Asia and the rest of the world for many years. Various structures such as reclamation bunds, highway and railway embankments, concrete LNG tanks, steel tanks, concrete buildings, airport taxiways and runways, mineral stockyards and container stacking yards have been supported. Vibro stone columns are ductile elements, providing a robust ground improvement solution. Well-calibrated design methods are crucial.

But particularly in the application of Vibro stone columns to soft soils, proper construction practises are critical. International construction standards exist, with EN 14731: 2005 being the most widely applied. Proper monitoring during column construction is important because of the limited applicability of direct testing via plate load tests. It is equally important to control post-column construction activities such as the construction or maintenance of the granular drainage layer, and where applicable the staged construction of the reinforced soil wall, embankment, tank hydrotesting, etc.

Finally, wherever possible long-term monitoring of the completed structure should be carried out, giving vital information back to the designers, allowing better calibration of design parameters, and validation of the design approach.

REFERENCES

Barksdale, R.D. & Bachus, R.C. 1983a. *Design and Construction of Stone Columns, Volume I*, FHWA/RD-83/026, US Department of Transportation, Federal Highway Authority

Barksdale, R.D.& Bachus, R.C. 1983b *Design and Construction of Stone Columns, Volume II, Appendixes*, FHWA/RD-83/027, US Department of Transportation, Federal Highway Authority

Building Research Establishment. 2000. *Specifying vibro stone columns, BR 391*, Construction Research Communications, London.

EN 14679: 2005. *Execution of special geotechnical works- Ground treatment by deep vibration*, European Committee for Standardization, Brussels, Belgium.

Hari Krishna, Y. & Yee, Y.W. 2006. Performance of a high reinforced soil wall supported on Vibro stone columns, *GSM-IEM Oktoberforum 2006 on Engineering Geology and Geotechnical Engineering*.

Kirsch, K. & Kirsch, F. 2010. *Ground improvement by deep vibratory methods*, Spon Press.

Leong, K.W. & Raju, V.R. 2007. Use of Vibro Replacement Method for the Stabilization of an Offshore Slope on Soft Clay, *Proceedings of the Sixteenth Southeast Asian Geotechnical Conference*, Yee, K., Ooi, T.A., Ting, W.H., Chan, S.F. (eds.), 547-550

Raju, V.R. & Sondermann, W. 2005. Ground Improvement using Deep Vibro Techniques, *Ground Improvement Case Histories*, Indraratna, B & Chu., J. (eds.), 601-638.

Raju, V.R., Yee, Y.W., Sreenivas, P. & Tam, E. 2004. Vibro replacement for the construction of a 15 m high highway embankment over a mining pond", *Malaysian Geotechnical Conference 2004*.

Sondermann, W., Raju, V.R., Daramalinggam, J. & Yohannes, M. 2016. Practical Design of Vibro Stone Columns, *Proceedings of the 36th Annual Seminar, Geotechnical Division*, *The Hong Kong Institution of Engineers.*

Evaluation of Liquefaction Potential of Reclaimed Land in Hong Kong

Erin Leung
Ove Arup and Partners Hong Kong Ltd

ABSTRACT

Liquefaction is one of the hazards associated with an earthquake event. Liquefaction has a potential to cause bearing capacity failure and settlements of shallow foundations, damage to piled foundations and waterfront structures such as seawalls and other types of retaining wall. Previous studies have shown that reclamation sites in Hong Kong with relatively clean sands as reclamation fill are potentially liquefiable. In this paper, liquefaction assessment is carried out for a number of reclamation sites in Hong Kong using an up-to-date method to evaluate the liquefaction potential under a seismic event. The critical SPT N values for the onset of liquefaction in the form liquefaction triggering curves are derived with respect to the seismic hazard and ground conditions of Hong Kong. The findings of this study provide some criteria for designers to conduct liquefaction screening for a site before considering to proceed with a detailed liquefaction assessment. Procedures of liquefaction assessment are also recommended.

1 INTRODUCTION

During an earthquake, the rapid shaking of the ground generates large pore water pressures in saturated granular soils under undrained condition which results in a reduction in effective stresses and subsequently a substantial loss in strength. This phenomenon is termed liquefaction. The variables that influence the onset of liquefaction include the presence of groundwater, the particle size distribution of the soil, the in-situ relative density of the soil, the effective confining stress and the amplitude and duration of ground motion. Liquefaction case histories have shown that loose and submerged clean sands, sands with fines and non-plastic or low plasticity silts are susceptible to liquefaction.

Liquefaction can lead to severe consequences in the cases of building or infrastructure damage. The potential types of damage include settlement and bearing capacity failure of shallow foundations, damage of pile foundations due to the loss of support in the liquefied layer, and failure of retaining structures due to an increase in earth pressure and a reduction of resistance against bearing and sliding failure. Notable examples are the extensive liquefaction and associated damage in buildings and civil engineering structures in the 1964 Niigata earthquake (Figure 1) and the 1995 Kobe earthquake (Figure 2) in which many of the affected areas involved reclaimed land and young sedimentary deposits with low density and shallow groundwater table. Previous seismic studies for Hong Kong have shown that there is a potential of liquefaction in reclaimed sites with fill comprising loose sands with low fines content (Pun 1992; Arup 2004).

This paper presents the liquefaction assessment for a number of reclamation sites in Hong Kong using an up-to-date method to evaluate the performance of the reclaimed sites under a seismic event. Based on the up-to-date method, the critical SPT N values for the onset of liquefaction are calculated with respect to the seismic hazard and ground conditions of Hong Kong. The results provide some guidelines for designers to conduct a preliminary screening of the liquefaction potential of a site and evaluate the need of further liquefaction assessment. Procedures of liquefaction assessment are also recommended.

Figure 1: Liquefaction-induced bearing capacity failure of building foundation in the Niigata earthquake in 1964 (Photograph from the Godden Collection, EERC, University of California, Berkeley)

Figure 2: Retaining wall damage caused by liquefaction in the Kobe earthquake in 1995 (Photograph from the Kobe Geotechnical Collection, EERC, University of California, Berkeley)

2 METHODOLOGY

Liquefaction assessment consists of the following three main steps (ASCE 2014):

1. Assessment of liquefaction susceptibility based on soil characteristics and depth of groundwater table;
2. Liquefaction triggering analysis on susceptible soils based on the capacity of soil to resist liquefaction and the seismic demand in terms of cyclic stress ratio; and
3. Evaluation of the consequences of liquefaction.

This paper focuses on the first two steps and the details are described below.

2.1 Susceptibility assessment

Liquefaction susceptible soils include uniform clean sands, silty sands and non-plastic/low-plasticity silts which are below the groundwater table. Plasticity index (PI) and clay content are the soil properties commonly considered in assessing liquefaction susceptibility. For example, soils with PI < 10% and clay content < 20% are considered as susceptible to liquefaction (Eurocode 8; ASCE 2014). In terms of common soil types in Hong Kong, liquefaction susceptible soils include Reclamation Fill, Alluvial Sands and Silts, and sandy or silty Marine Deposits. Public fill and marine sand fill are the most commonly used types of fill in local reclamation (CEO 2002). Public fill is variable in composition and contains construction debris and decomposed rock which has a wide range of particle sizes and is less susceptible to liquefaction compared to marine sand fill which has a fines content generally less than 10%.

The following common soil types in Hong Kong are considered not to be susceptible to liquefaction:

- Marine Clays and Alluvial Clays – the high clay content renders the soils not liquefiable.
- Colluvium – typically comprises gravel, cobbles, boulders in a silt/clay matrix and is rarely predominantly sand.
- Saprolite (Completely to Highly Decomposed Rocks) – the likelihood of liquefaction is very low due to their older age and high relative density, fines content and strength.

Only the soils that are susceptible to liquefaction are considered in the liquefaction triggering assessment.

2.2 Liquefaction triggering assessment

Common engineering practice in the liquefaction triggering assessment is to use one of many empirical relationships based upon case histories of liquefaction, or absence of liquefaction in earthquakes over the past 50 years approximately, and measured in-situ soil properties such as the penetration resistance in standard penetration test (SPT) or cone penetration test (CPT), or in-situ shear-wave velocity (v_s). The SPT based correlation of Seed et al. (1984, 1985) as shown in Figure 3 was one of the most widely applied relationships

for liquefaction triggering assessment. The deterministic triggering curves separate the occurrence of liquefaction and no-liquefaction cases. Cetin et al. (2004) proposed SPT based probabilistic relationships, as shown in Figure 4, which incorporates an expanded database of case histories and an improved assessment of the factors affecting liquefaction potential. The probabilistic relationships have been adopted in previous liquefaction assessment carried out for Hong Kong (Arup 2004; Arup 2012b). The most up-to-date method of SPT based probabilistic liquefaction triggering assessment is presented in Boulanger & Idriss (2012, 2014). It includes updated case histories from recent earthquakes such as the 2010 – 2011 Canterbury earthquakes in New Zealand and the 2011 Tohoku earthquake in Japan and revision of key parameters such as the magnitude scaling factor that is used to normalise the case history data for earthquake magnitude. The Boulanger & Idriss (2012, 2014) approach is adopted in this study.

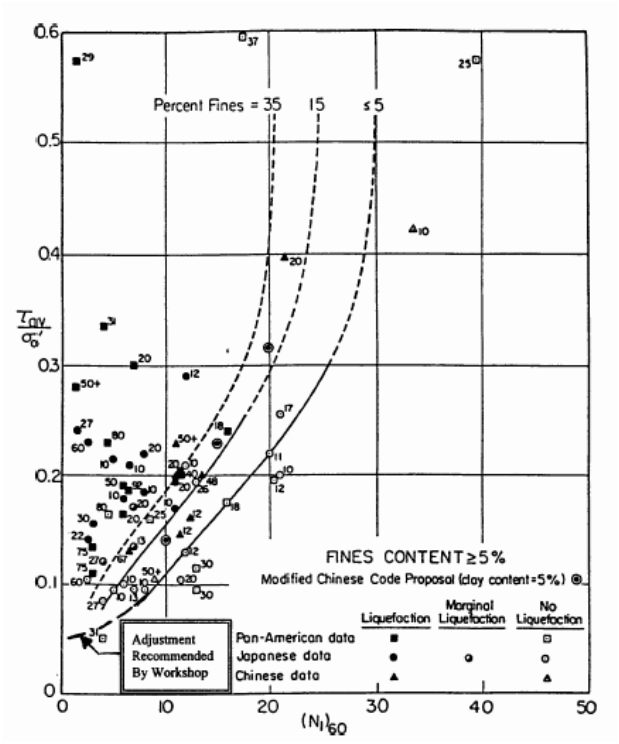

Figure 3: Correlation between equivalent uniform cyclic stress ratio and SPT data for M_W = 7.5 earthquakes with adjustments at low cyclic stress ratio (Seed et al. 1984 & 1985)

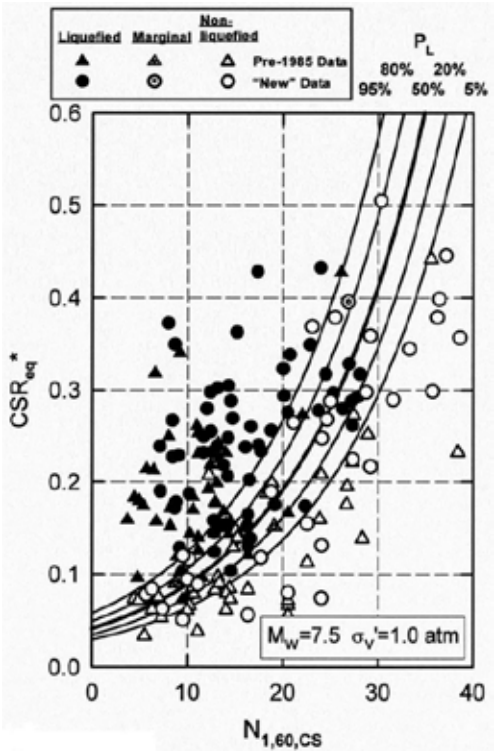

Figure 4: "Probabilistic" SPT-based liquefaction triggering correlation (for M_W = 7.5 and σ_v' = 1.0 atm) "clean sands" (FC ≤ 5%) (Cetin et al. 2004)

All of the above methods are stress-based approach which compares the earthquake-induced cyclic stress ratio (CSR) with the cyclic resistance ratio (CRR) of the soil. There is a potential of liquefaction if CSR > CRR. The determination of various parameters are presented below.

Cyclic stress ratio (CSR) –

The CSR is considered as an equivalent uniform cyclic shear stress ratio expressed in Equation (1).

$$CSR = 0.65 \cdot \frac{\tau_{max}}{\sigma_{v'}} \quad (1)$$

where τ_{max} is the peak shear stress of each soil element in the profile and is evaluated by means of site-specific seismic site response analysis in this study; and σ_v' is the vertical effective stress.

The triggering of liquefaction is affected by the duration of shaking and the amplitude of loading which are related to the earthquake magnitude. The stress-based approach for the liquefaction assessment is based on the CSR corresponding to an earthquake with a moment magnitude, M, of 7.5. For other earthquake magnitudes, an earthquake magnitude scaling factor (MSF) is applied to adjust the CSR to a reference M of 7.5 as expressed in Equation (2).

$$CSR_{M=7.5,\,\sigma'_v=1\ atm} = \frac{CSR}{MSF \cdot K_\sigma} \tag{2}$$

where K_σ is the overburden correction factor. The expression for K_σ is provided in Boulanger & Idriss (2014). An updated MSF relationship described in their study is adopted. It takes into account of the effects of soil type and density in addition to the earthquake magnitude.

Cyclic resistance ratio (CRR) –

The CRR is determined using the correlation proposed by Boulanger & Idriss (2012, 2014) expressed in Equation (3).

$$CRR_{M=7.5,\,\sigma'_v=1\ atm} = exp\left\{\frac{(N_1)_{60cs}}{14.1} + \left[\frac{(N_1)_{60cs}}{126}\right]^2 - \left[\frac{(N_1)_{60cs}}{23.6}\right]^3 + \left[\frac{(N_1)_{60cs}}{25.4}\right]^4 - 2.67 + \sigma_{\ln(R)} \cdot \Phi^{-1}(P_L)\right\} \tag{3}$$

where $CRR_{M=7.5,\,\sigma v'=1atm}$ is the cyclic resistance ratio of soil adjusted to a reference earthquake magnitude M = 7.5 and σ_v' = 1 atm; $(N_1)_{60cs}$ is the measured SPT blow count corrected for the effects of overburden stress, energy ratio of the SPT system and fines content, where the energy ratio is corrected to 60% and fines content = 0 (i.e. equivalent clean sand); $\sigma_{ln(R)}$ is the standard deviation of $\ln(CRR_{M=7.5,\,\sigma v'=1atm})$ and is equal to 0.13; Φ^{-1} is the inverse of the standard cumulative normal distribution; and P_L is the probability of liquefaction.

Corrected SPT blow count ((N1)60cs) –

The corrected SPT blow count $(N_1)_{60cs}$ is expressed in Equation (4).

$$(N_1)_{60cs} = (N_1)_{60} + \Delta(N_1)_{60} \tag{4}$$

$(N_1)_{60}$ and $\Delta(N_1)_{60}$ are expressed in Equations (5) and (6).

$$(N_1)_{60} = C_N C_E C_R C_B C_S N \tag{5}$$

$$\Delta(N_1)_{60} = exp\left(1.63 + \frac{9.7}{FC+0.01} - \left(\frac{15.7}{FC+0.01}\right)^2\right) \tag{6}$$

The correction factors are determined in accordance with Table 1.

Factor of safety against liquefaction triggering (FSLiq) –

The ratio between CRR and CSR indicates the factor of safety against liquefaction triggering (FS_{Liq}):

$$FS_{Liq} = \frac{CRR_{M=7.5,\,\sigma'_v=1\ atm}}{CSR_{M=7.5,\,\sigma'_v=1\ atm}} \tag{7}$$

Table 1: Correction factors for SPT N values

Correction factor	Description	Value(s)	Reference
C_N	Correction factor for overburden stress	$C_N = \left(\frac{P_a}{\sigma'_v}\right)^{(0.784-0.0768\sqrt{(N_1)_{60cs}})}$	Boulanger & Idriss (2014)
C_E	Correction factor for energy efficiency of SPT hammer	= ER_m/60%, ER_m is the measured energy efficiency ER_m = 60% (i.e. C_E = 1) for standard automatic trip hammers used in HK	Stroud (1989); Yang (2006)
C_R	Correction factor for short rod length	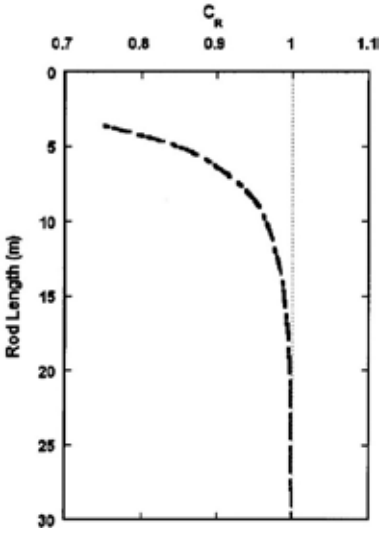	Cetin et al. (2004)
C_B	Correction factor for borehole diameters greater than 115 mm	= 1.00 for borehole dia. = 65 – 115mm = 1.05 for borehole dia. = 150mm = 1.15 for borehole dia. = 200mm C_B = 1 for standard procedures in HK	Skempton (1986)
C_S	Correction factor for using split spoons with room for liners but with the liners absent	$C_S = 1 + \frac{(N_1)_{60}}{100}$ where $1.10 \leq C_S \leq 1.30$ C_S = 1 for standard procedures in HK	Cetin et al. (2004)

3 LIQUEFACTION ASSESSMENT OF RECLAIMED SITES IN HK

3.1 Ground motion

Ground motion input is required to determine the seismic demand in the liquefaction assessment in terms of earthquake magnitude and cyclic shear stress in the soil profile. The latest seismic hazard assessment for Hong Kong (Arup 2012b; GEO 2015) has identified the de-aggregated earthquake magnitude and distance combinations that contribute most significantly to the seismic hazard in Hong Kong as shown in Table 2.

Table 2: De-aggregated combinations of magnitude and distance for UHRS (Arup 2012b)

Probability of the ground motion in the next 50 years	Return period (years)	Short period ground motion		Long period ground motion					
		0.2s		1 s (near field event, R < 250 km)		1 s (far field event, R > 250 km)		5s	
		M	R (km)	M	R (km)	M	R (km)	M	R (km)
10%	475	5.5	30	6.5	60	-	-	7	90
2%	2475	5.5	10	7	60	8	250	7.5	90

Based on the de-aggregated combinations, the following earthquake magnitudes are considered in the evaluation of liquefaction potential:

- '10% chance of being exceeded in the next 50 years' (return period = 475 years), near-field earthquake event at 60 km, Mw = 6.5
- '2% chance of being exceeded in the next 50 years' (return period = 2475 years), near-field earthquake event at 60 km, Mw = 7.0
- '2% chance of being exceeded in the next 50 years' (return period = 2475 years), far-field earthquake event at 250 km, Mw = 8.0

Earthquake time histories are developed from recorded strong ground motion records selected to match the de-aggregated combinations. The recorded strong ground motion records are modified by the spectral matching technique to match the uniform hazard response spectra for Hong Kong. The developed earthquake time histories are used in the site response analysis to calculate the maximum cyclic shear stress in the soil profiles.

3.2 Sites

Five sites on reclaimed land are evaluated for the potential of liquefaction. The soil profiles generally comprise Reclamation Fill overlying Marine Clay and/or Alluvial Sand/Silt, and decomposed rock. The fines content of the soils is about 10% for the Reclamation Fill and 20% for the Alluvial Sand. Table 3 summarises the details of the ground profiles.

Table 3: Details of ground profiles for liquefaction assessment

Site Name	Location	Rock Depth (m)	$\bar{N}$* (blows/300 mm)	$\bar{v}_s$** (m/s)
A	Tuen Mun	24	17	249
B	Kwai Chung	52	17	212
C	Central	75	14	216
D	Kowloon Bay	45	8	175
E	Tseung Kwan O	63	4	155

* $\bar{N}$: average value of blow counts required to drive the standard split spoon sampler a distance of 300mm in the upper 30m of the soil profile. $\overline{\mathrm{N}} = \frac{\sum_{i=1}^{n} d_i}{\sum_{i=1}^{n} \frac{d_i}{N_i}}$, where d_i is the thickness of layer i between 0 and 30m, N_i is the SPT N value at layer i, and $\sum_{i=1}^{n} \boldsymbol{d_i}$ = 30m.

** $\bar{v}_s$: average value of propagation velocity of S waves in the upper 30m of the soil profile at shear strain of 10^{-5} or less. $\overline{\mathrm{v}_S} = \frac{\sum_{i=1}^{n} d_i}{\sum_{i=1}^{n} \frac{d_i}{v_S}}$, where d_i is the thickness of layer i between 0 and 30m, v_s is the velocity of S waves at layer i, and $\sum_{i=1}^{n} \boldsymbol{d_i}$ = 30m.

3.2 Liquefaction triggering assessment

Liquefaction triggering assessment is carried out for the five reclaimed sites following the methodology described in Section 2. The CRR and CSR along the soil profiles are computed based on the SPT N values to calculate the factor of safety against liquefaction triggering. A probability of liquefaction is associated with the computation of CRR using Equation (3). The soil layer is considered to have a potential of liquefaction (FS_{Liq} < 1) when the probability of liquefaction exceeds 15% and 50% for ground motions having a return period of 475 and 2475 years respectively. In addition, Eurocode 8 (BS EN 1998-5:2004 Clause 4.1.4 (11)P) requires a safety factor of 1.25 in the evaluation of liquefaction triggering potential under a design ground motion with a return period of 475 years, i.e. a soil shall be considered as susceptible to liquefaction if the CRR is less than 1.25 times the CSR. The safety factor is applied to take into account the uncertainties of the field-based procedure in which no partial factor is applied to the SPT N values (Fardis et al., 2005).

Figure 5 shows the calculated factor of safety against liquefaction triggering along depth for 475-year and 2475-year return period ground motions. Two of the sites show a potential of liquefaction to a depth within 5m for both ground motions. Shallow foundations are potentially affected by a reduction of bearing capacity or an

excessive ground settlement due to liquefaction. In such case, ground improvement or deep foundations should be considered to ensure foundation stability. Piles are affected to a lesser extent unless there is lateral spreading associated with sloping ground resulting in a large ground displacement. The reduced strength and stiffness of the liquefied soil layer have to be considered in the design of piles.

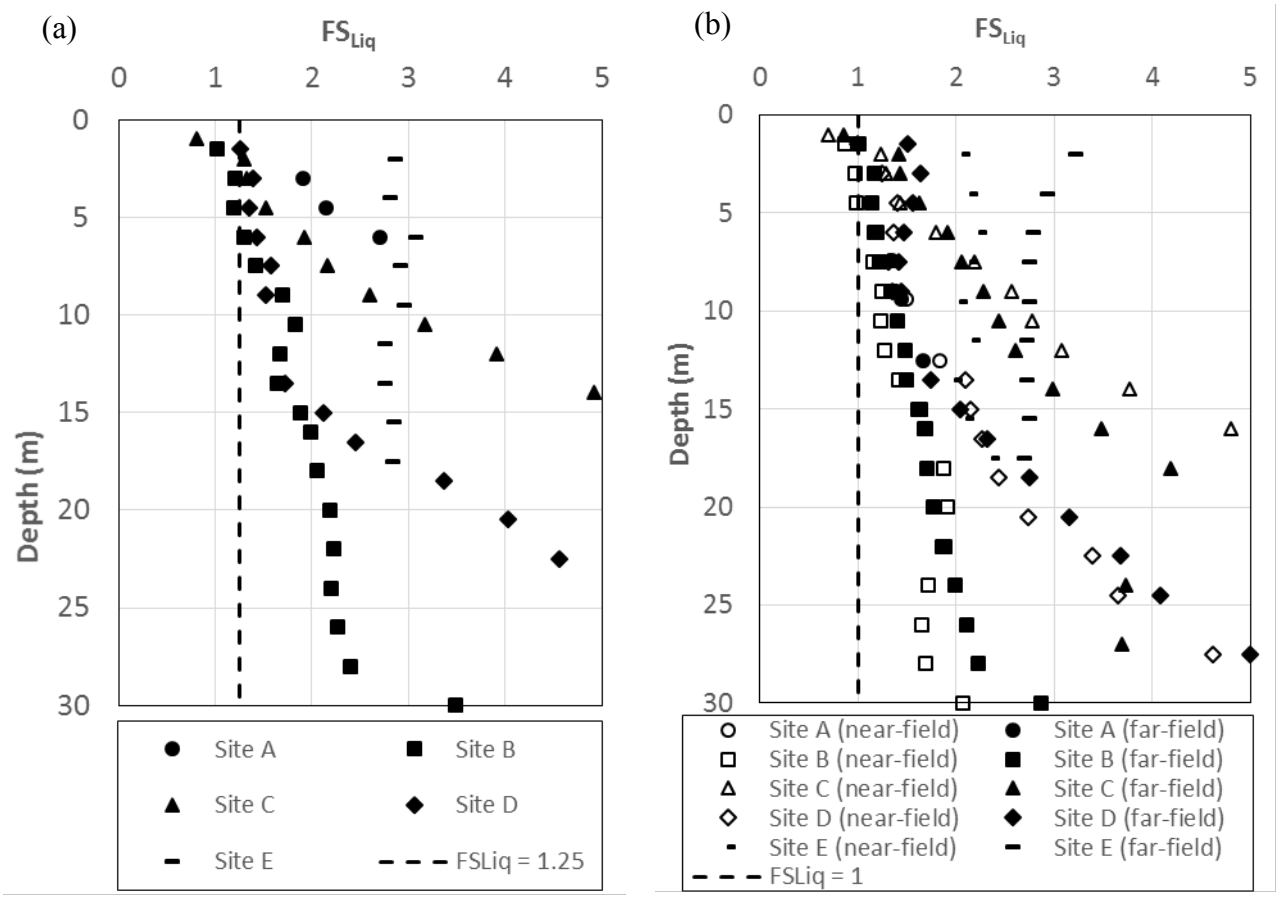

Figure 5: Factor of safety against liquefaction triggering of reclaimed sites in HK; (a) 475-year return period ground motion; (b) 2475-year return period ground motion

4 LIQUEFACTION SUSCEPTABILITY CRITERIA FOR HK

In order to facilitate designers to carry out a preliminary assessment of the liquefaction triggering potential of a site in Hong Kong, the critical SPT N values for the onset of liquefaction is calculated. Equations (2) and (3) are used to calculate the values of $(N_1)_{60cs}$ that result in $CRR_{M=7.5,\,\sigma v'=1atm} = 1.25 \cdot CSR_{M=7.5,\,\sigma v'=1atm}$ along the depth of a soil profile, with the consideration of $FS_{Liq} = 1.25$ under a design ground motion with a return period of 475 years. The critical $(N_1)_{60cs}$ profile is then converted to the uncorrected SPT N for soils of different fines contents using the correction factors shown in Table 1.

The adopted parameters are summarised in Table 4.

Table 4: Parameters for the calculation of critical SPT N values for the onset of liquefaction

Earthquake data –	
Earthquake scenario	'10% chance of being exceeded in the next 50 years', near-field earthquake event
Moment magnitude	6.5
Liquefaction criterion –	
Probability of liquefaction in CRR calculation	15%
Factor of safety against liquefaction triggering	1.25
Ground profile data –	
Groundwater level	2m below ground level
Unit weight of soil	19 kN/m^3

The peak shear stress (τ_{max}) of soil along depth is obtained from the envelope of τ_{max} calculated in the site-specific seismic site response analyses for 41 nos. of ground profile covering various parts of Hong Kong (Arup 2004; Arup 2012b). The variation of τ_{max} with depth is shown in Figure 6.

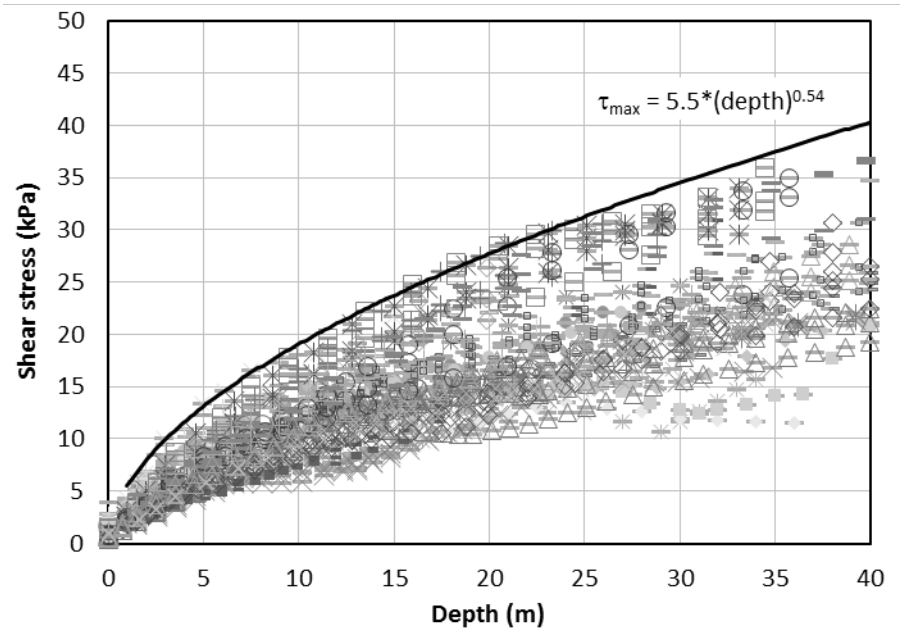

Figure 6: Peak shear stress vs. depth from seismic site response analyses for soil profiles in HK

Figure 7 shows the critical values of $(N_1)_{60cs}$ and the corresponding SPT N for different fines contents. Soils with SPT N values on the left of the corresponding curve are considered to have a moderate to high potential of liquefaction, while those on the right are considered to have a low potential of liquefaction. The result provides the criteria for designers to perform a preliminary assessment of the liquefaction potential of a site.

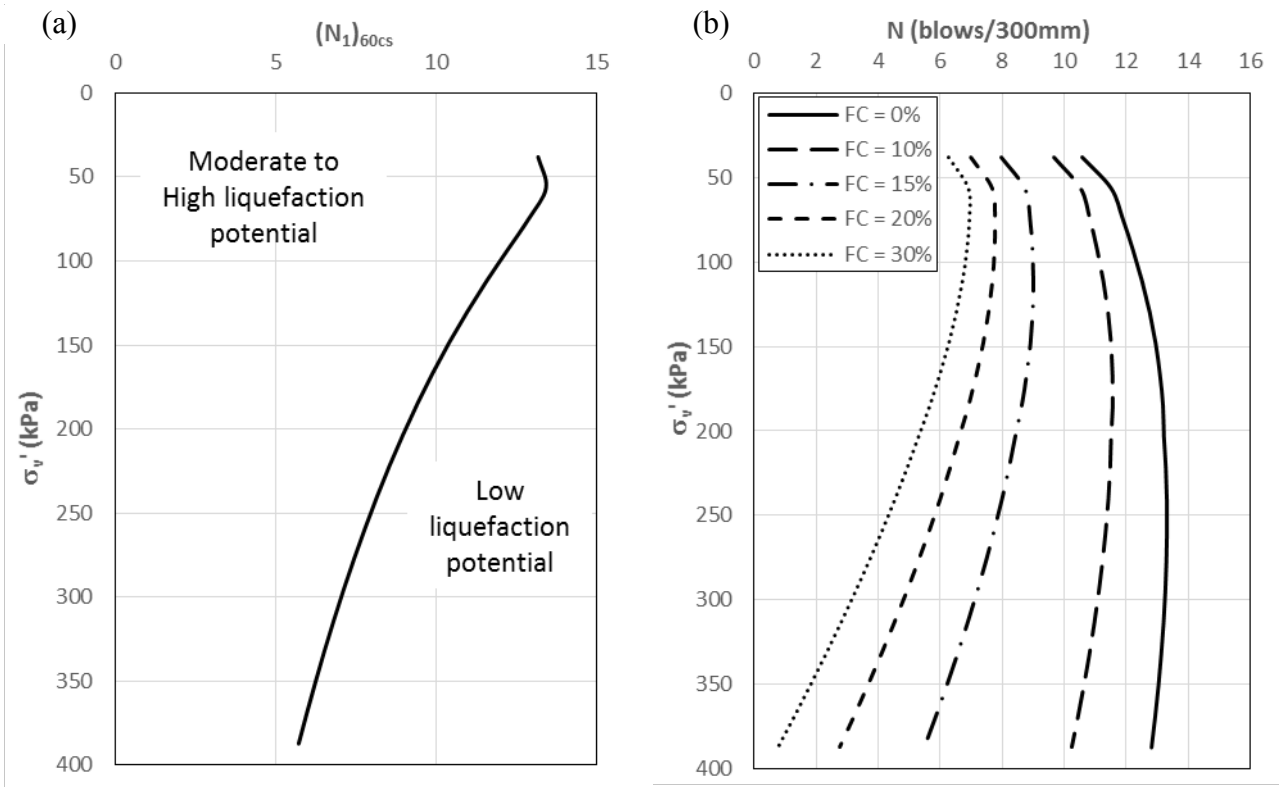

Figure 7: Liquefaction triggering curves for HK; (a) $(N_1)_{60cs}$; (b) SPT N

5 RECOMMENDED PROCEDURES OF LIQUEFACTION ASSESSMENT

Based on the discussion above, the following procedures are recommended for the evaluation of the liquefaction potential of a site in Hong Kong:

1. Susceptibility assessment
   a. Identify the existence of liquefaction susceptible soils which include Fill and superficial deposits comprising Alluvial Sands and Silts, and sandy or silty Marine Deposits.
   b. Check the Plasticity Index (PI) and clay content of the soils in Step 1a. The materials are considered as susceptible if PI < 10% and clay content < 20%.
   c. The above materials are considered as liquefaction susceptible if they are below the mean groundwater table.
2. Preliminary liquefaction triggering assessment
   a. Check the fines content and the SPT N values of the susceptible soils.
   b. Based on Figure 7, evaluate the potential of liquefaction triggering. The triggering curves are applicable to a design ground motion with a return period of 475 years in Hong Kong and correspond to a factor of safety against liquefaction of 1.25.
   c. If the SPT N values of the soils are on the right side of the triggering curves, the potential of liquefaction is low and further checking is not required. If the SPT N values lie on the left side of the triggering curves, proceed to Step 3.

3. Detailed liquefaction triggering assessment
   a. Carry out site-specific site response analysis to calculate the peak shear stress (τ_{max}) induced by the earthquake ground motion along the soil profile.
   b. Evaluate the potential of liquefaction triggering following established method of liquefaction triggering assessment such as the approach presented in Section 2.

6 CONCLUSIONS

Reclaimed sites in Hong Kong have been shown to have a potential of liquefaction in previous seismic studies. An up-to-date method of liquefaction triggering assessment (Boulanger & Idriss 2012 & 2014) is adopted in this paper to evaluate the liquefaction potential of reclaimed sites in Hong Kong. Two out of the five sites studied show a potential of liquefaction to a depth within 5m for both ground motions with a return period of 475 and 2475 years. The implications on the design of foundations are briefly discussed.

To facilitate designers to carry out a preliminary assessment of the liquefaction triggering potential of a site in Hong Kong, the critical SPT N values for the onset of liquefaction are calculated with respect to the seismic hazard and ground conditions of Hong Kong. Liquefaction triggering curves (critical SPT N values versus vertical effective stress) corresponding to a 475-year return period design ground motion are produced for soils with different fines contents. The curves serve as the criteria for designers to carry out a preliminary screening of the liquefaction potential of a site before proceeding to a detailed liquefaction assessment which may not be deemed necessary in some cases. Finally, a procedure of liquefaction assessment for sites in Hong Kong is recommended based on the findings of this study.

REFERENCES

Arup 2004. Evaluation of Site Response to Earthquakes. Consultancy Agreement No. CAO K49, Consultancy to Study the Seismic Effects on Buildings in Hong Kong. Buildings Department, Hong Kong.

Arup 2012a. Final Report on Overall Seismic Hazard Assessment, Landslip Prevention and Mitigation Programme, Pilot Seismic Microzonation Study in North-west New Territories for the Study of Potential Effect of Earthquake on Natural Terrain – Investigation, Agreement No. CE49/2008(GE), Ove Arup & Partners Hong Kong Ltd., Report prepared for Geotechnical Engineering Office, Hong Kong, 224 p.

Arup 2012b. Final Report on Seismic Microzonation Assessment, Landslip Prevention and Mitigation Programme, Pilot Seismic Microzonation Study in North-west New Territories for the Study of Potential Effect of Earthquake on Natural Terrain – Investigation, Agreement No. CE49/2008(GE), Ove Arup & Partners Hong Kong Ltd., Report prepared for Geotechnical Engineering Office, Hong Kong, 257 p.

ASCE/SEI 41-13 2014. American Society of Civil Engineers, seismic evaluation and retrofit of existing buildings.

Boulanger & Idriss 2012. Probabilistic standard penetration test-based liquefaction triggering procedure. *Journal of Geotechnical Engineering*, 138(10): 1185-1195.

Boulanger & Idriss 2014. CPT and SPT based liquefaction triggering procedures. Report No. UCD/CGM-14/01. Centre for Geotechnical Modelling, Department of Civil and Environmental Engineering, University of California at Davis.

Bray, J. D. & Sancio, R. B. 2006. Assessment of the Liquefaction Susceptibility of Fine-grained Soils, *Journal of Geotechnical and Geoenvironmental Engineering*, 132(9): 1165-1177.

CEO 2002. Port Works Design Manual Part 3 – Guide to Design of Reclamation. Civil Engineering Office, Civil Engineering Department, The Government of the Hong Kong Special Administrative Region, 60 p.

Cetin, K. O., Seed, R. B., Kiureghian, A. D., Tokimatsu, K., Harder, L. F., Kayen, R. E. & Moss, R. E. S. 2004. Standard Penetration Test-Based Probabilistic and Deterministic Assessment of Seismic Soil Liquefaction Potential, *Journal of Geotechnical and Geoenvironmental Engineering*, 130(12): 1314-1340.

Eurocode 8: Design of structures for earthquake resistance – Part 5: Foundations, retaining structures and geotechnical aspects, BS EN 1998-5:2004, European Committee for Standardisation.

Fardis, M. N., Carvalho, E., Elnashai, A., Faccioli, E., Pinto, P. & Plumier, A. 2005. Designers' Guide to EN 1998-1 and EN 1995-5 Eurocode 8: Design of structures for earthquake resistance. General rules, seismic actions, design rules for buildings, foundations and retaining structures. Thomas Telford, London.

GEO 2015. Seismic Hazard Analysis of the Hong Kong Region. GEO Report No. 311. Geotechnical Engineering Office, Hong Kong, 324 p.

Pun, W. K. 1992. Earthquake Resistance of Buildings and Marine Reclamation Fills in Hong Kong. GEO Report No. 16. Geotechnical Engineering Office, Hong Kong, 48 p.

Seed, H. B., Tokimatsu, K., Harder, L. F. & Chung, R. M. 1984. The Influence of SPT Procedures in Soil Liquefaction Resistance Evaluations, Earthquake Engineering Research Center Report No. UCB/EERC-84/15, University of California at Berkeley, October, 1984.

Seed, H. B., Tokimatsu, K., Harder, L. F. & Chung, R. M. 1985. Influence of SPT Procedures in soil liquefaction resistance evaluations, *Journal of Geotechnical Engineering*, 111(12): 1425-1445.

Skempton, A. W. 1986. Standard penetration test procedures and the effects in sands of overburden pressure, relative density, particle size, aging and overconsolidation, *Géotechnique*, 36(3): 425 – 447.

Stroud, M. A. 1989. The standard penetration test – its application and interpretation. *ICE Conf. Penetration Testing, Birmingham*. Thomas Telford, London.

Yang, W. 2006. Development and application of automatic monitoring system for standard penetration test in site investigation. PhD thesis, The University of Hong Kong.

Youd, T. L., Idriss, I. M., Andrus, R. D., Arango, I., Castro, G., Christian, J. T., Dobry, R., Finn, W. D. L., Harder, L. F., Hynes, M. E., Ishihara, K., Koester, J. P., Liao, S. S. C., Marcuson, W. F., Martin, G. R., Mitchell, J. K., Moriwaki, Y., Power, M. S., Robertson, P. K., Seed, R. B. & Stokoe, K. H. 2001. Liquefaction resistance of soils: summary report from the 1996 NCEER and 1998 NCEER/NSF workshops on evaluation of liquefaction resistance of soils, *Journal of Geotechnical and Geoenvironmental Engineering*, 127(10): 817–833.

Ground Improvement Works in Cotai, Macau SAR A Case Study Review

T.M.S. Sacadura
formerly Benaim Ltd (an AECOM company), currently Halcrow China Limited, Hong Kong
C.B. Turnbull & J.P.S. Case
Benaim Ltd (an AECOM company), Hong Kong

ABSTRACT

This paper focuses on the design and review of the ground improvement works using traditional surcharge preloading and prefabricated vertical drains undertaken on a reclaimed site in Cotai, Macau SAR. These works were required in order to facilitate the construction of a multi-level recreational and hospitality facility. The ground treatment was intended to improve the shear strength of the underlying Marine Deposits in basement excavation areas to a minimum undrained shear strength of 25+1.5z kPa, where 25kPa is the strength required at the top of the clay and z is the depth, and 20+1.5z kPa outside of the basement excavation. Typically, this required surcharge levels of 5m to 6m above existing ground levels with surcharge periods up to a maximum of 4 months to achieve 90% consolidation. Methods of evaluating the performance of the ground improvement during the construction stage are also discussed in the paper, i.e. review of instrumentation and monitoring data, Asaoka Analysis and verification *insitu* testing.

1 INTRODUCTION

A publicly listed international group has developed a prestigious 5-star fully integrated hotel and casino resort, at an estimated cost of 4.1 billion USD, on the Cotai Strip, located south of the Macau peninsula. The site was reclaimed between 2003 and 2007, in addition to the larger reclamation known as Cotai, which connects the islands of Coloane and Taipa. Extensive ground investigation was undertaken prior to construction, which revealed a range of ground conditions at the site. This included very soft Marine Deposits (MD) with significant thickness overlain by fill materials. These fill materials comprise man-made fill and dredged MDs from other construction sites.

The development incorporates a one-storey basement with localised deeper excavations, the construction of which required lateral support and excavations works. It was necessary to improve the properties of the very soft deposits over much of the site in order to avoid unacceptable deflections of the temporary walls and associated settlements. The Ground Improvement (GI) works also aimed at minimising lateral deflections of permanent piles during construction, mitigating negative skin friction loading within the basement area and providing a viable working platform for construction plant. Two methods of ground improvement were adopted to accelerate consolidation. Vacuum surcharging, where ground conditions suited, which was undertaken on the eastern end of the site by a specialist contractor and by traditional means, i.e. installing prefabricated vertical drains (PVDs) together with surcharge. The latter was the main methodology adopted across the site and is the focus of this paper.

2 SITE DESCRIPTION AND GROUND CONDITIONS

2.1 Site description

The site is roughly trapezoidal in shape with a plan area measuring about 22 hectares. The site's eastern edge was formerly a seawall, however, in recent years reclamation activities have moved the seawall out by approximately 230m. In June 2012, prior to the start of the GI works, the site topography varied between +2.0 mH_L and +4.5 mH_L.

The development's structural form comprises a 3-level podium structure, a tower complex of 29 storey's and a 70,000m^2 basement with localised horizontal utility tunnels and vertical shafts. Generally, excavation depths of 6m (-1.95 mH_L) were required for the basement with localised depths of up to 11.7m (-7.50 mH_L). Foundations comprised large diameter bored piles, under the tower footprint, and driven Pre-stressed Precast Concrete (PPC) piles for the remaining areas of the site.

2.2 Ground conditions

The site is located on an area of recently reclaimed land in Cotai, Macau completed around 2007. Past reclamation events in Macau were generally carried out using a 'drained' approach, i.e. no dredging of the very soft deposits was undertaken. Based on historical research, the reclamation at this site involved end tipping of uncontrolled construction waste and MDs from adjacent sites. In addition, sand, possibly hydraulically placed, was used as a fill material on its most southern end. These fill materials overlie the MD which in turn is underlain by Alluviums and bedrock, or completely decomposed granite, where present. Uncontrolled mud waves were assumed to have been generated during reclamation construction.

The main site investigation comprised 145 nos. boreholes, 23 nos. cone penetration tests, 7 nos. seismic cone penetration tests, 14 trial pits, 5 trial trenches, along with GCO probing and *insitu* CBR testing. Additionally, an environmental investigation was undertaken, which comprised shallow investigation holes for groundwater and ground gas monitoring purposes. The site investigation confirmed the highly variable geological conditions. Soil parameters were derived from the ground investigation and subsequent laboratory testing. From the data results reviewed, moderately conservative design soil parameters were adopted as shown below in Table 1.

Table 1: Summary of design soil parameters (moderately conservative values)

Stratum	Soil Type	Bulk Unit Weight (kN/m^3) (above GWL)	SPT 'N' Value	Cohesion, c' (kPa)	Angle of Internal Friction, ϕ' (°)	Unimproved Soil Undrained Shear Strength, c_u (kPa)	Improved Soil Undrained Shear Strength, c_u (kPa)	Unimproved Soil Young's Modulus E' (kPa) (5)	Improved Soil Young's Modulus E' (kPa) (5)	Typical Permeability k (m/s)
Fill	Rubble/ unsorted	19 / (18)	10	0	32	-	-	1N	-	1x10^{-6} to 1 x10^{-3}(1)
	Marine Fill	16.5		0-1	25 (12) (2)	7	20+1.5z 25+1.5z(3)	200c_u (350c_u)	260c_u (350c_u)	1 x10^{-8} to 5 x10^{-7}
	Sand	18.5	10	0	35	-	-	1N	-	1 x10^{-6} to 5 x 10^{-4}
Marine Deposits	Clay	16.5		0-1	25	10+0.4(-7-y)	20+1.5z 25+1.5z(3)	200c_u (350c_u)	260c_u (350c_u)	1 x10^{-8} to 1 x 10^{-7}
Alluvium	Silt/Clay	18.5		0-1	25	25+2(-15-y)	30+2(-15-y)	200c_u (350c_u)	260c_u (350c_u)	1 x10^{-8} to 1 x 10^{-5}
	Sand	19	20+1.5 (-30-y)	0	35	-	-	1.5N	-	5 x10^{-6} to 1 x 10^{-5}
CDG	-	19	40+3.7 (-60-y)	5	34	-	-	2N	-	

Notes:

1) Permeability for type 1 fill (unsorted construction waste) may be locally higher than tests indicate.
2) Residual values for the marine fill are provided – bracketed values.
3) Ground improvement designed to achieve a minimum of 25kPa at the top of the soft marine deposits along the ELS (excavation and lateral support)

perimeter and a minimum target of 20kPa at the top of the soft clay for the remaining areas.
4) y is elevation (mH_L), z is depth in m below top of horizon.
5) E' values for SLS conditions shown in brackets (i.e. $350c_u$).

Based on the ground water monitoring records a Serviceability Limit State ground water table was adopted at a level of +2.5 mH_L while the Ultimate Limit State was adopted at a maximum level of +4.0 mH_L or at ground surface, if lower.

3 GROUND IMPROVEMENT METHODOLOGY

Following a review of ground conditions and available ground improvement techniques, a combination of PVD's and surcharge preloading was selected as the most appropriate technique to improve the undrained shear strength of the underlying MDs. Vacuum preloading was applied to the eastern portion of the site (as shown in Plate 1) due to the extensive nature of MDs and to its proximal location to existing infrastructure.

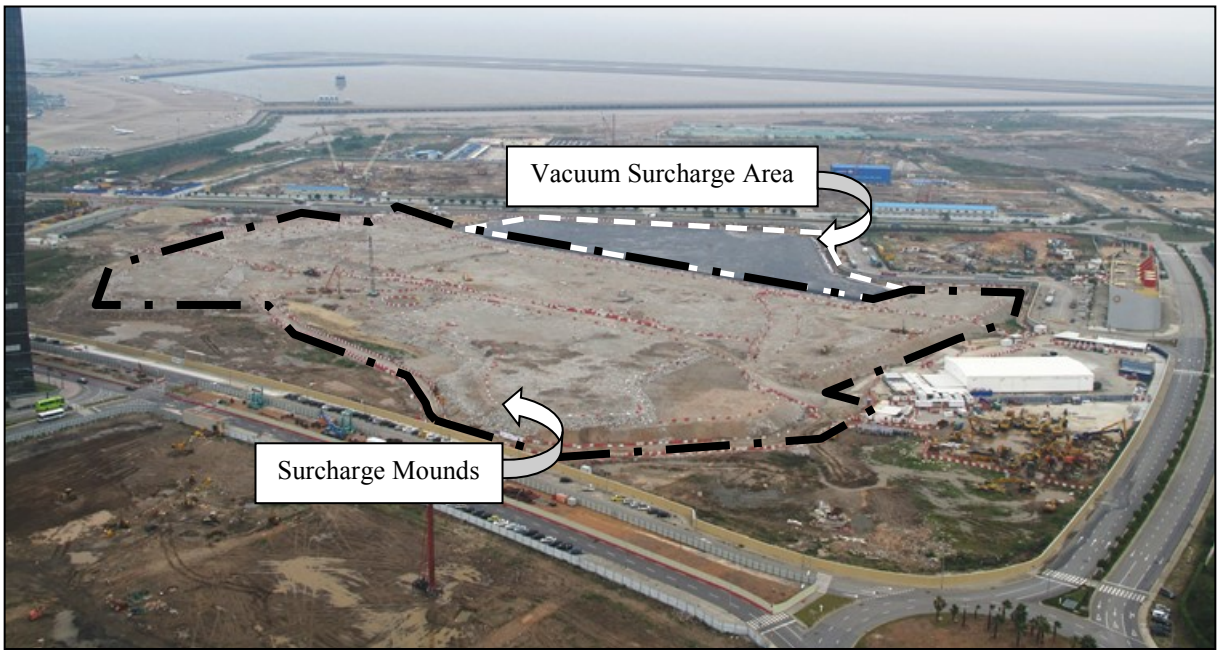

Plate 1: Site overview during ground improvement works (courtesy of Ban Lam)

The GI works were designed to improve the very soft MDs and achieve a minimum design undrained shear strength on the active and passive sides of proposed basement excavations of 25+1.5z kN/m^2, where 25 kN/m^2 is the strength required at the top of the clay and z is the depth. Elsewhere, a minimum design undrained shear strength of 20+1.5z kN/m^2 was to be achieved for temporary works including construction access and working platforms. Surcharge heights required, in order to provide the requisite increase in vertical stress were assessed based on the minimum estimated increase in undrained shear strength to 20-25kN/m^2 at the top of the clay layers. Typically, this represented an increase of 13-18kN/m^2 based on the baseline value of 7kN/m^2 assessed for the MDs.

The consolidation and surcharge requirements, in order to achieve the required increase in undrained shear strength, were assessed based on a review and an interpretation of the available geological distribution across the site.

3.1 Accelerated consolidation design

The basis of GI through surcharge/consolidation is a well-established theory which relies on the fact that the undrained shear strength of a fine-grained material can be related to its *insitu* effective stress and

consolidation history. The typical ratio undrained shear strength / *insitu* effective stress, c_u / σ_v', lies in the range of 0.2 to 0.3 (Fung et al. 1984). Skempton (Skempton 1957) suggested that this ratio can be related according to the following formula:

$$c_u = (0.11 + 0.0037 \cdot PI) \cdot \sigma_v' \quad (1)$$

where c_u = the undrained shear strength , σ_v' = effective vertical stress, PI = Plasticity Index.

For design purposes and, based on average PI values of 26% to 34% for the MDs and MD Fill, an estimate of $c_u = 0.22 \cdot \sigma_v$' was adopted. PVD's, with a minimum cross sectional length of 100mm and width of 3mm, were adopted in design to accelerate the consolidation and strength increase. The time for consolidation was estimated from consolidation theory assuming only radial, horizontal consolidation was effective. A spacing of 0.9m was considered as the minimum practical spacing for installation of the drains.
The degree of consolidation resulting from radial drainage is given by:

$$U_r = 1 \cdot e^{\left[\left(-8 \cdot c_h \cdot t\right) / \left(D^2 \cdot \mu\right)\right]} \quad (2)$$

where c_h = coefficient of horizontal consolidation (assumed to be equal to c_v as 1.3 m^2/yr), t = time for consolidation, D = drain influence zone as per formula (3) below, μ as per formula (4) below, n as per formula (5) below.

$$D = 1.05 \times L \quad (3)$$

where L is PVD spacing for triangular grids.

$$\mu = \ln\left(n/s\right) - 0.75 + \frac{k_h}{k_{h'}} \cdot \ln(s) \quad (4)$$

where s=1 and $\frac{k_h}{k_{h'}} = 1$

since zone of MD to be considered effectively remolded so smearing effects on c_h were considered to be low.

$$n = D / d_w \quad (5)$$

where d_w is the equivalent drain diameter as per $d_w = 2 \cdot (100 + 3) / \pi$

The value of c_h was assumed equal to c_v for the Marine Fill on the basis that no natural fabric or structure of the deposit would lead to an increased c_h value. It was also assumed that the effects of smearing did not affect the adopted value of c_v. The value of c_v was derived from laboratory oedometer and consolidated undrained triaxial testing based on log time methods.

From the above it was determined that in order to achieve 95%, 90% and 85% consolidation, 180, 138 and 114 days, respectively, would be required.

3.2 Surcharge calculation

The depth and thickness of the underlying MD varied significantly across the site, and due to the reclamation works it was considered that the deposit was under consolidated. The overlying, predominantly non-cohesive, fill capping, which had been in place since around 2007, was estimated to have contributed approximately 15% to 20% to the degree of consolidation of the MD at the time of resort development in mid-2012. It was considered that the installation of vertical drains would accelerate consolidation resulting from the existing capping layer loading. This effect was subsequently taken into account in assessing the additional surcharge

heights required. Where present, the overburden of the fill capping layer resulted in an increase in effective stress on the MD which resulted in an overall increase in undrained shear strength, depending on the degree of consolidation that had occurred. The theoretical c_u at the top of the MD may thus be represented by the following:

$$c_{u\,top} = 0.22 \cdot \sigma_v^{'} \cdot U \tag{6}$$

where U = the degree of consolidation

As discussed previously, the minimum design target undrained shear strength at of the MD, ranged between 20kN/m^2 to 25kN/m^2, hence the increase in vertical stress, i.e. additional surcharge, required may typically be estimated as follows:

$$H = \frac{\left(c_{u\,target} - \left(c_{u\,top} \cdot U\right)\right)}{0.22 * \gamma_f \cdot U} \tag{7}$$

where γ_f is the bulk unit weight of surcharge fill, taken as 18.5kN/m^3.

Due to the highly heterogeneous soil conditions, the methodology adopted was a "borehole by borehole" type assessment across the site, to calculate the height of surcharge as per formula (7). Then a simplified "grouping" surcharge arrangement was adopted as shown below in Figure 1, which shows surcharge elevations ranging from +5 mH_L to + 10 mH_L, (1m to 6m thick). Surcharging was concentrated in the area of the proposed basement excavation, and along the line of ELS / open cut as well as adjacent areas where working platforms for piling plants were required. The assessment of surcharge height requirements included an allowance for the existing fill cap thickness as well as its ongoing settlement.

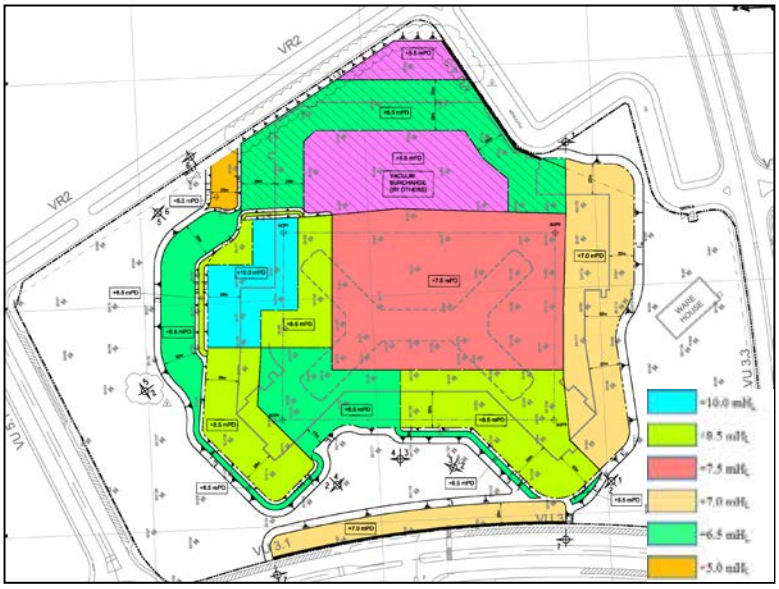

Figure 1: Grouped surcharge elevations for ground improvement works

3.3 Settlement calculation

Considerable settlements were expected as a result of consolidation of the underlying soft MDs. It should be noted that settlement of the surcharge mounds relative to the groundwater table would result in some loss of surcharge load due to buoyancy effects. During the design stage two alternatives were considered to compensate this effect, either by "topping up" the surcharge during the consolidation period or increasing the initial height of surcharge placed. The latter approach was assumed in deriving the design surcharge elevations. To compensate for the buoyancy effects an additional surcharge height equivalent to approximately 50% of the anticipated settlement was adopted, i.e. in the range 0.75m to 1.50m. It should be noted that predictive settlement estimates are generally inaccurate when compared to the actual field conditions, and particularly so when ground conditions are as variable as they were at this site. The expected major component of settlement resulted from the consolidation of the soft and very soft MDs, although it was highly likely that additional surface settlements would occur if any significant lateral squeezing took place.

An assessment of the likely consolidation settlements was made by considering the change in void ratio resulting from the increase in effective stress required to provide the target increase in c_u. The low undrained shear strength and oedometer and CPT test results suggested that significant portions of the clay were under consolidated, that is the *insitu* void ratio lied above the normally consolidated compression line. Therefore, some settlement was expected as the clay consolidated to the normally consolidated condition.

A moderately conservative value for coefficient of volume compressibility (m_v), which is the slope of the virgin compression line in the oedometer test, was adopted based on available laboratory test results for the MDs (both fill and *insitu* materials). The value adopted for design purposes was 0.44 m^2/MN. The outermost curve connecting the points when a soil specimen is in the loosest possible state is often called the virgin consolidation line, but will be referred to here as the virgin compression line. This is because it is strictly the line connecting equilibrium states whereas consolidation is a term used only for the time-dependent process between any pair of equilibrium states.

The initial void ratio was based on oedometer test results, and was taken as follows:

$$For\ c_u = 7kN/m^2, \sigma_v^{'} = {}^{7}\!/_{0.22} \approx 32kN/m^2 \rightarrow e_{07} = 1.499 \quad (7)$$

$$For\ c_u = 10kN/m^2, \sigma_v^{'} = {}^{10}\!/_{0.22} \approx 45kN/m^2 \rightarrow e_{10} = 1.431 \quad (8)$$

$$For\ c_u = 25kN/m^2, \sigma_v^{'} = {}^{25}\!/_{0.22} \approx 114kN/m^2 \rightarrow e_{25} = 1.255 \quad (9)$$

Based on the above, the change in void ratio necessary to reach the normally consolidated line could be calculated, considering the existing effective stress conditions. This component of settlement was expected to start immediately after the installation of the PVD's, and prior to surcharging. Additional settlement would then occur during and after placement of the surcharge, the value of which would depend on the change in vertical effective stress. Some consolidation settlement of the underlying Alluvial Clays was also expected as a result of the placement of surcharge and the installation of PVDs in the MD layer above and where possible on the top of the Alluvium. An assessment of the compressibility characteristics of the Alluvium indicated a value for the coefficient of volume compressibility in the order of 0.1 m^2/MN. Estimated settlements ranged up to 3m although such estimates were treated with caution given the uncertainty concerning the current consolidation state of the clay fill materials and that much of this settlement was anticipated to occur during surcharge placement.

It should be noted that settlements were observed to commence immediately after the installation of the vertical drains, which continued during surcharge placement. The magnitude of actual settlement compared with predicted values was not relied upon when assessing the degree of consolidation nor it was used as an indication that consolidation was occurring faster or slower than expected. Instead reliance was placed on rates of change with time as referred to in Section 4.1.

3.4 Site implementation

Instrumentation installation, to monitor conditions during construction, progressed in advance of the GI works in June 2012. The monitoring plan comprised inclinometers (Plate 2), rod and settlement gauges, extensometers, vibrating wire piezometers and standpipe piezometers. Some of the instruments were installed to monitor the surcharge stability, e.g. inclinometers, while others aimed at evaluating the GI performance, e.g. extensometers. There was the need to extend the instruments and keep them protected as the surcharge filling operations progressed, Plate 2.

The GI works started with the installation of a geotextile earthworks separator and the placement of a 1.0m thick drainage layer, Plate 3. PVD's with a minimum cross sectional length of 100mm and width of 3mm, were installed on a triangular grid at 0.9m c/c spacing over the majority of the site, Plate 4. In areas of the site where obstructions were expected, pre-drilling works through the unsorted fill layers were undertaken in advance of PVD placement, Plate 5. The drains extended to a maximum of 24m below working platform level, as this was the maximum depth that local sub-contractors could achieve. This was sufficient to reach the underlying Alluvial Clay over much of the site so it was considered sufficient to ensure treatment of the critical MDs.

Plate 2: Inclinometer with extendable steel casing

Plate 3: Earthworks separator and drainage layer placement

Plate 4: PVD installation in triangular grid

Plate 5: Pre-drilling to facilitate PVD installation

4 GROUND IMPROVEMENT PERFORMANCE REVIEW

4.1 Settlements and degree of consolidation

The magnitude of settlement over time was recorded at over 60 points located across the site area treated with traditional surcharging. Settlement curves vs time were plotted using data collected from rod and plate gauges, see Figure 2.

The resultant plots broadly exhibited "s" shaped curves with slow rates of settlement during installation of the drains, and rapid settlement during and soon after placement of the surcharge, steadily tailing off as consolidation neared design completion values. The total magnitude of settlement recorded at the markers varied considerably, ranging from about 0.15m to nearly 2.30m. This broad range is a reflection of the highly variable nature of the ground conditions found at the site.

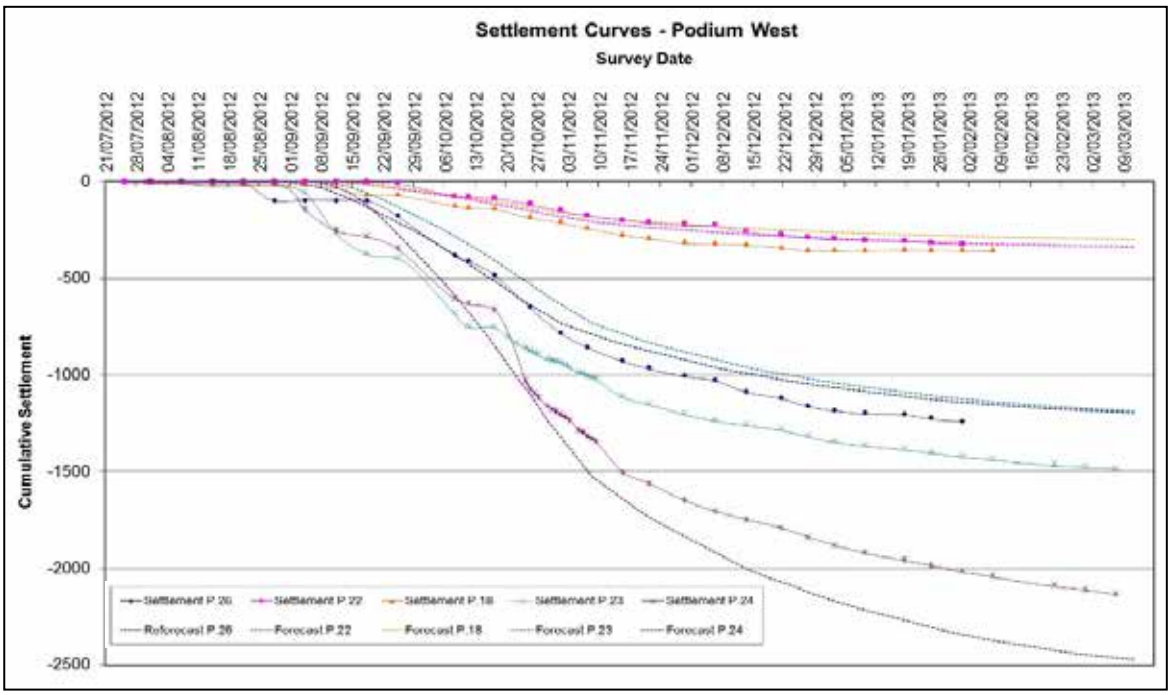

Figure 2: Settlement curves: predicted and monitored data

The trend of settlements in the underlying Maine Deposits, and the likely degree of consolidation that could be achieved, was predicted using the Asaoka Analysis method (Asaoka 1978). Selected analyses results are presented below in Figure 3. From these analyses, it was evident that the MDs along the line of the ELS had achieved 90% consolidation except in localised areas to the southeast of the site; where the predicted degree of consolidation was around 80%. Nonetheless, verification testing demonstrated that the required design strength had been achieved at the end of a 4-month consolidation period, see Section 4.2.

In certain areas where granular fill (unsorted and sand fill) overlaid the soft clays, the degree of consolidation was difficult to assess as a distinct trend, i.e. straight line, could not be defined. The *insitu* granular fill is likely to be partially densified due to surcharge placement.

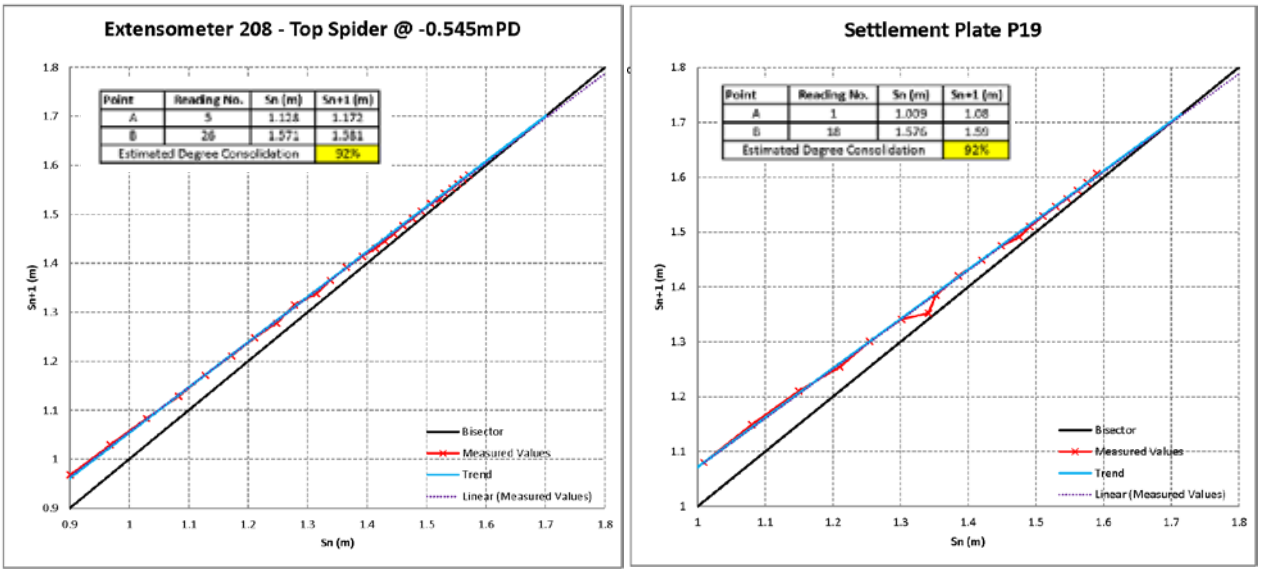

Figure 3: Determination of the degree of consolidation using the Asaoka analysis

Dilation effects of the densified granular fill may have meant that the plate gauges at top of the granular strata failed to register the effects of settlement at depth. This might suggest that an apparent "void" was created through the settlement of the underlying MDs which loosened the granular capping material by filling the "void". This phenomenon could possibly explain why some of the plate gauges records negligible settlement for a period and then suddenly settled by a significant amount. The difficulty of establishing a settlement trend made the assessment of the achieved degree of consolidation less reliable. To overcome this a broader assessment of adjacent areas was undertaken and was subsequently supported by the verification test results (see Section 4.2).

In general, the ground behaved reasonably in line with expectations in terms of predicted settlements and the time taken to achieve design consolidation values.

4.2 Verification testing

Verification testing comprised *insitu* vane shear testing along the line of the future ELS, at about 45m centres at over 30 locations and at depth intervals of 2m within the clay layers. These tests were conducted as close as possible to the existing boreholes so that the stratigraphy could be estimated accurately for testing purposes. Test results were corrected using a factor of 0.9 as suggested by Bjerrum (Bjerrum 1972) in conjunction with PI values.

In general, over 85% of all tests completed indicated that the minimum design strength requirement, 25+1.5z kPa, had been achieved. Two example plots are shown below in Figure 4.

The results marginally below the design line were assessed on a case by case basis. During the review stage it was found that there would be no adverse impacts to future design packages.

A summary comparison of the *insitu* vane shear testing results obtained within the clay layers and for adjacent boreholes, which were undertaken pre-ground improvement works (2011) and during the verification testing (2013), is shown below in Figure 5. It is evident that the MD had gained strength after surcharging.

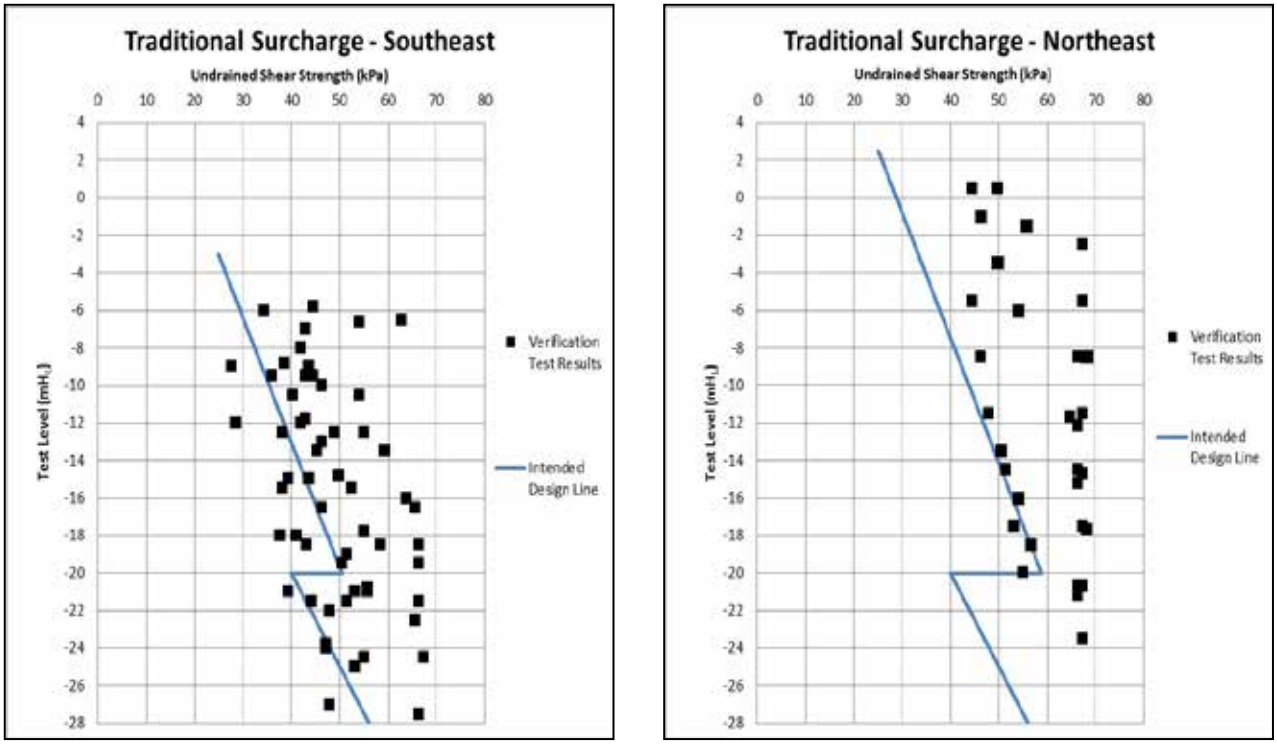

Figure 4: Verification testing results and intended ELS design line

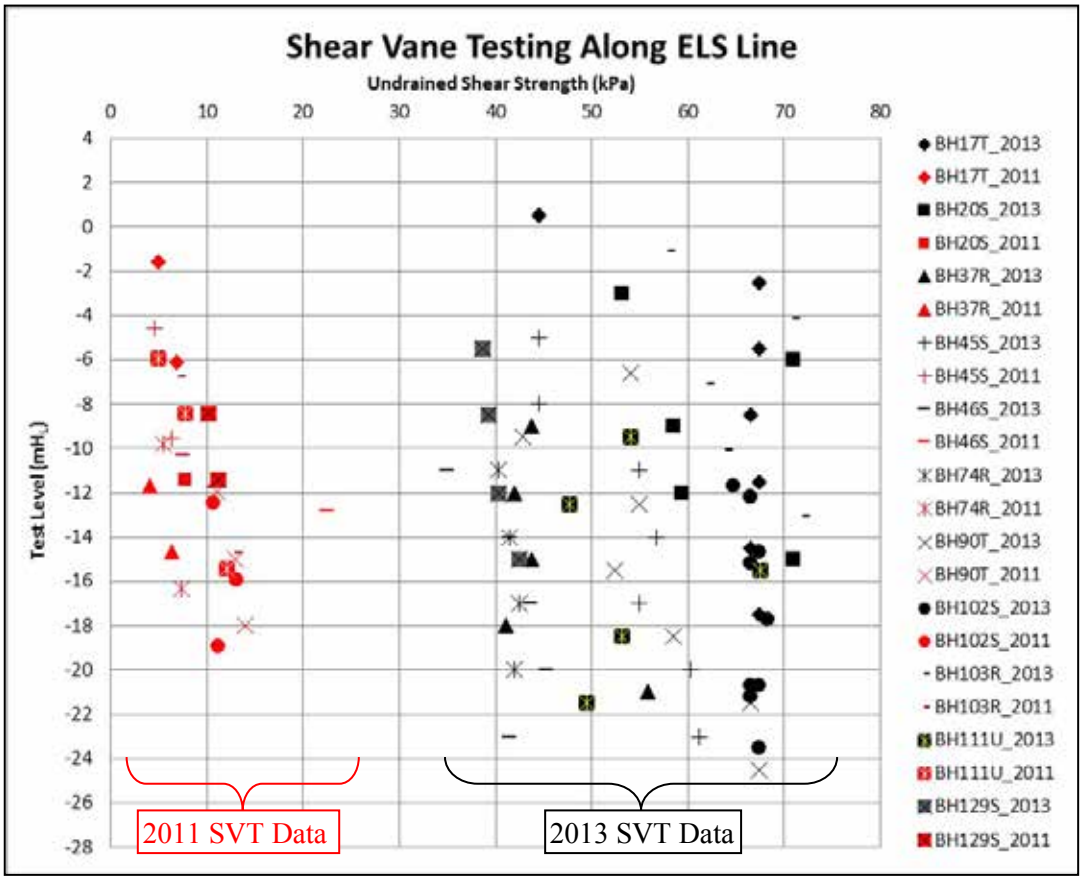

Figure 5: Comparison of undrained shear strength before and after the GI works

5 CONCLUSIONS

Ground improvement by means of PVDs together with surcharge preloading was carried out between June 2012 and March 2013 for the majority of the site. Generally, the ground behaved in accordance with expectations in terms of predicted settlement and time taken to achieve consolidation. This has been verified using the Asaoka Analysis method, based on monitoring results obtained from rod and plate gauges and extensometers. Although it was more difficult to predict settlement trends in areas of granular fill overlying MDs, best efforts were made to assess the achieved degree of consolidation. This was accomplished by reviewing the available data and comparing ground responses in adjacent areas, which was subsequently supported by the verification test results. These *insitu* shear vane tests, undertaken along the ELS perimeter, confirmed that the required design strength had been achieved for approximately 85% of all tests and that the undrained shear strength of the MDs was substantially improved. Therefore, it was concluded that the GI scheme had been successfully executed and achieved the design target requirements.

REFERENCES

Asaoka, A. 1978. *Observational procedure of settlement prediction. Soils and Foundations*, 18 (4): 87-101.

Fung, A.K.L., Foot, R., Cheung, R.K.H. & Koutsoftas, D.C. 1984. Practical conclusions from the geotechnical studies on offshore reclamation for the proposed Chek Lap Kok Airport. *Hong Kong Engineer,* 12(6): 17-26.

Skempton, A.W. 1957. Discussion on the planning and design of the New Hong Kong Airport. *Proc. Inst. Civil Engrs.*, 7:305-307.

Bjerrum, L. 1972. Embankments on soft ground. State-of-the-Art Report, *ASCE Specialty Conference on Performance of Earth and Earth-Supported Structures*, *June 11-14, Lafayette, Ind.*, 2: 1-54.

Jet Grouting Trial in Marine Environment

L.W. WONG
SMEC Asia Ltd, Hong Kong

ABSTRACT

Case histories on jet grouting on land and in marine environment have been conducted. The jet grout columns formed are 2 m in diameter and 10 m in depth below the seabed level. Ground movements due to jet grouting and the volume of return slurry were recorded. The extent of ground movements was found to be proportional to the distances to the centres of the jet grout columns. The magnitude of ground heaving could be related to the volume of the cement grout injected. The uniaxial compressive strengths of the jet grout columns, ranging from 1.1 MPa to 9.5 MPa, could be related to the cement content injected.

1 INTRODUCTION

Majority of the land reclamations in Hong Kong adopted the conventional method of removing the soft marine clay prior to constructing seawalls or placing fill materials. With the shortage of disposal sites, it has become more and more important to explore alternatives in dealing with marine clay other than the aforesaid conventional method. Ground treatment techniques such as sand drains, deep cement mixing, stone columns or sand compaction piling for strengthening the soft marine clay have been mentioned in Port Works Design Manual (Civil Engineering Office 2003) as potential alternatives.

During the construction of a reclamation project in Hong Kong, an alternative proposal for using jet grouting to strengthen the soft marine clay was critically studied. The seawall enclosing the reclamation area could be founded directly on the strengthened seabed. Dredging and disposal of marine clay and backfilling the trench with rock fill would become unnecessary. In order to prove the suitability of jet grouting, optimize the grouting parameters, verify the strength of the jet grout columns and to assess the ground movement control measures, two trial panels, one on-land and one in marine environment, were conducted. Results of the jet grouting trials are presented in this paper for future design and implementation reference.

2 JET GROUTING SYSTEM

The installation procedures for jet grout columns (JGC) have been described by Kauschinger & Welsh (1989) and Miki (1985). In general, the jet grouting process comprises 2 stages, the hole-reaming and the grouting stages. During the hole-reaming stage, the rotating monitor is lowered downward into the ground by breaking the surrounding soil with the water-jet sheathed with compressed air. When the monitor is lowered to the design depth, the cement grouting stage could commence. Water is then replaced with cement grout for injection. The monitor is withdrawn gradually upward from the bottom of the hole. By rotating the monitor the grout mixes with the pre-cut soil in-situ and a JGC is formed.

The Ultra Jetting System, a double-fluid system that utilizes compressed air, water and cement grout was used for the jet grouting trials. As shown in Fig. 1, three water-jets are spraying at the tip of the auger stem. The diameters for the flight auger and for the stem are 400 mm and 180 mm respectively. A pair of horizontal jetting nozzles, mounted at a radial distance of 150 mm to the axis of the stem, is located at approximately 1 m above the tip of the auger stem. The third nozzle, ejects fluid at an inclination of about 25^{o} to the horizontal, is located at about 0.8 m above the tip of the stem. The diameters of all these 3 nozzles are 2.8 mm. During hole-reaming the upper pair of nozzles injects water and compressed air while the lower inclined nozzle conveys only water. In the grouting stage water is replaced with cement grout. The upper nozzles inject cement grout sheathed with compressed air and the lower inclined nozzle injects cement grout without the compressed air sheath.

Figure 1: The nozzles mounted at the tip of the auger stem

3 SITE A – LAND TRIAL

3.1 Ground conditions at Site A

Site A for the on-land trial is located at the southern rim of the Yuen Long Basin, northwest Hong Kong. The subsoil is composed of 1.5 m of fill overlying the alluvial clay and the alluvial sand layers that underlain by completely decomposed granodiorite at the depth of 13.5 m. The groundwater level is encountered at 2.5 m depth. The soil profile is depicted in Fig. 2.

The alluvial clay layer located at the depths from 1.5 m to 6 m is composed of light grey and yellowish brown sandy clay. The *N* values increase with depth from 3 to 8. The alluvial sand layer encountered at the depths from 6 m to 13.5 m is composed of medium dense, yellowish brown, medium to coarse sand. There are some sub-angular gravel size quartz grains at the depths from 9 m to 13.5 m. The *N* values for the alluvial sand layer range from 6 to 15.

3.2 Jet grouting parameters

Three isolated jet grout columns, numbers A1 to A3, were installed at Site A. As depicted in Fig. 2, the depths of the toes of the JGCs vary from 5 m to 12 m. Due to bursting of the grout pipes, cement grout injection for JGC A1 terminated at the depth of 10.5 m. The grouted lengths for JGCs A1 to A3 range from 1.5 m to 4 m.

The jet grouting parameters adopted in the trial at Site A are summarized in Table 1. The pressures for injecting water and cement grout were 14 MPa and 28 MPa to 30 MPa respectively. Compressed air was applied at the pressure of 0.7 MPa with the flow rate of 10.6 m^3/min. The monitor revolved at 3 rpm and

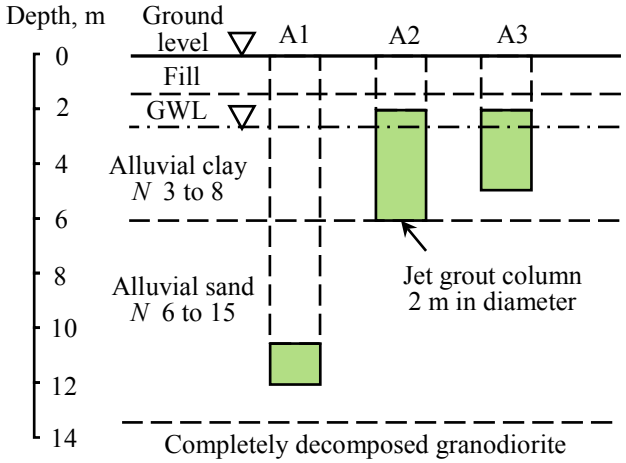

Figure 2: Section for jet grout columns at Site A

Table 1: Jet grouting parameters for the trial at Site A

Stage	Soil type	Water/Cement grout pressure MPa	Flow rate litre/min	Rotation speed rpm	Advance/ Withdrawal speed min/m	Theoretical cement content kg/m^3
Hole reaming	Alluvial clay	14	400	3	4	-
Grout injection	Alluvial clay	28 ~ 30	225	9	11	590

9 rpm in the hole-reaming and in the grout injection stages respectively. The cement grout had the mix proportion of water/cement ratio of 1 to 1 (in weight). The cement content in 1000 litre of grout is 750 kg.

The volume of the cement grout injected is the product of the injection rate and the withdrawal speed of the monitor. In the estimation for the theoretical cement content in a JGC, the target diameter of 2.0 m has been adopted. During the trial, specimens of water, fresh cement grout and return slurry were collected for flow consistency tests using the flow cone. The cement grout injected in the grouting stage had the flow time of 8.9 sec, which is comparable to that for water. The return slurry generated in the cement grout injection stage was so viscous that it did not pass through the flow cone.

3.3 Volume of return slurry

During the installation of JGC A3, it was observed that the return slurry emerged steadily from the grouthole. A sump pit was excavated to measure the volume for return slurry for JGC A3 in the hole-reaming stage. In the cement grouting stage the return slurry accumulated on the ground surface. As shown in Fig. 3, the heap of return slurry for JGC A3 had the geometry of a truncated cone, which had the base and the top diameter of 6.2 m and 2 m respectively, with a height of 0.8 m.

The results of return slurry measurements are summarized in Table 2. The volume of the return slurry (V_{sl}) emerged from the grouthole is related to the volume of the injected fluid (V_{fl}). As presented in Table 2, the V_{sl} / V_{fl} ratio in the hole-reaming stage was 0.53. In the grout injection stage, the V_{sl} / V_{fl} ratio was 0.95.

Table 2: Return slurry generated by the jet grouting process at Site A

Jet grout column no.	Reaming/ grouting fluid	Depth of grouthole m	Fluid injected V_{fl} , m^3	Volume of return slurry V_{sl} , m^3	Ratio of return slurry V_{sl} /V_{fl} , m^3
A3	Water	5	8.1	4.3	0.53
A3	Cement grout	2 ~ 5	12.3	11.7	0.95

3.4 Performance of jet grout columns

The upper portion of JGC A2 was exhumed on the seventh day after its installation. As marked with the red circle in Fig. 4, the target diameter of 2000 mm at the depths below 2 m was formed. At the depth above 2 m, the JGC had the diameter of about 900 mm. This column with a smaller diameter was formed by the hardened return slurry left in the grouthole. It was observed in the hole-reaming and in the grout injection stages that

Figure 3: Return slurry deposited at jet grout column A3

Figure 4: Exposed jet grout column A2

compressed air escaped from the perimeter of the well of slurry at the radial distances of about 450 mm and 1000 mm respectively from the hole centre.

Nine core holes, located at the radial distances of 0 m, 0.5 m and 0.8 m from the centres of the JGCs, were drilled at each jet grout column. Twenty-one core specimens of 78 mm in diameter were collected for uniaxial compression tests. A set of 5 cube samples of fresh cement grout was prepared in the moulds of 100 mm in size. The 28-day uniaxial compressive strengths, σ_c, of the JGCs range from 2.2 MPa to 7.6 MPa, with an average of 3.7 MPa. The average 28-day σ_c value for the cube samples of hardened cement grout is 17.5 MPa.

4 SITE B - MARINE TRIAL

4.1 Ground conditions at Site B

Site B for the marine trial is located at the northern shore of Hong Kong Island. As depicted in Fig. 5, the ground investigation drillholes TC1 and S10 show that the subsoil comprise the Holocene marine deposits of the Hang Hau Formation of 6 m in thickness underlain by completely decomposed granite (CDG). The alluvial sand layer of the Chek Lap Kok Formation is absent at the trial area. The bedrock of Granite Grade II is located at the level around -30 mPD. The cone resistance (q_c) values of the marine deposits are less than 0.3 MPa. The upper and the lower portions of the CDG stratum mainly comprise yellowish brown sandy to clayey silt and silty fine to medium sand respectively. The *N* values for the upper and the lower portions of CDG range from 6 to 10 and from 10 to 150 respectively. The seabed level is approximately -8.0 mPD (metre above Principal Datum). The mean sea level is 1.2 mPD.

4.2 Marine trial

A temporary platform of 8 m by 8 m was erected next to the shoreline to support the jet grouting machine as depicted in Fig. 6. A silt curtain surrounding the platform was installed down to the seabed level as the barrier for maintaining the water quality outside the trial area. A blanket of gravel layer of 700 mm in thickness underlain by a sheet of geotextile was laid on the seabed to provide additional overburden pressure in the trial area. As depicted in Fig. 7, six JGCs having the equilateral triangular spacing of 1730 mm were installed. Figure 8 shows that the JGCs of 10 m in length encountered marine clay and CDG in the upper and the lower portions respectively. These JGCs were installed in the period between 22 April and 28 May.

Due to machine breakdown in the grout injection stage, the cement grouting process was not fully implemented at JGCs B1, B3 and B6. The groutholes were abandoned and the reaming process for these JGCs repeated on the subsequent days. Only the bottom-most 1 m was grouted at JGC B1. For JGC B3, the portion from the depths of 5 m to 8 m below seabed was not injected with cement grout.

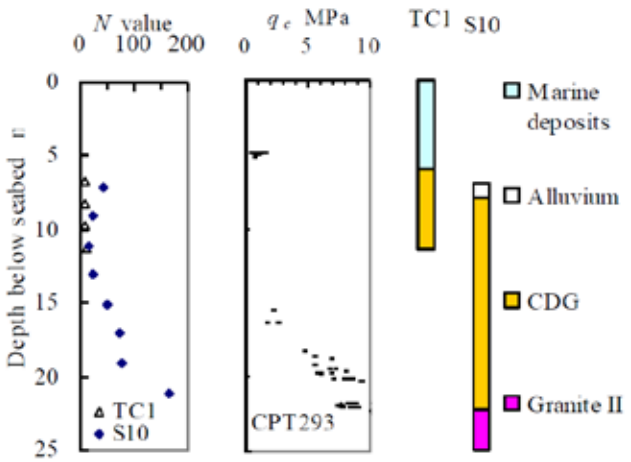

Figure 5: Typical subsoil condition at Site B

Figure 6: Marine trial at Site B

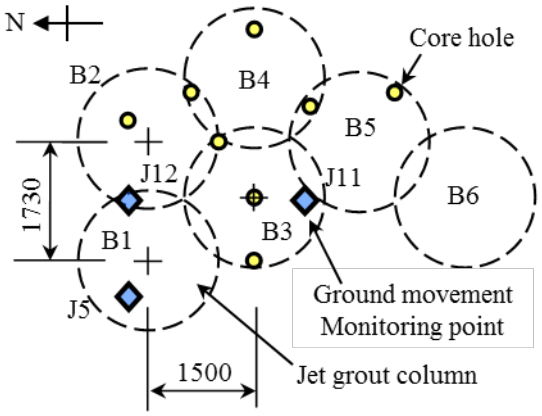

Figure 7: Layout of jet grout columns at Site B

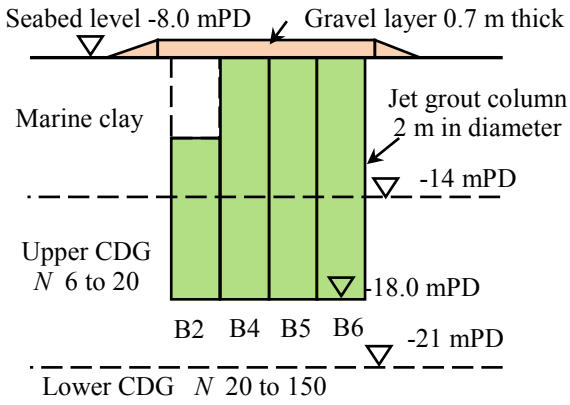

Figure 8: Jet grout columns at Site B

Twenty ground movement monitoring points, arranged at a rectangular grid pattern, were marked on the temporary platform. The seabed levels were monitored by chain sounding at these points prior to and after installation of each JGC. Eight core holes were drilled 4 weeks after completion of the jet grouting trial. As shown in Fig. 7, two of the core holes were within the radial distance of 0.5 m to the centres of the JGCs. The remaining 6 core holes, having the radial distances of 0.8 m to 1.0 m to the centres of the JGCs, were deployed around the edge, in the overlapping zone or at the intersecting point between the JGCs.

4.3 Jet grouting parameters at Site B

The jet grouting parameters adopted in the marine trial are summarized in Table 3. The pressures for injecting water to pre-cut the marine clay and the CDG strata were 10 MPa and 20 MPa respectively. Cement grout was injected at the pressures of 30 MPa and up to 40 MPa in marine clay and in CDG respectively. Compressed air was applied at the flow rate of 10.6 m^3/min with the pressure of 0.7 MPa. The monitor revolved at the rotation speed of 5 rpm in the hole-reaming and in the grout injection stages. Cement grout had the mix proportion of water/cement ratio of 1 to 1 (in weight). The fresh cement grout injected in the grouting stage had the flow time of 8.8 sec, which is comparable to that for water. Since grouting was conducted in submerged condition, the return slurry was not collected for viscosity measurement.

Table 3: Jet grouting parameters for the trial at Site B

Stage	Soil type	Water/Cement grout pressure MPa	Flow rate litre/min	Rotation speed rpm	Advance/ Withdrawal speed min/m	Theoretical cement content kg/m^3
Hole reaming	Marine clay	10	100 ~ 150	5	0.9 ~ 1.2	-
	CDG	20	160 ~ 200	5	2.7 ~ 2.9	-
	CDG	20	150 ~ 190	5	3.5	-
Grout injection	Marine clay	30	200	5	11.0	490 ~ 560
	CDG	40	220 ~ 285	5	11.5	600 ~ 780
	CDG	35	210	5	12.0	620 ~ 680

4.4 Volume of return slurry

At the marine trial at Site B, the volumes of the return slurry generated from each JGC are estimated from the heaving profile of return slurry, which are inferred from the results of seabed monitoring. The heaving profiles of return slurry for JGCs B4 and B5 are presented in Fig. 11. The estimated volumes of return slurry are summarized in Table 4. Comparing the volumes of return slurry with the fluid injected for JGC B4 and JGC B5, the V_{sl}/V_{fl} ratios range from 0.95 to 0.99. The low V_{sl}/V_{fl} ratio of 0.17 for JGC B2 could be attributable to the termination of cement grouting at the depth of 3.5 m below seabed. Some of the return slurry had to fill up the un-grouted portion before it emerged to the seabed surface.

It is observed that the core specimens recovered from the 8 core holes at Site B differ in colour between the upper and the lower portions. These cores preserved the colour of their parent materials. Orange and grey jet grouted cores were recovered in the CDG and in the marine clay strata respectively. The boundary of colour changing was located at the levels varying between -10.2 mPD and -13.0 mPD, with an average of -11.2 mPD. As shown in Fig. 8, the CDG stratum is encountered at -14.0 mPD. The 2.8 m rising, from -14.0 mPD to -11.2 mPD, of the CDG boundary in the cores is the positive evidence on generation of surplus return slurry. Since the toe levels of the JGCs were located at -18.0 mPD, the JGCs in CDG expanded from 4.0 m to 6.8 m in length. The inferred percentage of return slurry was about 70 % of the injected fluid.

The V_{sl} / V_{fl} ratio ranging from 70 % to 100 % estimated at Site B is consistent with those reported in the literature. Kauschinger and Welsh (1989) and Ueki et al. (1996) reported return slurry of 30 % to 90 % of the injected fluid for jet grouting with the double-fluid and the triple-fluid systems.

Table 4: Return slurry generated in cement grouting stage at Site B

Jet grout column no.	Fluid	Depth of column m	Fluid injected V_{fl} , m^3	Volume of return slurry V_{sl} , m^3	Ratio of return slurry V_{sl} /V_{fl} , m^3
B2	Cement grout	3.5 ~ 10	17.2	3.0	0.17
B4	Cement grout	0 ~ 10	22.8	21.6	0.95
B5	Cement grout	0 ~ 10	27.7	27.4	0.99

5 GROUND MOVEMENTS OBSERVATION

5.1 Settlement and heaving on seabed

The seabed levels within the trial area at Site B were monitored by 20 monitoring points. These points were measured on the preceding day prior to grouting and then on the following day after grouting. The locations for 3 monitoring points, namely, J5, J11 and J12 are shown in Fig. 7. Compared with the initial readings taken prior to the grouting trial, the negative and the positive vertical displacements presented in Fig. 9 denote settlement and heaving of the seabed respectively.

The jet grouting operation commenced on 22 April. Figure 9 shows that the cumulative settlements as large as 740 mm, 1000 mm and 1640 mm were observed at the monitoring points J12, J5 and at J11 respectively. These settlements were attributable to disruption of the jet grouting operation at JGC B1 on 23 April and on 5 May. The largest cumulative settlement of 1640 mm was caused by installing JGC B3 on 21 May.

After JGC B1 was reamed to the depth of 10 m below seabed on 22 April, the cement grouting operation began. As soon as the pumping pressure as large as 40 MPa was applied for cement grouting, bursting of the grout pipes occurred. The jet grouting operation was terminated. It was observed that the auger stem was withdrawn to the platform level. JGC B1 was re-installed on 3 May. Hole-reaming to the depth of 10 m below

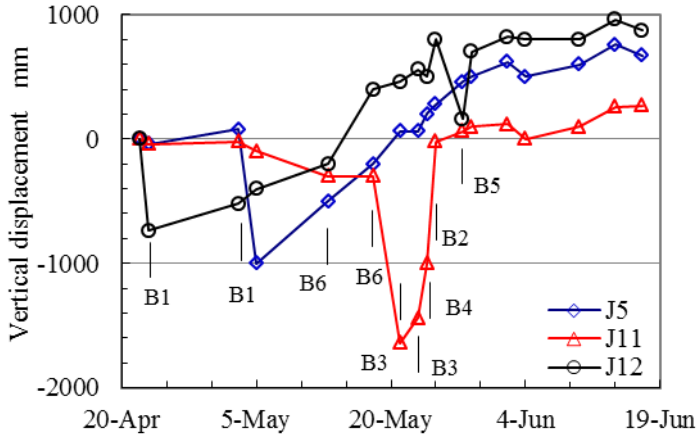

Figure 9: Ground movement monitoring at Site B

seabed was conducted again. After reaching to the bottom level, the cement grouting process however could not be conducted due to blockage of the mixing tank. Water jetting with compressed air continued for 2 hours until the blockage was repaired. Settlements of 740 mm and 1000 mm were observed at monitoring points J12 and J5 respectively on 23 April and on 5 May.

Similar to JGC B1, malfunctioning on the jet grouting system occurred on 18 May when JGC B3 was installed. The cement grout injection was not conducted in this JGC at the depths between 8 m and 5 m below seabed. Net seabed settlement of 1340 mm, from -300 mm to -1640 mm, was observed at the nearest monitoring point J11 on 21 May.

Figure 9 shows the occurrence of ground heave at Site B during the period between 18 May and 2 June. Unlike those conducted for JGCs B1 and B3, the grouting operation conducted after 22 May was less disruptive. Net seabed heaving of 980 mm, from the vertical displacement of -1000 mm to -20 mm, was observed at monitoring point J11 between 24 May and 25 May. Such heaving was caused by jet grouting for JGC B2. After completion of the jet grouting trial, cumulative heaving of 820 mm, 620 mm and 120 mm were observed at monitoring points J12, J5 and at J11 respectively on 2 June.

5.2 Settlement profiles

The settlement profiles of the seabed at Site B caused by installation of JGC B1 and JGC B3 are presented in Fig. 10, showing that the ground settlements were proportional to the radial distances to the JGCs. At the radial distance of 1 m to the centre of the JGC, the ground settlement was as large as 1340 mm.

As observed in the marine trial, the settlement of seabed was mainly attributable to withdrawal of the auger stem after the grouthole was reamed to the bottom level but cement grout injection was not conducted. In normal condition the wall of the grouthole would be supported by return slurry. Withdrawal of the auger stem due to malfunctioning of the jet grouting system at JGC B1 and JGC B3 created the holes of 10 m in depth below seabed. The seabed settlements were caused by close-in of the holes under earth and water pressures. The settlement profile could be expressed by the empirical Eq. 1:

$$S_v = \alpha H (r_o / r)^2 \quad (1)$$

where S_v is the ground settlement occurring at the radial distance r, r_o is the radius of the grout hole, H is the depth to the toe of the JGC below seabed level and α is an empirical factor.

The α value has been determined by fitting Eq. 1 with the settlement profiles summarized in Fig. 10. As described in Section 3.4 and shown in Fig.4, the grouthole formed by soil pre-cutting with water-jet had a diameter of 900 mm. The r_o value of 450 mm and the H value of 10 m are adopted in curve-fitting. Ignoring the data set of 40 mm settlement occurring at the radial distance of 0.5 m, an α value of 0.59 is obtained.

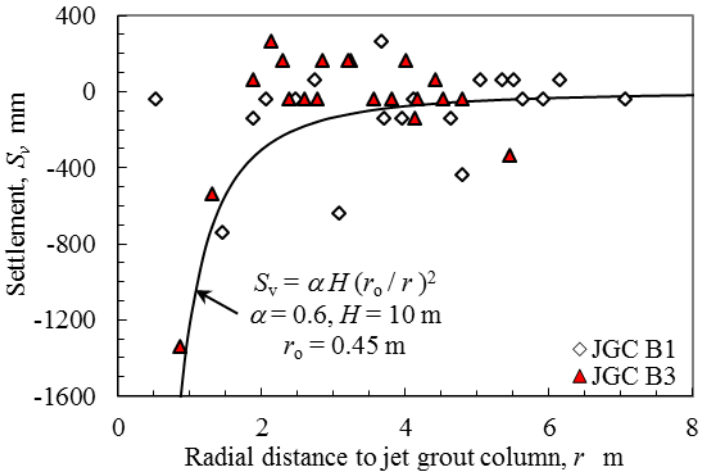

Figure 10: Settlement due to grouthole reaming

The correlation coefficient for the curve interpreted in Fig. 10 is 0.30. The weak correlation between the radial distances and the ground settlements is mainly attributable to the very limited number of data available within the radial distance of 1.5 m. The empirical Eq. 1 shall be applicable for the r / r_o ratios larger than 2.

5.3 Heaving profiles

The heaving of the seabed at Site B caused by the jet grouting operation for JGC B4 and JGC B5 are presented in Fig. 11. The magnitudes of heaving on seabed caused by installation of each JGC are inversely proportional to the radial distances to the JGCs. At the radial distance of 1.4 m to the centre of the JGC, the heaving of the seabed caused by JGC-B4 was as large as 980 mm.

As shown in Fig. 3, the heap of return slurry for JGC A3 had the geometry of a truncated cone. Based on this observation, the seabed heaving profiles for JGCs B4 and B5 are interpreted as conical surfaces. The inferred cone of return slurry for JGC B4 had the base and the top radius of 3.8 m and 1.4 m respectively, with a height of 0.96 m. The cone of return slurry for JGC B5 had the base and the top radius of 4.7 m and 3.3 m respectively, with a height of 0.55 m. The inclined surfaces of the return slurry had the angle of repose of about 21°. The volumes for the return slurry for JGC B4 and JGC B5 inferred from Fig. 11 are 21.6 m^3 and 27.4 m^3 respectively.

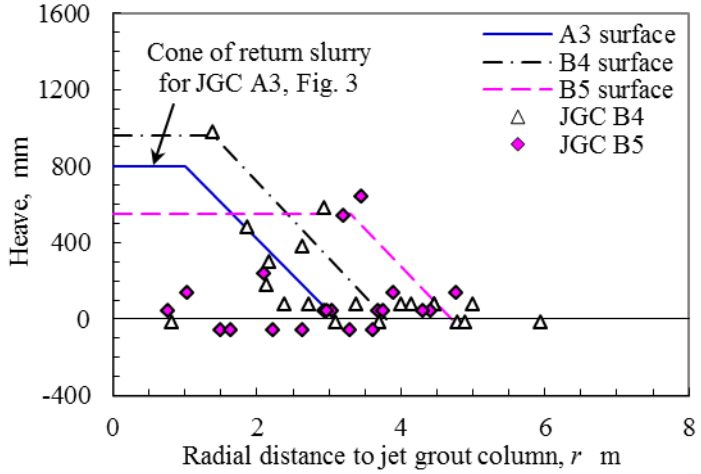

Figure 11: Heaving due to grout injection

6 STRENGTH OF JET GROUT COLUMNS

6.1 Uniaxial compressive strength

Eight core holes, located at the radial distances of 0 m, 0.5 m and 0.8 m from the centres of the JGCs, were drilled at Site B. Fifty-two core specimens of 78 mm in diameter were collected for uniaxial compression tests. Twenty-two point load index tests were conducted at regular intervals on the cores. A set of 5 cube samples of fresh cement grout were prepared in the moulds of 100 mm in size for compression testing.

Results of compression tests are presented in Figs. 12 and 13, which show the 28-day uniaxial compressive strengths, σ_c, of the JGC specimens collected from the central cores and from the outer cores respectively. There is the tendency of increase in σ_c values with depth. The σ_c values for the central cores, which have the radial distances within 0.5 m from the centres of the JGCs, range from 1.8 MPa to 7.5 MPa, with an average of 4.6 MPa. The σ_c values for the outer cores, which have the radial distances larger than 0.5 m from the centres of the JGCs, range from 1.1 MPa to 9.5 MPa, with an average of 5.3 MPa. The average 28-day compressive strength of the cube specimens of hardened cement grout is 24.5 MPa. The average σ_c value for the core specimens is approximately 20 % of that for the cube samples of hardened cement grout.

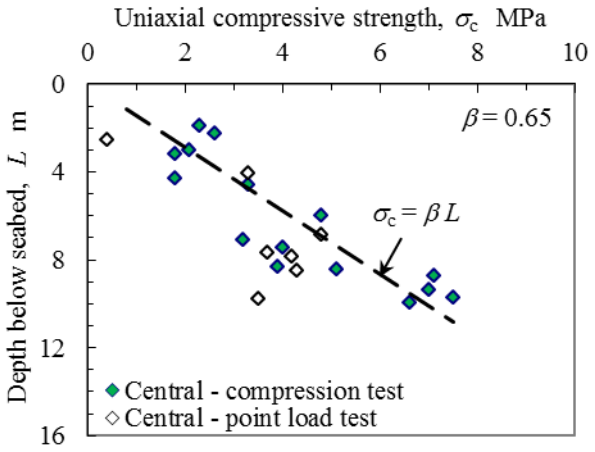

Figure 12: Compressive strength of central cores

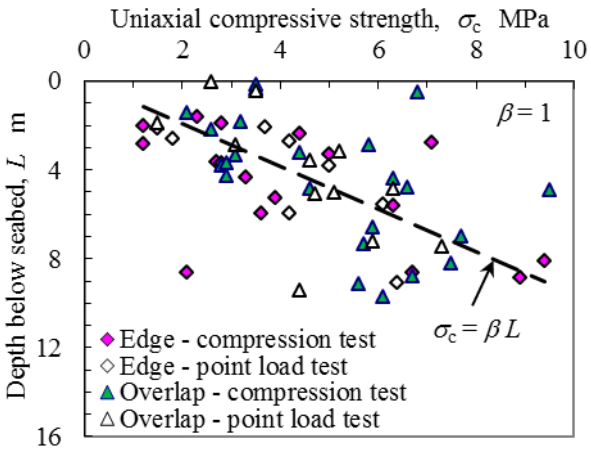

Figure 13: Compressive strength of outer cores

The point load index, I_p , of the grouted cores ranged from 0.14 to 0.66. The I_p values are correlated with the σ_c values. An empirical relationship between the σ_c and the I_p values could be expressed as:

$$\sigma_c = 11\ I_p \ \text{(in MPa)} \tag{2}$$

where σ_c is in MPa. The correlation coefficient for Eq. 2 is 0.31. Despite the weak relationship between the σ_c and the I_p values, Eq. 2 is adopted for estimating the σ_c values. Those σ_c values obtained from the compression tests and inferred from the point load tests are presented in Fig. 12 and Fig. 13. The trend of increase in σ_c values of the core specimens with depth could be expressed by the empirical Eq. 3:

$$\sigma_c = \beta L \ \text{(in MPa)} \tag{3}$$

where L is the depth of the core specimen below seabed in metre, β is an empirical factor and σ_c is in MPa.

The β values determined by regression analyses are 0.65 and 1.0 for the central cores and for the outer cores respectively. The correlation coefficients for the regression lines interpreted in Fig. 12 and Fig. 13 are 0.77 and 0.54 respectively. The correlation of the σ_c values with depths is strong for those of the central cores. Comparison between these two β values would indicate that the σ_c values for the central cores are about 2/3 of those for the outer cores. The larger in the σ_c values for the outer cores would likely be due to more effective mixing of cement grout with soil at the outer zone of the JGCs.

6.2 Relationship with cement content

The tendency of increase in the σ_c values with depth would be due to richer cement content of the soil-cement mixture in the lower portion of the JGCs. Figure 8 shows that the JGCs located at the depths below 6 m are installed in CDG. As summarized in Table 3, the theoretical cement contents for the JGCs in CDG range from 600 kg/m^3 to 780 kg/m^3 and those for the JGCs in marine deposits range from 490 kg/m^3 to 560 kg/m^3. The theoretical cement content of 590 kg/m^3 for the JGCs in alluvial clay is presented in Table 1.

Figure 14 shows the relationship between the theoretical cement contents and the average σ_c values of the outer cores formed in marine deposits, alluvial clay and in CDG. The trend of increase in σ_c value with cement content could be expressed by the empirical Eq. 4:

$$\sigma_c = 0.0067\ C_w \ \text{(in MPa)} \tag{4}$$

where C_w is the theoretical cement content of the JGC in kg/m^3 and σ_c is in MPa. It is noted that in the regression analysis for Eq. 4, the data set with the largest σ_c value of 7.3 MPa is ignored.

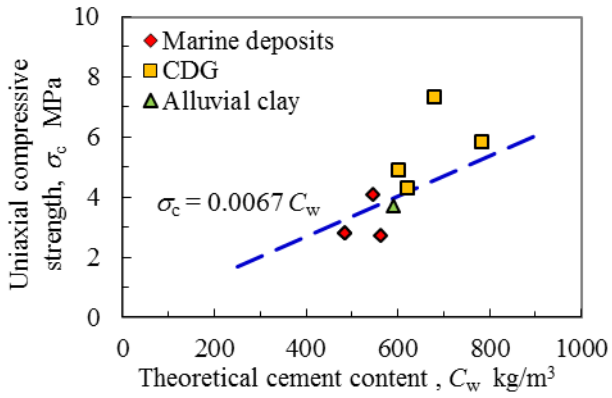

Figure 14: Relationship between cement contents and uniaxial compressive strengths of jet grout columns

Due to the very limited number of field data, Eq. 4 is indicative only to show the general trend of increase in compressive strength with cement content. The empirical factor of 0.0067 shall be reviewed when more case histories are available. As the σ_c values are proportional to the cement contents of the soil-cement mixture, they may not be related to the types of soil encountered by the JGCs.

7 CONCLUSIONS

A jet grouting trial programme comprising on-land and marine trials was conducted. Based on results of ground movement monitoring and on compression testing of the grouted specimens, the following concluding remarks could be drawn:

(1) Since jet grouting utilizes compressed air, water and cement grout for hole-reaming and for in-situ soil/cement mixing, it generates large volume of return slurry. The volume of return slurry would be 70 % to 100 % of the volume of the fluid injected.
(2) The return slurry emerged from the grouthole is so vicious that it accumulated on the ground or on the seabed surface, giving an apparent phenomenon of ground heave.
(3) Mainly attributed to withdrawal of the auger stem without backfilling with grout materials, ground settlements would occur in the hole-reaming stage. In order to minimize ground settlements caused by jet grouting, the groutholes shall be properly backfilled with cement grout.
(4) The uniaxial compressive strengths of the jet grout columns are proportional to the cement contents of the grout injected.

The generation of large amount of return slurry by the jet grouting process would be one of the considerations for design and implementation of jet grouting especially in marine environment. This case history on land and marine trials provides useful in-sights into the mechanism of ground movements caused by jet grouting.

REFERENCES

Civil Engineering Office 2003. *Guide to design of seawalls and breakwaters. Port Works Design Manual Part 4*. Civil Engineering Office, Civil Engineering Department, The Government of the Hong Kong SAR.

Kauschinger, J.L. & Welsh, J.P. 1989. Jet grouting for urban construction. *Proc. of the 1989 Seminar, Design, Construction and Performance of Deep Excavations in Urban Areas*, MIT.

Miki, G. 1985. Soil improvement by jet grouting. *Third Int. Geotechnical Seminar, Soil Improvement Methods*, *NTI, Singapore*, November, 45-52.

Ueki, H., Hasegawa, K., Suzuki, K & Bessho, M. 1996. Development of a high-pressure jet mixing method for displacement reducing. *Grouting and Deep Mixing, Proc. of IS-Tokyo'96, the 2nd International Conference on Ground Improvement Geosystems*, *Tokyo*, May, 767-772.

Reclamation over Soft Sediments with PVDs – Lessons Learnt

Suraj De Silva
SMEC Asia Ltd., Hong Kong

ABSTRACT

Many non-dredged reclamations, where the soft alluvial and marine clays & silts (marine muds) are left in-place and filled over have been carried out in Hong Kong. The marine mud in these reclamations has been improved by accelerating consolidation using the most common improvement technique - prefabricated vertical band drains (PVDs) and a wealth of experience has been gained by the geotechnical practitioners. This paper presents the experience gained from these reclamations here in Hong Kong and elsewhere, where PVDs have been used. The paper draws upon the lessons learnt from these experiences, and of others from published literature, and suggests how future reclamation design and construction practice can be further improved in order to minimise long term settlements, lateral movements and instabilities when PVDs are used. The paper focuses on issues related to design, installation and performance of prefabricated vertical band drains, and their testing requirements and suggests testing regimes for PVDs, considerations during design, PVD selection, and installation. The paper also suggests contingencies to be built into contracts when using PVDs.

1 INTRODUCTION

Since the establishment of Hong Kong in 1841, reclamation projects had created extensive developable land along the shoreline of the territory. The techniques of reclamation used in Hong Kong have changed since the early days. By the 1970's, the technique of drained reclamation, by installing prefabricated vertical drains (PVDs) into the marine mud was used to accelerate consolidation. The effectiveness of the drained method using PVDs was demonstrated by the construction of the test embankment at Chek Lap Kok in the early 1980s; and many reclamation projects using the drained technique was completed satisfactorily since. Cases history of some important drained reclamations using PVDs are discussed in the GEO Report No 93, dated 1997. The rate of reclamation in Hong Kong decreased in the last 16 years due to the public's preference to maintain the current shorelines and due to environmental considerations.

Figure 1 presents photographs of some distress caused to structures as a result of on-going settlement of reclamations. The on-going settlements have ranged from about 400mm to 1000mm over a period of 10 years where PVDs were used without surcharge. At some locations settlements of up to 2.2 m were experienced over a period of about 20 years.

Figure 1: Damage caused by on-going post reclamation settlement

2 TREATMENT OF MARINE MUD WITH PREFABRICATED VERTICAL BAND DRAINS (PVDs)

2.1 General

Prefabricated Vertical Band Drains (PVDs) are the most extensively used ground improvement method to accelerate the consolidation of marine muds and soft alluvial clays and silts in non-dredged reclamation in Hong Kong. The extensive use of PVDs is due to it being one of the most cost effective techniques of improving soft muds; the speed of installation; ease of securing plant to install; special know-how or training is not required of the plant operators. In the sections below the experiences and observations gained by using PVDs in the marine muds in Hong Kong are detailed, the lessons learnt are elaborated and from them the good practice when specifying, procuring, delivery, storage, installation, and when monitoring the progress of the consolidation are elaborated and recommendations for best practice identified.

2.2 Structure of PVDs

Generally most PVDs currently available in the market comprise a central core and an outer filter fabric that is wrapped around the core. Various PVD core profiles and photographs of PVDs are shown in Figure 2.

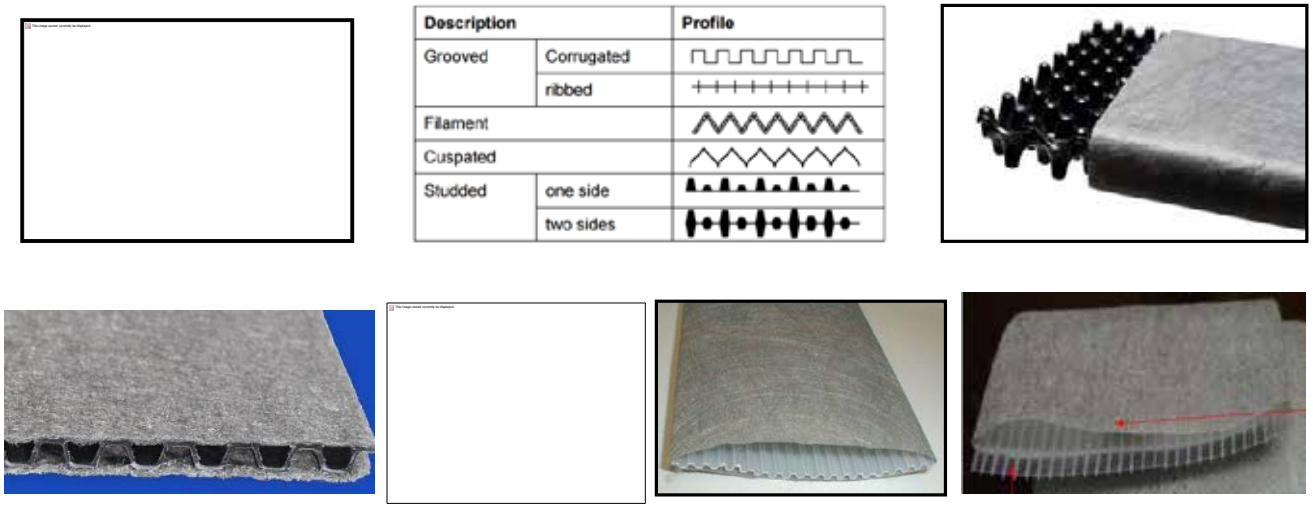

Figure 2: Various PVD core types

The width of PVDs is generally about 100mm and the thickness is generally about 3 - 5 mm. The choice of the band drain type, particularly the type of core is important when selecting the PVDs for a particular application. The aspects to be considered are, how flexible the PVDs are to bending and folding, the impact on core after bending/folding, the interaction between the core and the filter particularly when soil pressure is applied, the continuity of the drainage path along the core when bent/folded/spliced.

2.3 Rate of porewater discharge through PVDs

When consolidating very soft to soft marine muds, the vertical strain in the mud will be in region of the about 20% to 25%, for the fill thicknesses that are generally encountered in Hong Kong reclamations. Assuming the mud thickness is 15m, below a seabed elevation of -10mPD the settlement during reclamation will be about 3 – 4m; and 3 – 4m^3 of water will be discharged per square metre of reclamation area over the consolidation period - in about 6 to 9 months. This amounts to an average discharge rate of 11 to 22 litres/day. However, the rates of discharge at the initial stages of consolidation will be a few times higher than these rates. The volume of water discharge from one single band drain (assuming they are installed at 1.5 m centres) will be 25 to 50 litres/day,

or 0.29 to 0.58 x 10^{-6} m^3/s (or 9.12 - 18.2 m^3/year) as average rates. The initial rates of settlement will be about 3 to 4 times the average rate of settlement. Therefore, the discharge rates will be 1 x 10^{-6} m^3/s to 2.4 x 10^{-6} m^3/s (31.5 - 76 m^3/year) through one single band drain. The PVDs shall be capable of discharging water at these initial rates, to have no well resistance, and to achieve consolidation of the mud as predicted, while being subjected to large lateral confining stresses, bending and even twisting of the PVDs as the ground settles.

2.4 Lateral pressures imposed on PVDs

Assuming a seabed elevation of about -10 mPD, and a marine mud thickness of 15m, it can be shown that the total lateral pressure applied at the start of the reclamation is about 360 kPa at the middle of the layer, and about 460 kPa at the bottom of the layer assuming that the undrained shear strength values of 15 kPa and 25 kPa at the middle and bottom of the layer. If, say a 5m surcharge is placed these total lateral pressures will increase to 450 kPa and 550 kPa. Since the PVDs are installed rapidly, it is believed that the PVDs will be in an unsaturated state immediately after they are installed. Therefore, the total lateral pressure will be imposed immediately and this pressure will reduce as the PVD are saturated with the porewater entering the PVDs (note that due to the large pressure difference pore water will flow into the PVD very quickly upon installation, immediately after the initial application of total pressure). These pressures will then be reduced by the excess porewater pressure prevailing in the mud. These are large lateral pressures the PVDs will be subjected to and under these pressures the PVD cores can collapse or even close up significantly reducing the flow capacity. Figure 3 shows the impressions of the PVD core made on clay when subjected to effective lateral pressures of about 350 kPa. As it has made an accurate impression of the core, it is likely that the core was nearly completely closed due to the pressure. Moreover, if a ribbed type core is used the filter fabric will be stretched when forced into the core under the pressure (see sketch in Figure 3). The sharp corners of the ribbed structure of the core could also pinch or tear the filter fabric. The stretching, pinching and tearing of the filter will significantly change the filtering properties of the fabric to clay and silt particles; and will let the passage of fine clay and silt particles into the core causing the core to clog further.

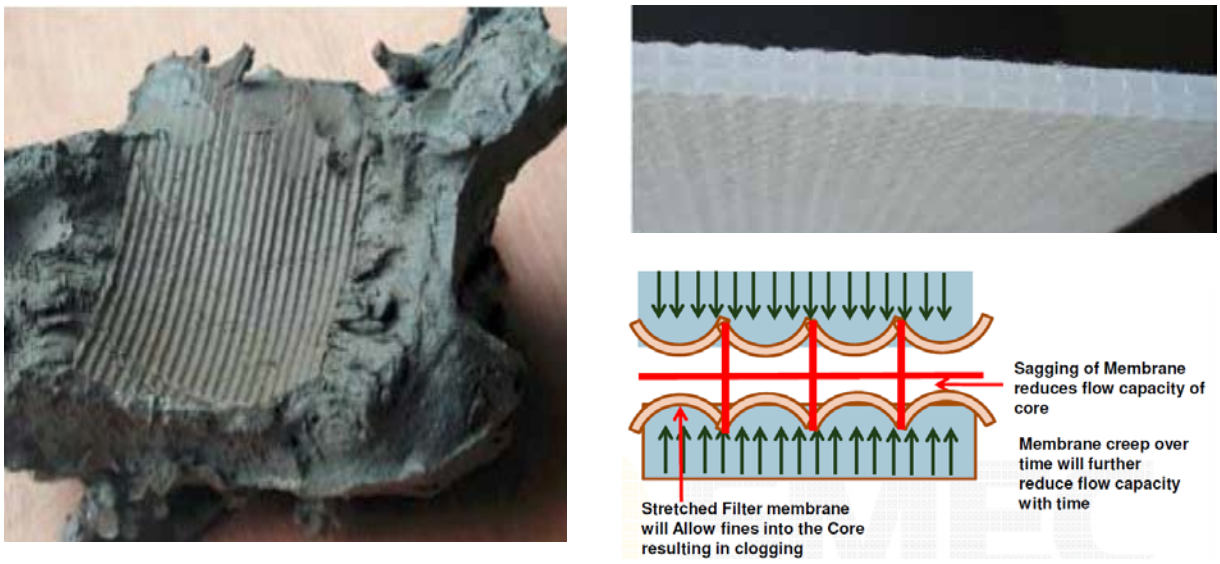

Figure 3: Impressions of PVD cores on mud due to high lateral pressures

2.5 Selecting PVDs with correct core type

The PVD core provides the conduit for the porewater that enters the core to be delivered to the drainage layer that is most often located at the top of the consolidating marine mud layer. Therefore, it is necessary to ensure that a conductive core is maintained throughout the whole of the consolidation period. As already explained in Section 3.4 above, if a ribbed core type PVD is selected for an application where the mud is very soft and large

fill height and surcharge load is to be placed resulting in large lateral pressures being imposed on the PVDs, the likelihood of the significant clogging of the PVDs will be high. Also such ribbed PVDs will not be very flexible and will not bend smoothly when large strains and settlements of the order of 3 - 5m occur. Hence, in such applications ribbed PVD core may not be very appropriate. Therefore, the PVD type and the PVD core type should be carefully selected with due consideration of all factors at site and the application.

2.6 Installation of PVDs

All PVDs should be installed to a specified depth or to refusal. The mandrel and anchor design are also important aspects of a PVD ground treatment assignment. They shall be such that the disturbance to the clay surrounding the PVD is kept to a minimum, thereby minimizing the smear zone around the installed PVD; and to ensure that the PVDs are installed as plumb as possible down to the bottom (else the drainage paths can be very large, particularly at the bottom). If the mandrel is not stiff enough they could bend as the stiffer/denser soils (such as dense sand lenses and layers) are encountered at depth while clay at the top is very soft. In Hong Kong, alluvial clay generally underlies marine mud, and a desiccated stiffer crust exists in the alluvial clay. The Engineer's specification generally requires that the PVDs are anchored 1m to 2m into the alluvium. If the mandrel is not stiff enough, the mandrel could bend under these pushing forces. Figure 4a shows a bent mandrel. Bent mandrels cause greater disturbance and smear zones in clay/silts. Mandrels come in two shapes rhombic and rectangular. See Figure 4b.

(a)

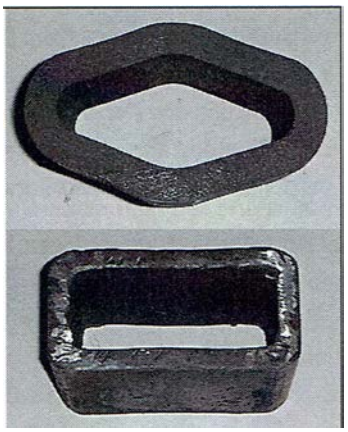

(b)

Figure 4: (a) A Bent Mandrel (b) Common cross-sections of mandrels (after Bo and Choa 2004)

The mandrel shoe cum PVD anchor shall also be designed with care to minimise the disturbance zone (the smear zone). The footprint of the anchor plate shall be as close as possible to that of the mandrel, but slightly bigger to ensure that mud and soil does not enter the mandrel. A V-shaped shoe/anchor plate is preferred as it could facilitate the penetration as well. An anchor plate that is too large compared to the footprint of the mandrel will form a void between the mandrel and the soil as the PVD is pushed, which will be immediately filled in with air (the inner space of the mandrel will be filled with air as the permeability of the clay is very low for any water to flow at the speed of penetration of the mandrel), and the volume of air trapped around the PVD after the mandrel is withdrawn will be larger. This air will be pushed out along the PVD as the soft marine mud squeezes in to close the void. Where the pressures are high the air will dissolve in the pore water but could be trapped as bubbles in the PVDs where the pressure is low at the upper reaches of the PVD. When the PVD (the core and the filter) is not fully saturated, the conductivity of the PVD will be less, affecting its performance. Figure 5 shows the time taken for saturation in a 1m length of PVD in an experiment. In actual field situation, it can take longer.

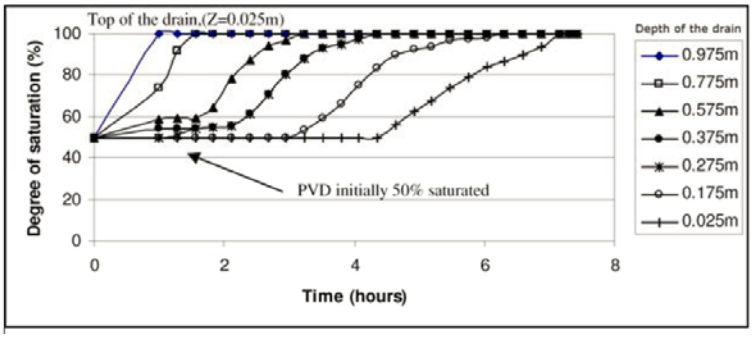

Figure 5: Laboratory experiment to demonstrate the time taken to saturate a 1m length of PVD (after Indraratne et al 2004)

2.7 Installation stresses and forces on PVDs

In addition to the stretching of the filter fabric caused by the structure of the core under lateral stresses, the PVDs are also subjected to stretching due to the forces imposed on it during installation. A photograph of a typical land based PVD installation rig is shown in Figure 6. When the marine mud layer is thick and the seabed is deep, the length of PVDs to be installed will be long. Considering a typical situation in Hong Kong, the length can be 30 – 35m. Therefore, to install them, if land based installation is opted for, will require a rig and a mandrel that is about 35 - 40m long. The PVDs, which are supplied to site on reels, are then mounted on the rig (see Figure 6) and the PVD is threaded around many rollers and then through the mandrel and an anchor plate or an anchor bar is attached at the point of exit from the mandrel. The mandrel is then pushed into the ground until the required installation depth is reached. Due to the inherent friction in the bearings on which the PVD reel is mounted, the rollers & guides and due to the acceleration when the mandrel is pushed tensile forces are imposed on the PVDs. Karunaratne (2003) measured the strain and the forces on a PVD during installation by attaching strain gauges. The results are shown in Figure 7. These measurements show that the maximum force is about 1000N during pushing of the mandrel. A force of about 600N is applied when the mandrel is withdrawn, and one of the strain gauges indicates that this force is locked-in in the PVDs. This could be due to the soil coming in contact with the PVD while the mandrel is being withdrawn. This indicates that he PVD and the filter fabric are permanently stretched longitudinally when in operation, particularly at their bottom end. As the surrounding soil settles, the vertical tensile strain in the PVDs will disappear along with tensile forces. Nevertheless, at the very initial stages, when the hydraulic gradient is at the largest, the PVDs are likely to be stretched and may allow clay and silt particles to get into the core. Therefore, when evaluating the performance of the PVDs, it is best that these actual site conditions are replicated to obtain the actual behavior and performance of the PVDs.

The PVD specifications normally require that the PVDs can withstand 1kN of tensile force and that the strains are less than 10%. The splices should also be able to withstand this force. Therefore, it is recommended that the splices are also checked before accepting the PVDs, and during construction. Another important consideration is the performance of the filter fabric after it is stretched. The AOS of the fabric, where an O_{95} value of 75μm is generally specified, will change when stretched and hence the filter characteristic will also change. If the change is significant the filter will allow clay and silt particles to get into the core and clog the core rendering the PVDs much less effective in discharging the porewater. Figure 8(a) shows the decrease of PVD discharge capacity when the PVDs are stretched by pulling them with a tensile force. Note that when 2.2 % of the ultimate tensile force is imposed, the flow capacity decreases by ½ and over time it will continue to decrease. Therefore, in the field during construction, it is important to ensure that the PVD rigs are well maintained. Particularly, all the relevant bearings of rollers and the mandrels are cleaned up regularly to minimize the tensile forces on PVDs and the consequential stretching of the PVDs.

Figure 6: The set-up at the land based PVD installation rig

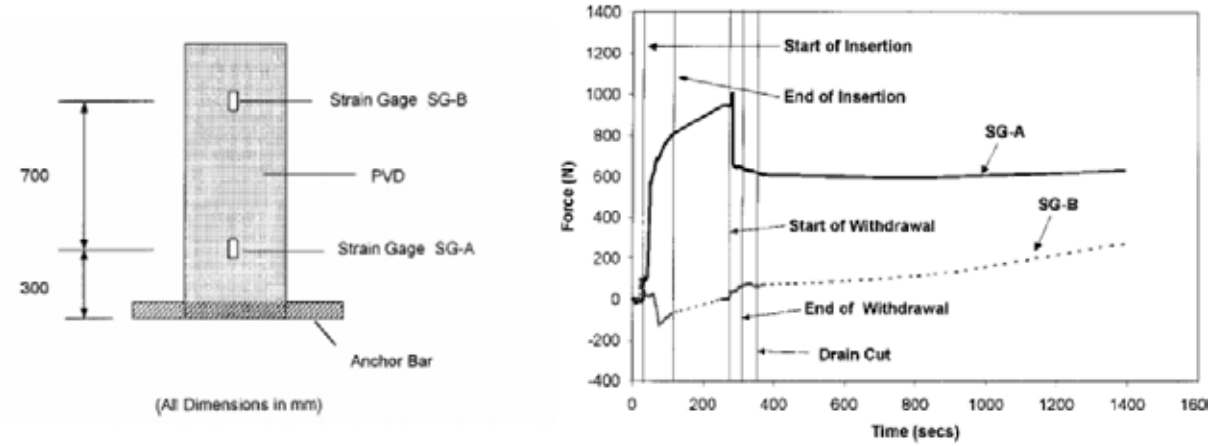

Figure 7: Measurement of tensile force on PVDs during installation and mandrel withdrawal (after Karunaratne et al 2003)

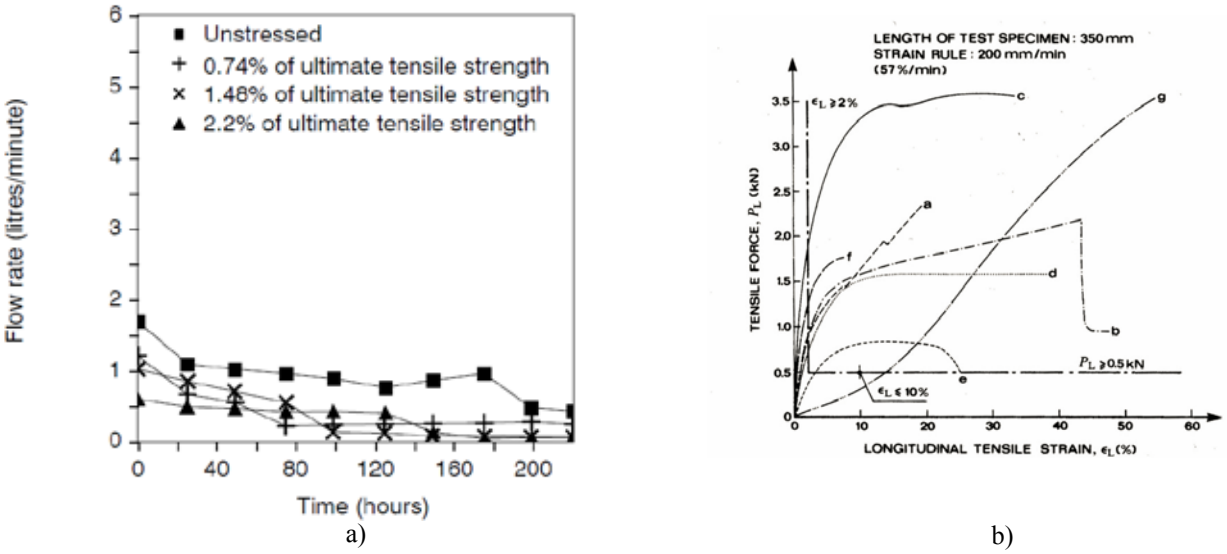

Figure 8: (a) Impact of tensile pulling force on discharge capacity of a PVD over time (extracted from Geosynthetics International, 1995 Vol 2 No.2. (b) Tensile force vs longitudinal strain of some typical PVDs

The tensile behaviour of some typical PVDs is shown in Figure 8(b). Note that most have an ultimate tensile capacity of about 1500N. If 600N is the locked in tensile force, it is 40% of the ultimate tensile strength and the discharge capacities could be less than that shown in Figure 8(a) above.

2.8 Tortuosity of PVDs and its impact

In Hong Kong's ground treatment context, as shown above, large settlements are expected to occur when reclaiming new land over soft marine muds. In the typical example considered above, the settlements are expected to be in the order of 3 - 4m. Moreover, as the water content of the marine mud is much higher when it is closer to the seabed, a larger proportion of this settlement will occur close to the seabed or close to the drainage layer at the top of the mud layer – the tortuosity of the PVDs will be much larger impeding the discharge. See Figure 9 showing a photograph of a bent form of a PVD extracted from a settling ground. Note the sharp bends in the folded PVD and the large number of them present. The PVDs is required to maintain flow across these bends over a period of more than 6 or even up to12 months (consolidation time depends on the PVD design – spacing and surcharge). Therefore, it is necessary to ensure that the core will not break under such bending and folding, and not block the flow. Also the filter will not tear and pinch letting fines to flow in and clog the core. It also demonstrates the importance of carrying out PVD flow tests under similar conditions – replicating the actual conditions that will be experienced on your site.

Figure 9: The bent shape of a PVD when subjected to large ground settlements (after Staplefeldt, T.)

2.9 Flow characteristics of PVDs under lateral confining stress

As can be seen from above many changes take place in a PVD when they are subjected to confining stress or pressures. The thickness of the PVD reduces and the space available to conduct water in the core reduces. Kamon et al (1994) has reported reductions of 55 – 90 % when subjected to confining pressures of 320kPa. However, the reductions depend on the PVD type and core type. Many PVD types were tested on 100mm x 100mm PVD sections using an hydraulic gradient of 0.5 and the results are shown in Figure 10 below. The results show that in wire mesh core type PVDs the reduction is more significant than in corrugated type cores.

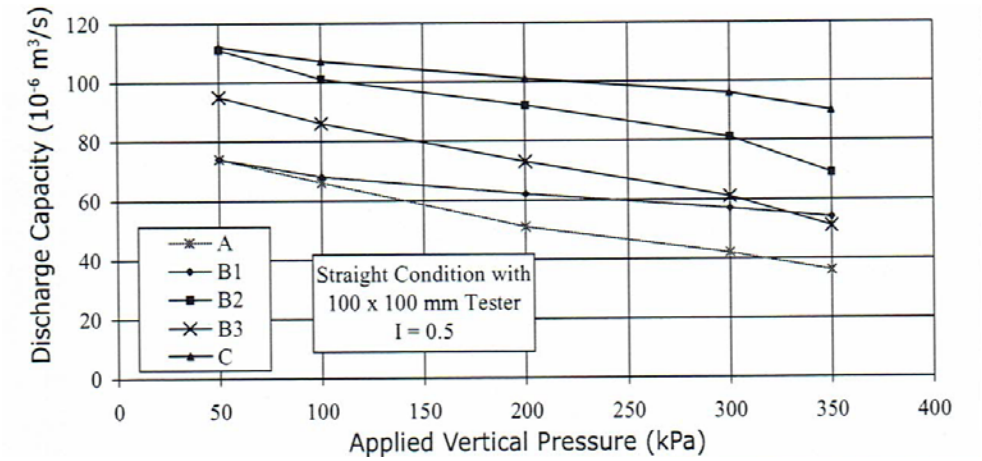

Figure 10: Tests showing the reduction in PVD discharge capacity, q_w, with confining pressure on various PVDs tested under a hydraulic gradient, i, of 0.5 (after Bo and Choa, 2004)

The above tests were conducted in a Straight Tester (no folds, bends or kinks in the PVD). Bergado (1994) has reported that a sharp bend can reduce the discharge capacity to 10% to 20% of the straight conditions. Some test results from Bergado (1994) are reported in Table 1 below. These results clearly demonstrate the significant effect bends, twists and folds have on PVD discharge capacity, and the importance of testing the PVDs under conditions that are most likely to be experienced by the PVDs at site when determining PVD discharge capacities. Test results have also demonstrated that the wire mesh type core PVDs have the most reduction when compared with corrugated core type PVDs.

Table 1: Reduction of discharge capacity of a PVD with bending, twisting and folding (after Bergado 1994)

Type of PVD Deformation	Discharge Capacity of PVD ($m^3/s \times 10^{-6}$)	Percentage Reduction from Non-deformed state (%)
Non-Deformed (Straight)	62	-
15% free bend	36	42
20% free bend	32	48
90 degree twist	31	50
180 degree twist	30	52
20% sharp folding	16	74
30% sharp folding in 2 locations	5.5	91

Bo and Choa (2004) have reported field measurements of PVD discharge capacities from a pilot test carried out in Singapore where a wire mesh type core and a corrugated type core PVDs have been installed in two pilot areas. These results are reported in Table 2 below. The results show a 10 folds decrease in the discharge rate in a period of 6 months. However, based on these results the performance of wire mesh and corrugated cores appears to be similar, even though the laboratory tests demonstrate the wire mesh performs worse compared to corrugated cores.

Table 2: Field measurement of PVD discharge capacities from pilot test in Singapore (after Bo and Choa, 2004)

		Discharge Capacity of PVDs installed in a 1.5 m x 1.5m grid (m^3/s x 10^{-6})	
Project	Measured Value or Time of Measurement	Wire Mesh Type Core	Corrugated Core
Phase 1C	Maximum Discharge	2.2	2.2
	At 3 Months	0.53	0.47
	At 6 Months	0.26	0.22
	Minimum Discharge	0.0198	0.018
Area A	Maximum Discharge		8.2
	At 3 Months		0.25
	At 6 Months		0.22
	Minimum Discharge		0.021

2.10 Required PVD discharge rates

Many researchers have studied the porewater discharge capacity of PVDs. One of the earliest studies conducted by Oostveen (1986) demonstrated, using actual site studies, that a maximum flow rate of 5 x 10^{-6} m^3/s existed in the PVDs investigated. Koerner (1994) summarised in service PVD flow rate data; the maximum flow rates ranged between 1.5 - 5 x 10^{-6} m^3/s (50 - 150 m^3/year). These flow rates are based on actual site conditions, and thus, reductions in the discharge capacity of the PVDs caused by installation damage are incorporated in the flow rate values. Therefore, factors of safety are required when specifying a minimum discharge rate at a particular pressure based laboratory determined discharge rates. Particular consideration should be given to the effects of the following three main factors that cause a potential reduction of flow capacity, as discussed before: (1) deformation and creep of the geotextile filter into the core profile; (2) reduction of the permeability of the geotextile filter (3) deposition of fine particles in the core structure; and (4) reduction of the flow capacity due to kinking and bending of the PVD during settlement. Van Santvoort (1994) recommends that a PVD have a discharge capacity of 10 - 50 x 10^{-6} m^3/s at a confining pressure of 300 kN/m^2 if the PVDs installed in the field are greater than 10m in length; and relative ground surface settlement is greater than 15% of the PVD length in less than 1.5 years.

Agaki (1994) carried out many analyses and tests on PVDs to determine the minimum discharge rates required in PVDs installed in various soil media with varying permeability for various lengths of PVDs installed in clays and silts. Figure 11(a) presents the results obtained by Agaki (1994) for PVD lengths embedded in clay/silts ranging from 5 - 30m where the horizontal permeability of the soil, k_h, ranging from 0.5 - 50 x 10^{-9} m/s. The permeability of Hong Kong marine mud have a permeability of about 1 x 10^{-9} m/s, and the length installed in it will range from about 15m to 25m in general. Therefore, the minimum discharge rates, $q_{w\min}$, required are in the range of 100 - 130 m^3/year or 3.2 - 4.1 x 10^{-6} m^3/s. based on the field results of Bo and Choa (2004), these discharge rates were not achieved in the field in his field test. This is likely due to well resistance that had developed due to clogging etc. The rate of consolidation will hence be influenced by the well resistance. Basu and Madhav (2000) studied the influence of clogging on time to consolidation. When designing PVDs, a factor of safety must be imposed on the measured flow rates - measured under the pressures that the PVDs will be subjected to using the specified flow rate measurement tests. This factor of safety is generally between 4 and 6 (Chu Jian et al 2004) to account for installation issues and deterioration of the flow rate with time when the NTU Buckled Tester is used. The FOS to be applied will depend on the type of test used. If the ASTM D 4716 standard test method is used FOS values of about 18 shall be used. The tests to measure discharge rate are discussed in the section below.

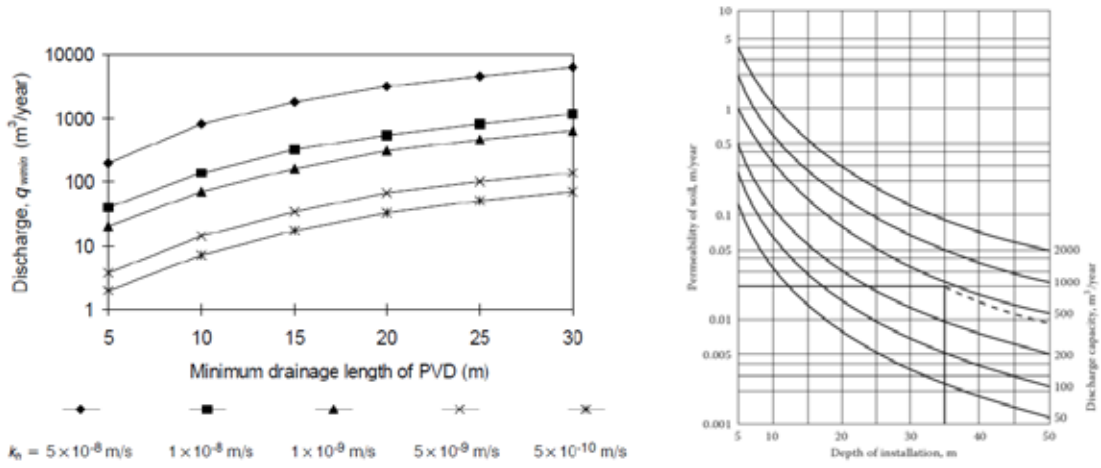

(a) (b)

Figure 11: Minimum discharge capacity required for negligible well resistance (a) After Agaki, (1994) (b) Extracted from BS EN 15237 (2007)

2.11 Tests for the determination of flow characteristics of PVDs

The main tests used to ascertain the PVD discharge capacities are (1) ASTM D 4716 standard test method, (2) Delft PVD discharge test; and (3) Singapore Nanyang Technological University's (NTU) simple discharge capacity tester for PVDs (Broms 1994) and (4) The NUS Tester.

2.12 Recommended tests for discharge capacity measurements

The preferred test is the Buckled Drain Tester because this test replicates closely the conditions that the PVDs will be experiencing in the field, especially if the tests are carried out with the soil sample obtained from the specific site. However, one of the difficulties is the need to provide the laboratory with the disturbed bulk soil samples to be used in the tests, along with the PVDs to be tested. Other difficulty is that these tests are not available in Hong Kong at present. The samples need to be sent to NTU laboratory in Singapore. These tests can be conveniently established in either commercial, Government or University laboratories in Hong Kong in the event of a major project here.

Other difficulty is that if minimum discharge rates are established based on these tests in the specification documents of a tender, it would be difficult for the contractors to obtain tests results in time using soil samples from the site or using soil samples close to that on site. One way around this problem is to test the PVDs immediately after award of contract with the PVDs proposed by the contractor with soil retrieved from site before the PVDs are accepted by the Engineer. It is best if the NTU Buckled test is amended by testing PVDs that are initially subjected to tensile loads of about 600 kN to replicate the stresses imposed in the installation process.

3 SUMMARY AND CONCLUSION

The following lessons were learnt from the experience gained in carrying out reclamations over soft sediments in Hong Kong, and in other places where prefabricated vertical band drains have been used as the technique to accelerate the consolidation of soft compressible sediments;

a. PVDs are the most common and extensively used ground improvement technique for soft compressible sediments all over the world as it is cheap, effective and quick to install. A wealth of knowledge is currently available with regards to the behaviour of PVDs and PVD treated ground. This wealth of knowledge must be exploited when designing new reclamations and ground treatment projects. PVDs have been used in drained reclamations in Hong Kong since the late 1970s.

b. The selection of the PVD type is an important aspect of the reclamation design process. The following aspects need to be considered;
    a. The characteristics of the soft sediments to be improved – Index properties including particle size distribution, compressibility, coefficients of consolidation - c_v, c_h, c_r, coefficient of secondary consolidation, structure of the clay, clay sensitivity, and activity.
    b. Depth to seabed and depth of the soft sediments and the length of PVDs required.
    c. The fill thickness, and the surcharge height to be placed; and the resulting total settlements and the vertical strain to be experienced by the clays and the lateral stresses PVDs will be subjected to.
    d. The method of installing the PVDs – with marine plant (before reclamation) or land plant (after reclamation).
    e. Estimated time required to achieve consolidation (as the performance of PVDs deteriorate with time).
    f. The residual settlement to be achieved.

c. The main function of the PVDs is to efficiently discharge the pore water from the compressible soft clays/silts, without well resistance, and reduce the water content, thus consolidating it. Therefore, during the consolidation period, the PVD discharge capacity should be higher than the minimum discharge rate required to avoid well resistance, $q_{w\min}$.
d. The PVD discharge capacity after applying the appropriate Factor of Safety to the discharge measured in the specified laboratory test shall be higher than the minimum discharge capacity required.
e. The method of measuring the discharge capacity is very important. The test used shall replicate as closely the conditions that the PVD will be subjected to in the field. The test that closely replicates is the Buckled Drain Tests developed by Nanyan Technological University (NTU) and National University of Singapore. These tests are preferred.
f. The selection of the type of PVD is important considering its core structure, the filter and how the filter interacts with core when it is subjected to lateral pressure, when bent/folded and spliced. These play an important part in its flow capacity.
g. It is recommended that tests with the NTU Buckled Drain tester are conducted with soil from the site before PVDs are accepted for installation; but after award of contract (before the contractor orders the PVDs in bulk).
h. Regular QA tests shall be carried out to ensure consistency of quality of drains supplied.
i. The field PVD discharge rates deteriorate quickly – in about 6 months – with the well resistance increasing – leading to 'stagnant' excess pore pressures which is commonly observed in many reclamation projects. The way to discharge these 'stagnant' excess pore pressures is to re-install PVDs. Therefore, provisions should be made in contract documents for re-installation of PVDs as a contingency measure.
j. Even if primary consolidation is complete significant settlements occur post primary due to secondary consolidation. Long term residual settlements can be controlled by overconsolidating the Marine Muds by additional surcharging.
k. The smear and other effects due to soil disturbance must be considered in the PVD design in determining rate of consolidation. This can be taken account of by adopting the field coefficient of horizontal consolidation $c_{h(field)}$, which is back calculated from past similar sites, in design.
l. Mudwaves shall be prevented at all costs as the disturbance of the mud will render PVDs useless.

REFERENCES

Akagi, T., 1994. Hydraulic Applications of Geosynthetics to Filtration and Drainage Problems - with special reference to Prefabricated Band - Shaped Drains, *Proceedings of the Fifth International Conference on Geotextiles, Geomembranes.*

ASTM D 4716. *Standard Test Method for Constant Head Hydraulic Transmissivity (In-Plane Flow) of Geotextiles and Geotextile Related Products*, American Society for Testing and Materials, West Conshohocken, Pennsylvania, USA.

Basu, D. and Madhav, M.R., 2000. Effect of Prefabricated Vertical Drain Clogging on the Rate of Consolidation: A Numerical Study, *Geosynthetics International*, Vol. 7, No. 3, pp. 189-215.

Bergado, D. T., Manivannan, R., Balasubramaniam, A. S. 1996. Proposed criteria for discharge capacity of prefabricated vertical drains. *Geotextiles and Geomembranes* 14 (1996), 481-505.

Broms, B.B., Chu, J. and Choa, V., 1994. Measuring the Discharge Capacity of Band Drains by a New Drain Tester, *Proceedings of the Fifth International Conference on Geotextiles, Geomembranes and Related Products*, *Vol. 2, Singapore*, pp.803-806.

Chua K.T., and Lee J.S.S.. Evaluation of Discharge capacity of prefabricated vertical drains. PSB, Singapore.

Fourie, A.B. and Kuchena, S.M., 1995. The Influence of Tensile Stresses on the Filtration Characteristics of Geotextiles, *Geosynthetics International, Vol. 2, No. 2*, pp. 455-471.

GEO. 1997. *GEO Report No. 63. 1997. Review of Some Drained Reclamation Works in Hong Kong*, The Government of the Hong Kong Special Administrative Region.

Indraratna, B, Rujikiatkamjorn, C, Wijeyakulasuriya, V, McIntosh, G & Kelly, R. 2010. Soft soils improved by prefabricated vertical drains: performance and prediction, In Almeida, M (ed), *Symposium on New Techniques for Design and Construction in Soft Clays, 2010,* 227-246, Brazil: Officna de Textos.

Indraratna, B., and Redana, I. W. 2000. Numerical modeling of vertical drains with smear and well resistance installed in soft clay. *Canadian Geotechnical Journal*, Vol. 37, pp. 132-145.

Karunaratne, G. P., Chew, S. H., Leong, K. W., Wong, W. K., Lim, L. H., Yeo, K. S., Hee, A. M. 2003. Installation stress in prefabricated vertical drains. *Journal of geotechnical and geoenvironmental engineering*, Vol. 129, No. 9, September 2003, 858-860.

Klaus Kirch Editor and Allan Bell. Editor (ed.). *Ground Improvement*. 3rd Edition

Oostveen, J.P. and Troost, G.H., 1990. Discharge Index Tests onVertical Drains, *Proceedings Fourth International Conference on Geotexiles, Geomembranes and Related Products*, Vol. 1, *The Hague, Netherlands*, pp. 345-350.

Rawes, B.C. 1997. Critical Parameters for Specification of Prefabricated Vertical Band Drains. *Geosynthetics International*, *Vol. 4, No. 1*, pp. 51-64.

Stapelfeldt, T.. "Preloading and vertical drains"

GROUND ENGINEERING SPECIALIST PROVIDING INNOVATIVE SOLUTIONS

Intrafor - specialist contractor on the **Tuen Mun-Chek Lap Kok Link Northern Connection** project.
Our scope of works includes:

Cone Penetration Testing
Vibro Compaction
Jet Grouting
Diaphragm Wall
Cutter Soil Mixing
Geotechnical Instrumentation
Ground Investigation

For further information please contact:
Email: northasia@vsl-intrafor.com
Phone: (+852) 2590 2288
www.intrafor.com

VSL INTRAFOR

Keller Group is the world's largest independent ground engineering specialist. With 150 years of service to the construction industry, Keller is renowned for providing a full range of technically advanced and cost-effective foundation solutions across the entire construction spectrum. The Keller group has a strong profile in Asia and the Middle East, and unrivalled coverage in Europe, North America, Australia and South Africa.

Capabilities:

- Vibro Compaction
- Vibro Stone Columns
- Specialist Grouting
- Deep Cement Mixing
- Ground Anchors & Micropiles
- Dynamic Compaction &
- Dynamic Replacement
- Soil investigation
- Prefabricated Vertical Drains
- Diaphragm Walls
- Foundation Civil Works
- Testing & Monitoring
- Foundation Bored Piles

Unit A, 27th Floor, Billion Plaza II
10 Cheung Yue Street, Cheung Sha Wan
Kowloon, Hong Kong

Tel: +852 3959 3353 | Fax: +852 3584 7990
E-mail: info@kellersing.com.sg
www.kellerasean.com